BODLEIAN LIBRARY OXFORD
DEPOSITED
THESIS
10·12·73

KINEMATICS OF THE LOWER LIMBS IN HUMANS

by

J.R.W. MORRIS, B.Sc.

A thesis submitted for the degree of Doctor of Philosophy.

July, 1973

University of Oxford.

ABSTRACT

Kinematics of the Lower Limbs in Humans

A history is given of the experimental techniques used in gait analysis. There follows a description of the phasic activity of various musculo-skeletal elements of lower limbs during a step of normal walking.

Equations are derived, relating the output signals of accelerometers, fixed to a moving body, to the motion of that body. Methods of solution to these equations are given, taking into account various approximations and simplifications. A suitable form is suggested for an accelerometric measurement system for studying the movement of the shank.

Computer programs, which analyse the signals from such a system, are explained. The following variables are found as functions of time: translational acceleration, angular and translational velocity, and angular and translational displacement.

Those features of the above variables which are characteristic of certain types of gait are discussed. The clinical usefulness of a selection of these variables is also examined. The development of a tape-recorder for use with the accelerometers is explained.

It is concluded that accelerometry is a useful technique for the study of human body movement.

TABLE OF CONTENTS

		Page
ABSTRACT		i
TABLE OF CONTENTS		ii
LIST OF FIGURES		iv
ACKNOWLEDGEMENTS		vii
CHAPTER 1	INTRODUCTION	
1.1	The Purpose of Research	1
1.2	A History of Orthopaedic Biomechanics Research up to 1945	2
1.3	Gait Analysis since 1945	5
1.4	A Summary of Current Knowledge - The Step	9
1.5	Accelerometry v. Cine photography; Project Development	16
CHAPTER 2	KINEMATIC ANALYSIS	
2.1	Introduction	20
2.2	The Effect of Gravity on Measurements of an Acceleration Field	21
2.3	The Techniques of Inertial Navigation	23
2.4	The Six Accelerometer System	26
2.5	Determination of Initial Conditions, and Offset Compensation	30
2.6	Simplifying Approximations, Methods of Solution and Errors	37
CHAPTER 3	EXPERIMENTAL PROCEDURES AND PROGRAM DESCRIPTIONS	
3.1	Introduction	44
3.2	The Transducers and Associated Electronic Circuits	45
3.3	Leg Mounting	50
3.4	Double-Buffered Data Input DATIN	53
3.5	General Structure of the Analysis Routines START,HOP,MAIN1,MAIN2,MAIN3	56
3.6	Kinematic Analysis Routines MAIN4,M4EXT, MAIN5,MAIN6	59
3.7	Graphs and Moving Pictures MAIN5 and MOVE; Summary	66

		Page
CHAPTER 4	EXPERIMENTAL RESULTS	
4.1	Introduction	69
4.2	Comparisons with Cinephotographic Results	71
4.3	Accelerations	76
4.4	Velocities	80
4.5	Displacements	85
4.6	Summary of Clinically Relevant Variables	90
4.7	Heel-Strike	92
CHAPTER 5	THE TAPE RECORDER	
5.1	Introduction	94
5.2	Possible Recording Systems	95
5.3	The MRC/Oxford Instruments Tape Recording System	97
5.4	Duplexing Pulse Width Modulation Encoding	101
5.5	Decommutation and Decoding; Characteristics	106
5.6	Future Systems - The Resistance Ratio Controlled Oscillator	109
CHAPTER 6	DISCUSSION AND SUMMARY	
6.1	Introduction	115
6.2	A Comment on Methods Describing Gait	116
6.3	The Advantages of Accelerometry	117
6.4	The Disadvantages of Accelerometry	118
6.5	Extensions of the Present System	119
REFERENCES		122
APPENDICES		
A	A Glossary of Anatomical Terms	A1
B	Specifications of the Pixie Transducer	A4
C	Specifications of the Aakers Transducer AE 801	A6
D	Block Diagram and Program Listings (folding out)	A8
E	Errors	

LIST OF FIGURES

Figure Number	Title	Page Number (opposite
1.1	from 'de Motu Animalium'	2
1.2	A Stick Diagram by Braune and Fischer	3
1.3	Frequency Spectrum of a Limited-Bandwidth Procedure	17
2.1	Measurement Points in a Moving Frame of Reference	27
2.2 2.3 2.4	{ Removal of Zero and First Order Polynomial Components from a Periodic } Variable	31
2.5	Transducer Platform	39
2.6	A Typical Transformation Matrix	42
3.1	Accelerometer Schematic	45
3.2	Accelerometer Drift	47
3.3	Transducers and Amplifiers	48
3.4	Cast on Leg	50
3.5a)&b)	Oscillograph showing Platform Movement	51
3.6	START v.d.u. message	56
3.7	START constants entry	56
3.8	HOP steering message	56
3.9	MAIN1 2.56s data window	57
3.10	MAIN2 calibrated data set	57
3.11	MAIN4 OM1 and OM2	59
3.12	MAIN4 operator error message	59
3.13	MAIN4 filtered angular velocities	59
3.14	MAIN6 translational components of the origin movement	65

3.15	MAIN5 display choice	65
3.16	MAIN5 display OM1 and OM2	66
3.17	MAIN5 display DC	66
3.18	MAIN5 display DC detail	66
3.19	MOVE view and speed selection	66
3.20	MOVE frame from lateral view	67
3.21	MOVE frame from anterior view	67
3.22	MOVE 4 lateral frames	67
4.1	Cine camera locations	71
4.2	Lateral camera frame	72
4.3	Anterior camera frame	72
4.4	Two typical sets of parallax-corrected data	73
4.5 4.6	Comparison of Accelerometric and Cine Displacement Data.	74
4.7	Runs 4,5 and 13	
4.8	Representative Normal Data Set. Accelerations	76
4.9	Accelerations. Subject D.B.	77
4.10	Accelerations. Subject G.F.	77
4.11	Accelerations. Subject G.P.	77
4.12	Representative Normal Data.Angular Velocity	80
4.13	Representative Normal Data Set. Velocities	81
4.14	Angular Velocities. Subject D.B.	83
4.15	Angular Velocities. Subject G.F.	83
4.16	Angular Velocities. Subject G.P.	83
4.17	Velocities. Subject D.B.	83
4.18	Velocities. Subject G.F.	83
4.19	Velocities. Subject G.P.	83
4.20	Representative Normal Data Set. Direction Cosines	85

4.21	Representative Normal Data Set. Displacements	86
4.22	Direction Cosines. Subject D.B.	87
4.23	Direction Cosines. Subject G.F.	87
4.24	Direction Cosines. Subject G.P.	87
4.25	Displacements. Subject D.B.	87
4.26	Displacements. Subject G.F.	87
4.27	Displacements. Subject G.P.	87
4.28	A table indicating how the kinematic variables provide clinically relevant data	on page 89
4.29	Comparisons of ankle anterior accelerations found by two methods (after Paul)	92
5.1	The M.R.C./Oxford Instruments Cassette Recorder	96
5.2	Servo Motor Speed Control	98
5.3	Mark/Period Ratio Encoding	99
5.4	Duplexed M/P Ratio Signal	101
5.5	Duplexer Block Diagram	102
5.6	Duplexer Waveforms	102
5.7	Duplexer Schematic Circuit Diagram	103
5.8a)&b)	TTL logic Transfer Characteristics	104
5.9	Tape Recorder Interior	105
5.10	Decoder Block Diagram	106
5.11	Decoder Waveforms	106
5.12	Resistance-Ratio Controlled Oscillator	111
5.13	Voltage Waveforms for Fig.5.12	111
5.14	A Family of Hyperbolae. $\Delta f/k_1$	112
D1	Program Flow Block Diagram	A9

ACKNOWLEDGEMENTS

I should like to express my gratitude to the following :

Dr.J.J.O'Connor, my supervisor, who directed some naive ideas into a feasible project and who has been a true teacher.

Dr.C. Ruiz, who acted as supervisor for a year and helped particularly with the layout of this thesis.

Professor R.D. Duthie for offering employment within the Nuffield Dept. of Orthopaedic Surgery while this project was in progress and for training an engineer on the 'shop-floor' of clinical orthopaedic medicine.

Dr.D.W. Clarke and members of the Control Group of the Engineering Science Dept. for assistance in the operation of the computer.

Members of the Department of Engineering Science and the Nuffield Department of Orthopaedic Surgery, in particular Mr.D. Haynes, Mr.P. Flint and Mr.M. Lawrence for help with the photography and reproduction of this thesis.

Mrs.M. Miles for her excellent typing.

The Trustees of the Trust Fund of the Nuffield Dept. of Orthopaedic Surgery for financial support.

Professor J.P. Paul, Mr.N. Jacobs and Mr.G. Ishai of the Bioengineering Unit of the University of Strathclyde for their generosity in offering their time and facilities for the experiments using cinephotography.

CHAPTER 1

INTRODUCTION

1.1 The Purpose of the Research

1.2 A History of Orthopaedic Biomechanics Research up to 1945

1.3 Gait Analysis since 1945

1.4 A Summary of Current Knowledge - The Step

1.5 Accelerometry v. Cinephotography; Project Development

1.1 The Purpose of the Research

The conception of this project was the result of a clearly defined need. A description of that need should indicate the purpose of the research.

The need was for a new method of making kinematic measurements of the locomotion of human subjects. The existing methods of measurement are inadequate on two counts. First, there are certain facets of the human locomotion process which it has been difficult or impossible to study, and second, there is no measurement system which is properly suited to routine use in a clinical orthopaedic environment. In order to justify this definition of the need, this chapter will first report on past developments which have allowed our current knowledge of human locomotion to be acquired.

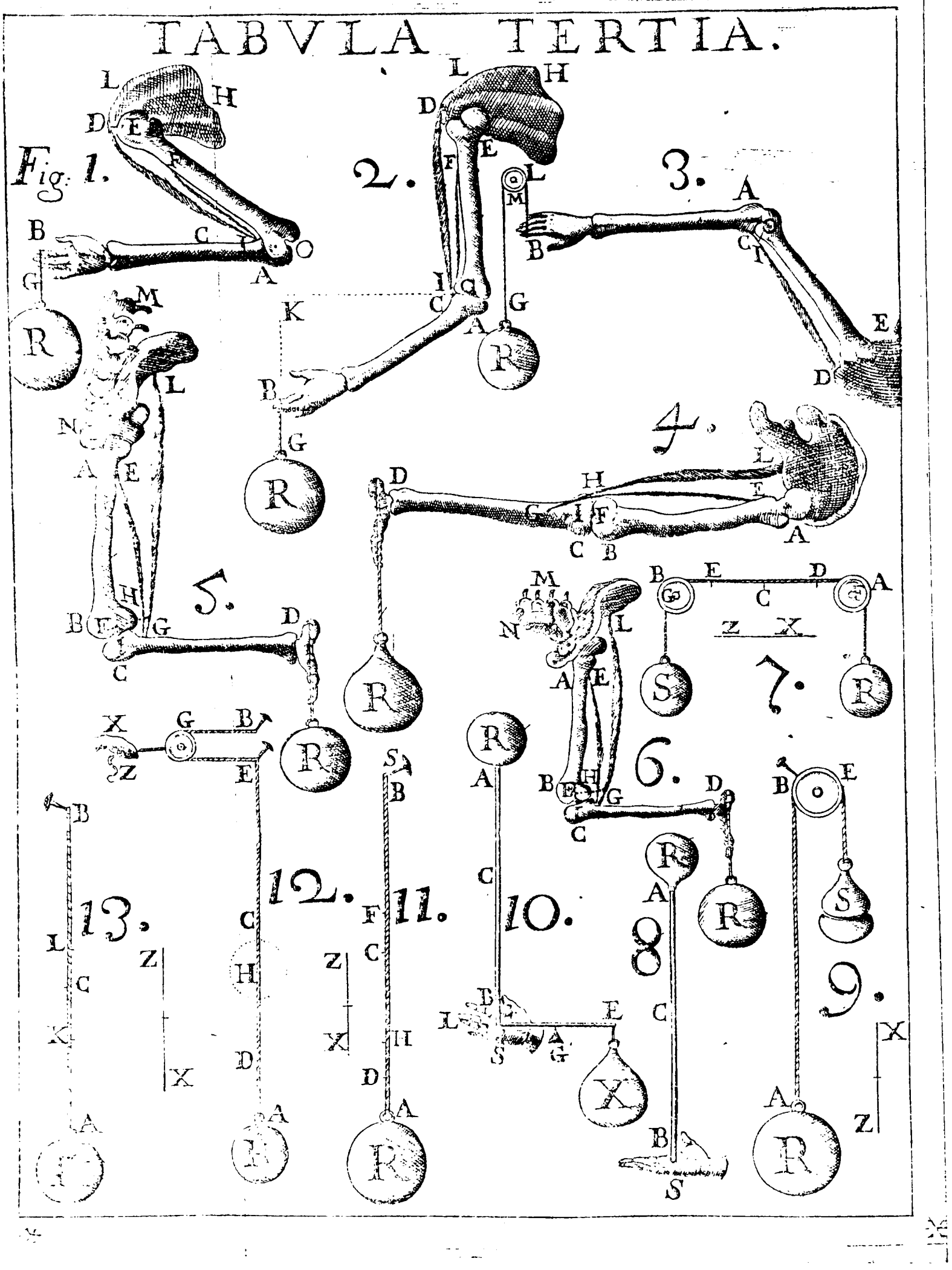


Figure 1.1 from 'de Motu Animalium'

1.2. A History of Orthopaedic Biomechanics up to 1945

The essence of the study of movement is the experimenter's ability to record parameters of that movement. Without such a record, further analysis is impossible. The first students of human movement were forced by the techniques available to them to rely almost exclusively on what they could remember of what they had seen. They could make static measurements of relative length and, since the human body was the most common object of convenience, they used anthropometric quantities as their first absolute standards of length. The Romans used the length of a marching soldier's pace and the Norse used the span of a warrior's outstretched arms. Long before Leonardo da Vinci showed the geometry of idealised human proportions, men would have been aware of the approximate equality of armspan and height, and probably tried to relate height to length of pace. The lack of any record of such an attempt may be due to the poor correlation between the two variables (an early case of not reporting an unexpected result).

Later, as accurate measurements of time were made available, it became possible to study cadence and this study has continued until the present day. Borelli's book, De Motu Animalium[1], which is widely credited with being the earliest study in biomechanics, deals extensively with the statics of the body (see Fig.1.1) and gives a description of walking as a process of continuous, interrupted falling. This qualitative description is, rightly, still popular.

It was the development of photography in the nineteenth century which provided the first accurate method of recording

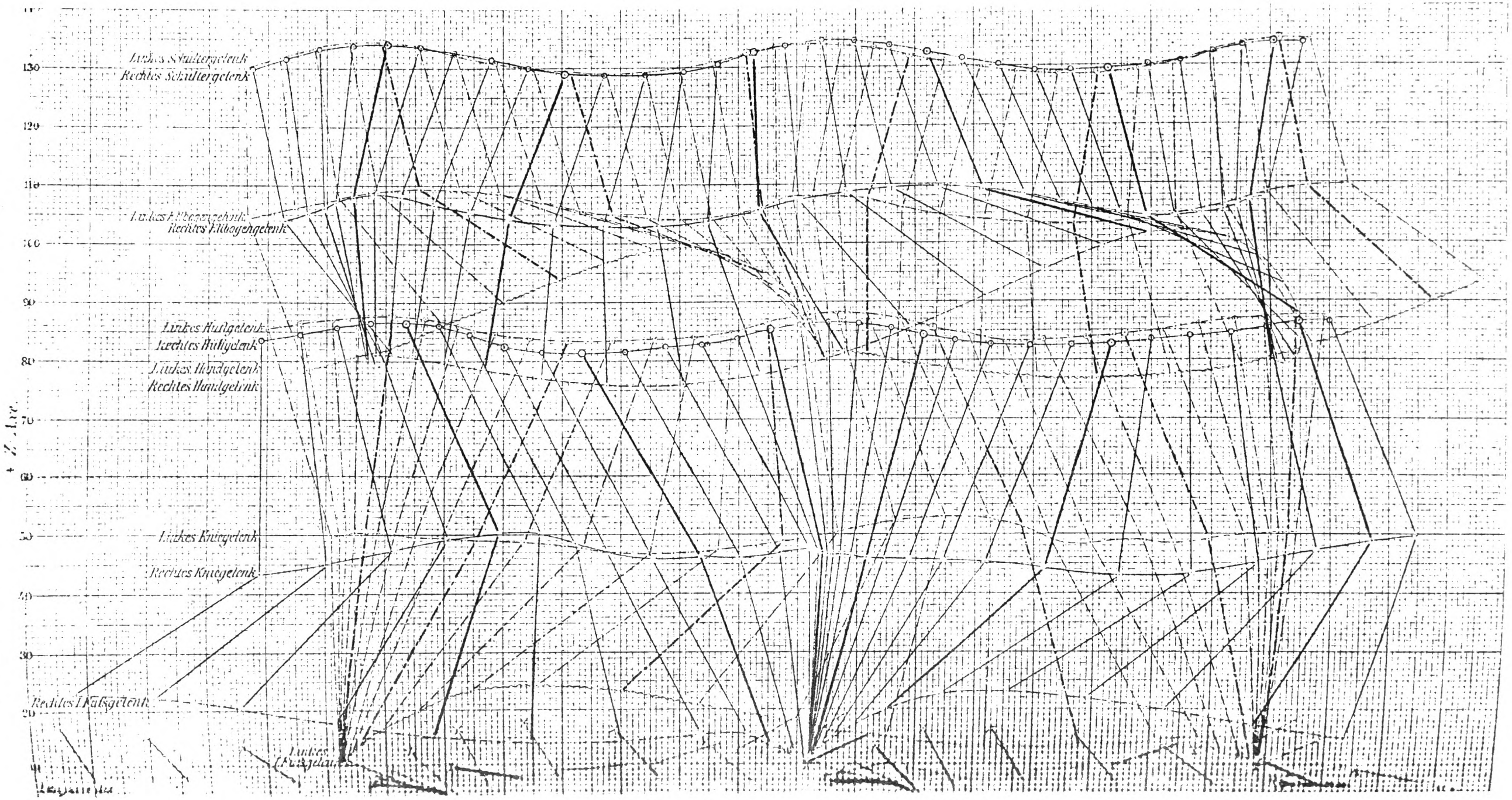


Figure 1.2 A Stick Diagram by Braune and Fischer

animal kinematics. Soon after man had devised machines which were capable of locomotion without animal or other natural motive power, he was able to freeze movements in stationary, pictorial records. Quite naturally, animal movement, which for so long had been the only consciously-directed locomotion in nature, was studied photographically as soon as the technology allowed. The resulting pictures were used both as curiosities[2] and for more serious purposes, most notably by Marey[3], and by Braune and Fischer. The research of these last two men covered an enormous area. They made measurements on the physical dimensions of the human body, identifying the axes of rotation of the joints[4]. They segmented four cadavers and measured the weights and mass distributions of the separate segments of the body, calculating the centres of mass and radii of gyration of all limb elements. Finally they photographed[5] moving human subjects to produce some of the first 'stick-diagrams', one of which is shown in Fig.1.2. From the abovementioned items, it was possible for them to calculate, for part of the walking cycle, the forces and moments required at the joints to produce the resulting motion. The results for which they are most remembered are the static anthropometric studies which were not duplicated or expanded until 1955, when Dempster[6] made similar tests on a larger number of cadavers.

Throughout the period up to the advent of modern orthopaedic surgery, medical interest in human kinematics came primarily from the need to duplicate lower limb movements in total, ectoprosthetic limb replacements. The "artificial leg"

was recognised as having to simulate normal leg movements if it was not to disturb the gait of the wearer. Various designs resulted but shorter life-expectancy meant that the problem was less acute than it is today, with more than 80% of all amputations now due to geriatric vascular disease, rather than to trauma.

During the first part of the twentieth century, orthopaedic surgery began to treat disabling disease by surgical procedures which altered the functional requirements of various muscles. The mechanical requirements of the muscles after these surgical procedures were largely unknown, with the result that there were many failures. In U.S.S.R.[7], and in U.S.A.[8], photographic methods were improved and the study of phasic muscular activity began, both by palpation[9] of muscles on a subject walking on a moving treadmill, and later using electromyography.[10] The forces between the foot and the ground were measured on load sensitive shoes.[11] By 1945, the basic techniques of gait analysis were available although they were used in only a few centres throughout the world. The knowledge which had been obtained prior to this time was neither widely known nor used. After the Second World War, public outcry in the United States against the poor services available for amputees who had suffered their injuries during the fighting prompted the American government to support a programme of research in biomechanics on a larger scale than had ever before been attempted. This research, carried out in the University of California, Berkeley, marks the beginning of modern gait analysis.

1.3. Gait Analysis Development since 1945.

The Berkeley study of the kinematics and dynamics of the lower limbs in 1945 - 1947 used most of the techniques of gait analysis which were available at the time. It also introduced the force-plate as a device for measuring all six components of the load transmitted between a foot and the ground. The phasic activity of synergistic muscle groups was studied using electromyography and, for some experiments, marker pins were fixed transcutaneously to the bones of ambulant subjects. The main body of experimental results was published privately,[12] but the understanding of gait which the project provided was translated into terms which a clinician might appreciate and was reported in 1952.[13] In particular, the group made a study of the transverse rotations of the lower limbs[14] and these results are used later in the research reported here.

Subsequently, the interest of the orthopaedic profession in the information which bioengineers could provide encouraged research in many centres. Generally, the methods of investigation remained unchanged, but attempts to use walkways, force-plates and cinephotography in routine clinical circumstances were usually shortlived.

In the 1950's a new type of orthopaedic surgery was developing very rapidly - that of total joint replacement. When biochemical treatments were perfected for the two major diseases of the musculo-skeletal system, poliomyelitis and tuberculosis, surgeons discovered that the largest group of patients still requiring treatment were suffering from diseases

of the joints. In the U.K., the two main pathologies in this category are rheumatoid arthritis and osteoarthrosis The only effective treatment for the advanced stages of these degenerative diseases is the replacement of the entire diseased joint. The first attempts at total hip replacement, made by the Judet brothers in France,[15] were not backed by any engineering knowledge at all, and failed disasterously. However, Charnley, after initial problems with materials, perfected a hip replacement.[16] He had a secure knowledge of the likely mechanical loads which the prosthesis would be expected to bear. In a parallel development, McKee[17] produced an equivalent device.

Estimates of the static forces through the hip joint were made by McLeish and Charnley[18] and of the dynamic forces by Paul.[19] The estimates by Paul were a significant advance in the knowledge of locomotor dynamics. Although the experimental methods used were very similar to those used in Berkeley, the forces derived were 'internal' joint and muscle forces, not the 'external' resultant forces which had been calculated previously. At the same time, Rydell[20] measured hip joint forces directly using instrumented endoprostheses and obtained results comparable to Paul's. The methods developed by Paul were extended by Morrison[21] to provide estimates of the dynamic forces acting in and around the knee joint.

One clear difference between gait studies before and after the 1950's was the increasing interest in the detailed kinematics of joints and muscles, rather than of the limb as a whole. All three major joint complexes of the lower limb

have been examined by a technique known as electrogonimetry. This involves the direct measurement of the angular displacement of the joint using potentiometers across the joint. The hip joint was studied by Johnston and Smidt[22], the knee joint by Kettlekamp[23] et al., and the ankle/subtalar compound joint by Wright[24] et al. These studies introduced this new system of measurement to satisfy the need for detailed joint kinematics. Besides some attempts to use polarised light goniometry, the success of which is unknown, electrogoniometry is the only new kinematic tool which has been made available to the gait analyst in the last eighty years. A single isolated report of the use of accelerometers was made by Gage[25] in 1965, but the analysis to which the signals were subjected was very limited.

An outstanding problem in the analysis of limb kinematics, since the time of Braune and Fischer, has been the difficulty of obtaining accelerations from photographic position measurements. Because of this and other inaccuracies, the estimates which have been made of the forces in the joints of walking subjects are possibly in error by up to 50%.[26] This fact, in itself, is not of any great consequence since the estimates of these forces are used only to provide order-of-magnitude parameters. But in many movements other than walking, the inertial forces are likely to be considerably larger than gravitational forces and, in these cases, photography is an inadequate means of obtaining data. This matter is discussed further at the end of this chapter.

This concludes a summary of the current state of experimental method in gait analysis. As far as is known, there are very few orthopaedic centres which are using any form of gait study in routine clinical orthopaedics. The exceptions to this statement use either cinephotography[27] or simple vertical reaction force walkways.[28] However, the past century has provided an accumulation of information on gait, gathered by each of the methods described above. This information is summarised in the next section.

1.4. A Summary of Current knowledge - The Step.*

As a format for presenting the current understanding of gait, the sequential events occurring during one step of normal walking, through swing and stance phases, are described below.

The cycle under consideration begins at the start of the swing phase, just after the toe has left the ground. The angular positions of the pelvis and elements of the leg are taken relative to their positions at stationary, neutral stance. The pelvis is externally rotated about 4^{o}[14] and is stationary in a transverse plane. It is also tilted downwards by 5^{o}[13]. The hip joint is just past the point of maximum extension at 12^{o}, abducted 3^{o} and externally rotated 7^{o}[22]. The knee is approaching the point of maximum flexion at 40^{o}, adducted 5^{o} and beginning the only short period of internal rotation which reaches a peak of 2^{o} a few milliseconds later[23]. The ankle joint has approximately 20^{o} of plantar flexion[24]. The initiation of the swing phase is brought about by the hip flexors, primarily by a short burst of activity by iliopsoas[29]. However, the compressive force in the hip joint is low, dropping rapidly to zero[19] since the weight of the limb is balancing the flexor force. Biceps femoris is active in the first part of the swing phase[30], keeping the knee joint flexed above about 40^{o}. However, Morrison[21] records no e.m.g. activity in the hamstrings during this part of the swing phase.[23] Certainly, knee flexion is not fixed in this period of the phase. The main area of muscular activity is in the region around the

---

* A Glossary of anatomical terms may be found in Appendix A.

the ankle joint. The foot must be moved from its position of plantar flexion to a neutral, or slightly dorsiflexed state, if the toe is to clear the ground. A failure to achieve this movement is clinically recognisable as 'foot-drop' and this indicates some abnormality of tibialis anterior, with extensor hallucis longus and extensor digitorum communis, or the popliteal nerve which supplies them. These muscles are active throughout the swing phase[31], keeping the foot dorsiflexed against the posterior ligaments of the ankle.

The sinusoidal nature of graphs of hip flexion during most of the swing phase[23] indicate that the movement of the leg is largely pendulous. Examination of recorded muscular activity confirms this. Only semitendinosus and semimembranosus show signs of action in the thigh[29], delaying knee extension.

During the swing phase, the pelvis returns to its neutral position and moves into internal transverse rotation[27], while pelvic tilt is reduced by the abductor group on the opposite side. The transverse rotations of the femur and tibia accelerate inwardly to a neutral position prior to heel strike[14]. About three-quarters of the way through the swing phase, the hip reaches 30^{o} flexion and maintains this angle until heel-strike,[22] by the action of the vasti in the quadriceps group.[29] This action is of particular interest. The leg as a whole has a certain angular momentum in the sagittal plane, and this momentum can only be changed by external moments applied to the system. Since the hip muscles are quiet, only the weight of the limb acting about the hip joint can provide such a moment. The action

of the vasti, which are single joint muscles, merely transfers the angular momentum of the thigh down to the shank. The hip therefore slows its flexion and the knee is rapidly moved into full extension prior to heel-strike. The quadriceps action is reflected by a compressive force in the knee joint which increases from zero to around body weight before heel-strike.[21] A load of up to 200 N in the posterior cruciate ligament controls the backward gliding of the tibia relative to the femur.[21]

That the whole leg is normally stabilised before heel-strike is well demonstrated by the sensation of collapse which is felt when heel-strike comes before it is expected. The hip, after reaching a maximum flexion of 30° begins to extend[22] under the action of biceps femoris, long-head, and possibly gluteus maximus.[30] The load in the joint is still low, less than body weight.[19] Depending on the individual case, the knee may hyperextend before heel-strike because of the angular momentum of the shank.[22] In any case, the movement of the shank is halted by the passive extension of the hamstrings and the posterior cruciate ligament.[21] The 'screw-home' mechanism of the knee is inoperative as the load on the joint is too low. About the ankle joint, the dorsi-flexors of the foot continue their activity up to and through heel-strike.[29] Plantar flexion of the joint, brings the foot down, flat onto the ground after heel-strike in less than 100 ms, under muscular control. This movement appears to be the main energy sink for the excess of energy produced by the leg in the transition from a swing to a stance role. Estimates of both the knee and hip loads show a

rise-time of approximately the same duration for the rapid increase in load which occurs after 'heel-strike'. To date, no published estimates have been made of the loads occurring in the ankle and subtalar joints, but they are certainly high. Surprisingly, however, these joints are relatively free of the degenerative changes which occur in the cartilage of other joints of the limb. No current theory of the aetiology of the disease can account adequately for this difference.

As is mentioned above, the loads in the hip and knee joints rise rapidly a short time after heel-strike, from about body weight, to peak values of about 2½ times body weight for the knee[21] and to 5 times body weight for the hip.[19] There is a reflex contraction of the hamstrings and quadriceps together, stabilising the knee. Simultaneously, there is an antagonistic contraction of the muscles around the hip, including gluteus maximus, the largest hip extensor, which is usually conspicuously silent for the rest of the step.

The role of the limb changes dramatically from providing balancing forces during the swing phase to become a supportive and propulsive member in the stance phase. During the first half of the stance phase, the shear force between foot and ground in an antero-posterior direction acts so as to remove forward momentum from the body, reaching a peak of approximately 100 N[32]. The integral over time of this force should be zero for the complete stance phase in symmetrical gait.

The progressive extension of the hip joint in the stance phase is an approximately linear function of time up to 'toe-off' and this extension is effected initially by biceps femoris.[30]

Once the toe on the opposite leg has left the ground, this muscular activity ceases and the trunk is carried forward by its own momentum until the femur is aligned with the trunk. Meanwhile the body weight is transferred gradually from one leg to the other and the line of action of this load exerts an increasing, adductive moment about the hip joint. This moment reaches a peak at opposite 'toe-off' of around 170 Nm[19] corresponding to the peak compressive load on the joint. The moment is balanced by the abductor group of muscles, primarily by gluteus medius.

The knee joint, rather than extending, flexes from 0^{o} to 10^{o} during the first half of the stance phase.[23] The purpose of this flexion is to provide an effective shortening of the whole limb which reduces the distance through which the body mass must be raised.[13] The flexion is controlled by a force applied by the quadriceps, reaching a peak of about 800 N.[21] With the knee near full extension, the change in length of this muscle group is relatively small for a given angular displacement of the knee, so the muscle action is approximately isometric.[33] The line of action of body weight passes much closer to the knee joint than to the hip and the adduction moment is correspondingly lower. However the moment is sufficient to move the centre of pressure in the joint onto the medial condyle and to produce a tensile force in the lateral collateral ligament of up to 350 N.[21]

After 'foot-flat' the foot is normally immobilised until the heel leaves the ground and the muscles of the ankle may

therefore be regarded as inserting into ground-fixed points. The movement of the ankle joint complex is a gradual dorsiflexion from 10^{o} plantar flexion to about 30^{o} dorsiflexion[27] after which point the heel leaves the ground. Some of the plantar flexors of the ankle begin to act soon after 'foot-flat'[34], before the 'weight-line' has passed anterior to the joint. The most likely explanation for this is that the centre of pressure between the foot and the ground can be moved anterior to the heel by the resulting moment.

As has been stated, up to half-way through the stance phase the body has been losing forward momentum by the conversion of a part of its kinetic energy into potential energy in raising the centre of mass. The second half of the stance phase is characterised by the increase of forward momentum. The leg comes closest to the stationary, stance position half-way through the 'foot-flat' period. Beyond this point the leg acts as a falling, inverted pendulum which gradually increases its length due to the extension of the knee and to the plantar flexion of the ankle and foot.

Knee extension is accomplished by the vasti[21], but since gastrocnemius, one of the most powerful plantar flexors of the ankle, is also active[29], there is some antagonistic activity around the knee. This activity has the effect of stabilising the joint but also means that the joint load increases dramatically to its highest values of up to four times body weight.[21] Soleus and tibialis posterior assist in the plantar flexion of the ankle until the heel leaves the ground.[31] After this point

the foot itself becomes a complex linkage with many degrees of freedom. 'Push-off' is due primarily to the intrinsic muscles of the foot, most notably by abductor hallucis, flexor digitorum brevis, and flexor hallucis brevis.[35]

During 'push-off' the hip joint returns to the neutral positions of ab/adduction and rotation and, indeed, hip-flexion begins before 'toe-off'.[22] Hip extension is limited by a passive stretching of the hip flexor muscles and the ischio-femoral ligament.[36] The very sharp peak which occurs in hip joint load during 'push-off'[19] is due to the storing of elastic strain energy in the structures around the hip joint. As long as the knee remains fully extended, this energy store continues to draw on the body's kinetic energy. When the knee is allowed to 'break', hip flexion begins with an elastically applied moment. The antero-posterior shear force between the foot and ground drops rapidly at the same instant.[32] Thus it could be said that the swing phase begins before the toe actually leaves the ground. The 'vigorous push-off' encouraged by some people in the rehabilitation of gait is a functional myth.

This concludes a largely qualitative description of the internal and external mechanical events which occur in a leg during one normal step cycle. While the physical dimensions and even the anatomy of normal adults may vary from case to case, there seems to be general agreement on the definitions of 'normality'. The remainder of this thesis deals primarily with kinematics alone but, since all voluntary body movements are under the control of the body's musculature, a sound understanding of the internal mechanics of the limb is essential.

1.5. Accelerometry v. Cinephotography; Project Development.

It might appear, from the long history of gait analysis, that the action of the legs is well understood. This is not the case. Without exception, every fact which was presented in the previous section was obtained from the study of subjects walking in a biomechanics laboratory. Experiments can often take several hours to set up and some workers report that changes in gait were observed due to subject fatigue, indicating the abnormality of the circumstances which prevail in the laboratory.[32] Furthermore, it is clear from the outset that the amount of time which an individual normally spends walking steadily over smooth, flat surfaces, concentrating on his or her gait, is very small. The self-referenced nature of accelerometry immediately indicates the possibility of measurements taken outside the laboratory. It was with such a possibility in mind that this project was conceived. For reasons which are explained later, this objective has not yet been achieved, but there is nothing to show that the method is unsuitable for this sort of use.

Besides the inherent portability of accelerometers, there is an additional advantage over other forms of kinematic data acquisition. As was mentioned in section 1.3, a major source of error in the dynamic analysis of gait is the difficulty of double-differentiating position data with respect to time in order to derive accelerations.[37] Gutewort lists shutter timing, measurement inaccuracies from film, camera vibration, and a

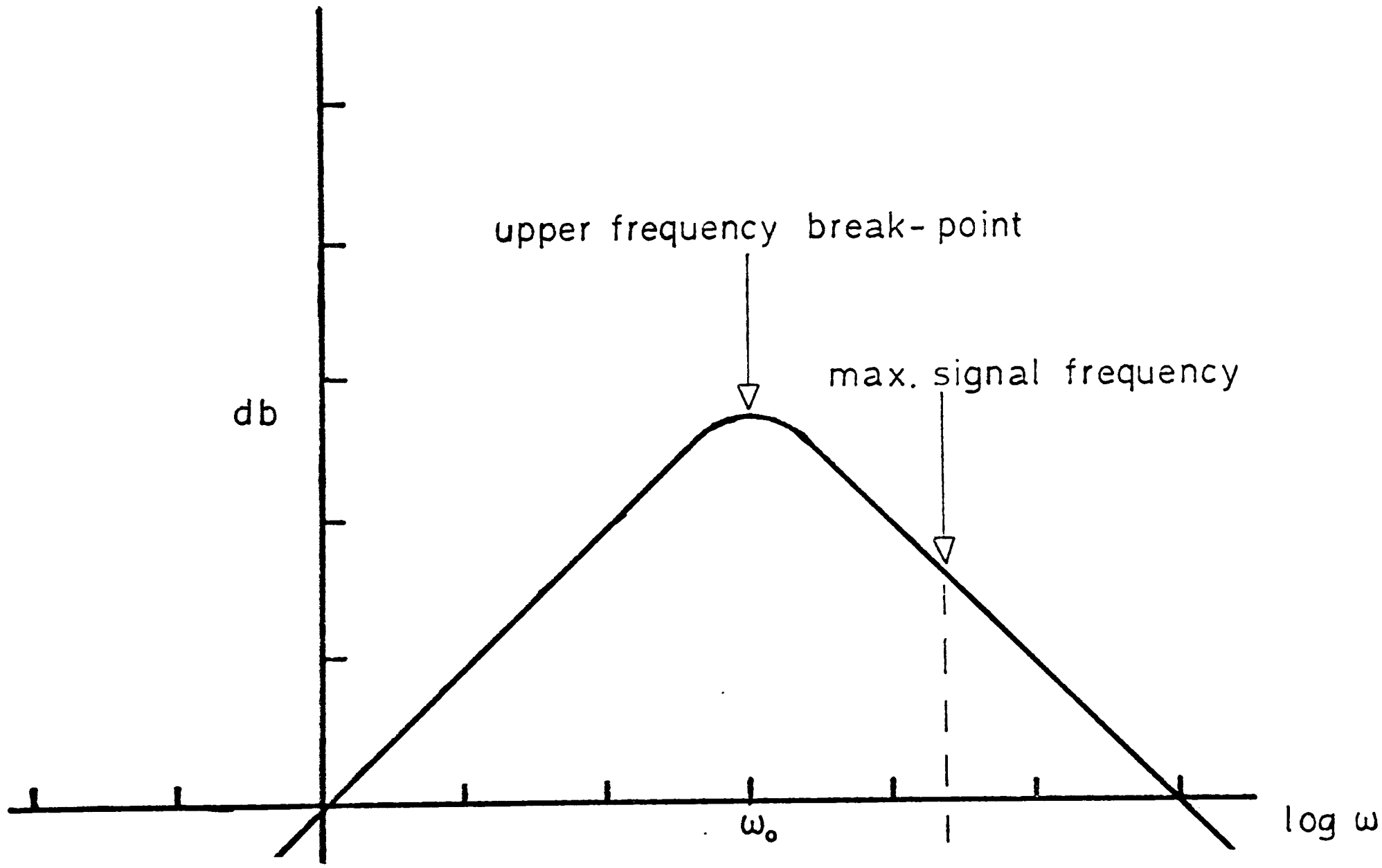


Figure 1.3 Frequency Spectrum of a Limited-Bandwidth Differentiation Procedure

number of other sources of error as potential noise producing factors in the measurement of position in cinephotography. Perhaps with undue pessimism, as the purpose of the article was to sell a new camera, the maximum relative error for accelerations determined from movie-cameras of the type frequently used in gait analysis is given as 300%. The usual way to avoid such gross inaccuracies is to band-limit the differentiation process. The choice of a suitable break-point is influenced by subjective impressions of the speed of the faster sequences in gait and by the sampling rate imposed by the camera. High frame rates usually mean less accurate shutter timing or expensive cameras, so that the commonly used rates are 50 or 64 f.p.s. At these rates, the number of frames which occur, for instance, during the important period from 'heel-strike' to 'foot-flat' may be as low as 2 or 3. In this circumstance, the highest frequency component of the movement may be higher than the highest signal frequency which is differentiated by the numerical procedure used. This is demonstrated in Fig.1.3. As will be shown later, no such problem exists in filtering out low frequency noise in an integration procedure.

Another difficulty exists in the use of cinephotography. Although the means are available for the automatic, numerical quantification of film position data[38], the process is complex and expensive. Sometimes, a semi-automatic frame-by-frame digitisation is employed, using movable cursors linked to a paper-tape punch. While this is considerably faster than transcribing measurements from film by hand, it is still a slow, laborious process.

Accelerometry is most unlikely ever to replace photography completely. The amount of data available in a single frame of film is very large and cinephotography has the advantage of presenting a record of the movement which is immediately comparable with the mental record remembered by the experimenter. But the very fact that photography has been available for so long and has still not become a means of keeping quantified records of gait in clinical orthopaedics underlines the weakness of the method.

With the background given in this chapter, the project was initially conceived as the development of a system with a number of accelerometers, sufficient to define the movement of all seven segments of the lower limbs and pelvis.[48] If the joints are assumed to have six degrees-of-freedom, the total number of transducers required is 42(6x7). If certain assumptions are made about the joints (hip 3 d-o-f.; knee 1 d-o-f.; ankle 2 d-o-f.) the number of transducers needed can be reduced to 18. However, before this could be attempted, it was necessary to show that the hardware and analytical algorithms could be applied to the study of the movement of one limb element.

The chapters which follow this introduction will discuss the analytical methods employed, the experiments which have so far been carried out and the conclusions drawn from those experiments. Details will also be given of the portable tape-recording system which is to be used with the transducers, and the interactive computer programs which allow the experimenter to change the course of the analysis to suit the characteristics

of the data. The research, as a whole, is nowhere near complete. Indeed, the hope is that, now the feasibility of the techniques has been demonstrated, work may continue and the method be used and extended.

CHAPTER 2

KINEMATIC ANALYSIS *

2.1 Introduction

2.2 The Effect of Gravity on Measurement of an Acceleration Field

2.3 The Techniques of Inertial Navigation

2.4 The Six Accelerometer System

2.5 Determination of Initial Conditions, and Offset Compensation

2.6 Simplifying Approximations, Methods of Solution, and Errors.

2.1 Introduction

The first chapter introduced, without an explanation, the possibility of estimating time-dependent functions of the movement of a rigid body in space from measurements of its acceleration. This chapter will attempt to show how this may be accomplished by solving a set of well-known vector equations, and how the process of solution may be greatly simplified by making certain assumptions. However, before these vector equations are derived, it is worth examining the nature of the quantity which is to be measured, since it will be shown that the transducer's output signal contains a component which is due to gravity.

---

* An article, based primarily on Chaps.2 and 3, has been accepted for publication by Journal of Biomechanics.

2.2 The Effect of Gravity on Measurements of an Acceleration Field

The output of the transducer which is used to measure acceleration will contain a component due to the effect of gravity. It will be necessary, later, to assume that this gravitational effect can be represented as a uniform vector field of acceleration. The vector magnitude is numerically equal to the force (g) per unit mass which acts on a body close to the surface of the earth and the direction of the vector is vertically upward, along a radius-line from the centre of the earth.

The simplest representation of the gravitational effect is a vector field which is dimensionally equivalent to acceleration. Indeed, an isolated observer, although he may be able to detect the field, is unable to identify it as a gravitational field, as opposed to an acceleration of his frame of reference with respect to another frame of reference in which the measured field at the same point is zero. This is a statement of the Principle of Equivalence in the General Theory of Relativity.

For present purposes, we need to study only the local movements of bodies near the surface of the earth. We find empirically that the field (known from now on as the acceleration field) is zero only in bodies which are moving in trajectories corresponding to a 'downward' acceleration of magnitude g, perpendicular to the surface of the earth. We also find that the field of trajectorial acceleration vectors is approximately uniform. We may therefore define an unusual

Newtonian frame of reference, where the measured acceleration field is zero, in which all bodies, 'unless subject to an external force, will continue in a state of rest or of uniform motion in a straight line'. All such bodies are described as being in a state of 'free-fall'.

The more usual Newtonian frame of reference, which is fixed to the surface of the earth, is clearly accelerating 'upwards' relative to the reference frame defined above. As a result, the acceleration field, measured in this ground-fixed frame of reference, is uniform, has a direction which is vertically 'upwards', and has a magnitude equal to the relative acceleration of the two frames of reference. Thus gravity is seen to have a measurable effect which is equivalent to the effect of this uniform acceleration field. All deviations of the measured acceleration field from this locally invariant field must be due to accelerations of the point of measurement relative to the ground-fixed frame of reference.

2.3 The Techniques of Inertial Navigation

A rigid body moving freely in three-dimensional space has six degrees of freedom, usually represented as three orthogonal translations and three orthogonal rotations. Estimation of a movement with unknown components for each of these six degrees of freedom requires six independent measurements of the movement to be made. The rotational components of the movement may be measured by gyroscopes; instruments which produce a torque which tends to keep them aligned with an output axis. The output torque can be used to preserve the orientation of the instrument directly. Alternatively, the torque may be measured and used as the error signal in a closed-loop control system which moves the gyroscope until the torque is reduced to zero. The output torque is proportional to the angular velocity of the instrument and so the latter system can be made considerably more accurate for changes in angular position. Three gyroscopes are mounted on a gimballed platform with their output axes orthogonal and are used to preserve the initial angular position of the platform whatever movements may occur in the body on which the platform is mounted.

In this gimballed system, three acceleration field transducers, known as accelerometers, also with their measurement axes orthogonal, are mounted on the stable platform. Thus the acceleration field of the platform is measured in the form of components whose orientations are fixed throughout the duration of the body's movement. Analytically, the determination of translational displacements with this apparatus is very simple,

involving only double integration of each component of the difference between the measured acceleration field and the known gravitational field. (In aircraft or spacecraft flights, the simplifying assumptions made in the last section about the gravitational field will not apply). This gimballed, gyroscopic system is characterised by high mechanical complexity and analytical simplicity.

A modification of the 3-gyroscope, 3-accelerometer system which affords a simpler mechanical realisation is that known as the 'strapped-down' system.[39] In this system, the gyroscopes are 'strapped-down' to the body and the output torques are used to determine an angular velocity vector for the body. From this angular velocity vector, a numerical representation of angular displacement (e.g. a direction cosine transformation matrix) is estimated. This representation is stored electronically and is used to transform the components of the measured acceleration field into the reference frame of the body's movement. Thus the gimballed platform of the original system is metaphorically replaced by the continuously updated, numerical representation of the body's angular displacement.

In the past, the gimballed system had advantages both of size and accuracy, but modern, real-time, digital computation is developing so rapidly that the extra calculations required by the 'strapped-down' system are ceasing to be a problem. Indeed, the most advanced 'strapped-down' system is now probably the equal of the gimballed system in terms of accuracy, and is certainly the smaller and lighter of the two systems.

The ultimate rationalisation of a position estimation system is one in which gyroscopes are not used. Since accelerometers can be made without bearings and almost 'without moving parts' a gyroscope-free system can be kept mechanically simple. Such a system, which has been shown in this section to be a logical development of modern inertial navigation systems, was used in this study of human gait.

2.4 The Six Accelerometer System

The estimates of displacement made in this study are not used, as in a navigation system, while the movement is taking place. In other words, there is no real-time requirement on the analytical computer. The other definitive characteristic of the problem is that the transducing elements need to be as small as possible. Clearly, a system which would operate without gyroscopes was indicated. As was mentioned in the previous section, six independent measurements of acceleration are sufficient to define the movement of a single, rigid body. The current literature contains almost no references to the technique, although a few authors[40] intimate that such a method should be feasible.

The lack of previous interest in the method is explained by the nature of the movements which had been measured. In the aerospace industry, movements are primarily translational, with rotational components of moderate magnitude usually introduced only to impart stability (as in the 'roll' of a missile). The component of the measured acceleration field which is due to rotation is relatively small. In the movement of the lower leg, however, the movement is as much rotational as translational. Analytically, the accelerometric system is similar to the 'strapped-down' system described in the previous section except that the angular velocity vector is not found from gyroscopes.

Referring to Fig. 2.1, consider the acceleration of a point fixed in a body reference frame. The position of the point from the local frame origin is $\underline{r}$. The body reference frame

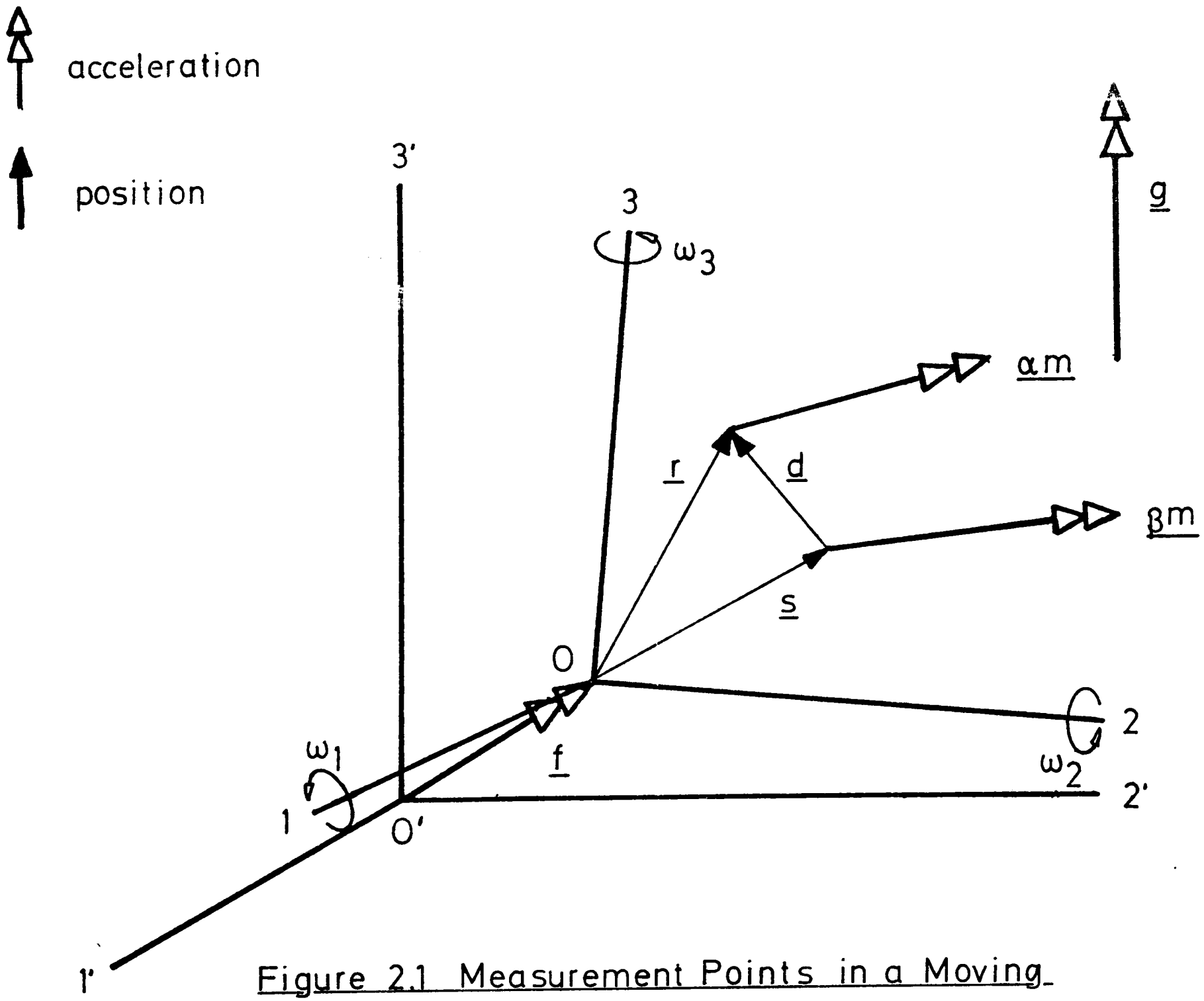


Figure 2.1 Measurement Points in a Moving Frame of Reference

is rotating with angular velocity $\underline{\omega}$ and the acceleration of the body origin O, with respect to the fixed reference frame, is $\underline{f}$. The acceleration vector $\underline{\alpha}$ of the point is given by:

$$\underline{\alpha} = \dot{\underline{\omega}} \times \underline{r} + \underline{\omega} \times (\underline{\omega} \times \underline{r}) + \underline{f} \qquad 2.1$$

(two additional terms, $2\,\underline{\omega} \times \dot{\underline{r}}$ and $\ddot{\underline{r}}$ would be needed if the point were not fixed to the body reference frame)

As was shown in section 2.2, the measurable acceleration field vector $\underline{\alpha m}$ at the same point will be:

$$\underline{\alpha m} = \underline{\alpha} + \underline{g} \qquad 2.2$$

where $\underline{g}$ is the field component due to gravity.

Two similar equations exist for the acceleration $\underline{\beta}$ and the acceleration field $\underline{\beta m}$ of another point fixed in the body.

$$\underline{\beta} = \dot{\underline{\omega}} \times \underline{s} + \underline{\omega} \times (\underline{\omega} \times \underline{s}) + \underline{f} \qquad 2.3$$

$$\text{and} \quad \underline{\beta m} = \underline{\beta} + \underline{g} \qquad 2.4$$

Subtracting equation 2.4 from equation 2.2.

$$\underline{\alpha m} - \underline{\beta m} = \underline{\alpha} - \underline{\beta} = \dot{\underline{\omega}} \times \underline{d} + \underline{\omega} \times (\underline{\omega} \times \underline{d}) \qquad 2.5$$

where $\underline{d} = \underline{r} - \underline{s}$

Equation 2.5 is a first-order, differential vector equation for $\underline{\omega}$, which may be rewritten in integral form:

$$\underline{\omega} \times \underline{d} = \int ((\underline{\alpha m} - \underline{\beta m}) - \underline{\omega} \times (\underline{\omega} \times \underline{d})) + \underline{C} \qquad 2.6$$

where: $\underline{C}$ is a vector, independent of time, and the integral is over time.

The equation is non-linear and consequently it is not possible to solve it analytically. It would be difficult to arrive at

an approximate solution by numerical methods.

It will be shown in section 2.7 that a careful choice of the components of vector $\underline{d}$ can be used to simplify equation 2.6 to produce an analytical solution for $\underline{\omega}$.

When $\underline{\omega}$ has been estimated as a function of time, the angular displacement of the body may be derived. It is convenient to represent the angular displacement of the body by the direction cosine transformation matrix. This matrix $[\lambda]$ is related to $\underline{\omega}$ by the equation:

$$[\dot{\lambda}] = [\omega][\lambda] \qquad 2.7$$

where $[\omega]$ is the skew-symmetric matrix
defined by : $\omega_{ij} = \omega_k \varepsilon_{jik}$
where : ε_{jik} is a permutation symbol
and : ω_k is the angular velocity vector.

[39,40,41]

Equation 2.7 is well known and is used in the 'strapped-down' gyroscopic systems described in the last section. It should be noted that the direction cosine matrix is not unique as a representation of relative angular displacement. The matrix is redundant and over-determined since a minimum of four elements is sufficient to define the others. Alternative representations are equivalent Euler Angle rotations, or Quaternions.[39] The use of these alternatives would effect a saving in computer storage since they are canonical forms, but the analytical complexity of the program would be increased and it was therefore decided to use the direction cosine representation. The method of solution of equation 2.7 is explained in section 2.6.

$[\lambda]$ transforms vectors in local, body coordinates into the fixed coordinate system. The acceleration field, interpolated from the points of measurement to the body origin, may

be transformed into the fixed coordinate system, using $[\lambda]$. Since the gravitational component of the acceleration field is known for all possible positions of the body origin, the vector of the gravitational component may be subtracted from the transformed, measured field vector. The difference vector, as was explained in section 2.2, is the acceleration of the body origin with respect to the fixed reference frame ($\underline{f}$ in Fig. 2.1). Simple integrations then lead to the translational velocity and displacement of the body origin.

Thus the movement of a body, with six degrees of freedom relative to a fixed frame of refemence, can be calculated from six acceleration field measurements made on the body.

2.5 Determination of Initial Conditions, and Offset Compensation.

It can be shown[42] that the translational displacement of a body is a fourth-order integral function of body-fixed measurements of acceleration field. These integrals arise as follows.

1) from the solution of equation 2.6 for angular velocity;
2) from the solution of equation 2.7 for angular displacement;
3) from the determination of body origin translational velocity;
4) from the determination of body origin translational displacement.

Each of these four integrations introduces a time-independent term corresponding to the initial conditions of the integral functions: 1) initial angular velocity; 2) initial angular position: 3) initial translational velocity; and 4) initial translational position. Each of these initial conditions must be specified before a solution can be obtained to the equation from which it arises.

The simplest set of initial conditions occurs when the rigid body whose movement is to be determined is initially at rest. In the present case, however, the kinematic analysis was to be performed for short time intervals taken from a continuous stream of recorded data. Clearly, this simple set of initial conditions is inapplicable.

In walking, most kinematic variables are approximately cyclic functions of time. There may be small variations from one step to the next, but the instantaneous value of a variable, at a point in the cycle when it is not changing rapidly, is generally constant from one cycle to the next. (An obvious

Figure 2.2

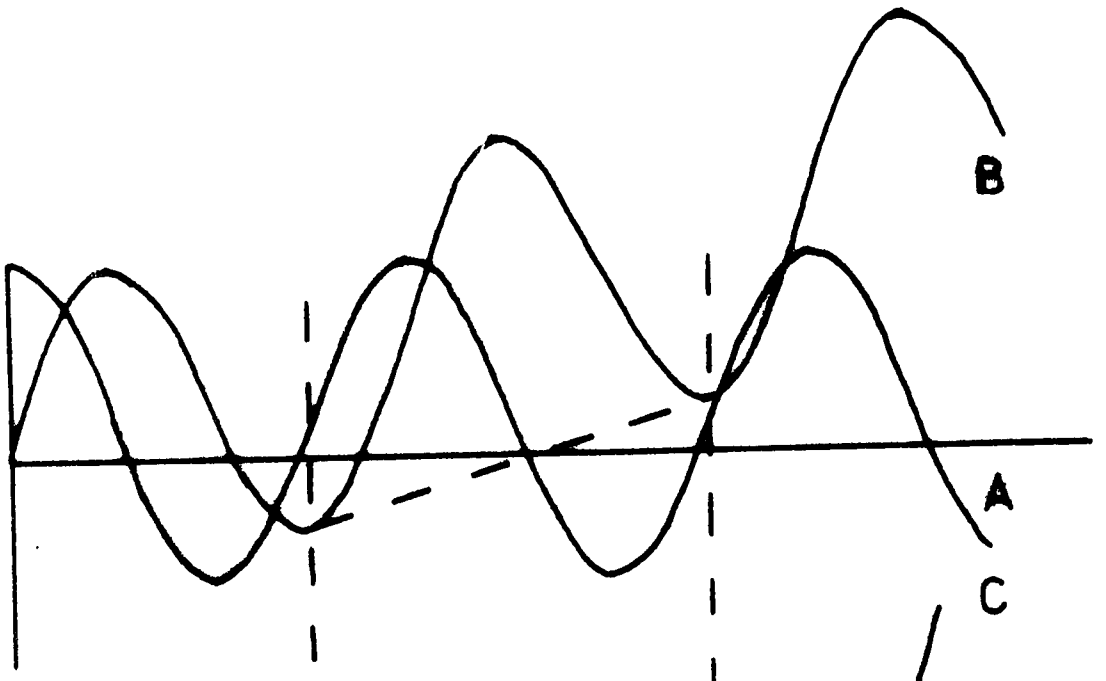


Figure 2.3

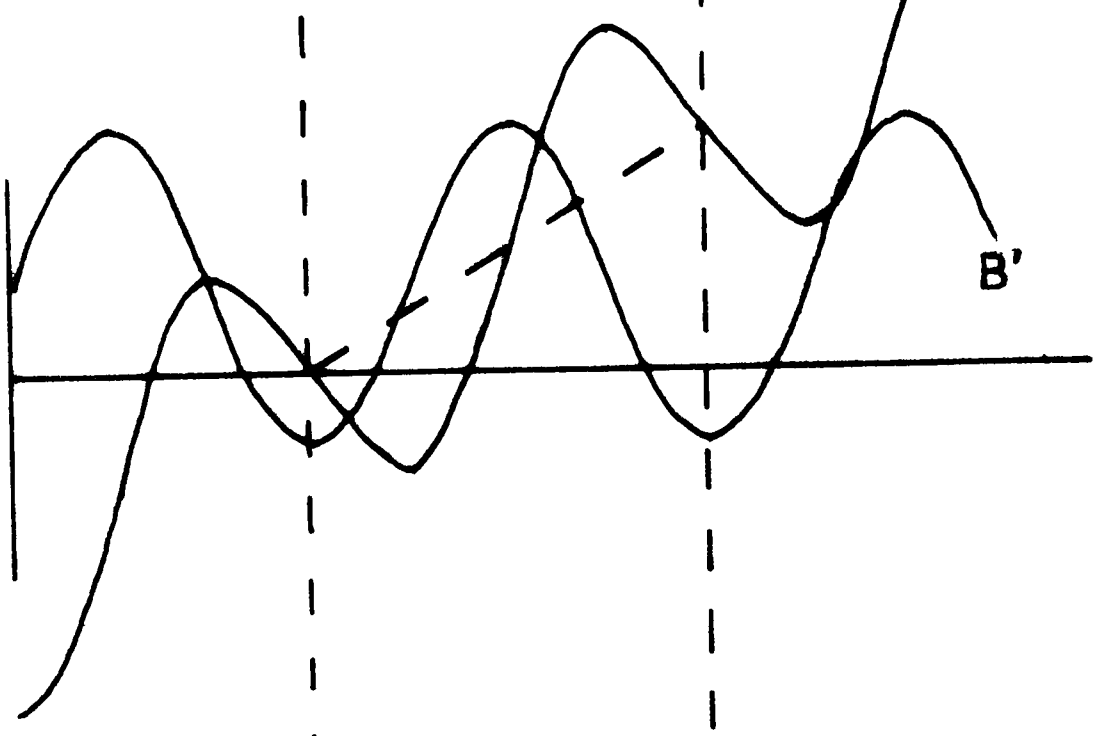
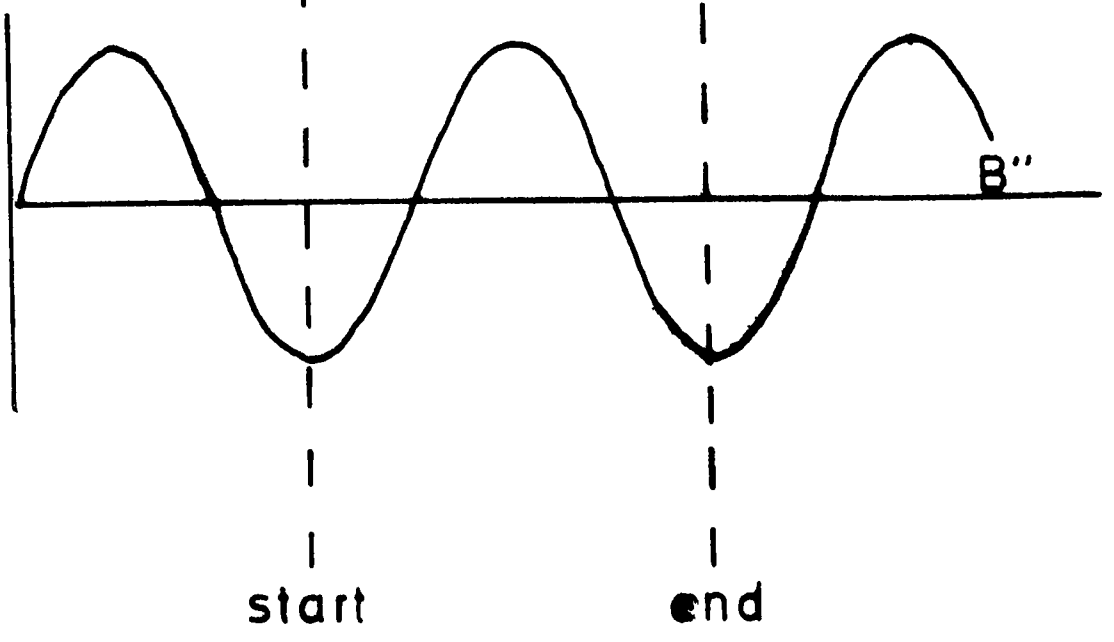


Figure 2.4



Removal of Zero and First Order Polynomial Components from a Periodic Variable

exception to this generalisation is translational displacement which is clearly not periodic.)

Fig. 2.2 shows a hypothetical function of time B which is expected to be periodic. Clearly, this variable is superimposed on a linear ramp. The ramp may be removed very simply from the variable. Two points are selected to mark the beginning and the end of the expected cycle and the difference between their actual values is noted, as well as the period of the cycle. From these two quantities the slope of the ramp is estimated and the ramp may be subtracted from the original function of time.

This process does not allow the determination of the initial value of B, but enables one to find the initial value of the function A from which B was obtained by integration. For instance, if B represents a periodic velocity, the acceleration A from which it was derived must have had a constant initial condition error which, when integrated with respect to time, produced the ramp. Once the equation for the ramp is known, the acceleration initial condition error may be found and removed.

Fig. 2.3 shows the result of subtracting a ramp function of time from the variable shown in Fig. 2.2. If this function B' is itself integrated with respect to time, the integral function C will also be a periodic function superimposed on a ramp. This may be the correct form of C (for instance, if it represents the forward displacement of the ankle over one step). However, if B' represents a component of angular velocity, the integral function C will be an angular displacement which should

be truly periodic. We can then find the initial value of B' by subtracting a constant from all values of B' such that the cumulative integral of B' over the cycle period is zero. The resulting function of time B'' is shown in Fig. 2.4.

The process described in the preceding three paragraphs allows the initial values of two of the four sets of variables listed at the beginning of this section to be found. These are the angular velocities and the translational velocities (except for the forward velocity which, as has been explained, will not produce a purely periodic integral). This leaves the initial values of the angular displacement function (the direction cosine matrix) and the initial translational displacement function. The latter set of functions may be dealt with very simply.

Since this kinematic study is concerned with the gait of human subjects, it is only the relative translational displacements of various points on the legs during a step which are of interest. The geographical location of the leg at the start of the cycle is of no relevance whatsoever. The initial values of all translational displacements are therefore made zero. This is not true of the angular displacements which must be known absolutely if the correct components of the gravitational field are to be subtracted from the acceleration field measurements. Before the process of finding the initial values of the elements of the direction cosine matrix can be described, a few details must be given of the physical nature of the problem

The limb element, whose movement was studied, was the shank, (or anatomically, the leg), which lies between the knee

and the ankle joints. The two frames of reference shown in Fig. 2.1 correspond to a frame fixed to the ground and an equivalent, moving frame fixed to the shank. The origin of the shank frame of reference is arbitarily chosen to lie at a point approximately half way up the shank and the corresponding axes of two frames of reference are parallel when the shank is vertical.

The stance phase of the walking cycle can generally be divided into three distinct periods. The first, immediately following heel-strike, is short (see Chap.1) and lasts until the foot is flat on the ground. The second, or 'foot-flat' period lasts until 'heel-off' and is of approximately the same duration as the third period, which lasts from 'heel-off' to 'toe-off'. During the second period the shank of the leg moves with pure rotation about a point whose position, relative to the ground, is known.[24] This point lies within the talus (a bone in the ankle joint complex), between the axes of the ankle and subtalar joints. Since the position of this origin of rotation is known, knowledge of the motion of the shank becomes mathematically redundant. The six measurements of the acceleration field are not then independent. Their interdependence allows the angular position of the shank to be found directly. Referring again to Fig. 2.1, the body-fixed origin O, if transformed to the origin of rotation (a purely translational transformation), is fixed with respect to O'. The term $\underline{f}$ in equations 2.1 and 2.3 is therefore zero. The expression for $\underline{a_m}$ becomes:

$$\underline{a_m} = \dot{\underline{\omega}} \times \underline{r} + \underline{\omega} \times (\underline{\omega} \times \underline{r}) + \underline{g} \qquad 2.8$$

Since $\dot{\underline{\omega}}$, $\underline{\omega}$ and $\underline{r}$ are known, $\underline{g}$ may be expressed in terms of $\underline{\alpha m}$ for the duration of the 'foot-flat' period. The start and finish of the cycle defined for analysis purposes are chosen to lie within this period.

Vector $\underline{g}$, found from equation 2.8, is the gravitational field vector in body coordinates. The transformation of this vector may be equated to the fixed reference frame gravity field vector.

$$\begin{bmatrix} & \lambda & \end{bmatrix} \begin{Bmatrix} g_1 \\ g_2 \\ g_3 \end{Bmatrix} = \begin{Bmatrix} 0 \\ 0 \\ 1 \end{Bmatrix} \qquad 2.9$$

(N.B. the vertical component is +1, not -1. This was explained at some length in section 2.2)

From equation 2.9, we find that:

$$\lambda_{31} = g_1 \qquad 2.10$$

$$\lambda_{32} = g_2 \qquad 2.11$$

$$\lambda_{33} = g_3 \qquad 2.12$$

This is not a sufficient number of terms to define $[\lambda]$ but relative rotation of the two reference frames in a horizontal plane (1'2') is of no particular importance. It is therefore convenient to make:

$$\lambda_{12} = 0 \qquad 2.13$$

This has the effect of making axis 2' perpendicular to axis 1 (see Fig. 2.1). The matrix is now defined.

$$\lambda_{22} = +\sqrt{1 - \lambda_{32}^2} \qquad 2.14$$

(The square root is positive since λ_{22} is always approximately equal to +1)

$$\lambda_{21} = -\lambda_{31}\ \lambda_{32}/\lambda_{22} \qquad 2.15$$

$$\lambda_{13} = \lambda_{21}\ \lambda_{32}-\lambda_{22}\ \lambda_{31} \qquad 2.16$$

$$\lambda_{23} = \lambda_{32}\ \lambda_{13} \qquad 2.17$$

$$\lambda_{11} = \lambda_{22}\ \lambda_{33}-\lambda_{23}\ \lambda_{32} \qquad 2.18$$

(Any element of the matrix is equal to its first minor in the determinant of the matrix)[43].

The redundancy during 'foot-flat' could also be used to check the correctness of λ_{31}, λ_{32} and λ_{33} at the end of the step cycle, but this has not been tried. This is a specific example of the double-checking which is possible whenever the number of degrees of freedom of a moving body is temporarily reduced. The motion of other intermittently free-moving bodies can be checked in the same way.

All the required initial conditions have now been found. Furthermore, any offsets in the transducers may be removed by an analogous process. It is worth speculating, at this point, as to how aperiodic movements might be analysed.

However accurately the transducers are calibrated before the start of an experiment, in common with most semiconductor strain gauge devices, they are subject to "zero-drift" due to changes in temperature. For the transducers which are currently in use (see Appendix B) the nominal characteristic of this drift is $\pm$ 0.05 g/^{o}C. This corresponds to a position error of approx. $\pm$ 25 mm/^{o}C. over 1 second or 1.25 m/^{o}C. over 5 seconds. While the thermal environment of the transducer is stable in a site

of close proximity to the body, the local thermal changes in the strain-sensitive elements themselves give measurable offset drifts of up to $\pm$ 0.1g.

Since the project began, a new type of transducer has become available with a different form of construction (see Appendix C). These transducers have a zero-drift characteristic which is about 100 times lower than that of the present transducer. With such a device, the possibility exists of making precalibrated aperiodic measurements. In the arm, for instance aperiodic movements are usually started and end with a zero-velocity state-of-rest. If the components of velocity were known to be zero at the beginning and end of the movement, and the initial position was known, the kinematics could be analysed.

2.6 Simplifying Approximations, Methods of Solution and Errors.

It was stated in section 2.4 that the relative position vector $\underline{d}$, which appears in equation 2.6, could be manipulated to allow an analytical solution to be found for $\underline{\omega}$. Equation 2.6:

$$\underline{\omega} \times \underline{d} = \int((\underline{\alpha m} - \underline{\beta m}) - \underline{\omega} \times (\underline{\omega} \times \underline{d})) + \underline{C} \qquad (2.6)$$

assumes that it is possible to measure all three components of $\underline{\alpha m}$ (or $\underline{\beta m}$) at a single point. Since the accelerometers each measure only one component of the acceleration field and have a finite size, it is clearly not possible to use equation 2.6 as it stands. If this equation is expanded into matrix form, the resulting equation contains components derived from $\underline{d}$ which are specific for a particular measurement direction, as well as for a particular body reference frame coordinate. The components derived from $\underline{d}$ are labelled d_{pq} , where p indicates the field measurement direction, and q is the number of the coordinate of the transducer. d_{pq} is a second-order tensor developed from a first-order tensor (vector) by the cross-products which occur in equation 2.6. The matrix equation is:

$$\begin{bmatrix} 0 & d_{13} & -d_{12} \\ -d_{23} & 0 & d_{21} \\ d_{32} & -d_{31} & 0 \end{bmatrix} \begin{Bmatrix} \omega_1 \\ \omega_2 \\ \omega_3 \end{Bmatrix} = \begin{Bmatrix} \int((\alpha m_1 - \beta m_1) + d_{11}(\omega_2^2 + \omega_3^2) \\ \quad -d_{12}\omega_1\omega_2 - d_{13}\omega_1\omega_3) + C_1 \\ \int((\alpha m_2 - \beta m_2) + d_{22}(\omega_3^2 + \omega_1^2) \\ \quad -d_{23}\omega_2\omega_3 - d_{21}\omega_2\omega_1) + C_2 \\ \int((\alpha m_3 - \beta m_3) + d_{33}(\omega_1^2 + \omega_2^2) \\ \quad -d_{31}\omega_3\omega_1 - d_{32}\omega_3\omega_2) + C_3 \end{Bmatrix} \qquad 2.19$$

where the integrals are w.r.t.time.

The simplification of this equation starts from a consideration of the physical realisation of the measurement system. The measurements are to be made on the shank, which is prismatoid, with its major axial length considerably larger than any dimension in a perpendicular plane. Any component of d_{pq} which is of the form d_{p1} or d_{p2} will be considerably smaller than a component of the form d_{p3} . Furthermore, experiments previously conducted by other researchers[14] have shown that ω_3 , the transverse plane angular velocity of the shank, reaches a maximum value of only about 1 rad/s just after heel-strike and shortly before toe-off. At the start of the experiments, no information was available on the likely value of ω_1 , the coronal plane angular velocity, but, considering the lack of movement of the knee in this plane, it would be likely to have a value comparable to or slightly higher than ω_3 . ω_2 the sagittal plane angular velocity, is quite obviously the largest component of $\underline{\omega}$. Bearing in mind that ω_1 and ω_2 could be measured quite accurately but that ω_3 could not, because of the constraints on $\mathbf{d}$, it was decided to make the approximation that ω_3 was zero. With this simplification, equation 2.19 reduces to:

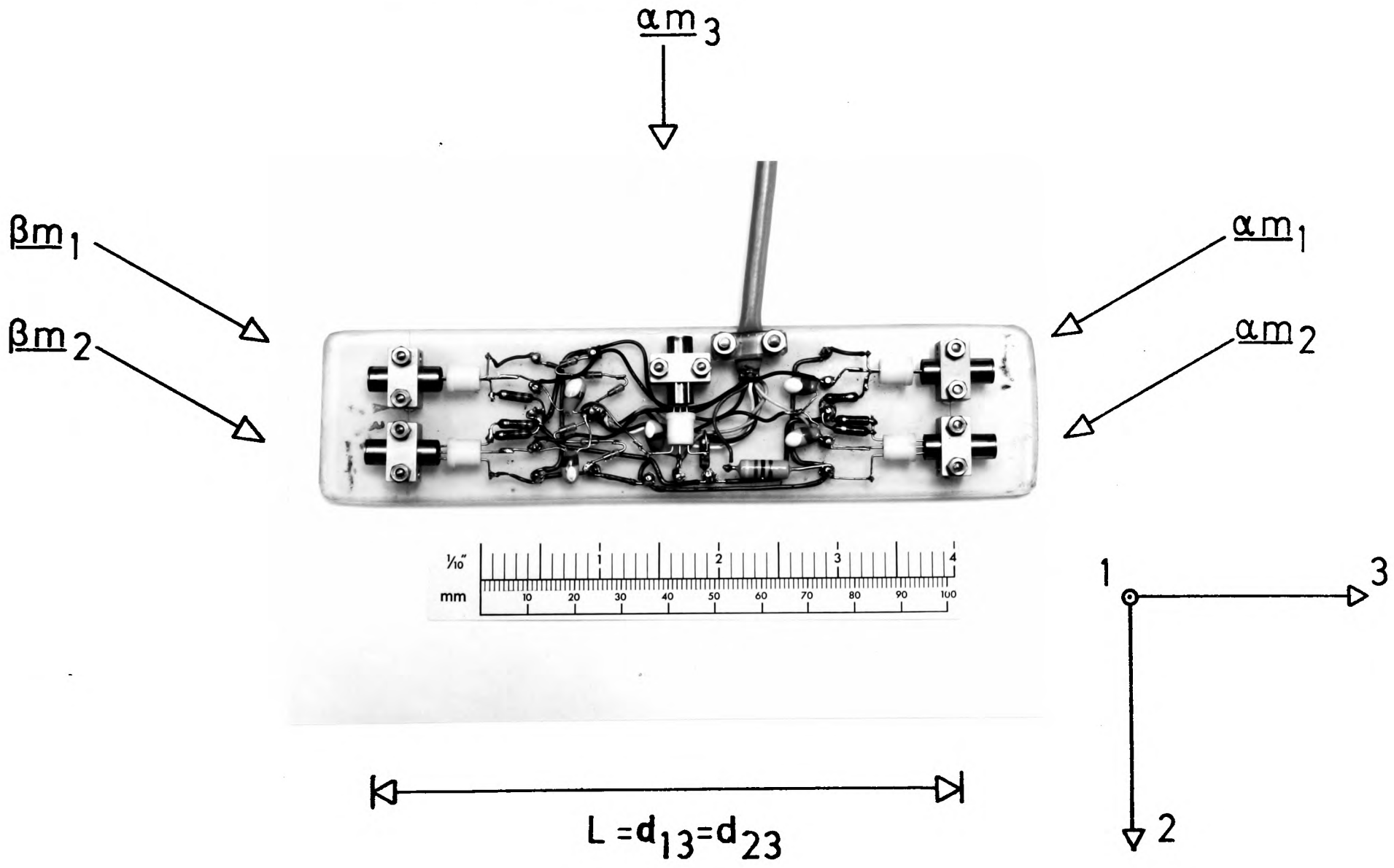
$$\begin{bmatrix} 0 & d_{13} \\ -d_{23} & 0 \end{bmatrix} \begin{Bmatrix} \omega_1 \\ \omega_2 \end{Bmatrix} = \begin{Bmatrix} \int((\alpha m_1 - \beta m_1) + d_{11}\omega_2^2 - d_{12}\omega_1\omega_2) + C_1 \\ \int((\alpha m_2 - \beta m_2) + d_{22}\omega_1^2 - d_{21}\omega_2\omega_1) + C_2 \end{Bmatrix} \qquad 2.20$$

This equation may also be considerably simplified, by making:

$$d_{11} = d_{12} = d_{21} = d_{22} = 0 , \qquad 2.21$$

Figure 2.5

TRANSDUCER PLATFORM



into a linear form:

$$\begin{bmatrix} 0 & d_{13} \\ -d_{23} & 0 \end{bmatrix} \begin{Bmatrix} \omega_1 \\ \omega_2 \end{Bmatrix} = \begin{Bmatrix} \int((\alpha m_1 - \beta m_1) + C_1 \\ \int((\alpha m_2 - \beta m_2) + C_2 \end{Bmatrix} \qquad 2.22$$

If: $L = d_{13} = d_{23}$ 2.23

then: $\omega_1 = (\int(\beta m_2 - \alpha m_2)) / L + D_1$ 2.24

and: $\omega_2 = (\int(\alpha m_1 - \beta m_1)) / L + D_2$ 2.25

where: D_1 and D_2 are constants of integration.

These are solutions for ω_1 and ω_2. Fig.2.5 is a photograph of the actual accelerometer platform, showing the arrangement of transducers which produced the values of d given in equations 2.21 and 2.23.

The assumption that $\omega_3 = 0$ introduces error terms into the estimates of ω_1 and ω_2. Substituting from equations 2.21 and 2.23 into equation 2.19;

$$\begin{bmatrix} 0 & L \\ -L & 0 \end{bmatrix} \begin{Bmatrix} \omega_1 \\ \omega_2 \end{Bmatrix} = \begin{Bmatrix} \int((\alpha m_1 - \beta m_1) - L\omega_3\omega_1 + C_1 \\ \int((\alpha m_2 - \beta m_2) - L\omega_2\omega_3 + C_2 \end{Bmatrix} \qquad 2.26$$

$$\therefore \quad \omega_1 = \int(\beta m_2 - \alpha m_2) / L + \int \omega_2\omega_3 + E_1 \qquad 2.27$$

and $$\omega_2 = \int(\alpha m_1 - \beta m_1) / L - \int \omega_3\omega_1 + E_2 \qquad 2.28$$

where E_1 and E_2 are constants of integration.

The error terms, $\int \omega_2\omega_3$ and $\int \omega_3\omega_1$, are the result of the double cross-product term in equation 2.19, all other components of this term having been previously multiplied by zero. The effect of $\int \omega_3\omega_1$ on the value of ω_2 will be small since both $\omega_3 \ll \omega_2$ and $\omega_1 \ll \omega_2$, but $\int \omega_2\omega_3$ may have a considerable influence on the estimate of ω_1.

Since, in equations 2.24 and 2.25, the only physical dimension used is d_{p3} (a measurement along the long axis of the shank), the transducers may all be mounted in a plane, as is shown in Fig.2.5. Four accelerometers are needed to estimate ω_1 and ω_2. A fifth, situated in the centre of the platform, is used to measure translations in the 3-axis direction.

Equations 2.24 and 2.25 express ω_1 and ω_2 in terms of integrals of time-dependent functions whose sampled values are known. Numerical approximations to the integral function values might be found by any of a large number of numerical analysis procedures, the best-known of which is Simpson's Rule. This second-order polynomic approximation procedure assumes that the integrable function is twice differentiable[44], i.e. that the rate of change of slope of the function does not become infinitely large. In practice, the rate of change of slope of $(\alpha m_1 - \beta m_1)$ and $(\alpha m_2 - \beta m_2)$ is extremely large at heel-strike, and it was found that this produced an oscillatory instability in the Simpson's Rule procedure.

Integration procedures based on a trapezoidal approximation (first-order) require the function to be differentiable only once. The integral accuracy is determined by the sample rate. Since this is high (100 Hz.), compared with all expected frequency components of the acceleration signal, the use of a low-order approximation is justified. The step size is kept constant since there is little or no time-saving to be gained by 'doubling and checking' with this low-order approximation.

Equation 2.7 can be rewritten in repeated subscript notation:

$$\dot{\lambda}_{pq} = \omega_s \lambda_{rq} \varepsilon_{psr} \qquad 2.29$$

where: ε_{psr} is the Levi-Civita Density, or Permutation Symbol.

This form of the equation is easily expanded to give three sets of three simultaneous, differential equations for the elements of $[\lambda]$.

$$\dot{\lambda}_{11} = \omega_2 \lambda_{31} - \omega_3 \lambda_{21} \qquad 2.30$$

$$\dot{\lambda}_{21} = \omega_3 \lambda_{11} - \omega_1 \lambda_{31} \qquad 2.31$$

$$\dot{\lambda}_{31} = \omega_1 \lambda_{21} - \omega_2 \lambda_{11} \qquad 2.32$$

$$\dot{\lambda}_{12} = \omega_2 \lambda_{32} - \omega_3 \lambda_{22} \qquad 2.33$$

$$\dot{\lambda}_{22} = \omega_3 \lambda_{12} - \omega_1 \lambda_{32} \qquad 2.34$$

$$\dot{\lambda}_{32} = \omega_1 \lambda_{22} - \omega_2 \lambda_{12} \qquad 2.35$$

$$\dot{\lambda}_{13} = \omega_2 \lambda_{33} - \omega_3 \lambda_{23} \qquad 2.36$$

$$\dot{\lambda}_{23} = \omega_3 \lambda_{13} - \omega_1 \lambda_{33} \qquad 2.37$$

$$\dot{\lambda}_{33} = \omega_1 \lambda_{23} - \omega_2 \lambda_{13} \qquad 2.38$$

Here again, the equations may be rewritten in integral form and solved by groups of three. All nine solutions are affected, to differing degrees, by the assumption that $\omega_3 = 0$. In equation 2.34, for instance, ω_3 is multiplied by λ_{12} which will generally be small, so that λ_{22} will not be greatly in error. In equation 2.33, however, ω_3 is multiplied by λ_{22} which is approximately equal to unity, so that the error in

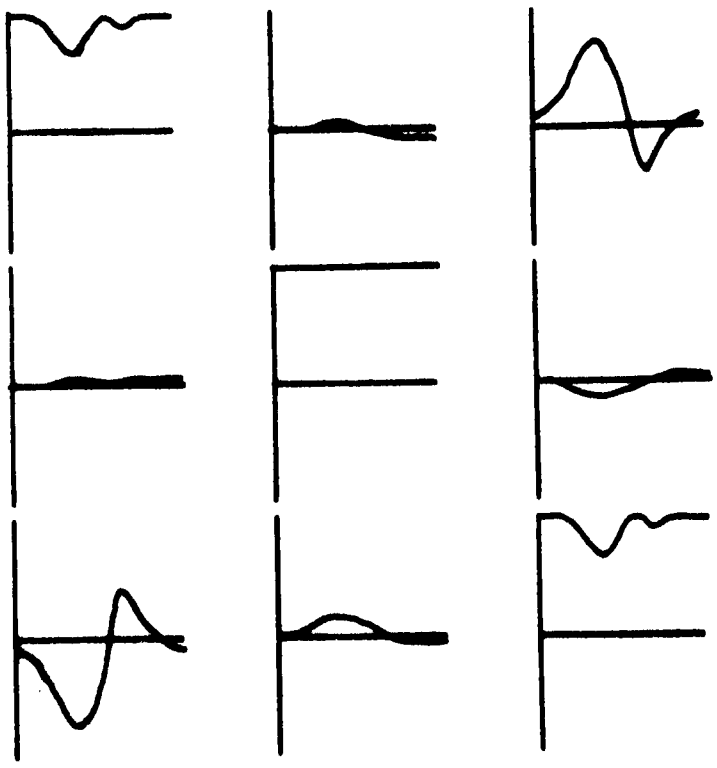


Figure 2.6 A Typical Transformation Matrix

will be larger.

One indication of the effect of errors is the amount by which the elements of $[\lambda]$ differ at the beginning and end of a cycle. Fig. 2.6, which shows $[\lambda]$ for an actual step, indicates that there are slight errors in λ_{12} , λ_{21} , λ_{23} and λ_{32} , but these correspond to angular displacements of 5^{o} over one cycle. It should be noticed, in this context, that the drift compensation procedure mentioned in the last section was not applied to $[\lambda]$ because of the difficulty of the non-commutativity of angular displacements.

There is one corrective procedure which can be applied to $[\lambda]$. This is a check on the orthogonality of the matrix.[45] As may readily be shown[43], a direction cosine matrix is the inverse of its transpose.

$$\text{i.e.} \quad [\lambda][\lambda]^{T}=[I] \qquad 2.40$$

If errors have been introduced into the estimate of $[\lambda]$ particularly due to approximate integration procedures, these errors may be partly corrected by an iterative process based on equation 2.40. The iterative equation is:

$$[\lambda]_{n+1} = [\lambda]_{n}([I]-([\lambda]_{n}^{T}[\lambda]_{n} - [I])/2) \qquad 2.41$$

This technique has been carefully analysed elsewhere[45] and is found to offer particular advantages in situations where the sample rate is slow compared with the rotational speed. Although this procedure is applied at each step of the solutions of equations 2.30 - 2.38, it has been found that only one or two iterations are required to make:

$$\left|[\lambda]^{T}[\lambda] - [I]\right| < [0.01] \qquad 2.42$$

This has been taken as an indication of the adequacy of trapezoidal integration.

The next development of the kinematic analysis will come with the inclusion of a sixth transducer. With the more accurate accelerometer mentioned in section 2.5, the relatively small values of transducer separation available in the transverse plane will be less of a problem in the measurement of ω_3. The analysis will be performed using equations described in this chapter and the results can be expected to be good.

CHAPTER 3

EXPERIMENTAL PROCEDURES AND PROGRAM DESCRIPTIONS

3.1 Introduction

3.2 The Transducers and Associated Electronic Circuits

3.3 Leg Mounting

3.4 Double Buffered Data Input : DATIN

3.5 General Structure : Data Selection : START,HOP,MAIN1, MAIN2,MAIN3

3.6 Kinematic Analysis Routines : MAIN4,M4EXT,MAIN6

3.7 Graphs and Moving Pictures : MAIN5,MOVE : Summary.

3.1 Introduction

This chapter will describe the experimental apparatus, its use, and the experimental procedures which lead to the results presented in the next chapter.

The experiments have been performed in a variety of environments, ranging from biomechanics laboratories to hospital corridors. The subjects, in every case, were prevented from moving completely freely by a cable which connected them to a tape recorder. However, this cable was the only feature of the experiments which was likely to disturb their gait since they were able to be fully clothed and to move wherever they wished within the area allowed by the cable.

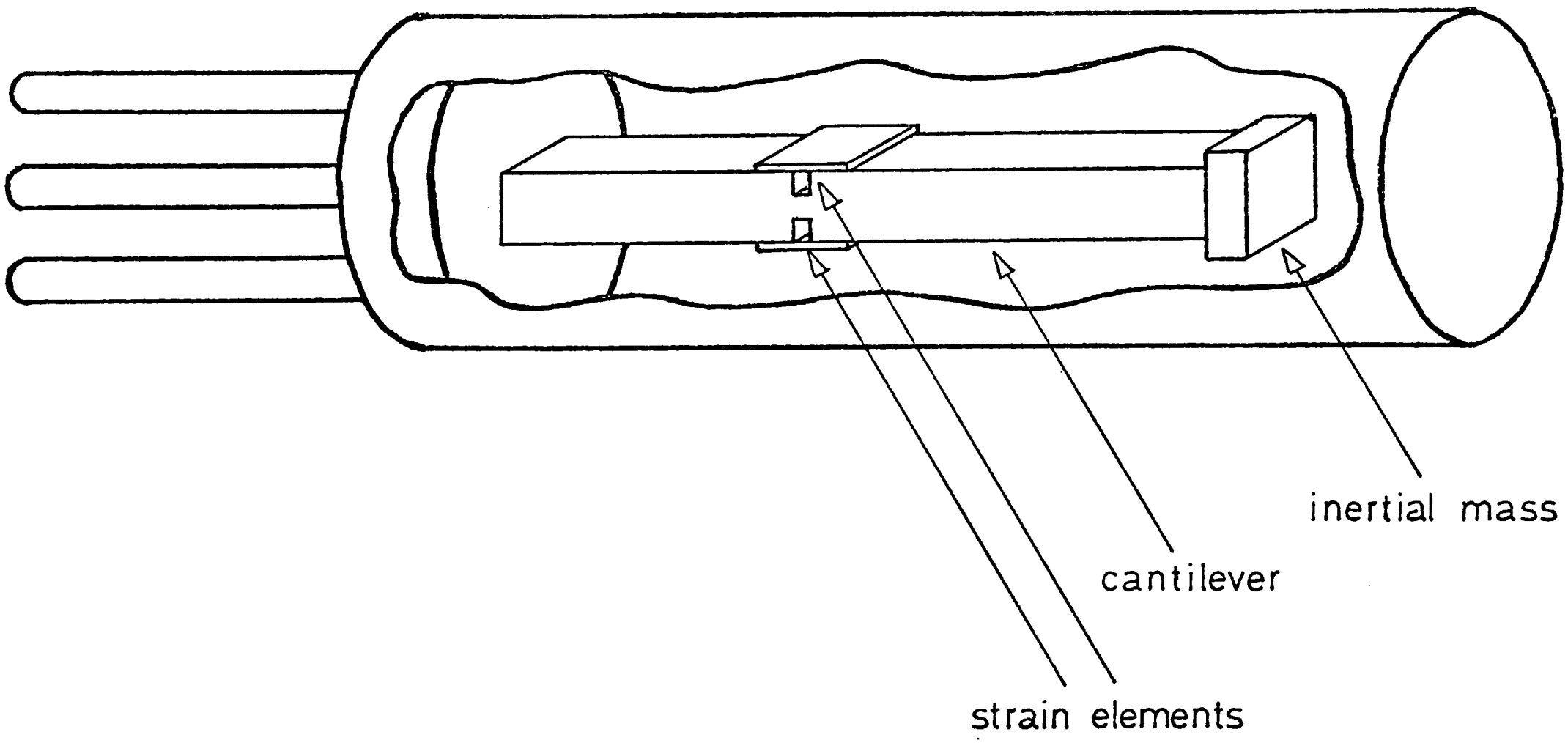


Figure 3.1 Accelerometer Schematic

3.2 The Transducers and Associated Electronic Circuits

The transducer used in this project is the Endevco 8210 vibration sensor and the data sheet for this device is included in Appendix B. As its name implies, the normal use of this transducer is the detection of vibration and the manufacturers are careful not to call it an accelerometer, although it does indeed measure the acceleration field as a variation of electrical resistance. The reason for this nomenclature is presumably the relatively poor zero-drift characteristic of the device compared with other devices with otherwise similar characteristics. However, after a thorough search through the range of accelerometers available in 1970, it was decided that this one would be the most suitable for the application. The criteria which were of primary importance were small size, low weight, low cost and high sensitivity. The data sheet gives all these details except cost, which was £80 for one off, or £50 for quantities over 9. This cost may seem high but, for comparison, the cost of a small force-feedback accelerometer* was £750. Fig.3.1 shows a schematic representation of the construction of the transducer, based on the manufacturer's written description. (Knowledge of the details of the internal dimensions would have required the sacrifice of one device and, in view of the cost, this was not considered). A cantilever, made up of two Endevco Pixie Elements mounted back-to-back, supports a mass at the free end. At some point along the cantilever, narrow slits are cut into opposite sides and doped. Silicon slabs are cemented

---

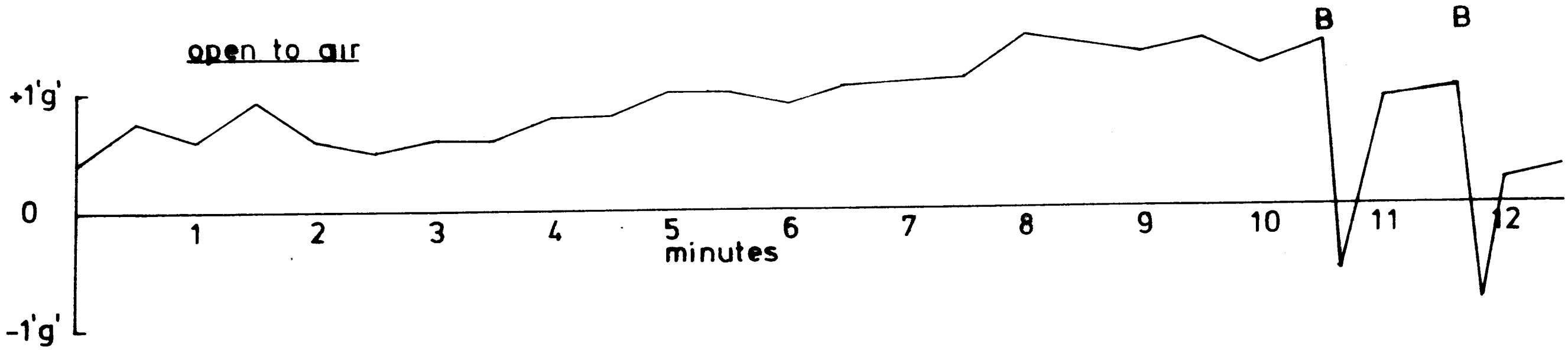
* Ferranti FA.3.

across the slits. A metallic, conducting pathway, interrupted by these strain-sensitive elements, runs around the cantilever with the point electrically between the elements also brought back to the fixed end. Thus the transducer takes the form of a resistive ½-bridge. Bending of the cantilever in the direction of the sensitive axis causes one strain-element to be in tension and the other to be in compression. Assuming a linear stress/strain characteristic for the semiconductor in tension and compression, the resistive changes in the elements should be equal and opposite. Furthermore, the temperature characteristics for the two ¼-bridge arms are nominally equal, providing a degree of thermal compensation. In practice, the two pieces of semiconductor are not identical and this results in a poor drift characteristic. The cantilever is mounted in a cylindrical case (14 mm.x 5 mm. diam.) and electrical contacts are brought out by three pins. The maximum deflection of the cantilever is limited by 'end-stops' within the case which protect the device from excessive accelerations, such as might occur were it dropped.

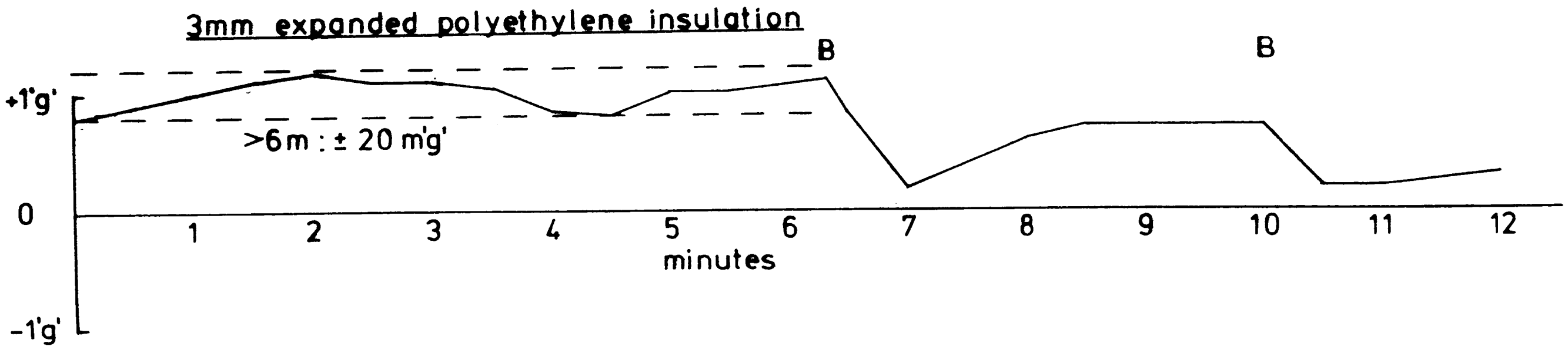
While the manufacturers quote a nominal sensitivity of ½% resistance change in each element for each 'g' of acceleration, the calibrated sensitivity, zero inbalance and direction of the sensitive axis were not given. The sensitive axis is approximately in line with the pins at the end of the transducer and measurements showed that careful visual alignment, using these pins, was accurate to $\pm 2^{o}$.

Initial attempts at calibration of the transducers were carried out on the bench but it was soon clear that changes in

Figure 3.2 Accelerometer Drift



B - blew on transducer

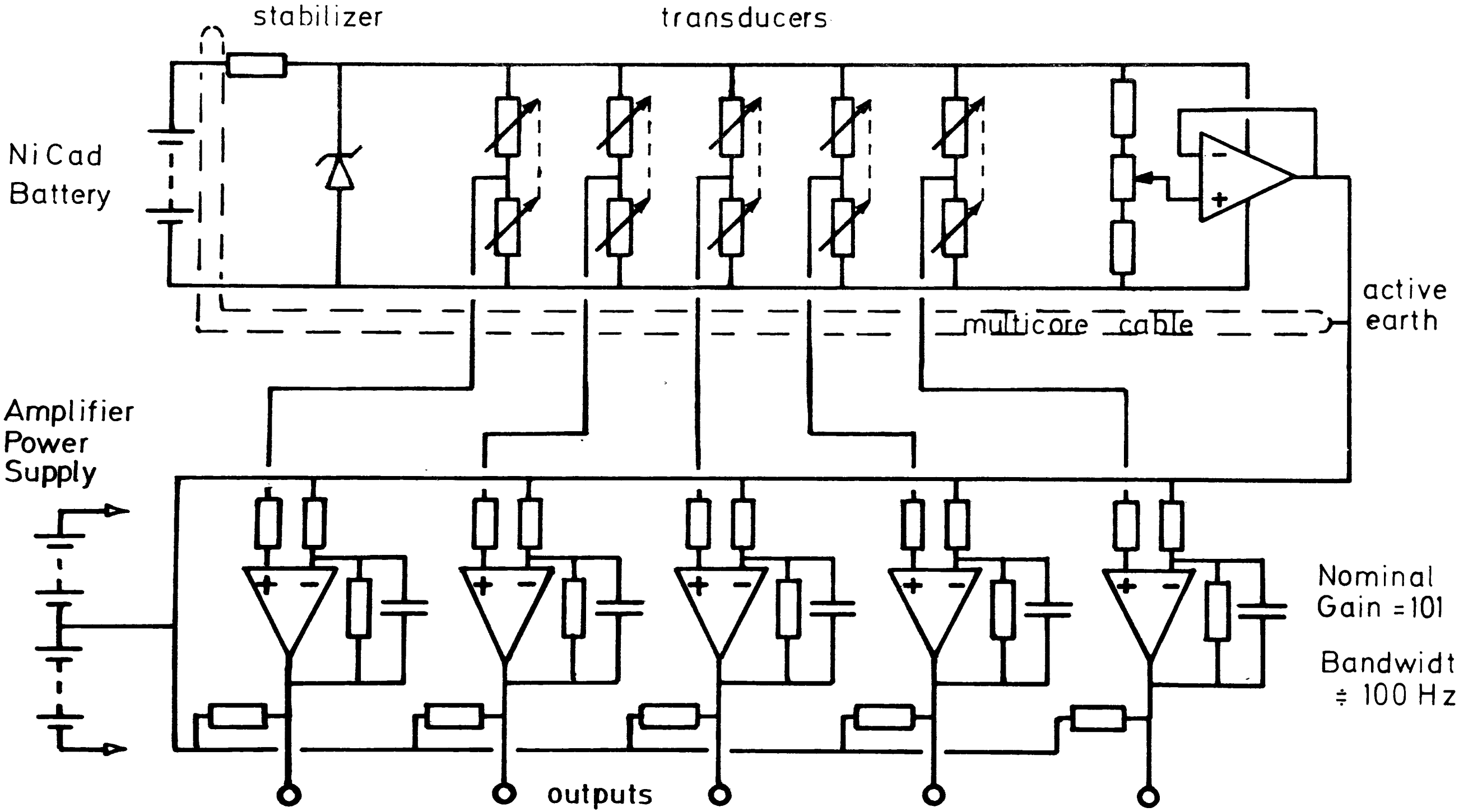


ambient temperature were sufficient to cause unacceptable changes in the zero-offset measurements. Final calibration was therefore deferred until the transducers were mounted next to the body. The mechanical aspects of the method of mounting the transducers on the limb are the main topic discussed in the next section, but the thermal environment of the transducers is also greatly influenced but the mounting. As well as the constant-temperature, heat source provided by the body itself, the mounting provides thermal insulation (3 mm. of expanded polyethylene) over the transducers. Under these conditions, transducer zero-drift is much reduced, once 5 minutes of warm-up time have elapsed. Fig.3.2 compares the zero-drift of a transducer with and without insulation.

Calibration entails a determination of the sensitivity (V/g) and the zero g offset (V). A sensitivity test can be made very simply by rotating the transducer about an appropriate axis so that the output voltage passes through a maximum and then a minimum. These two points will correspond to 1'g' of acceleration field in either direction along the sensitive axis. The derived sensitivity ((maximum voltage-minimum voltage)/2) is a function of the supply voltage, but varies only slightly with temperature (5% average for $10^{o}C$ temperature change). Checks on sensitivity are made, therefore, at periodic intervals as the battery supply voltage goes down, but not while the transducers are attached to the subject. (Few subjects can comfortably rotate any limb through 2π about three, orthogonal axes).

The zero offset voltage, on the other hand, is relatively independent of the supply voltage, but varies greatly with

Figure 3.3 Transducers and Amplfiers



temperature. These measurements must be made on the subject. This is usually done immediately before a test run when the subject's leg is held vertical and all the transducers, save that measuring vertically, should sense zero acceleration. The vertical transducer will indicate +1g.

The transducer output is of the order of 5 mV and since a long, multicore, lightweight cable would attenuate this signal while introducing noise, it was decided to provide amplifiers which could be carried by the subject. A power supply for the transducers and another for the amplifiers would also be carried. The transducer platform itself needed to be of as low a mass as possible and only a minimum amount of electronic apparatus, consistent with a noise-free signal, was to be mounted on the platform.

Fig.3.3 shows the circuit of the components carried by the subject. A battery of Nickel Cadmium cells supplies a reference diode voltage stabilizer. The reference diode voltage is 5.6, since this voltage corresponds to the zero temperature coefficient of such diodes. In addition to supplying the five transducers, this voltage is symmetrically divided and the mid-point passed to a voltage follower. The follower output provides a low-impedance 'active'earth line about which the whole transducer circuit is forced to 'float'. The voltage stabilizer, the transducers, the voltage divider and the voltage follower are carried on the platform.

A screened, multicore cable carries signals to a small, die-cast box (60mm.x 110mm.x 30mm.) which contains the two sets of

batteries and five amplifiers. These amplifiers (twin 741s in eight-pin, dual-in-line packets) have a nominal gain of 101 and feedback capacitors to provide a pole of the voltage transfer function corresponding to a frequency of around 100 Hz. This limitation of the signal bandwidth is necessary because the transducers are mechanically underdamped with a natural frequency of vibration at around 350 Hz. The amplifiers attenuate any mechanical ringing at this frequency. The output impedance of the amplifiers (2Ω) is low enough for them to drive the capacitance loading of a cable many times the length of that used (10m.) Battery life is 2 hours for the NiCad cells (20 minute recharge) and 10 hours for the dry cells which supply the amplifiers.

Clearly, although the present system does function satisfactorily, the two weak points of the system are the transducers and the trailing cable. The transducers will be replaced and the resulting, anticipated improvements are discussed in the previous and the final chapters. The replacement of the trailing cable by a portable tape recorder is examined in detail in Chap.5.

Figure 3.4 Cast on Leg

The moulded Plastazote cast is held in place by Velcro straps. The transducer platform (Fig.2.5) lies beneath the cast on the antero-medial surface of the tibia. Three sizes of cast are used to accomodate all sizes of adult limbs.

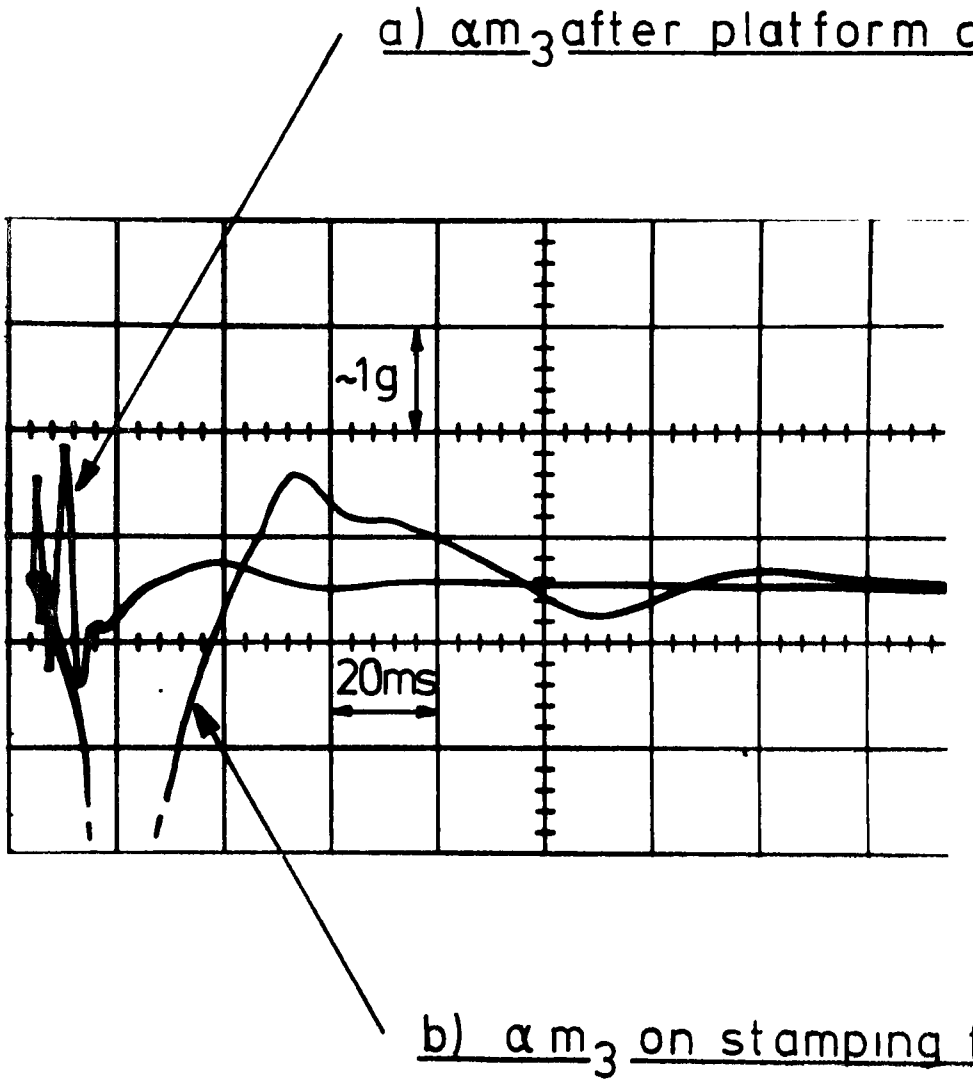


3.3 Leg Mounting

From the outset, it was realised that the method of mounting the transducers on the leg was of primary importance. The mass-centre of any section of the limb moves about within that section due to soft tissue displacements. So the assumption that the leg consists of a set of linked, rigid bodies is an approximation common to all methods of kinematic measurement. It is usual in gait analysis to attempt to determine the movement of the skeleton, since the positions of joints are known functions of bone position. The movement of soft tissue over the skeleton, so obvious in the buxom or obese, clearly introduces errors in measurement. It is worth noting, however, that such movements cause errors in cinephotographic, as well as accelerometric, measurement.

It was decided to study the movement of the shank, or lower leg, for two reasons. First, the movements of that limb element appeared to promise a considerable amount of useful data on gait, and second, a site suitable for the mounting of transducers is available on all likely subjects. This site, on the antero-medial surface of the shank, extending over more than half the length of the tibia, is free from subcutaneous musculature, and is relatively flat. A transducer platform, mounted on this site, will move relative to the bone only as its own inertia deforms the skin covering the tibia. The perspex platform, already shown in Fig.2.5, fits over this site in the majority of adults. The inner surface of the platform, which is in contact with the skin, is coated with silicone rubber caulking to provide a high-friction interface. The stress applied

Figure 3.5 a & b Oscillograph (retouched) showing platform movement



to the skin by the inertia of the platform is inversely proportional to the area over which the stress is applied. By making this area as large as possible, the deformation of the skin can be minimised. This is the purpose of the expanded polyethylene cast surrounding the platform and shown in Fig.3.4. This material, manufactured in sheet form for the production of moulded, semi-rigid casts, may be heated to approximately 70^{o}C and then wrapped around a limb. The low thermal capacity of the material prevents burns. In cooling, it takes on the shape into which it has been deformed and maintains this shape. When wrapped around the shank over the transducer platform, the cast is indented by the accelerometers. The cast and platform may then be removed. After the inside of the cast has also been smeared with silicone rubber and Velcro straps glued in place, the whole assembly can be reapplied to the leg. Because the cast is accurately shaped to the leg and held to the platform by the indentations, shear stresses due to the inertia of the system are distributed over a wide area. Fig.3.5a shows the long axis acceleration of the platform in response to a step displacement applied directly to the platform in situ beneath the cast. A length of thread was fixed to the platform and then pulled to displace the platform, producing an elastic shear deformation of the skin. When the thread was cut, the platform returned to its original position. Fig.3.5b shows the acceleration measured by the same transducer on stamping the foot. The resonance frequency in case (a) is much higher than that in case (b) so that the resonating structures in the two cases are clearly different. Undesirable movements of the platform over

the soft tissues are not occurring in case (b). All movements in this case are large, soft tissue movements which are a normal, unavoidable feature of the structure of the body. The mounting technique is thus demonstrated as optimal, short of direct fixation to bone.

Finally, three measurements are made on each subject for later use in the analysis of the data. The tibia rotation is the angle which the flat surface on the bone makes with the antero-posterior direction. The platform-ankle distance is measured from the ankle-joint line to the centre of the platform, and the shank length is measured from the ankle-joint line to the knee-joint line.

Note The remainder of this chapter traces the analysis through a series of computer programs. These programs, written in FORTRAN, are contained in Appendix D, which may be folded out for reference. A flow chart is also included in the appendix.

3.4 Double-Buffered Data Input. DATIN

All the experiments discussed in the next chapter used an Ampex SP300 FM Tape Recorder to record the signals from the transducers. A trailing cable approximately 10m. long allowed the subject to move in the vicinity of the recorder. A transient view of the data played back from the recorder onto an oscilloscope does not provide a satisfactory means of selecting data sets for analysis. Instead, a period of several minutes of data is replayed to the computer where it is stored on the disk file. Subsequently, stationary graphs of data representing any 2.56 second time interval may be viewed on the computer visual display unit. The transfer of data from the analogue recorder to the computer disk is accomplished by the program DATIN.

The IBM 1130[46] (16k) computer has a Storage Access Channel (SAC) which allows a fixed set of core-store locations to be read or loaded directly by an external device. In the present case, the device is the Oxford University Interface (OUI) which contains an Analogue-to-Digital Converter (ADC), an analogue multiplexer, Digital-to-Analogue Converters (DACs), a crystal-controlled clock which provides pulses at adjustable time intervals, and a number of other facilities. The computer disk store has a moving head and the maximum rate at which data may be written on the disk continuously is limited by the time taken

for the head to move from track to track across the disk. However, disk writing may occur simultaneously with other events in core and this facility is used by DATIN.

The clock is set to provide a pulse every 10 ms. If the computer is in a WAIT condition (i.e. not running) when an interrupt pulse arrives from the clock, the computer will jump to a predetermined point in the program. In DATIN, this point is the statement following CALL SINT2 (point A). After checking the position of a switch, the program reaches CALL SCAN (point B). This is the subroutine which instructs the multiplexer to make one pass and loads the digitised data into the first five elements of an array, ISCAN. Depending on the value of a variable, ISW, the program will branch to statement 100 or statement 200. The five data words are transferred to one of two buffers, L1 or L2, and the computer then waits (point C or C') for the next interrupt from the clock. When the appropriate buffer is full, the program reaches the statement CALL FILER (point D or D') which initiates the writing of the relevant buffer onto the next sector of the disk. Without waiting for this transfer to be completed, the program will jump, at the next clock pulse, to CALL SINT2 and, since the value of ISW has been changed, will begin to fill the other buffer. Thus one buffer is always being filled while the other is transferred to the disk and the sampling of data may be made continuous. The program ends either by the setting of a switch or when the allocated area on disk is full. The double-buffering used in DATIN is not an original method but the program has been explained here for the sake of completeness.

The choice of 10 ms. as the sampling period warrants some explanation. Examination of records presented later will indicate that fairly large changes in acceleration can occur within 10 ms. However, experiments with higher sampling rates show little significant improvement in the definition of results. The rate of 100 samples/second was chosen as a compromise between poor definition and the generation of excessive quantities of digitised data and a subsequent increase in the execution time of the analysis programs. It is worth noting that this sampling rate is considerably faster than the highest frame rates used in cinephotography.

Figure 3.6

```
PROGRAM <START> SETS UP INITIAL CONDITIONS
AND THEN LINKS TO PROGRAM <HOP>

<HOP> IS THE MASTER STEERING PROGRAM FOR
ANALYSIS OF DATA FILED BY <DATIN>

PRESS PROG START TO CONTINUE
```

START
v.d.u. message

Figure 3.7

```
ENTER FIXED PARAMETERS FOR THIS RUN

A0S1,B0S1,A0S2,B0S2,A0S3

-0.55,-0.54,-0.40,-0.50,-0.30

AG1,BG1,AG2,BG2,AG3

1.11,1.05,0.69,0.64,-0.54

ADC SENSITIVITY <VOLTS>, TIBIA ROTATION <DEG>,
SAMPLE TIME <SEC>,SHANK LENGTH <MM>,
PLATFORM/ANKLE DISTANCE <MM>

5.0,32.0,0.01,430.0,250.0

CHECK     THEN, PRESS START
```

START
constants entry

Figure 3.8

```
FILES 1 AND 2 UPDATED
IF NEW DATA IS REQUIRED,  TYPE 1
IF KINEMATICS ARE REQUIRED,  TYPE 2
IF HARD COPY OF FILES 1 AND 2 IS REQUIRED,
TYPE 3
OTHERWISE,  TYPE 0
```

HOP
steering
message

3.5 General Structure of the Analysis Routines. START,HOP, MAIN1,MAIN2,MAIN3

The purpose of the kinematic analysis programs is to generate graphical records of various kinematic variables and to produce a simulated moving visual picture of the limb in motion. To this end, the programs follow the sequence of the analytical algebra explained in the last chapter.

The first task for the operator is the selection of a period of data suitable for analysis and the calibration of the data. Program START allows calibration constants to be entered and filed for subsequent use. The only explanation of this program which should be necessary is provided by Figs. 3.6 and 3.7. AOS1,BOS1,AOS2,BOS2,AOS3 are the total, zero 'g', voltage offsets introduced by a combination of offsets in the transducers, the tape recorder and the ADC. AG1,BG1,AG2,BG2 and AG3 are the net gains of the five channels in volts per 'g'. Other calibration variables are explained in Fig.3.7. All data entries demanded by the display are entered on the computer keyboard.

Program HOP performs no analytical functions but is used to call the other mainline programs, on demand, from the disk file into core storage for execution. A typical HOP v.d.u. request is shown in Fig.3.8.

If program HOP interprets a request for new data it will call up MAIN1. This program allows a search to be made through the file of data loaded by DATIN. A period of 2.56 seconds (2^7 samples) of uncalibrated data is displayed on the computer visual display unit. (v.d.u.). This display window may be held stationary or moved at various speeds through the file in either

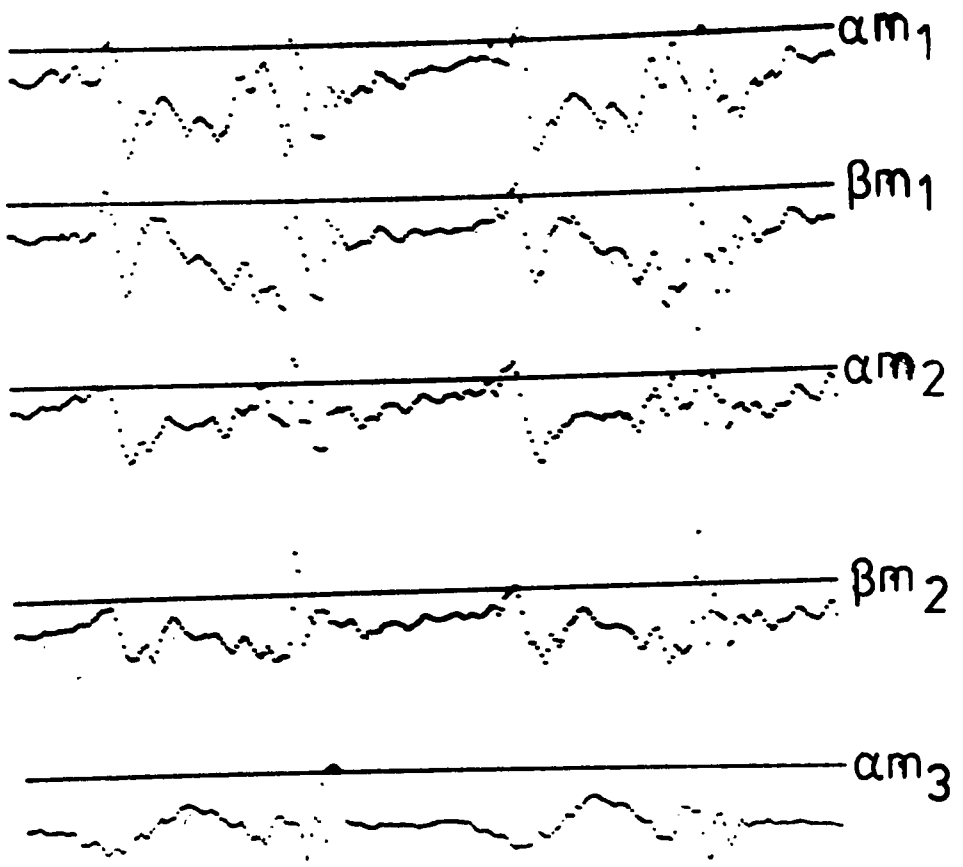


Figure 3.9

MAIN1 2.56s data window

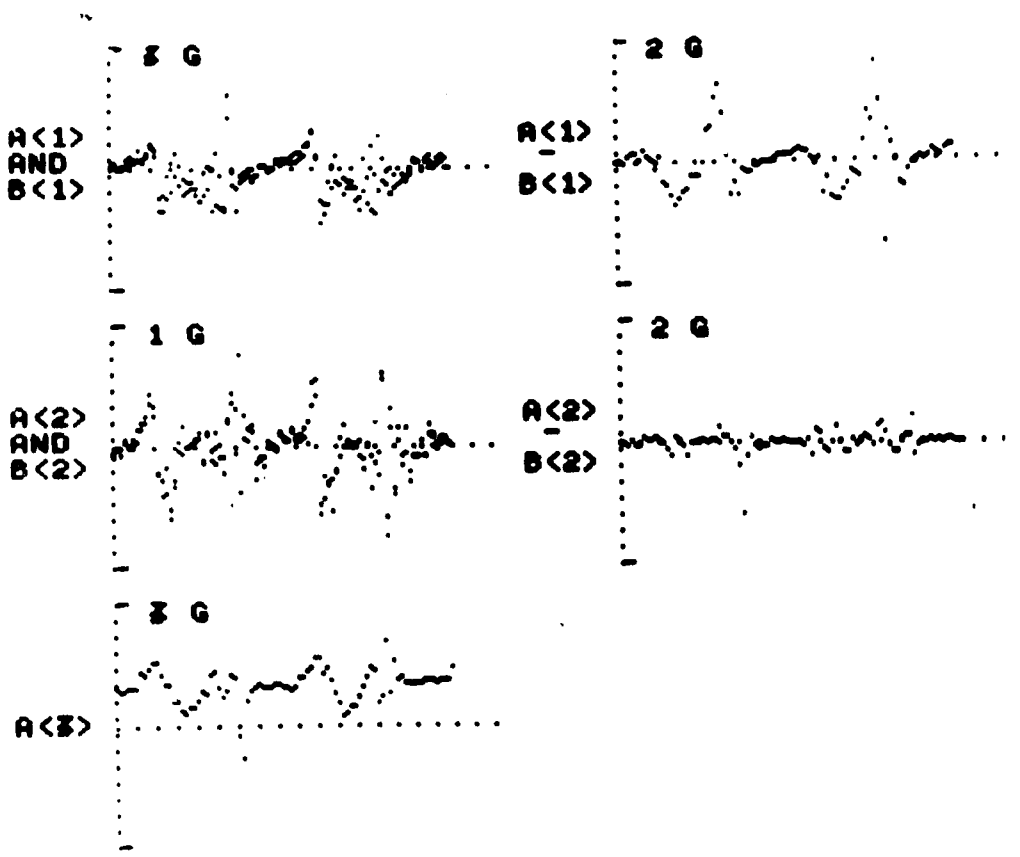


Figure 3.10

MAIN2 calibrated data set

direction. Fig.3.9 is a composite picture of the five graphs available in MAIN1. They represent, from top to bottom, AM1, BM1,AM2,BM2,AM3, corresponding to $\alpha m_1, \beta m_1, \alpha m_2, \beta m_2, \alpha m_3$. The stance phases of three steps are easily recognised from the lower graph as periods of relatively constant axis 3 accelerations. The ability of the operator to select a particular set of steps for analysis is useful, both to avoid data which would be unsuitable for analysis, and to select steps typical of the subject. Experience has shown that the operator quickly learns to interpret graphs such as those in Fig.3.9 in this way. An explanation of the operation of MAIN1 is not given since it relies heavily on system-specific subroutines.

Program MAIN2 takes the uncalibrated data from MAIN1 and, using parameters from the file generated by START, scales, dimensionalises and displays the results. It should be noted that the tibia rotation angle, THETA, is used to transform the accelerations by rotating the local axes about the long axis of the shank. (See sections A and B in MAIN2). The accelerations displayed by MAIN2 (Fig.3.10) are therefore in the antero-posterior and the medial-lateral directions with respect to the shank. The difference signals between parallel pairs of acceleration signals are also displayed in Fig.3.10. These give an indication of the angular accelerations in two planes. After seeing the calibrated signals, the operator has the choice of filing them for analysis or of returning, via HOP, to MAIN1 in order to select more data. If the choice is to update the acceleration files, HOP will display the message shown in Fig.3.8.

The remaining program in this group is MAIN3 which prints out the calibrated accelerations of Fig.3.10. on the line printer. This program is used very little as the numerical values of accelerations have little intrinsic significance. There is one application, however, for which accurate acceleration values are needed and this is the calibration of the transducers. Only by making zero 'g' offset error measurements after digitisation can every potential source of error be accounted for. It has been found useful to make periodic checks on zero-offsets by standing the subject stationary with the shank vertical. All the signals should then be zero except for the vertical measurement of +1'g'. If they are not, the offset voltages can be reset using START.

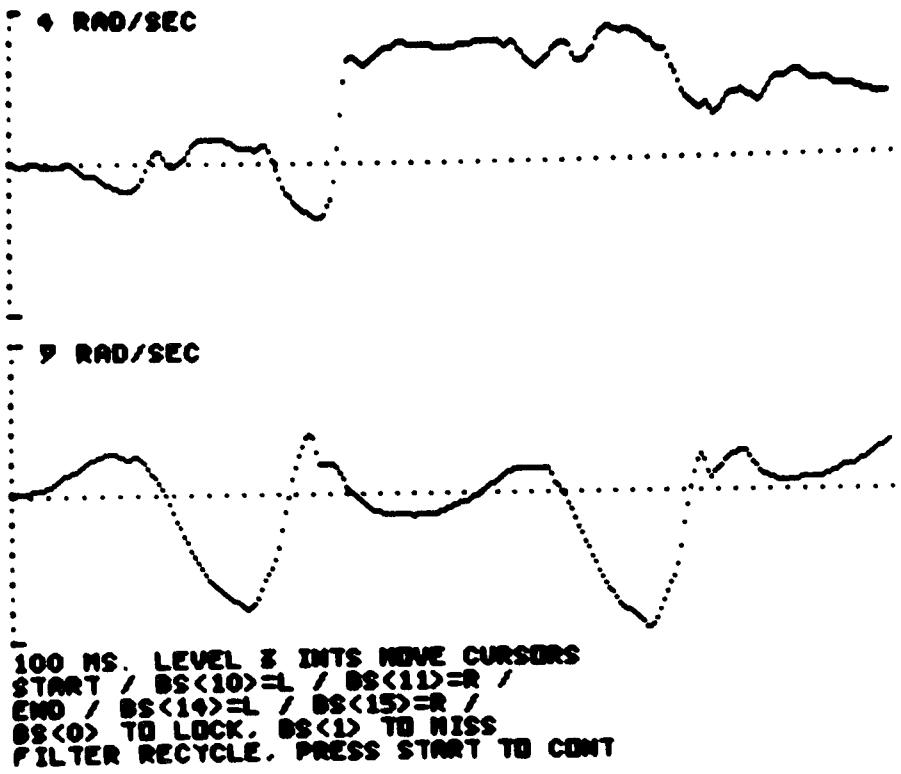


Figure 3.11

OM1

MAIN4

OM2

Figure 3.12

```
YOU'VE GOT YOUR CURSORS OVERLAPPED.
BACKWARDS. OR OFF-SCALE.
PRESS PROG START
```

MAIN4 operator error message

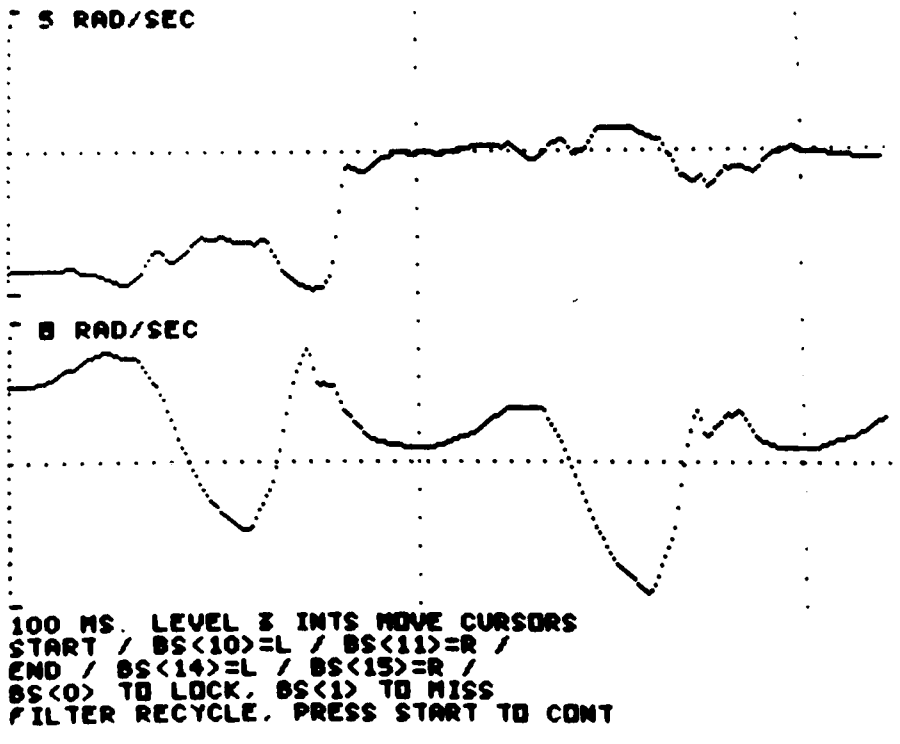


Figure 3.13

OM1

MAIN4 filtered angular vels.

OM2

3.6 Kinematic Analysis Routines.MAIN4,M4EXT,MAIN5,MAIN6.

The programs MAIN4,M4EXT and MAIN6 calculate the solutions to the integral equations used to estimate the translational and rotational positions of the limb element. As was mentioned in Chapter 2, section 6, a first-order integration procedure is used. Subroutine TRAP performs the integration on an array A, putting the integral in array B. This subroutine is called by MAIN4 and MAIN6.

MAIN4 begins by reading the acceleration files generated by MAIN2. Using the known value of $d_{13} = d_{23}$ (the distance separating parallel pairs of accelerometers, equal to 125 mm.), it solves equations 2.24 and 2.25 for ω_1 and ω_2, which are known in the program as OM1 and OM2 (see points A and B). It will be remembered that ω_3 is assumed to be zero. The next section of the program is concerned with plotting the graphs of OM1 and OM2 which are shown in Fig.3.11. On these graphs it can be seen that the initial values of both functions have been made zero. The message below the graphs refers to a pair of cursors both of which are initially placed over the left-hand axes. On receiving an interrupt pulse from the OUI, the program will move the cursors in either direction according to a code set up on the computer handkeys. As the cursors move, the program keeps track of the sample numbers (II and JJ) at which the cursors lie. The operator needs to move the cursors to find two points during foot-flat in adjacent stance phases which will be used to define the beginning and end of a step. The procedure is fairly fool-proof but the program may give the warning shown in Fig.3.12.

There are three reasons why foot-flat is chosen as the point for defining the beginning and end of a step. At first sight, the instant of heel-strike might seem a more obvious point to choose since it is more clearly defined. The filtering process which is applied takes the values at the cursors and from these calculates linear functions which are added to each angular velocity to make the initial and final values equal. If heel-strike were taken to indicate extent of the step, the above process would be most inaccurate since the values of angular velocity are most variable at this point. On the other hand, during foot-flat the angular velocities are almost constant and are very consistent from step to step. Point C in MAIN4 marks the beginning of the filtering cycle. Two variables, DIF1 and DIF2, are calculated as the difference between initial and final values of the angular velocities divided by the intervening number of samples. The appropriate ramps are then added to the original functions, removing the errors due to accelerometer zero drift.

Suitable values for the mean level are next found, in the manner outlined in Chapter 2, section 5. First OM1 and OM2 are transferred to arrays, BUF1 and BUF2, of the appropriate size (point D). Next subroutine TRAP is called to find the integrals of the angular velocities. Using these integrals, the mean levels are calculated (variable names DIF1 and DIF2 are again used). The subtraction of the mean levels from each element of OM1 and OM2 generates angular velocities whose mean levels are zero over the defined step. Fig.3.13 shows the same angular velocities as those in Fig.3.11 after the completion of the processes just

described. The cycle may be repeated, if necessary, with new cursor positions.

The second reason why foot-flat is chosen is indicated by Fig.3.13. If the positions of the cursors are slightly in error, the mean level will not be greatly affected. The values of angular velocities are invariably low during this period, so the errors in the integral functions used to find the mean levels will be very small. Once the operator is satisfied that the angular velocities have been satisfactorily corrected, they are filed, along with the sample numbers given by the final cursor positions. The analysis then continues in program M4EXT.

After reading the necessary arrays and other variables from files, M4EXT calculates the initial element values of the transformation matrix of direction cosines, DC. To do this, the foot-flat condition is again used. At point B, the non-vertical acceleration signals at the start of the cycle are subject to five-point, first-order smoothing which produces AA1, AA2, BB1 and BB2. It has been shown (Chap.2, sect.5), that the solution of the equation:

$$\underline{\alpha m} = \dot{\underline{\omega}} \times \underline{r} + \underline{\omega} \times (\underline{\omega} \times \underline{r}) + \underline{g} \qquad (2.10)$$

for $\underline{g}$ will allow three elements of the matrix to be found, from which the rest may be derived. If instead of $\underline{\alpha m}$, the mean of $\underline{\alpha m}$ and $\underline{\beta m}$ is used, equation 2.11 can be simplified to:

$$g_1 = (\alpha m_1 + \beta m_1)/2 - \dot{\omega}_2 r_3 \qquad 3.1$$

$$g_2 = (\alpha m_2 + \beta m_2)/2 - \dot{\omega}_1 r_3 \qquad 3.2$$

$$g_3 = \alpha m_3 + (\omega_1^2 + \omega_2^2) r_3 \qquad 3.3$$

r_3 is the distance to the centre of rotation; the platform/ankle distance.

$$\therefore \quad g_1 = \alpha m_1 (1/2 - r_3/d) + \beta m (1/2 + r_3/d) \qquad 3.4$$

$$\text{and} \quad g_2 = \alpha m_2 (1/2 - r_3/d) + \beta m_2 (1/2 + r_3/d) \qquad 3.5$$

where: d is the distance between parallel pairs.

In the program, BIT and BOT, derived at point A, are the coefficients of αm and βm in the calculation of DC(3,1,1) and DC(3,2,1). Rather than find DC(3,3,1) from αm_3 with equation 3.3, the program uses the orthogonality condition. This is because the sensitivity of a near vertical acceleration measurement to small angular changes is very low. ($d(\cos\theta)/d\theta \doteq 0$ when $\theta \doteq 0$). The remaining elements of the initial value of the matrix are then found according to equations 2.14 to 2.18.

The evaluation of the transformation matrix, from the components of the angular velocity vector, is found from the following equation from Chap.2:

$$\dot{\lambda}_{pq} = \omega_s \lambda_{rq} \varepsilon_{psr} \qquad (2.29)$$

In the usual manner for the solution of differential equations, it can be rewritten in integral form:

$$\lambda_{pq} = \int \omega_s \lambda_{rq} \varepsilon_{psr} \qquad 3.6$$

This equation splits up into 3 sets (i=1,2,3) of 3 equations:

$$\lambda_{1i}(t) = \lambda_{1i}(t-\Delta t) + \int_{t-\Delta t}^{t} (\lambda_{3i}(t)\omega_2(t) - \lambda_{2i}(t)\omega_3(t))\, dt \qquad 3.7$$

$$\lambda_{2i}(t) = \lambda_{2i}(t-\Delta t) + \int_{t-\Delta t}^{t} (\lambda_{1i}(t)\omega_3(t) - \lambda_{3i}(t)\omega_1(t))\, dt \qquad 3.8$$

$$\lambda_{3i}(t) = \lambda_{3i}(t-\Delta t) + \int_{t-\Delta t}^{t} (\lambda_{2i}(t)\omega_1(t) - \lambda_{1i}(t)\omega_2(t))\, dt \qquad 3.9$$

Assuming $\omega_3 = 0$ and using trapezoidal approximations to the integrals:

$$\lambda_{1i}(t) - \lambda_{3i}(t)\omega_2(t)\Delta t/2 = \lambda_{1i}(t-\Delta t) + \lambda_{3i}(t-\Delta t)\omega_2(t-\Delta t)\Delta t/2 \qquad 3.10$$

$$\lambda_{2i}(t) + \lambda_{3i}(t)\omega_1(t)\Delta t/2 = \lambda_{2i}(t-\Delta t) - \lambda_{3i}(t-\Delta t)\omega_1(t-\Delta t)\Delta t/2 \qquad 3.11$$

$$\lambda_{3i}(t) + \lambda_{1i}(t)\omega_2(t)\Delta t/2 - \lambda_{2i}(t)\omega_1(t)\Delta t/2 =$$

$$\lambda_{3i}(t-\Delta t) + \Delta t(\lambda_{2i}(t-\Delta t)\omega_1(t-\Delta t) - \lambda_{1i}(t-\Delta t)\omega_2(t-\Delta t))/2 \qquad 3.12$$

These equations are in a suitable form for numerical solution since the left-hand sides are functions of the current values of variables and the right-hand sides are functions of the previous, known values of the variables. In matrix form, the equations become:

$$\begin{bmatrix} 1 & 0 & \frac{-\Delta t\omega_2(t)}{2} \\ 0 & 1 & \frac{\Delta t\omega_1(t)}{2} \\ \frac{\Delta t\omega_2(t)}{2} & \frac{-\Delta t\omega_1(t)}{2} & 1 \end{bmatrix} \begin{Bmatrix} \lambda_{1i}(t) \\ \lambda_{2i}(t) \\ \lambda_{3i}(t) \end{Bmatrix} =$$

$$\begin{Bmatrix} \lambda_{1i}(t-\Delta t) + \Delta t\lambda_{3i}(t-\Delta t)\omega_2(t-\Delta t)/2 \\ \lambda_{2i}(t-\Delta t) - \Delta t\lambda_{3i}(t-\Delta t)\omega_1(t-\Delta t)/2 \\ \lambda_{3i}(t-\Delta t) + \Delta t(\lambda_{2i}(t-\Delta t)\omega_1(t-\Delta t) - \lambda_{1i}(t-\Delta t)\omega_2(t-\Delta t))/2 \end{Bmatrix} \qquad 3.13$$

It is this matrix equation which is solved in M4EXT.

The coefficient matrix is B, the nine elements stored by columns. At point C in the program, the four changing elements of this matrix are refreshed. The driving vector is known as RKAPP, and, when array B has been written onto array A, subroutine SIMQ is called to solve the equation. On reentry from SIMQ, array A has been overwritten and the solution vector is stored in RKAPP. RKAPP is then written onto the appropriate elements of DC. After three calls of SIMQ, the nine elements of the current transformation matrix, DC, are known.

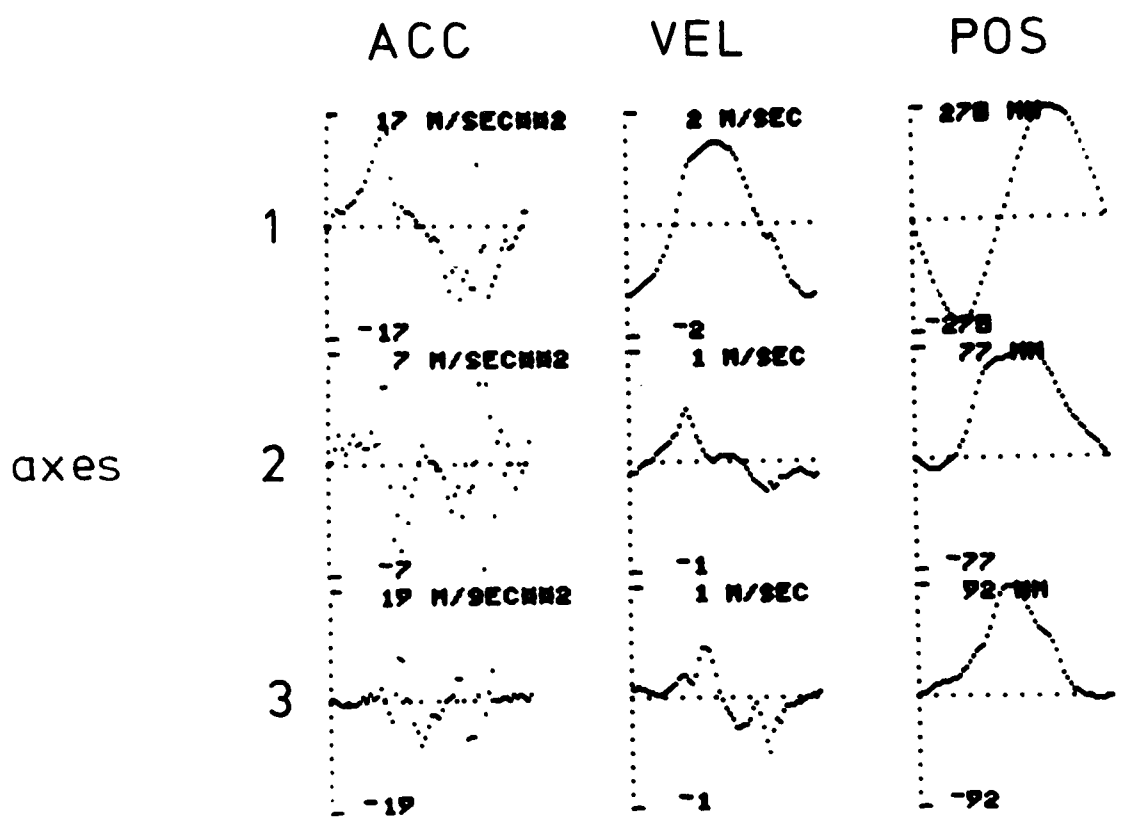
The orthogonality of DC is then checked by subroutine ORTHO. The current value of DC is written onto a dummy array, DIRC, which is tested. Subroutine ORTHO (listed at the beginning of Appendix D) calculates a matrix, PROD, which is equal to the product of the transformation matrix and its transpose. If PROD differs from the unity matrix, in any element, by more than twice an amount QTEST (in this case, QTEST = 0.005), the corrective procedure explained in Chap.2:

$$[\lambda]_{n+1} = [\lambda]_n([I] - ([\lambda]_n^T[\lambda]_n - [I])/2) \qquad (2.42)$$

is applied. The test is then made again. ORTHO returns to the mainline program either with a corrected matrix or when more than NMAX (=50) corrections have been made without success. In this latter case, execution will stop and the computer will display the sample number of the failure. In the usual event where this does not occur, M4EXT calculates the elements of each transformation matrix up to the end of the step, and files the results.

Figure 3.14 Translational components of the origin movement

MAIN6



Chap.2 indicated that, once the rotational position of the limb element was known, the translational parameters could be estimated. This is the task of program MAIN6. (The numbering of the mainline programs is simply an accidental result of the order in which they were written). First, the calibrated accelerations, the sample time and the transformation matrix are read from their respective files. The acceleration of the centre of the platform, denoted ALPHA, is calculated from the following equation:

$$\alpha_j = 9.81(\lambda_{ji}\ (\alpha m_i - g_i)) \qquad 3.14$$

where: αm_i represents the acceleration in body coordinates.

$g_i\ (=\lambda_{3i})$ is the component of the gravity vector in the i^{th} body-axis direction.

λ_{ji} is an element of the transformation matrix

α_j is in metres/second.

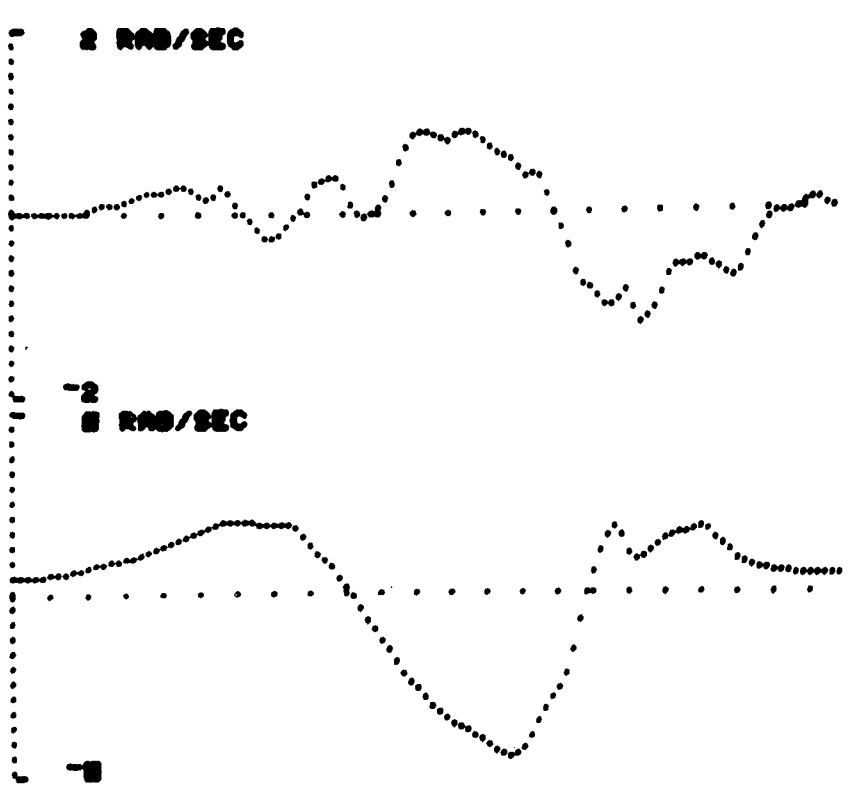
From ALPHA are found VEL, the translational velocity, and POS, the translational displacement of the platform centre. MAIN6 has an option whereby the displacements can be returned to zero, simulating a forward-moving ground-fixed reference frame (see Fig.3.14). The variables ALPHA, VEL and POS are then filed on the disk.

DISPLAY PROGRAM

CHOICES - ANGULAR VELOCITIES. TYPE 1
DIRECTION COSINES. TYPE 2
MOVEMENT SIMULATION. TYPE 3
PROGRAM END. TYPE 0

Figure 3.15

MAIN5
display choice



OM1

Figure 3.16

MAIN5
display

OM2

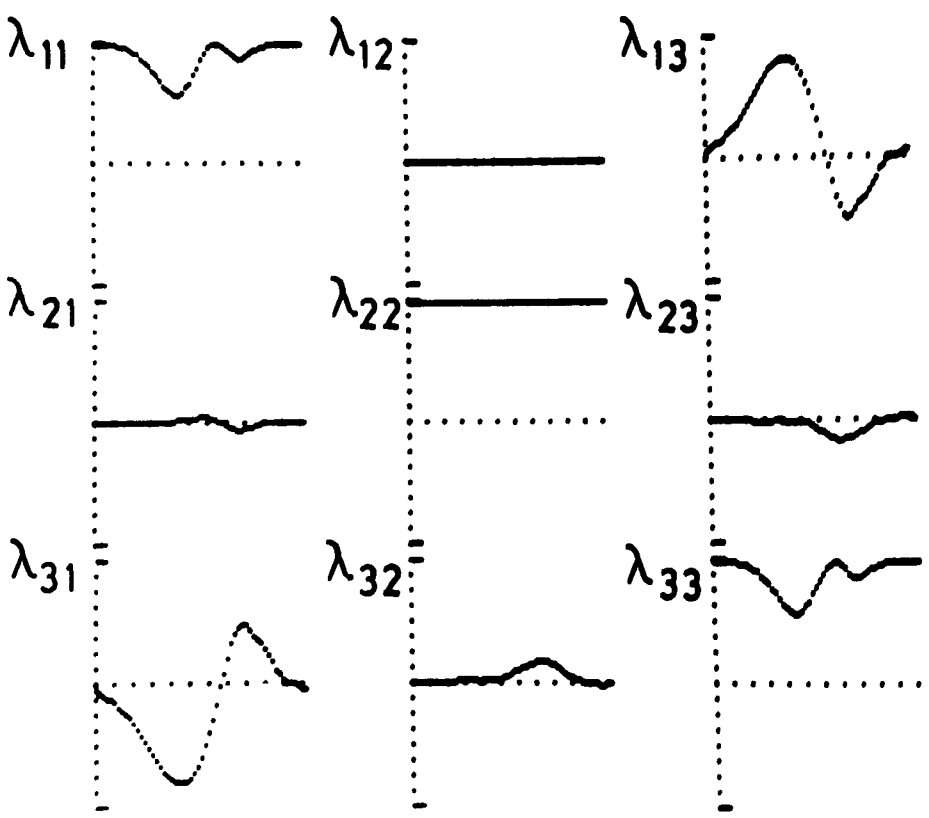


Figure 3.17

MAIN5
display

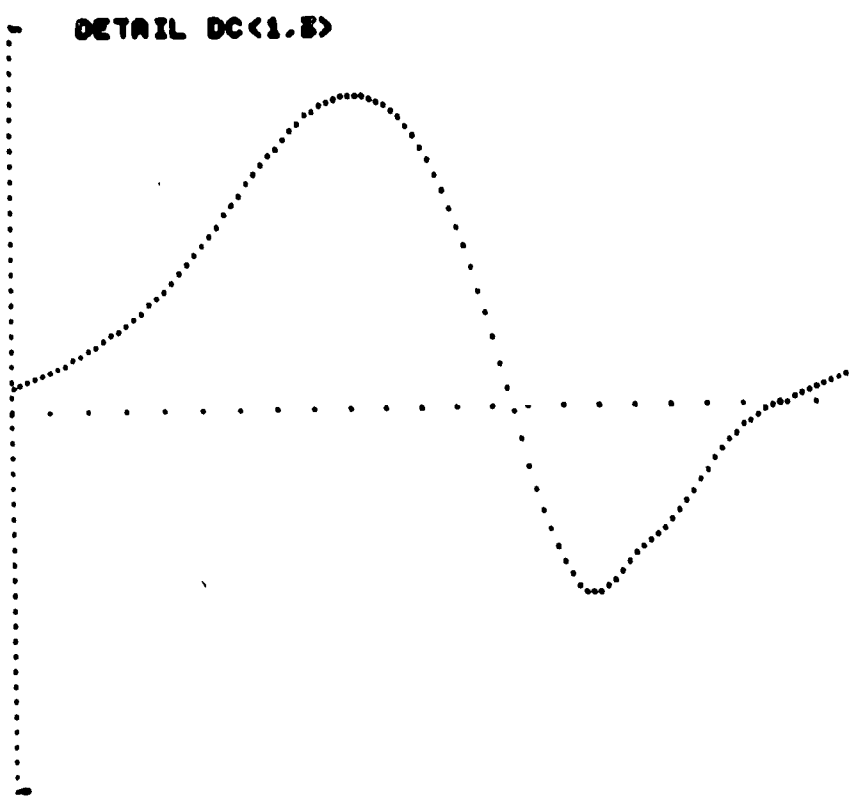
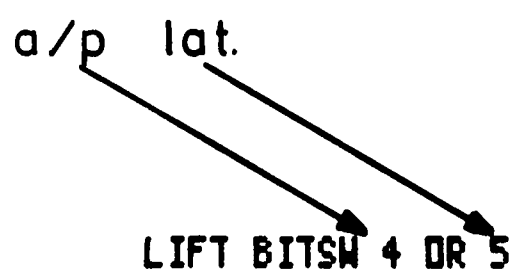


Figure 3.18

MAIN5 display



PROVIDE 40 MSEC LEVEL 3 INTERRUPTS

Figure 3.19

MOVE view and speed selection

3.7 Graphs and Moving Pictures: MAIN5 and MOVE:Summary

MAIN5 and MOVE, the two remaining programs of the set, are both concerned with the graphical and pictorial representation of the results which have been obtained by the analysis. MAIN5 presents the operator with a choice (see Fig.3.15) of viewing the angular velocities (Fig.3.16) or the transformation matrix (Fig.3.17). Since the definition of the display will not permit every sample point of the transformation matrix to be seen in this complete picture, the operator may also choose to see a graph of any particular element of the matrix (Fig.3.18). Finally, the choice may be made to use a combination of the results to generate a moving picture of the shank. In this case, the program MOVE will be called into core.

MOVE first generates a mathematical representation of a shank and foot. This representation, stored in array P, consists of 26 points, each defined by three coordinates corresponding to the moving axes fixed to the shank. A foot is included to add to the realism of the picture, but the motion of this foot, relative to the shank, is not known.

The position of the leg is known at every 0.01s, but to display each of these positions would be superfluous. Instead, elements of an array IPIC are found for every 4th.sample, at each 0.04s (point A in MOVE). IPIC has three subscripts, I,J and K. These represent, respectively, frame number, point number and fixed axis number. The coordinates of P are transformed by DC, and the movement of the shank origin, POS, is added to the result. The appropriate scaling is made on the picture for different knee/ankle distances. Thus IPIC contains

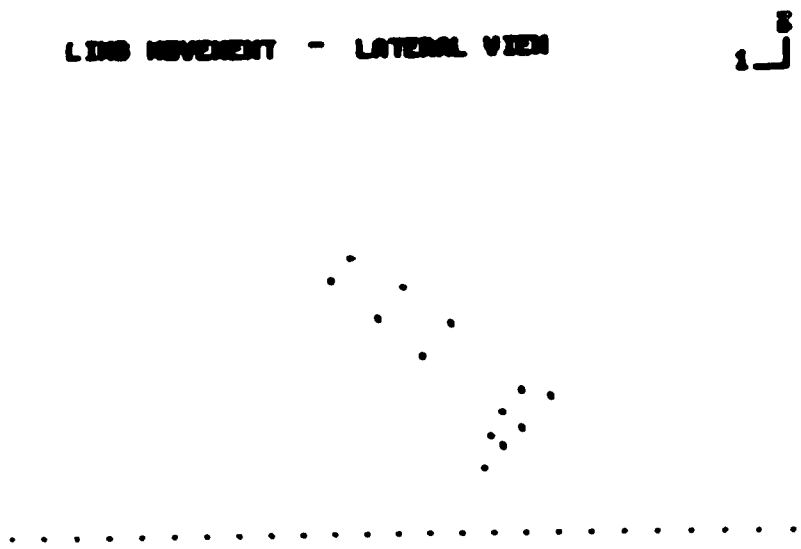


Figure 3.20

MOVE frame from lateral view

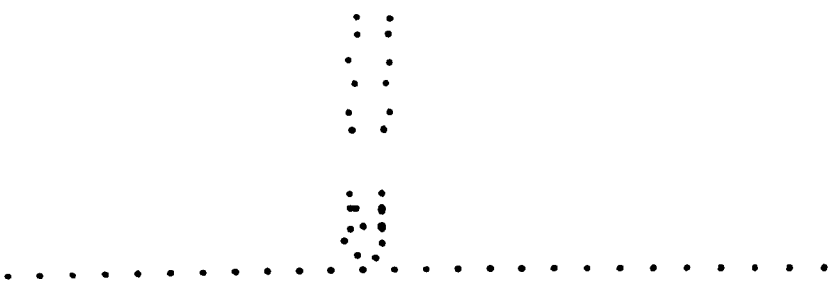


Figure 3.21

MOVE frame from anterior view

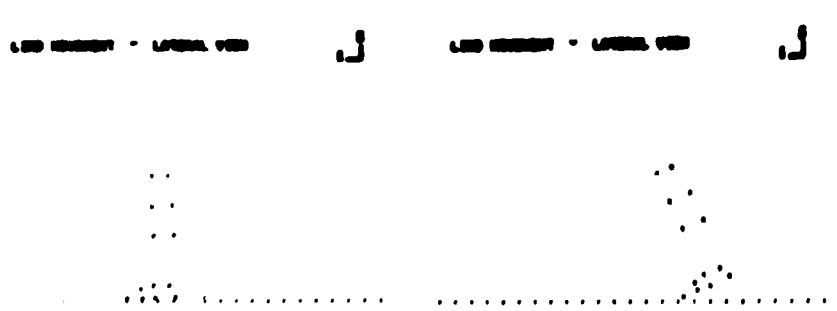
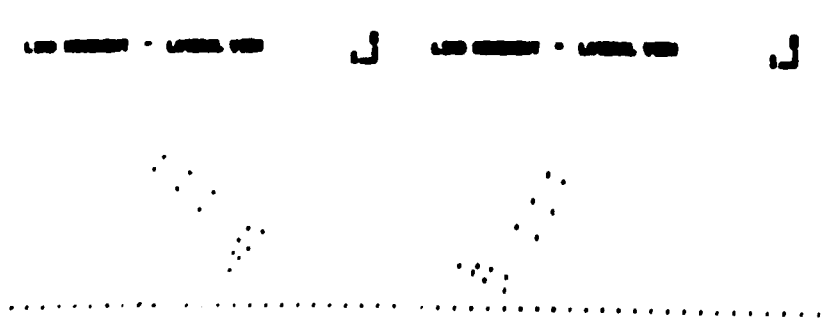


Figure 3.22

MOVE 4 lat. frames



every coordinate of every point of every frame in the step. A final correction is made to the coordinates of the foot. The "ground" is defined as being the level of the lowest excursion of the "heel". If any other part of the "foot" is found to go below the "ground", the shape of the "foot" is changed to simulate dorsi-flexion. This will occur in the latter part of the stance phase. At all other times the "foot" is kept in the neutral position.

The operator selects the viewing plane on the handkeys and provides 40 ms. interrupt pulses from OUI (Fig.3.19). Only two viewing planes are normally provided, namely, a lateral view and an antero-posterior view. Other viewing planes would be simple to incorporate but when these were tried, the results were found to be of little additional interest. Since the display is to occur at a real-time rate, the amount of computation which occurs between frames must be minimised. To this end, two one-dimensional arrays, IQUIX and IQUIY are generated from the three-dimensional array, IPIC (point B in MOVE). With time thus saved, due to the simpler addressing of IQUIX and IQUIY, only integer additions occur within the loop (point C to point D). Fig.3.20 and 3.21 show typical frames in either viewing plane and Fig.3.22 shows a frame from each quarter of the cycle. Since the rotational and translational positions of the shank can be returned to their initial values by the analysis, the "leg" appears to be walking on a steadily moving platform. This keeps the picture on the screen and allows the step to be recycled without any discontinuities.

This completes the description of the experimental procedure and the analysis programs. It will be seen that the performance of a test, from measurement, through analysis, to graphical results is simple. This supports the original intention of the development of a system, simple enough for clinical use, which is still capable of providing quantified, repeatable results.

Appendix E contains a quantitative assessment of the errors which arise with this method.

CHAPTER 4

EXPERIMENTAL RESULTS

4.1 Introduction

4.2 Comparisons with Cinephotographic Results

4.3 Accelerations

4.4 Velocities

4.5 Displacements

4.6 Summary of Clinically Relevant Variables

4.7 Heel-Strike

4.1 Introduction

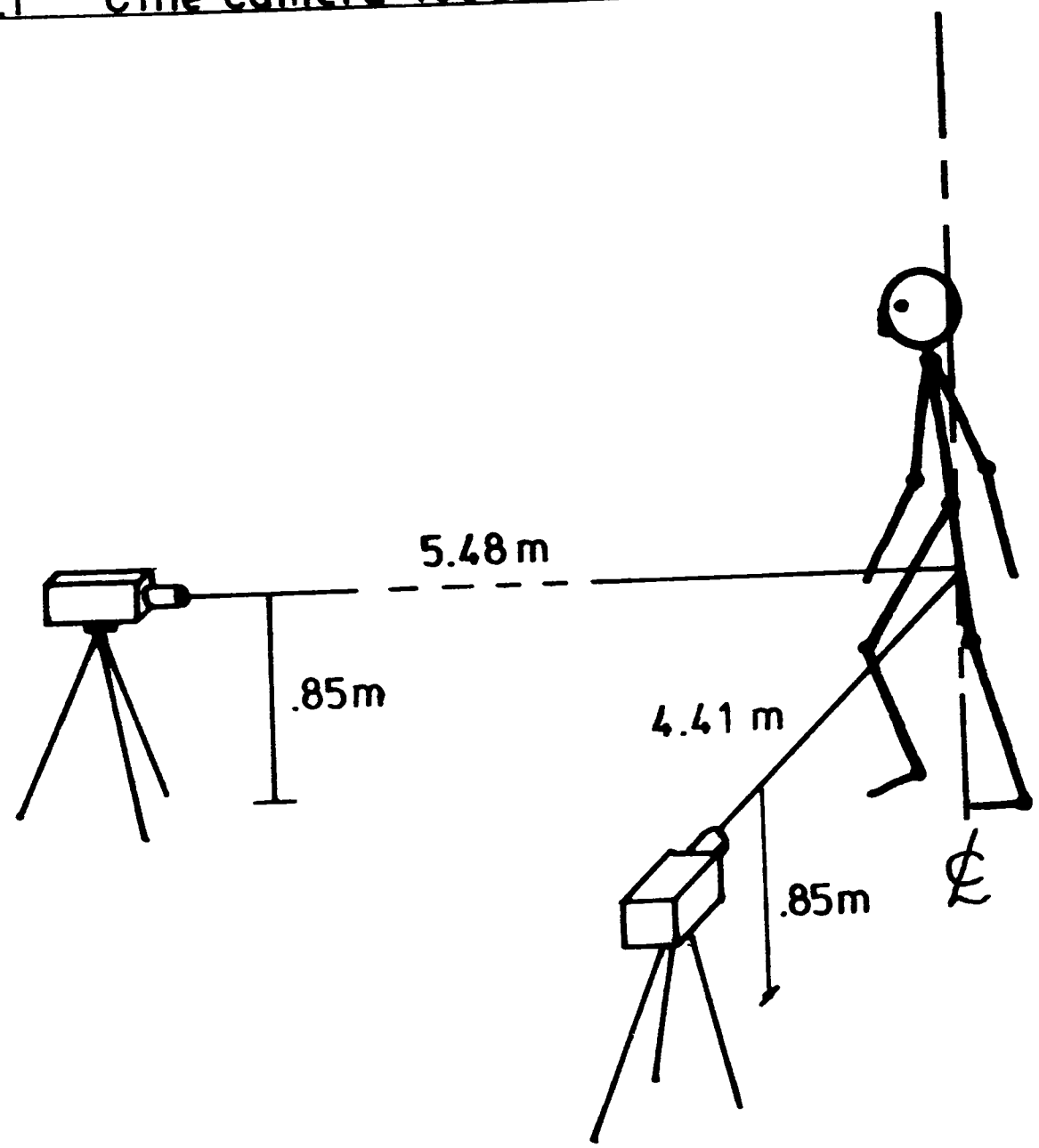
The objectives of the project up to the point where this report is made are twofold. First, to demonstrate that accelerometry is a feasible method for obtaining kinematic data on the movement of an ambulant subject's leg, and second, to study gait in this way and, from a limited number of observations, to select those parameters which most clearly demonstrate the particular characteristics of a subject's gait.

The absolute numerical values of most biological, kinematic functions are too widely varied to allow comparisons to be made between individuals in numerical terms. For this reason, comparisons are made between graphical representations of the time-dependence of such functions.

The meaning of the word normal is potentially ambiguous when used to describe mathematical variables which may be either normal (typical of a generally accepted norm) or abnormal (atypical of a generally accepted norm). It is therefore

necessary to state that, whenever the word normal is used in this chapter, it is intended to have the non-mathematic meaning given above. There has not been the opportunity to establish the normal patterns of any kinematic variables by a statistical study of a large, random population of subjects. The graphs of normal gait, used in Sections 4.3, 4.4 and 4.5 as the basis for comparison, are subjective impressions of the normal patterns for these variables, obtained from the analysis of six healthy subjects (four male and two female, ages 18 - 30). The variations from normality so defined, which are examined later, are sufficiently large to justify this form of comparison.

Figure 4.1 Cine camera locations



4.2 Comparison with Cinephotographic Results

Cinephotography may be considered as the traditional method for gait study and it has therefore been used as a yardstick in the assessment of the accuracy and limitations of accelerometric measurement. Due to a lack of facilities, it was not possible to use cinephotography until the accelerometric studies had virtually been completed. The experiments which were needed for the comparison were performed at the Bioengineering Unit, University of Strathclyde, using apparatus developed by Prof. J.P. Paul. The cinephotographic apparatus was operated by members of the Bioengineering Unit and the subsequent analysis of the films was carried out in Oxford according to the methods used in Strathclyde.

Two synchronised 16 mm. cine cameras were placed laterally and anteriorly to the path of a walking subject (Fig.4.1). In addition to the five accelerometric signals which were recorded as for a normal experiment, a set of pulses from the synchronous drive motors of the cameras was also recorded, as well as a pulse whose leading edge indicated the moment when a firing voltage was applied to a flashbulb. The light from this flashbulb was recorded on both camera films and thus a time reference point was provided on both recording media. Each subject, after standing for a few seconds while the tape recorder speed became steady and transducer zero-calibration records were taken, walked towards the anterior camera. The cameras were started as soon as the walk began, and came up to speed (50 f.p.s) in approximately 400 ms. During the walk the flashbulb was fired. The

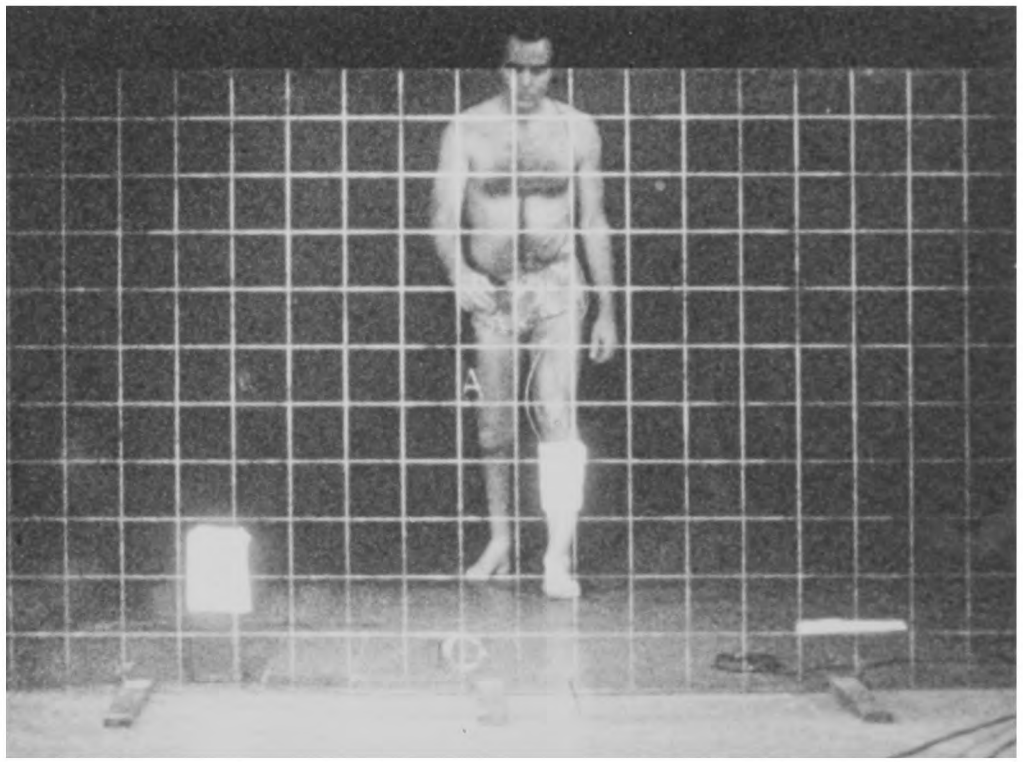
Figure 4.2 A Frame from the Lateral Camera

Marker dots are visible on lateral knee-joint line and on the lateral malleolus.



Figure 4.3 A Frame form the Anterior Camera

Marker dots are just visible on the patellar tendon and on the anterior ankle-joint line.

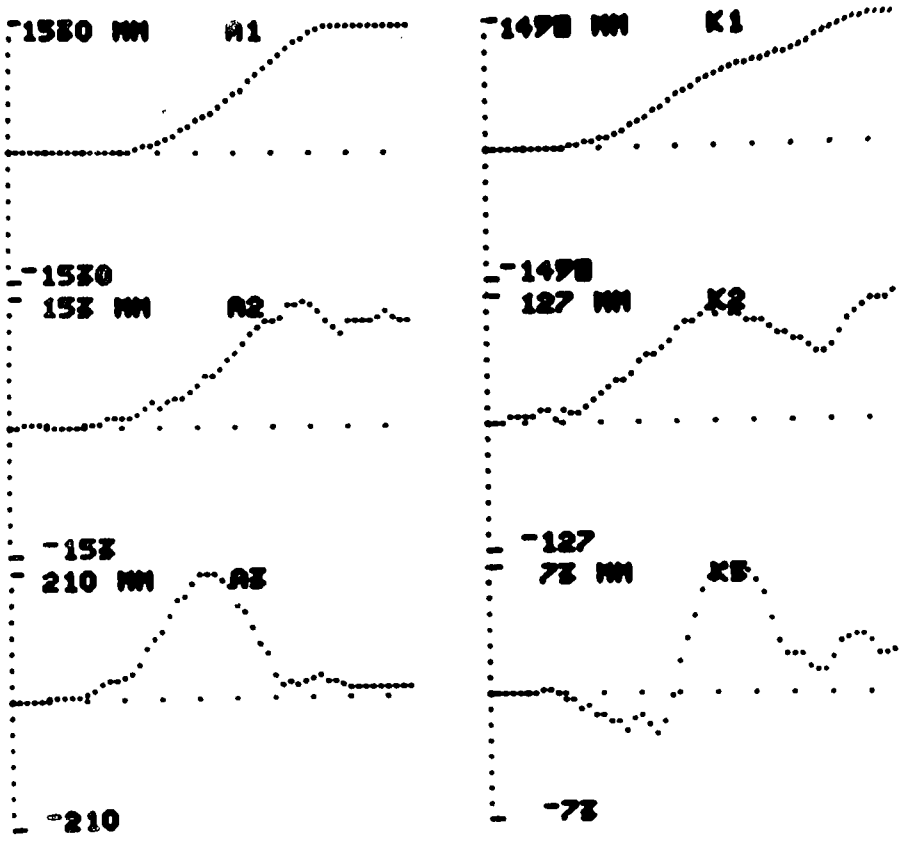


subjects made several passes and were not restrained in relation to gait cadence or stride length. The resulting records showed that each subject took approximately 10 paces/run of which the lateral camera recorded the fourth or fifth pace. After the film had been exposed, it was rewound and reexposed with a 5 inch grid placed at the intersection of the centrelines of the cameras, first perpendicular to one camera axis and then to the other. This provided a reference grid on each frame of the film against which measurements could later be made. Typical frames from the two cameras are shown in Figs.4.2 and 4.3.

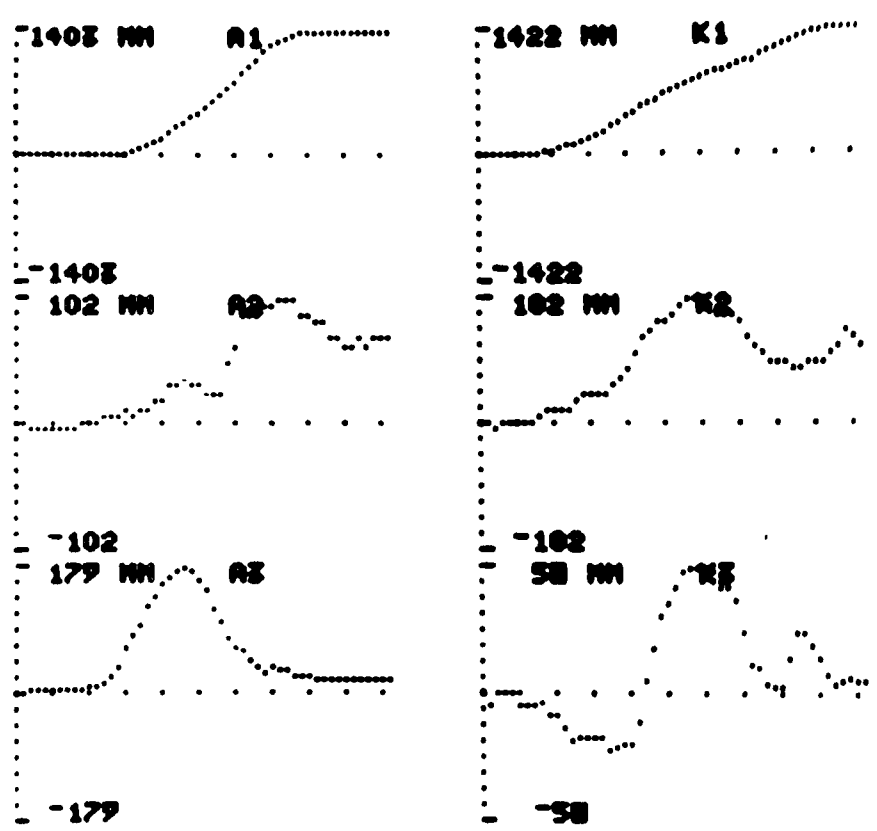
The film records, when analysed, showed that some of the passes were more suitable than others for the purpose of comparison. A suitable pass showed foot-flat to foot-flat on the lateral camera, for the leg on which the transducers were mounted, allowing the two measurement methods to be compared for a complete cycle. Using an analysing projector, the two films were, in turn, projected onto a sheet of graph paper so that the 5 inch grid on the film coincided with a 2 cm grid on the paper. Measurement of the position of marker dots on the legs of the subjects was usually possible to better than ½ inch, true displacement. These marker dots, shown in Fig.4.2, which were placed at four sites on the shank of the subjects, allowed the vertical and antero-posterior positions of the knee and ankle to be measured from the lateral camera, and the medio-lateral positions of these joints to be measured on the anterior camera.

For each film sample (sample period:20 ms) six measurements were made, making a total of approximately 300 measurements per step-cycle. This was found to take about 1 hour. The method of

Figure 4.4 Two typical sets of parallax-corrected cine film data



A1 ankle forwards
A2 ankle sideways
A3 ankle upwards
Kj knee ....



correcting film data for parallax errors is explained elsewhere.[47] A short computer program, FILM, (see Appendix D) was written to make the corrections. This program prints out the corrected coordinates and displays a continuously updated graph of the variables. It is therefore very easy to see when a major transcription error has been made. Such errors can be immediately put right. Fig.4.4 shows two typical graphs of parallax-corrected data. The largest parallax error was 5%. Certain features are immediately apparent from the graphs. The accuracy of measurement of the position of a dot in the centre of a frame was ¼ - ½ inch, depending on the speed at which the dot was moving. Near the edge of the frame the accuracy is reduced, due to lens distortions and less adequate lighting. These sources of error may account for the non-return-to-zero of the vertical ankle displacement which occurred on some sets of corrected data. Some of the quantization steps in the graphs are due to the visual display unit accuracy, but the larger steps on the A2,K2 and K3 traces are due to the limiting accuracy of measurement.

The corresponding analysis of the accelerometric data was made as described in the last chapter with slight differences. The frequency of the shutter synchronisation pulses recorded on tape were checked for each of the passes to be analysed by sampling the pulse train as though it was a typical data signal. The slow beat frequency (0.2 Hz) of the resulting aliased signal showed that the film and tape time-base rates were accurately matched. Where the flash bulb pulse occurred prior to the start of the cycle to be analysed (no great care had been taken during the experiments to ensure that this was so), it was possible to trigger the start of the signal sampling and digitisation from

Figure 4.5 Comparison of Accelerometric and Cine Displacement Estimates

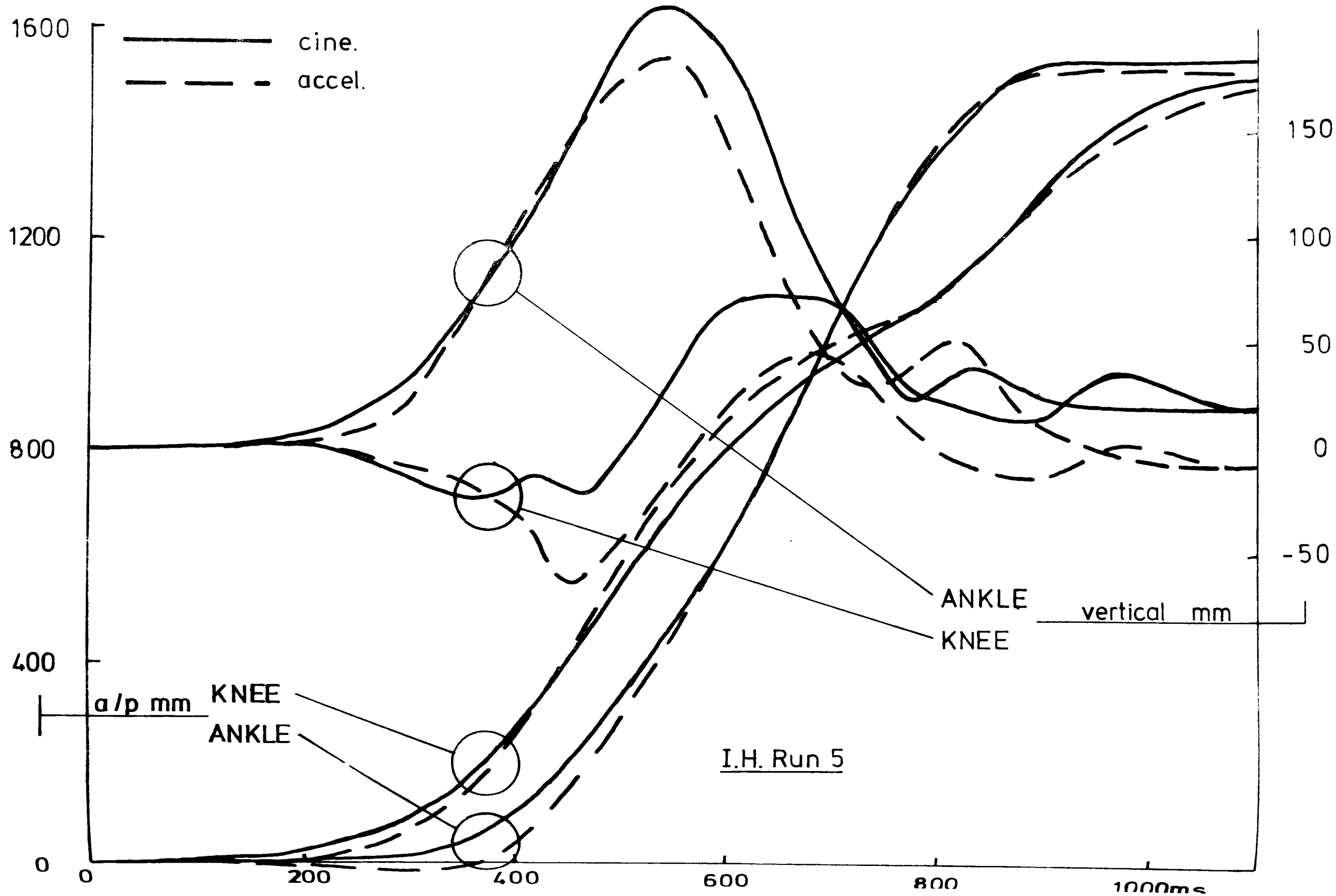


Figure 4.6 Comparison of Accelerometric and Cine Displacement Estimates

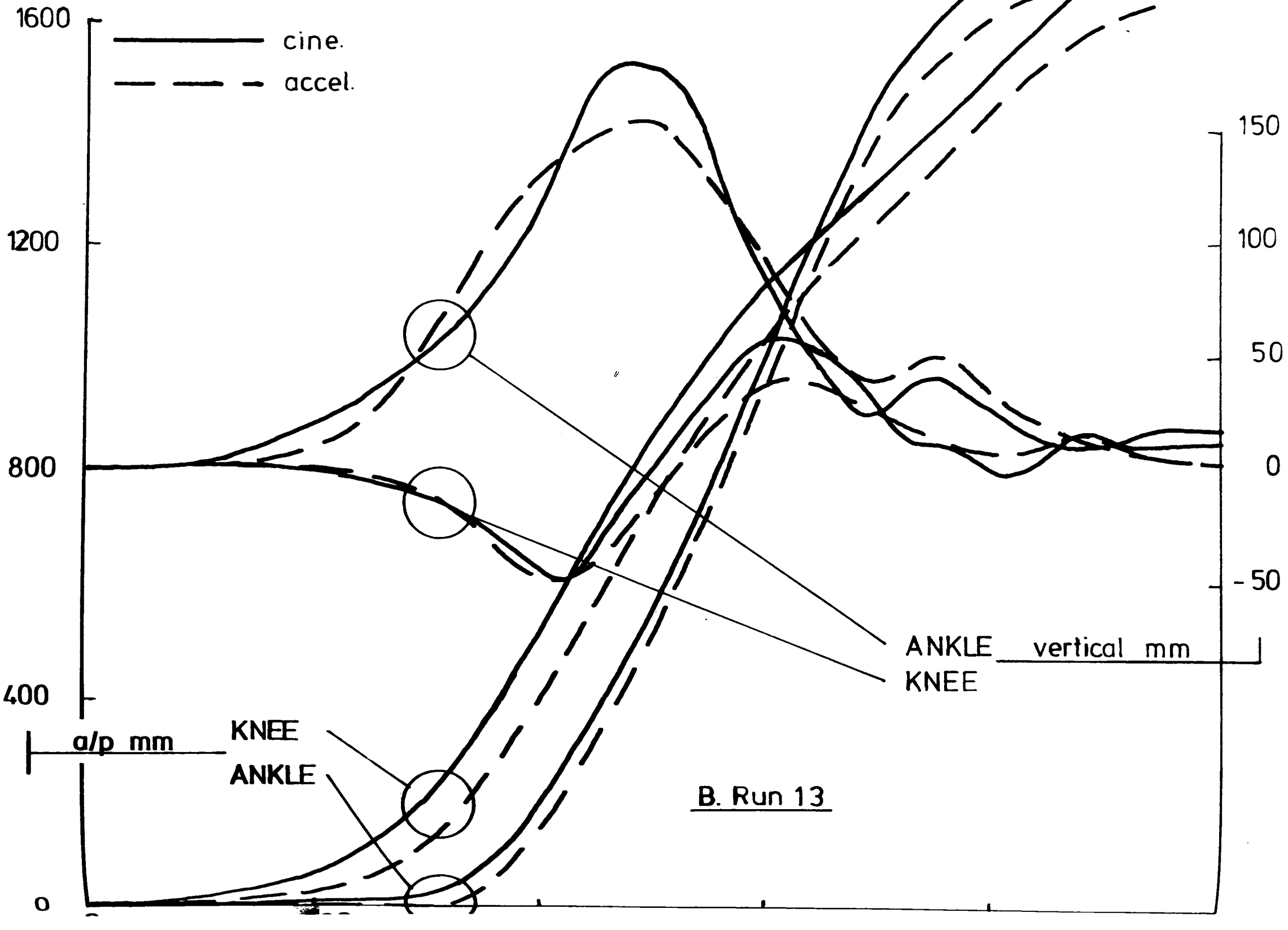
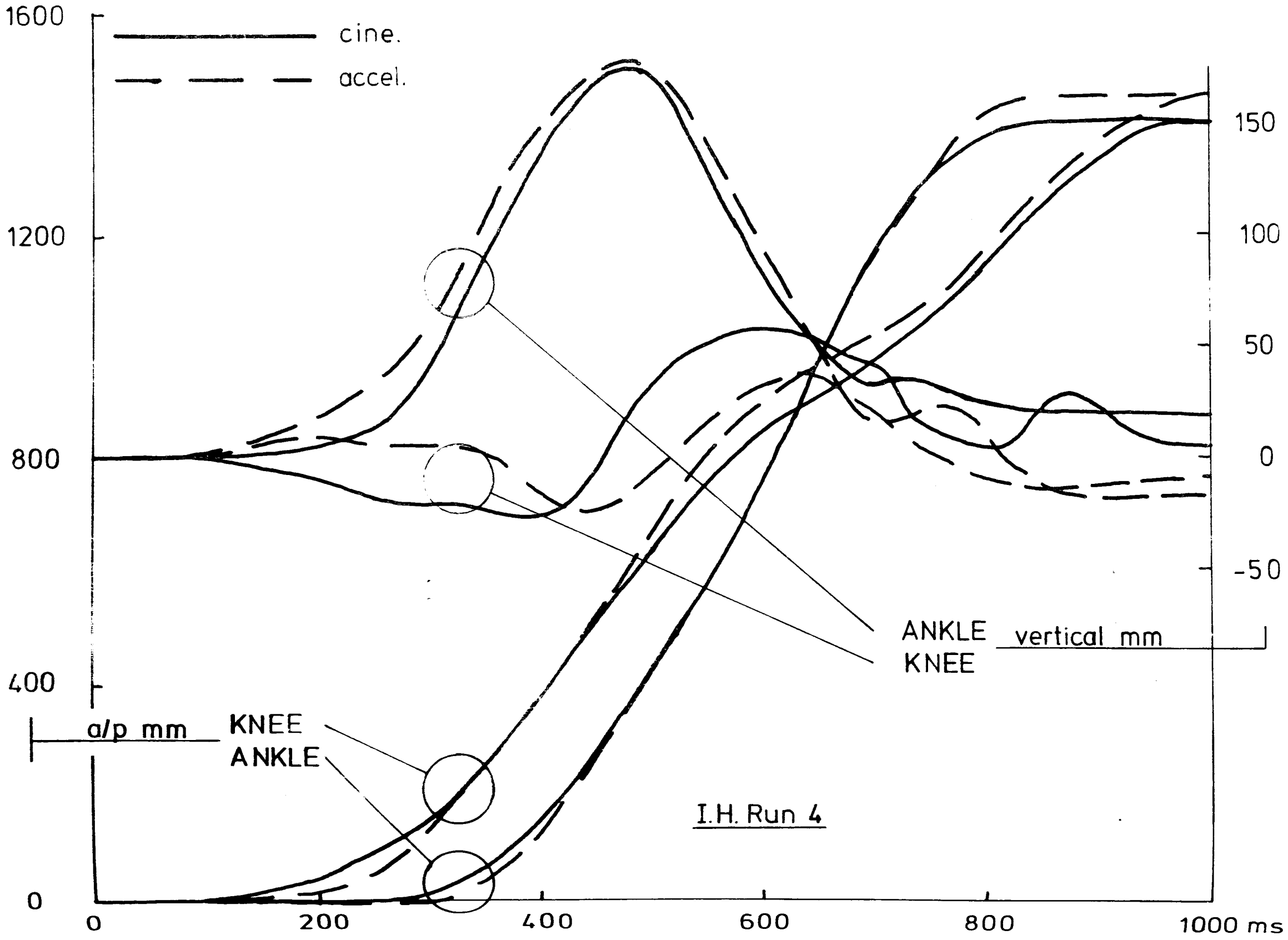


Figure 4.7 Comparison of Accelerometric and Cine Displacement Estimates



the leading edge of this pulse. The start of the cycle at foot-flat could therefore be located exactly, being a known time after the flash.

After the usual analysis, another short program, WHERE, (see Appendix D) was used to estimate, from the movement of the shank, the resulting displacements of the knee and the ankle. The display graphs and print-out allowed direct comparison with the output of FILM for the corresponding step.

Fig.4.5,4.6 and 4.7 show the superimposed graphs of antero-posterior (a/p) and vertical positions of the knee and ankle joints for three separate steps for which complete suitable data sets were available. Each of the graphs starts arbitrarily from zero. Not surprisingly the a/p movements show the closest apparent agreement since the displacement scales are four times coarser than those for vertical movement. The a/p displacement disparity is between zero and 70 mm, the largest values usually occurring at the end of the cycle. This is a relative disparity of between zero and 5%. The general shape of these a/p graphs is the same for both systems of measurement. The forward displacement of the knee is already increasing with an approximately constant slope when the ankle begins to move. The knee velocity drops during the third quarter of the swing phase while the ankle velocity increases. Ankle velocity then drops quickly, but smoothly, to zero while the knee velocity increases once more and then itself slows, sometimes to zero during the stance phase.

The relative disparity between the two methods of measurement is much larger in the vertical displacement graphs, rising

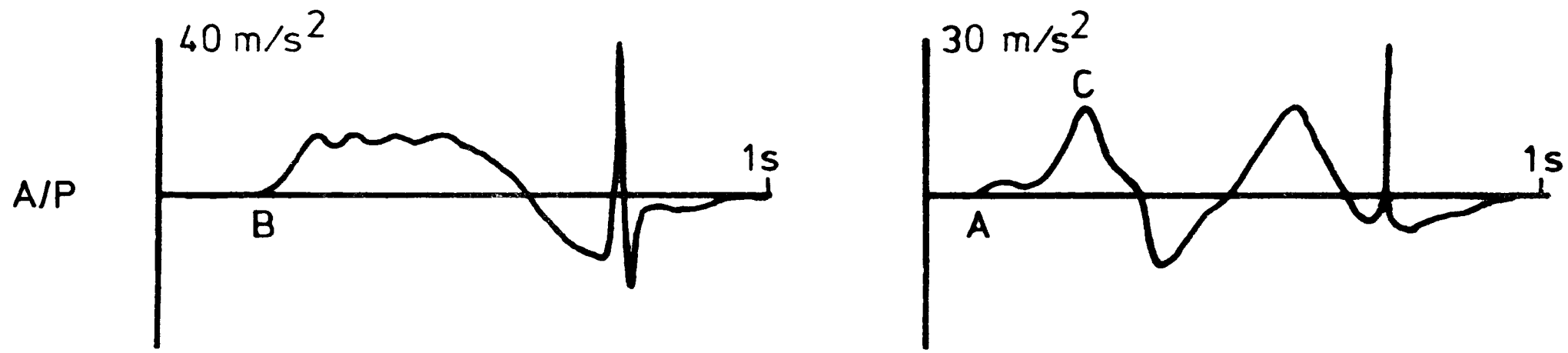
to 50% during some parts of the cycle. But the absolute disparities are of the same order as in the a/p graphs.

The knee vertical displacement first falls, reaching a minimum 1/3 of the way through the cycle, just before the ankle reaches its highest point. The knee then rises slowly and falls as slowly until heel-contact. Just prior to heel-contact, the ankle rises again with the forward swing of the leg. Finally the knee may be seen to rise over the fixed ankle during the stance phase. In these graphs, the general shape again shows agreement between the two methods.

The two predictable sources of error in the position graphs derived from accelerometric data are phase error and drift, due to the integration procedures. Both these effects are clearly apparent. The cine-film data, although itself subject to errors (for instance, the knee and ankle suffer net vertical displacements above a flat floor), is the nearest approach that is possible to an absolute reference.

The experiments have demonstrated that accelerometry can give sensible values of displacement, subject to the expected errors. It is felt, for reasons stated in section 1.5, that the relative errors of displacement derived from accelerometry will be lower than the errors of acceleration derived from cinephotography. Although several investigators have used cine-photography to make estimates of acceleration, there is only one published result with which a comparison of accelerations can be made. This comparison, in particular as it relates to heel-strike accelerations, is discussed in the final section of this chapter.

Figure 4.8 Representative Normal Data Set



ACCELERATIONS

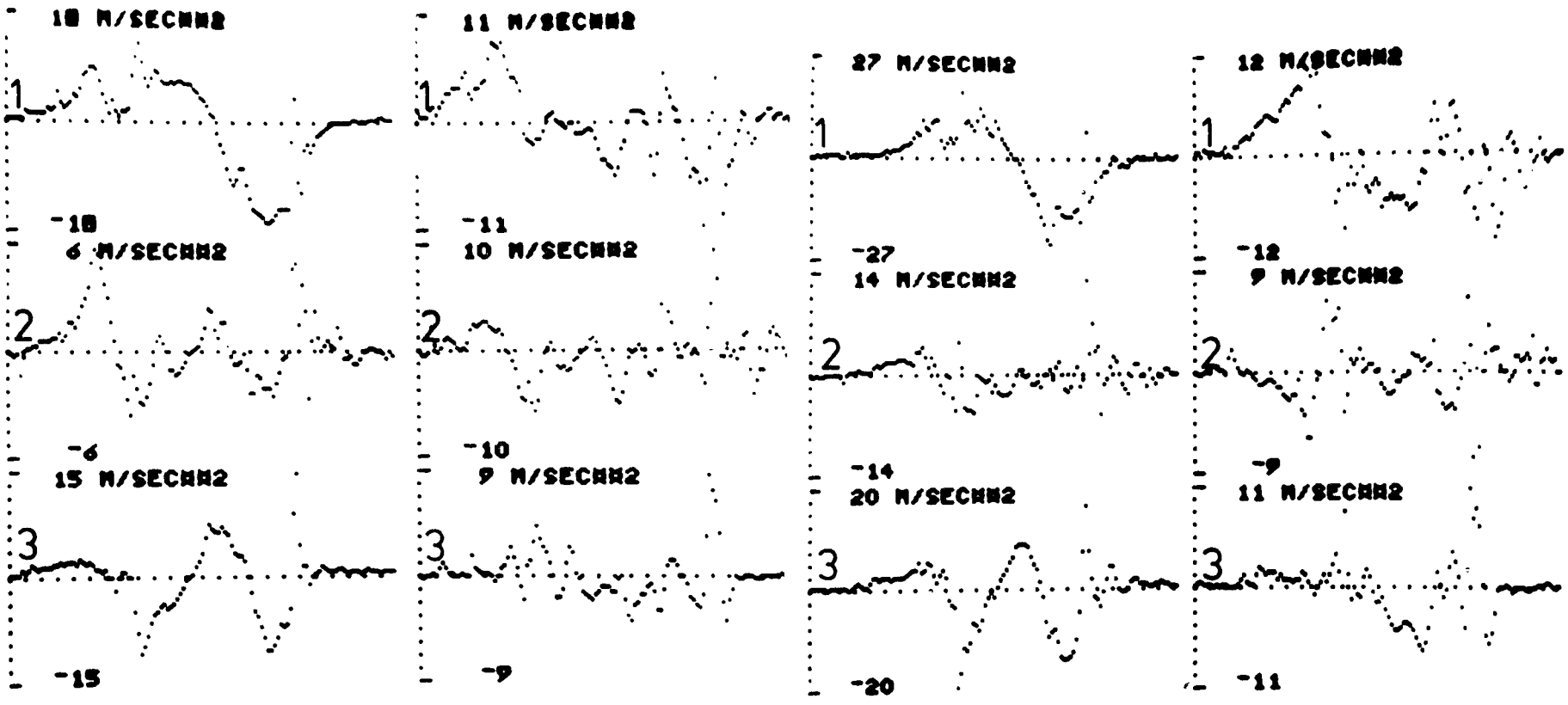
4.3 Accelerations

As was indicated in section 4.1, the results of only a number of the experiments which have been performed will be presented and discussed. The first variable to be examined is translational acceleration.

The acceleration measurements were made at a point which lies approximately mid-way along the shank, but since the precise location of this point will vary from subject to subject and from experiment to experiment, the measured data itself is not useful for comparison purposes. The translational accelerations of the ankle and knee joints provide more useful comparisons. Since the calculation of these quantities is simple and linear, the data is not smoothed and retains the sharp transients which are seen in the raw data. (c.f.Figs.3.9 and 3.10).

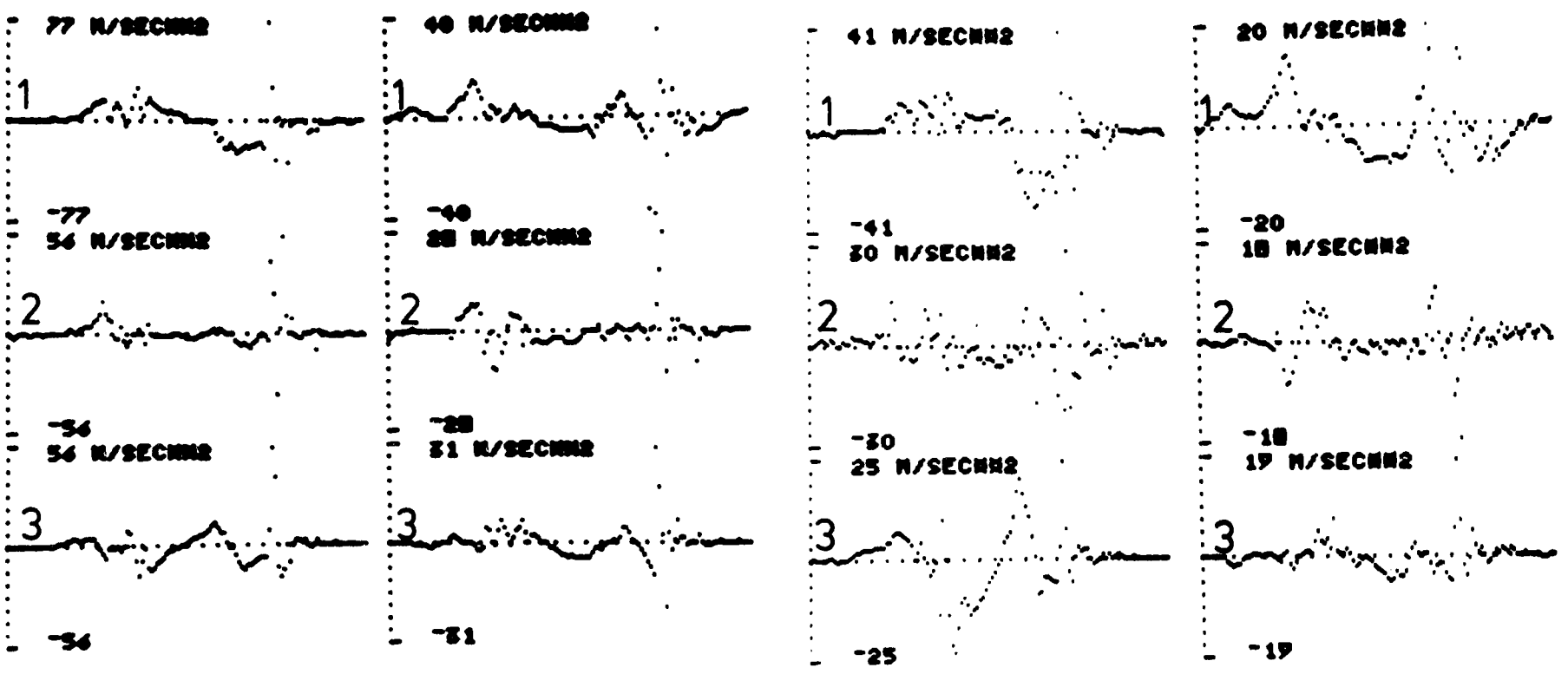
Fig.4.8 is a diagramatic representation of a typical cycle of a/p and vertical accelerations obtained from a normal subject, showing features of particular interest. Each graph is separately scaled and this should be remembered when examining any of the computer display results. As usual, the cycle begins during foot-flat when all accelerations are near zero. The knee accelerates first, forward and downward (A), with the heel leaving the ground shortly afterwards (B). Thereafter, the forward acceleration of the ankle is, for a time, constant at around 1.5g. Meanwhile, the knee reaches a peak (2g) of forward acceleration due to the muscular initiation of hip-flexion at toe-off (C). There is a corresponding peak of downward acceleration of the knee. The vertical acceleration of the ankle oscillates about zero, reaching a peak of around -2g,

Figure 4.9 (D.B.) Accelerations



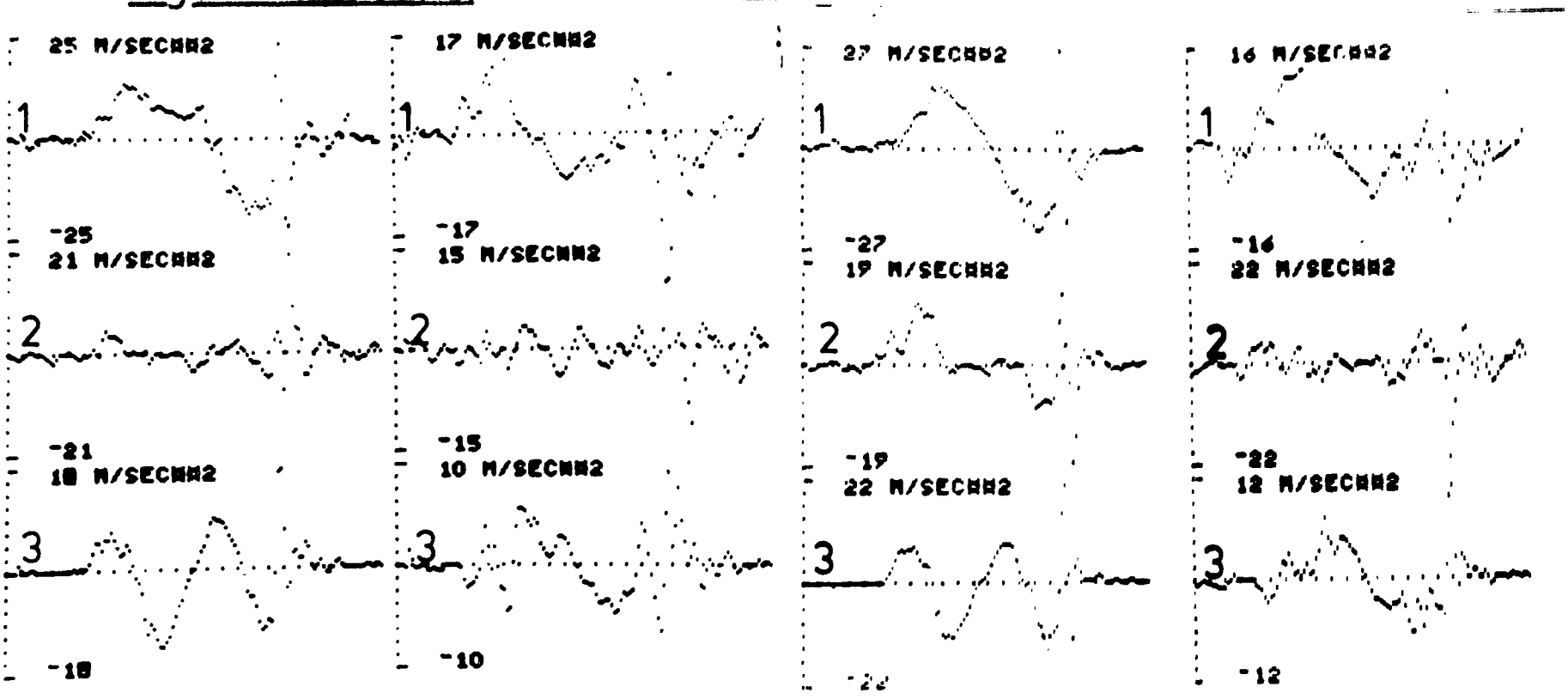
L Ankle L Knee R Ankle R Knee

Figure 4.10 (G.F.)



L Ankle L Knee R Ankle R Knee

Figure 4.11 (G.P.)



L Ankle L Knee R Ankle R Knee

all graphs for one step - cycle (~1s)

due to the large centripetal term, at the point of highest angular velocity (D).

The predominant feature of the acceleration traces is the spike which occurs at heel-strike. It is sometimes suggested that heel-strike is an inappropriate term to describe the initial contact of the heel with the ground. Certainly, the velocity traces, which are described in the next section, show how ankle velocity is brought down to zero in a controlled manner before this contact occurs. Nevertheless, we find accelerations of 3g, or more, in the ankle at heel strike. This is for normal gait in rubber soled shoes. Without shoes, or with certain types of abnormal gait, this peak value sometimes increases by 2 or 3 times.

Fig.4.9,4.10 and 4.11 show acceleration traces for three subjects whose gait is abnormal for known reasons. Subject D.B., a woman of 50, was admitted to hospital with diagnosed osteo-arthrosis in the left-hip. She was otherwise fit and had no pain in the right hip. Her gait, although visibly antalgic, was not grossly abnormal and she suffered less pain when walking than when sitting. Her gait (cadence 100 ppm) was measured on the day before she was operated on for a total hip replacement (THR). Subject G.F., a man of 70, was measured approximately 4 weeks after a left T.H.R. He was fit, active and was considered to have rehabilitated extremely well. The only obvious abnormality in his gait (cadence 106 ppm) was a slightly louder audible click at heel-strike on the operated leg. He had no pain in his left leg. Subject G.P. was a diagnosed rheumatoid arthritic, a woman

of 50, who had been treated biochemically as an inpatient. She had evolvement of both knees but suffered no pain at the time of measurement. Her gait (cadence 94 ppm) appeared slow and deliberate, but with no recognisable abnormalities.

Considering first subject D.B. and Fig.4.9, we may note that the overall magnitude of the ankle accelerations are 25-50% lower on the left, as compared with the right. This is the first indication of an asymmetric gait. The heel-strike peaks are abnormal on both sides, being much higher in a vertical direction than in an a/p direction. This suggests a high-stepping, precise gait; a fact which will be borne out later when displacements are considered. All the traces are noisy, indicating that there is a degree of muscular spasm preventing the free, pendulous nature of a normal swing phase. The jerk of left ankle at toe-off is low compared with the right side, indicating a low-impulse push by the left foot.

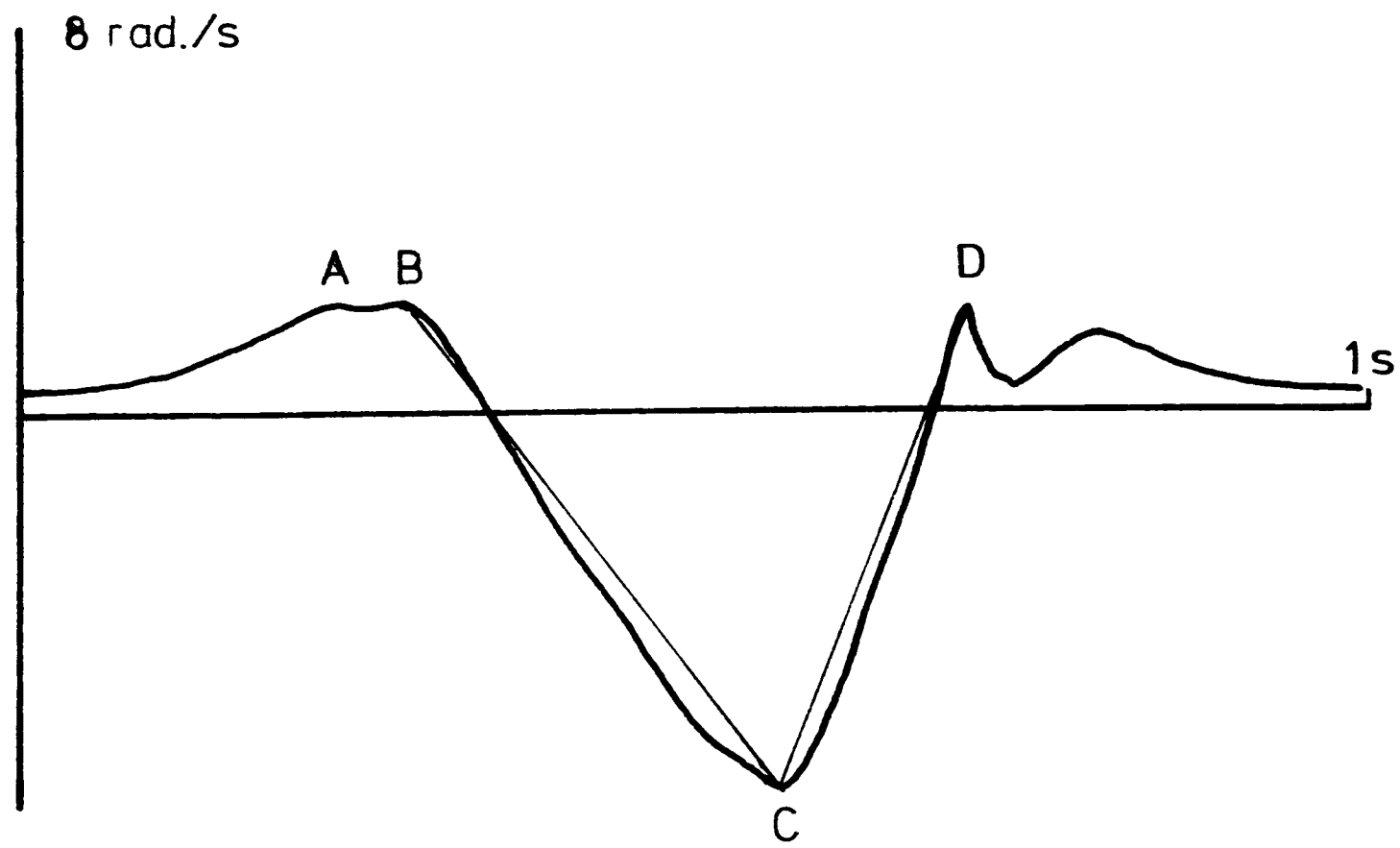
Next, we may consider Fig.4.10 and subject G.F. Here the findings are surprising. The louder,audible clicks on the operated side were indeed evidence of a hard heel-strike. The vector sum of the ankle accelerations on the left leg shows that a peak of more than 10g. occurs at this point. This is well in excess of normal values, and about double the value for the other leg. In other respects, the traces show no particular abnormalities.

Finally, subject G.P. in Fig.4.11 shows no particular abnormalities other than slightly lower accelerations in the

right leg. No asymmetry was visibly evident in her gait.

In summary; the graphs of acceleration at the knee and ankle are difficult to interpret. High-impulse heel-strikes and toe-offs may be recognised, as well as a general jerkiness in the movement of the leg. For the purposes of routine clinical assessment, however, it would seem unnecessary to present results in the detailed form shown here. It should be sufficient to indicate the values of the maximum accelerations and whether, or not, these peak values occur at heel-strike, for this is not always the case.

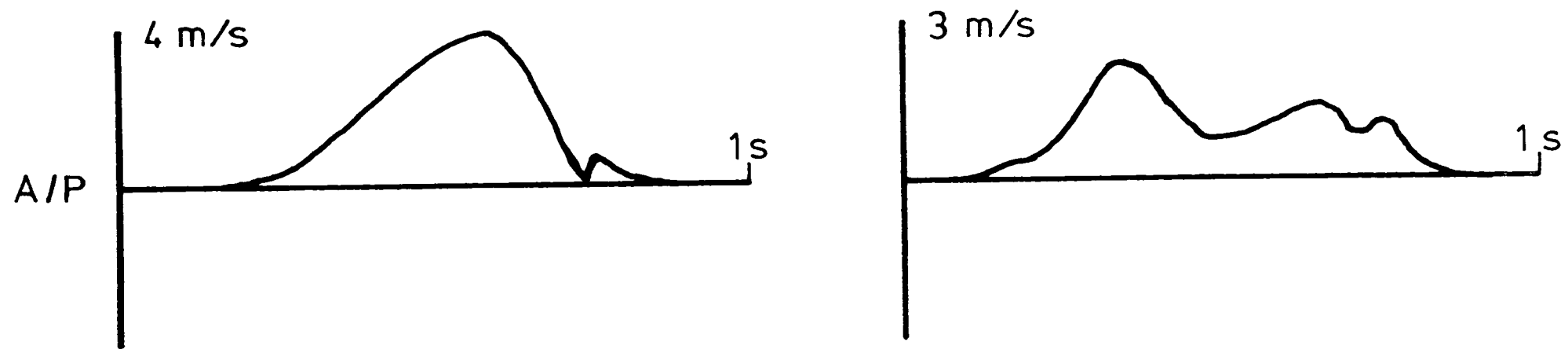
Figure 4.12 Representative Normal Data



4.4 Velocities

The angular velocities of the shank and the translational velocities of the ankle and knee are certainly the most useful assessment parameters to be derived from the analysis. Fig.4.12 shows, diagramatically, a normal, sagittal plane, angular velocity graph. The angular velocity in a coronal plane has no recognisable pattern in normality. Its magnitude is usually of the same order (<1 rad/sec r.m.s) as the transverse angular velocity, which is assumed to be zero. Any coronal plane angular velocity which exceeds 2 rad/sec. may be considered abnormal. In the sagittal plane, however, there are very clear patterns of normality. At the start of the cycle, during foot-flat, the angular velocity is on, or just past, a positive-valued minimum. The value increases approximately linearly to around 3 rad/sec. (point A) as the heel rises off the ground. In vigorous gait, push-off may produce a short, positive pulse (point B) before the angular velocity drops rapidly through zero. At a cadence of 110, the process of push-off, continuing until the forward swing commences, lasts around 0.1s. There is no sudden change in the slope of the curve as the toe leaves the ground. The angular velocity becomes increasingly negative, reaching a peak amplitude of around -7 rad/sec., two-thirds of the way through the swing phase (point C). At this point there is a rapid change of slope, as the knee-flick mechanism operates, and the angular velocity thereafter increases quickly to around +2 rad/s at heel-strike (point D). A useful measure in the swing phase is the ratio of the slopes of the lines BC and CD. In a normal subject, this ratio has been found to be 0.5 - 0.6 (the minus sign is omitted). This will be known as the swing-phase ratio (SPR) and

Figure 4.13 Representative Normal Data Set



VELOCITIES

it provides an indication of the stiffness of the knee joint; the higher the value of the SPR, the longer it takes to straighten the knee and, the stiffer the joint.

For a low impulse heel-strike to occur, the control mechanisms of the limb must match the backward speed of the ankle (backward, relative to a moving body origin) with the speed of the passing ground. It has been found that the shank usually rotates very slightly faster than is necessary to give a low impulse heel-strike, so that a slight drop in angular velocity occurs immediately after heel-strike. When the speed match is poor, this drop in angular velocity can be greatly increased (as will be shown later). As the knee flexes against the quadriceps muscle group which is stabilising the joint, the shank angular velocity increases once more during the active damping of heel-strike to foot-flat. The angular velocity then slowly decreases almost to zero at the positive-valued minimum from which the cycle began.

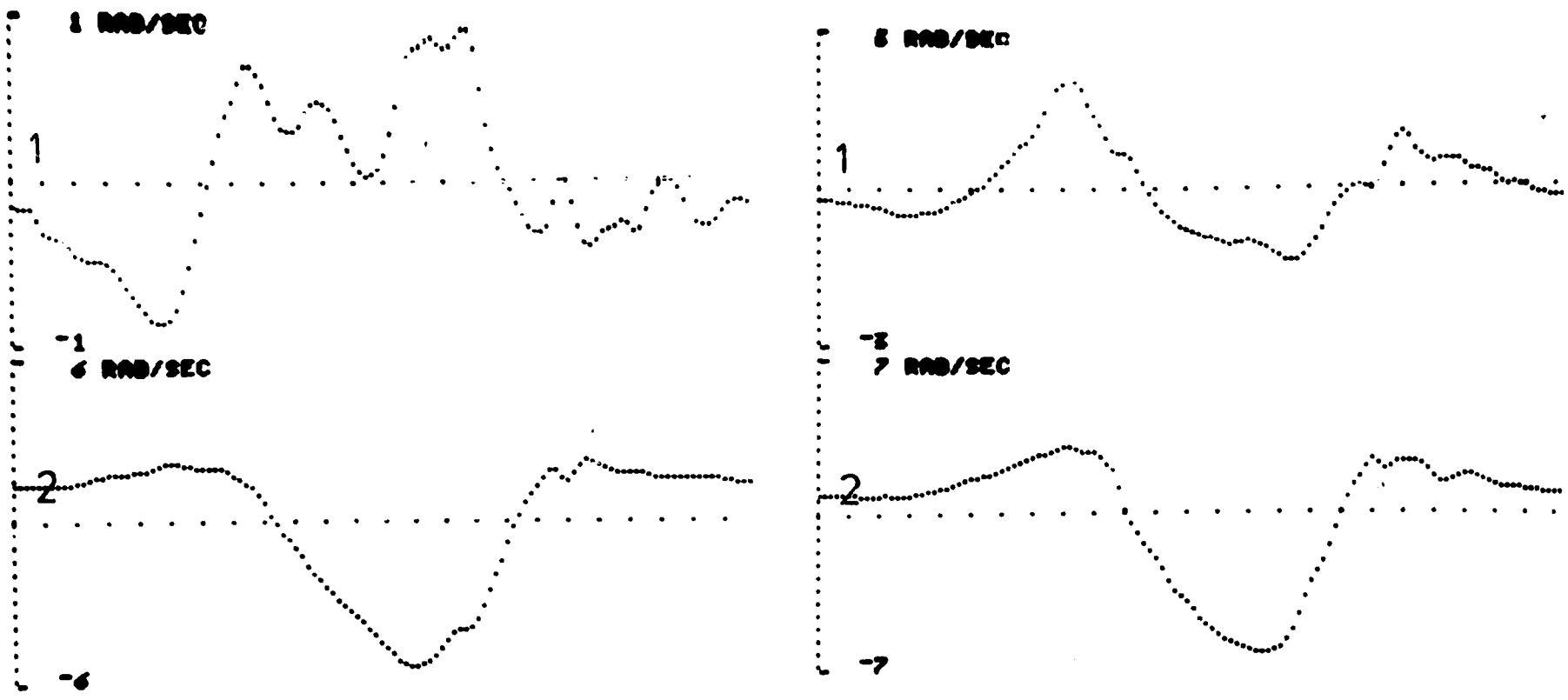
The translational velocities of the knee and ankle are considered next. Fig.4.13 shows ankle and knee movements in the velocities in the a/p and vertical directions. The forward velocity of the ankle shows an approximately linear rise to a peak, whose value depends on the stature and cadence of the subject, followed by a steeper linear fall to zero at heel-strike. After heel-strike, there is a small positive pulse of forward velocity as the ankle rotates about the point of contact with the ground at the heel. The absence of this pulse indicates a flat-footed gait. In a vertical sense, the ankle velocity has

the appearance of a damped oscillation; a positive half-cycle as the ankle accelerates upwards during and after toe-off; a negative half-cycle as it swings back down, close to the ground; a further, smaller, positive half-cycle as the foot swings forward; and a small negative quarter-cycle, which is interrupted by heel-strike. The two characteristics of this graph which are most clearly recognisable are its oscillatory nature, and the magnitude of negative peak at heel strike.

The knee forward velocity usually has two positive peaks, the first corresponding to hip flexion during the swing phase. Hip flexion reaches a maximum of around 30^{o} (viz. Chap.1, section 4) and maintains this angle until heel-strike. While hip flexion is constant, the knee velocity should be equal to the velocity of the pelvis and trunk. This velocity, of course, depends on the mean speed of progression but typically is about 1 m/s. The second, smaller peak, which occurs just prior to heel-strike cannot be explained by hip flexion and is probably due to the rotation of the pelvis. Finally, it should be noted that, during walking the knee forward velocity cannot be zero or negative, since hip extension occurs during the stance phase when the foot, with zero velocity relative to the ground, is moving backwards relative to the knee.

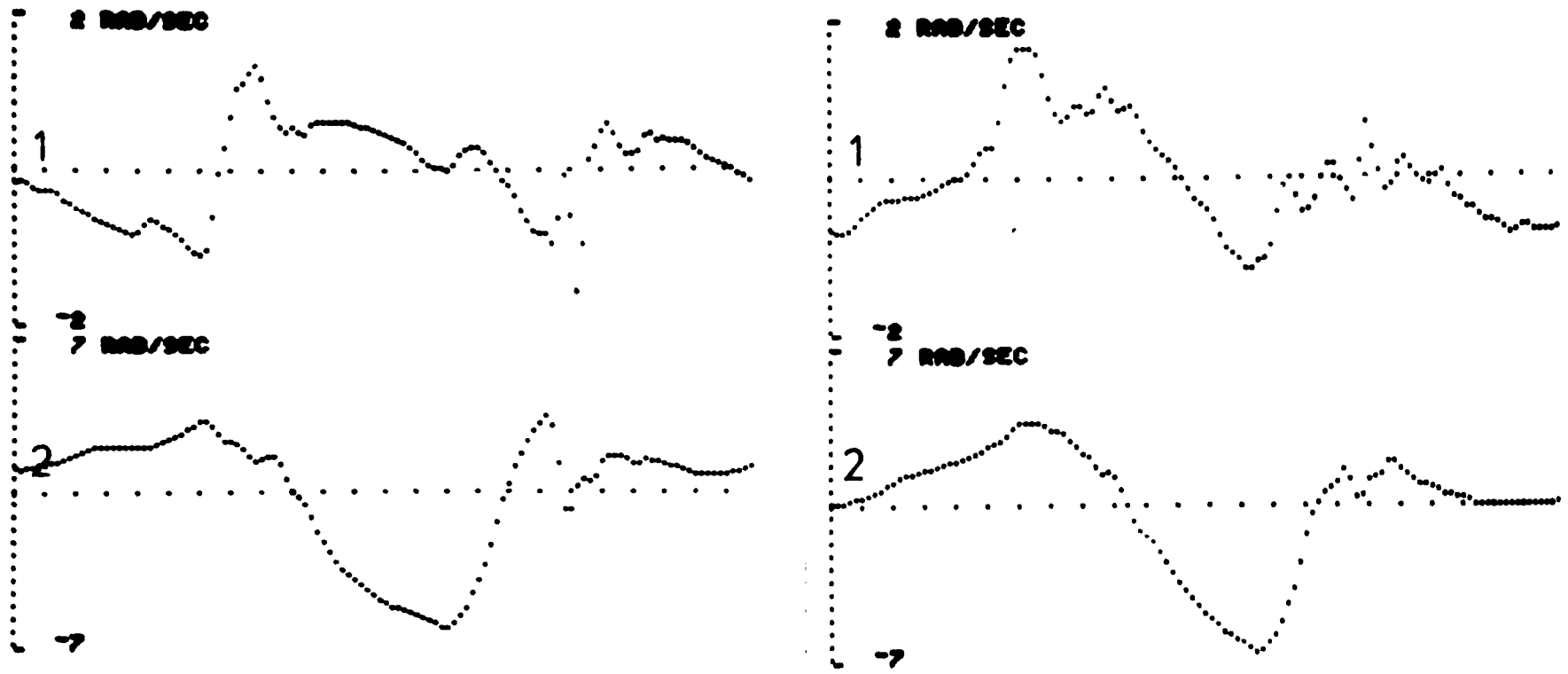
Lastly, the vertical velocity of the knee is slightly negative at the beginning of the cycle and then becomes positive as the hip flexes and is hiked by the contralateral abductor muscles. The velocity will fall to become negative before heel-strike, at which time it will be forced to zero and then become positive as the knee rises over the foot in the stance phase.

Figure 4.14 (D. B.) Angular Velocities



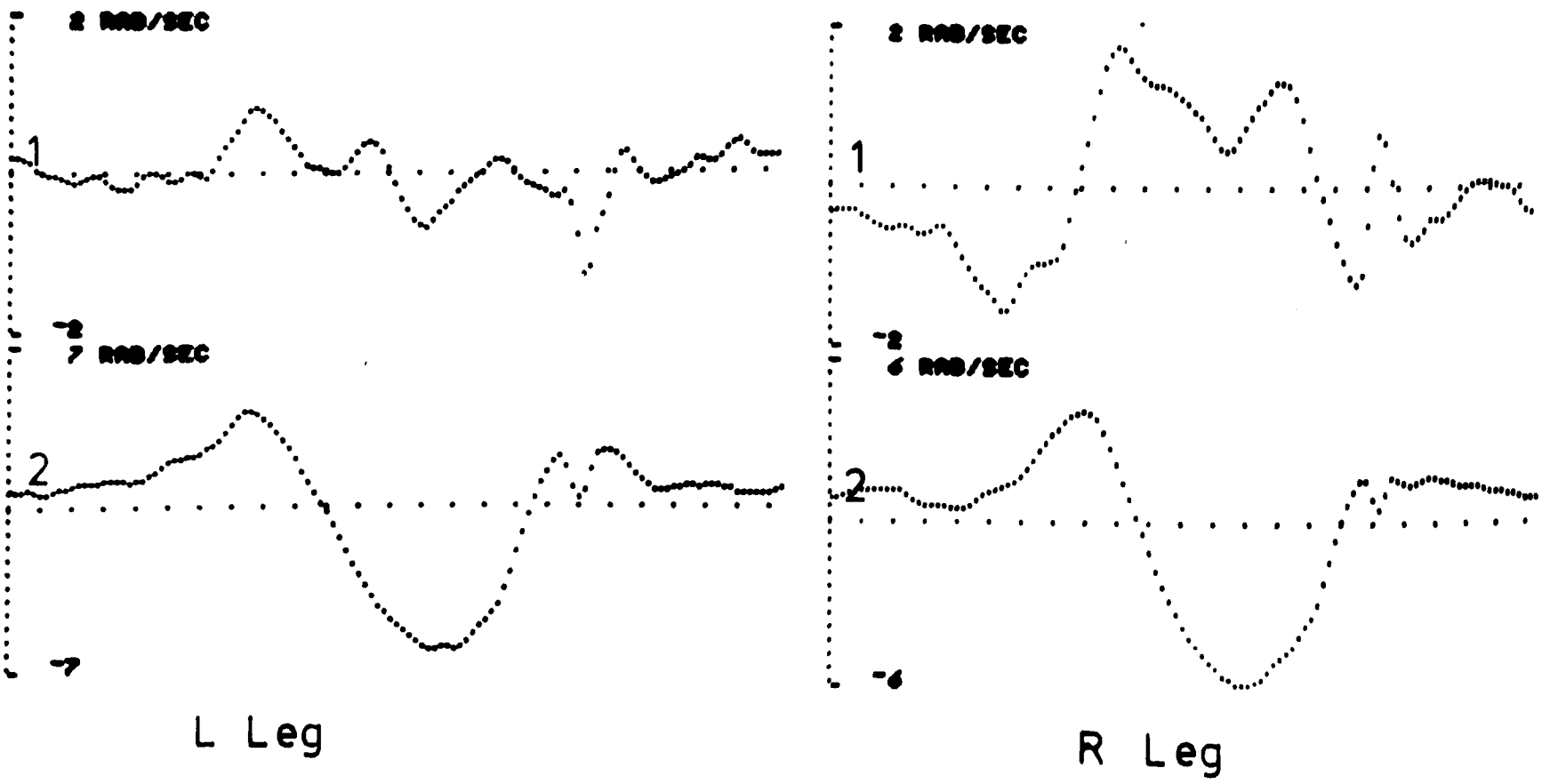
L Leg R Leg

Figure 4.15 (G. F.)



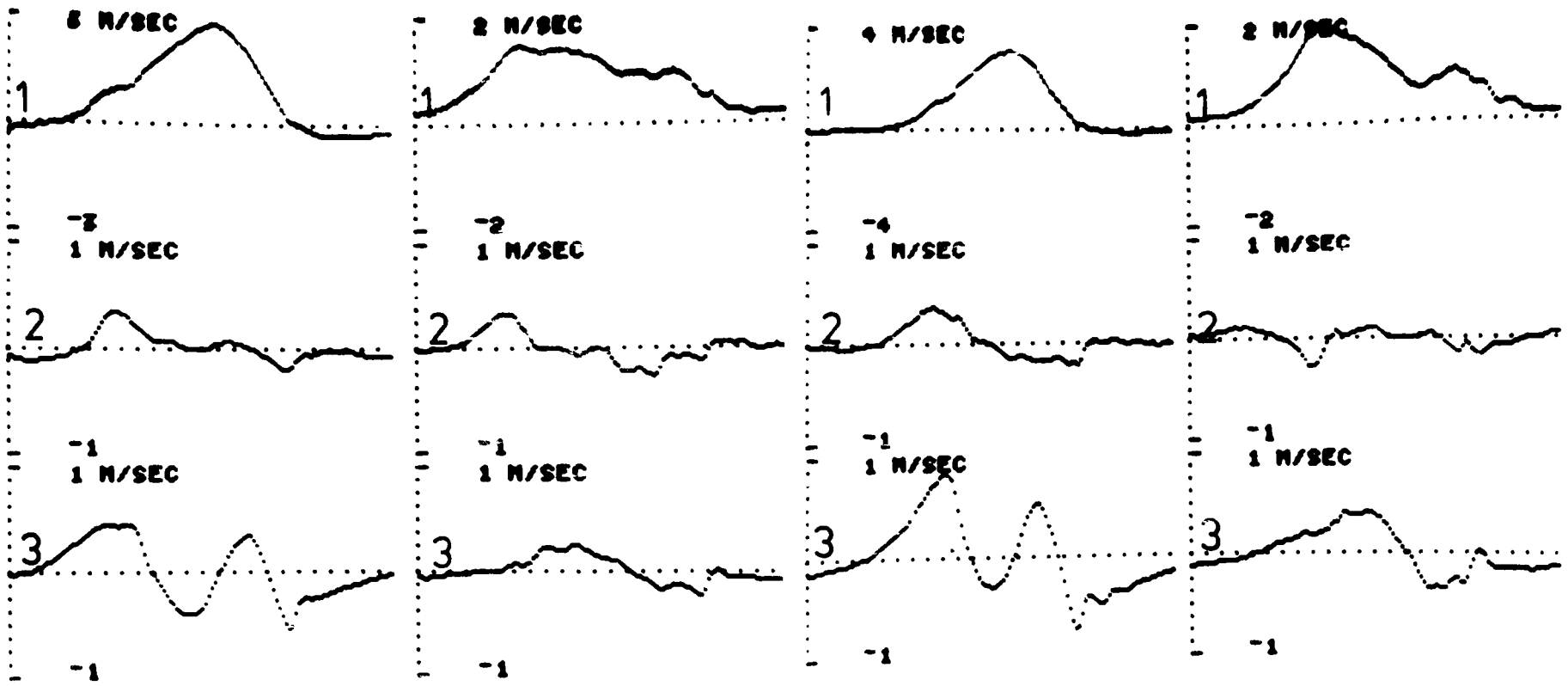
L Leg R Leg

Figure 4.16 (G. P.)



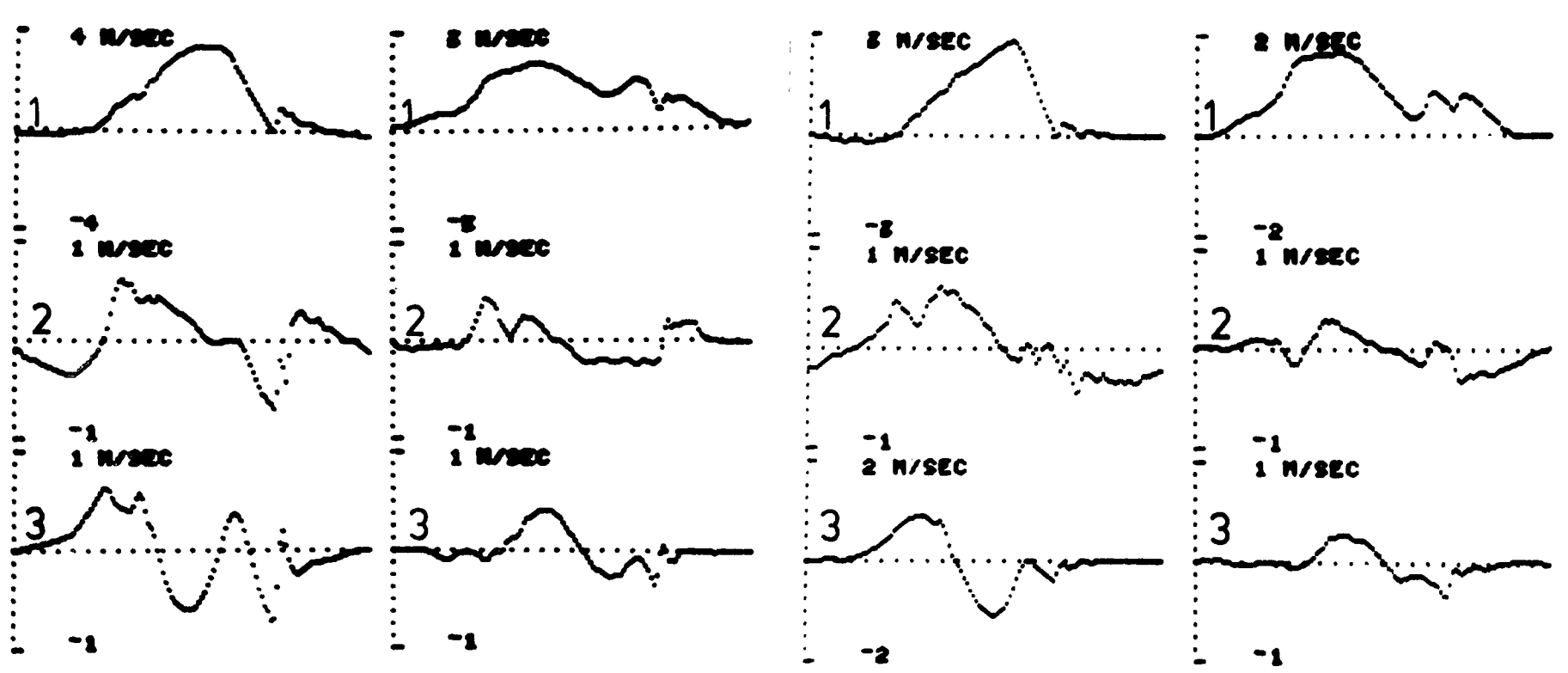
L Leg R Leg

Figure 4.17 (D.B.) Velocities



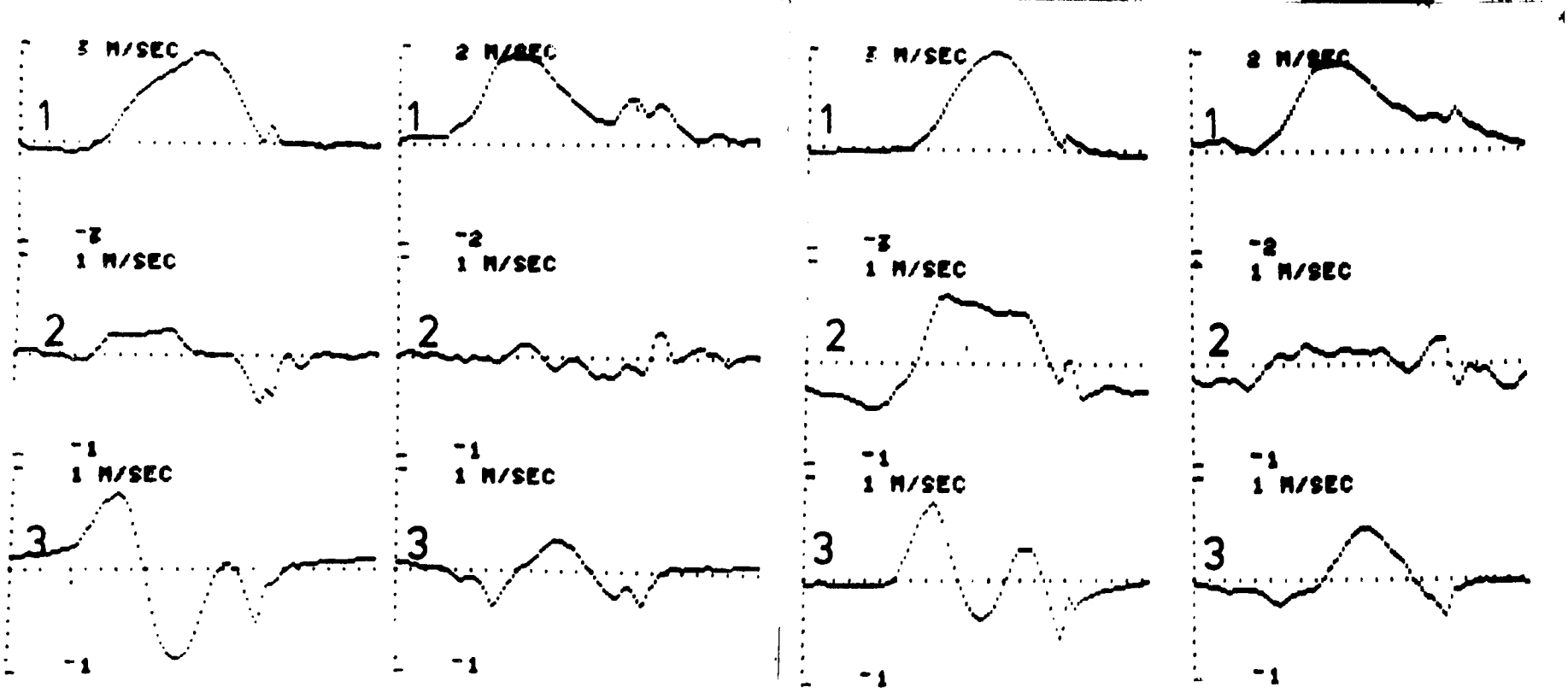
L Ankle L Knee R Ankle R Knee

Figure 4.18 (G.F.)



L Ankle L Knee R Ankle R Knee

Figure 4.19 (G.P.)



L Ankle L Knee R Ankle

The three subjects may now be examined to see how their velocities differ from the normal forms just described. Taking the cases in the same order as before, Figs.4.14 and 4.17 show the angular and translational velocities of subject D.B., the woman with an arthrotic left hip. The lower traces in Fig.4.14, the sagittal plane angular velocities, show some abnormalities. The stance phase velocity is almost constant on the left side, instead of having peaks at heel-strike and toe-off, showing that the knee is held in a flexed position throughout the stance phase, since the normal trough in this graph is due to knee extension in the mid-stance phase. The same graphs also show a particularly weak push-off on the left side. To compensate for the apparent shortening on the left side, due to the flexed knee, the right shank shows abnormally high coronal plane angular velocities as the right leg is swung around the shortened supporting member. Swing phase ratios are 0.62 on the left and 0.57 on the right. Both these values are within the normal range, although the left knee is somewhat stiffer than the right, probably because of muscular spasm.

The translational velocities show a flat-footed gait for both legs, with the feet placed carefully on the ground. The knee vertical velocity on the left side is particularly low-peaked, indicating a cautious flexion/extension movement of the left hip.

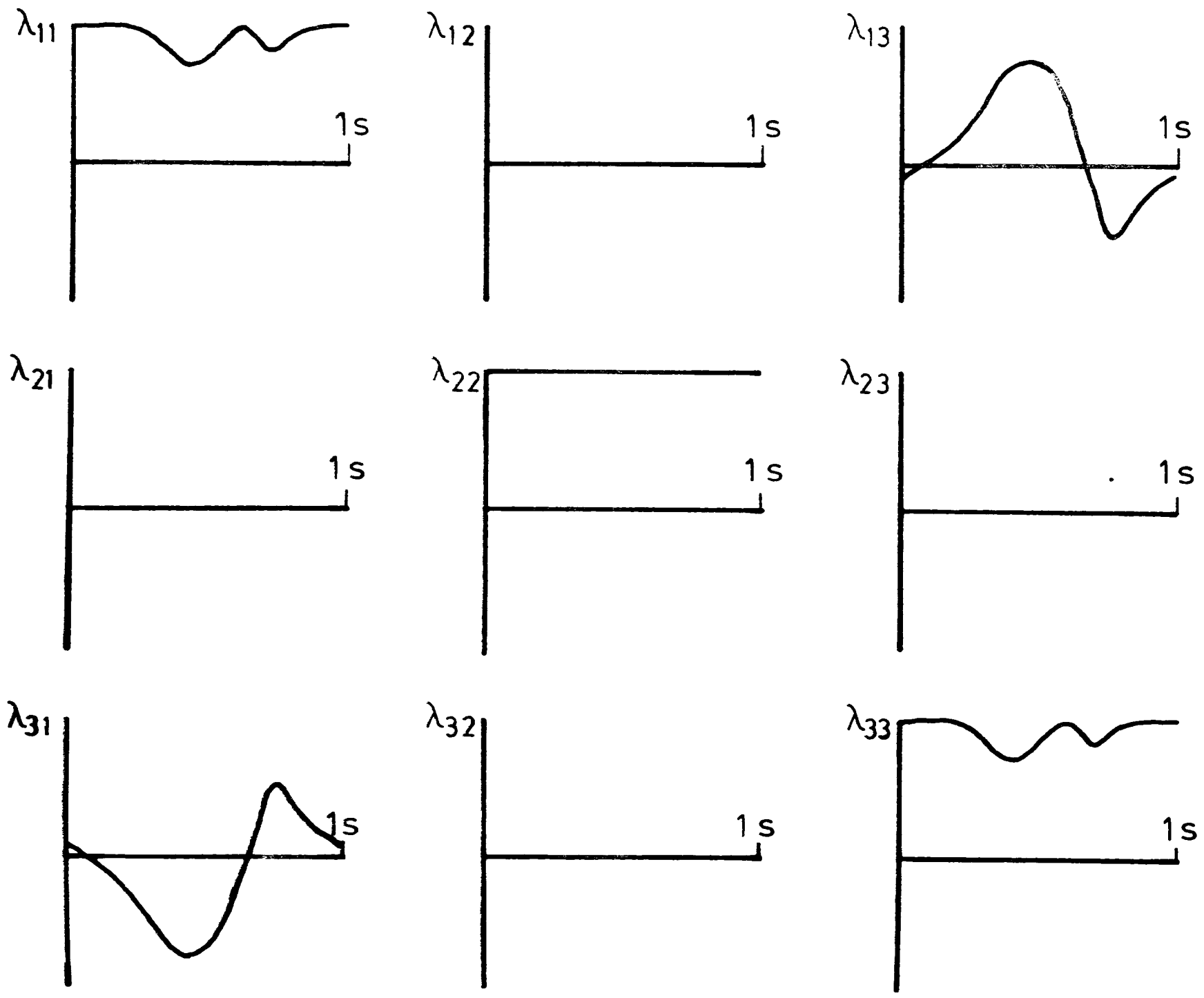
Subject G.F., the man with a left THR, recorded the angular and translational velocities shown in Figs.4.15 and 4.18. The sagittal plane angular velocities are obviously asymmetric and, once again, the most prominant feature is the large change in angular velocity on the left side which occurs at heel-strike.

The left shank is rotating at 4 rad/sec when the heel makes contact with the ground. The swing phase ratios are 0.45 on the left side and 0.55 on the right. This indicates that the left knee is flicked with considerable vigour. The translational velocities are almost normal except that the right ankle vertical velocity has only one positive peak. The second peak, which produces the forward rise of the foot, is missing.

Finally, Figs.4.16 and 4.19 show the velocities of the shank of subject G.P., the rheumatoid arthritic with envolved, but pain-free, knee joints. The rounded, symmetrical shape of the swing phase angular velocities suggests high values of the SPRs, 0.83 on the left and 0.95 on the right. These values indicate very stiff knee joints. The peak swing phase angular velocities are normal, but these peaks occur much earlier in the swing phase than is usual, probably before full hip flexion. The translational velocities in Fig.4.19 are quite normal except that, as in the last subject (G.F.), the vertical velocity of the left ankle has no second positive peak.

The examination of the velocity graphs of these three subjects shows how much information may be gleaned from this group of movement variables. The coronal plane angular velocity is not useful for comparison purposes, but the sagittal plane graph contains a great deal of interest. Of the translational velocity components, the ankle velocities in the a/p and vertical directions are the most distinctive and, indeed, the full significance of the information they hold may not yet have been realised.

Figure 4.20 Representative Normal Data Set



DIRECTION COSINES

4.5 Displacements

The graphs of displacement data embody all the assumptions and approximations made in the analysis whereas the calculated velocities and accelerations depend on only some of them. Displacement data is therefore the least reliable of all the presentations of a subject's gait. The most inaccurate assumptions are those made to determine the initial value of the transformation matrix of direction cosines. (viz.Chap 2, section 3). The errors introduced at this point are not primarily due to approximate analytical procedures, but to the fundamental dependence of the initial conditions on the zero points of the transducers. Errors in these initial conditions result in odd discrepancies such as an ankle which 'moves' while the foot is flat on the ground, or a knee having a lower net forward displacement in one step than the ankle to which it is attached. Nevertheless, there are some important features of gait which are easily seen from displacement graphs.

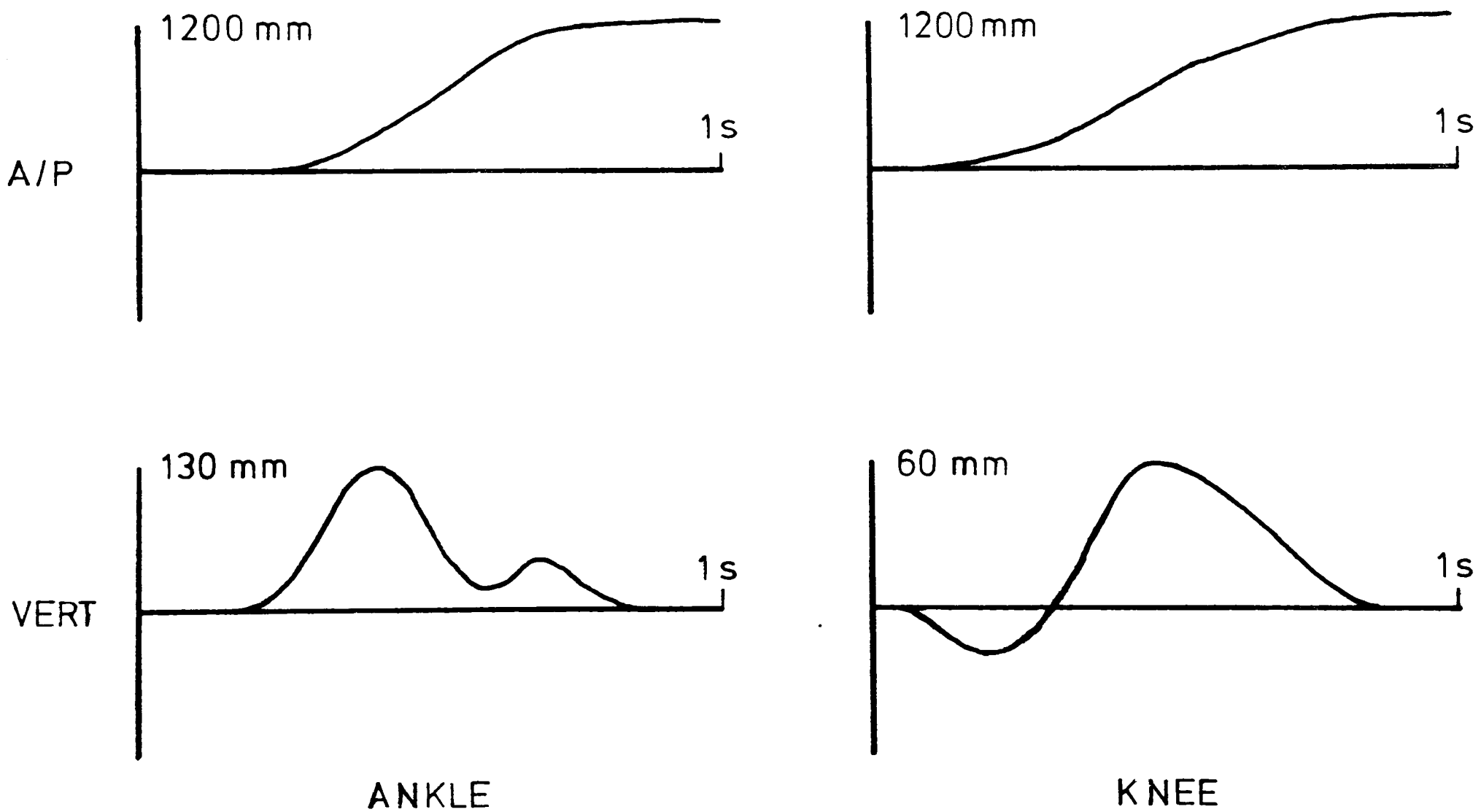
Fig.4.20 shows a typical set of direction cosines for one normal step. Four of the components of the matrix, λ_{12}, λ_{21}, λ_{23}, λ_{32}, are always zero and one, λ_{22}, is always equal to one because coronal plane angular velocity is near-zero and the transverse plane angular velocity is assumed to be zero. Since any element in the matrix is equal to its co-factor;

$$\lambda_{33} = (-1)^{3+3}(\lambda_{11}\lambda_{22} - \lambda_{12}\lambda_{21}) = \lambda_{11} \qquad 4.1$$

$$\lambda_{31} = (-1)^{3+1}(\lambda_{12}\lambda_{23} - \lambda_{13}\lambda_{22}) = -\lambda_{13} \qquad 4.2$$

The matrix is therefore skew-symmetric. λ_{11} and λ_{31} are the cosine and sine, respectively, of the angle which the shank major axis (3) makes with the vertical. λ_{31} is therefore a sufficient

Figure 4.21 Representative Normal Data Set



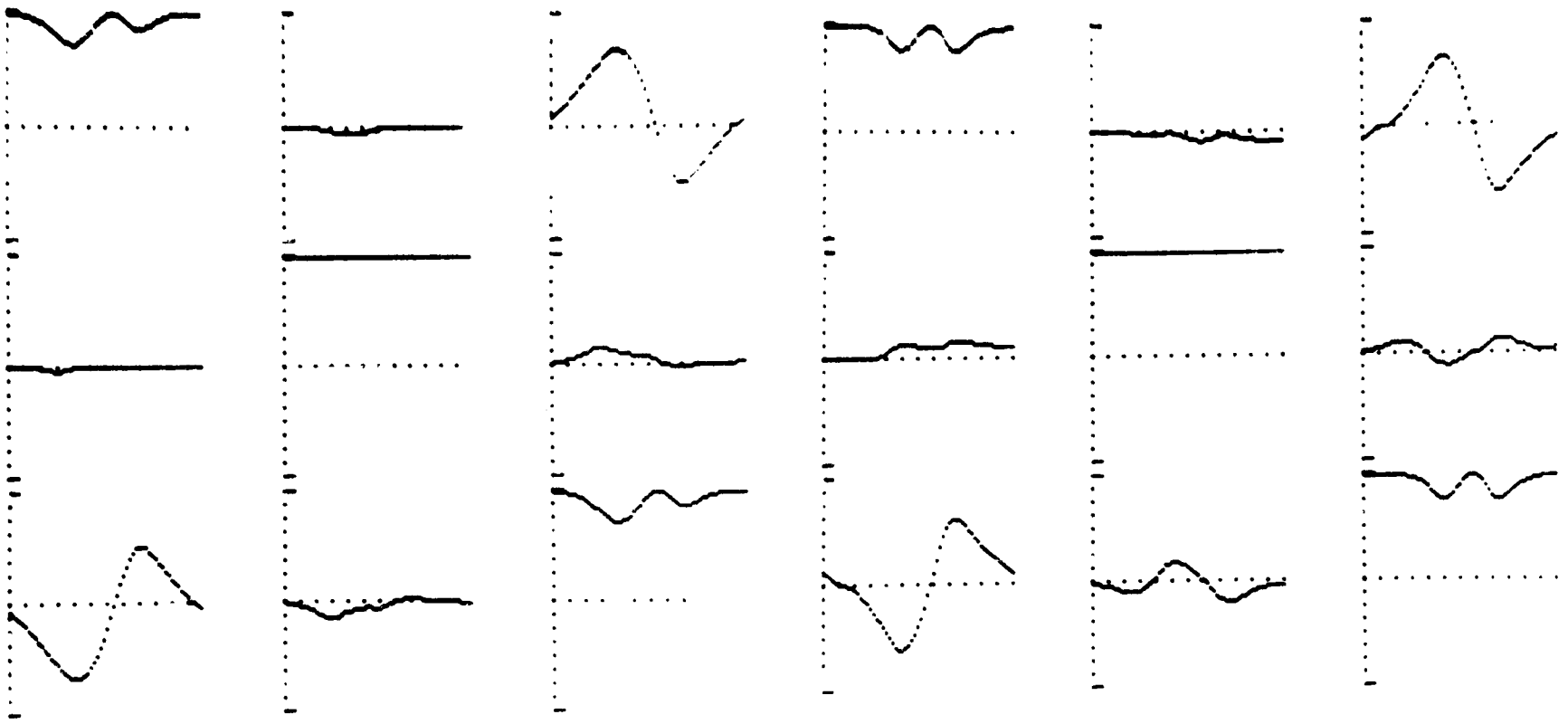
DISPLACEMENTS

characterisation of the whole matrix. The negative portion of the cycle may reach a peak of -0.7, (i.e. a backward swing of 45°) and the forward swing produces a peak of about 0.6 (35° forward). Heel-strike normally occurs at the positive peak.

Fig.4.21 shows the displacement functions which are the integrals of the graphs in Fig.4.13. These normal graphs may be compared with Figs.4.5,4.6 and 4.7, where displacement data from film records is shown. The knee begins to move forward before the ankle. The ankle displacement during the swing phase is a monotonic function with a steeper mean slope than the knee displacement. The knee displacement graph is also monotonic for the first two-thirds of the swing phase, but then decreases in slope and continues as a linear function to heel strike. The linear portion of the graph corresponds to the near-linear forward movement of the pelvis while the hip joint is held near maximum flexion. The vertical displacement of the ankle, is a double-peaked curve, with the first peak (backward swing) usually much larger than the second (forward swing), which may sometimes even be absent. The trough between the peaks shows the height above the ground of the foot in mid-swing. The knee first drops by 20-30 mm as the hip flexes through a neutral position. As the flexion continues to 30°, the knee moves up to 60 mm above the stance phase level.

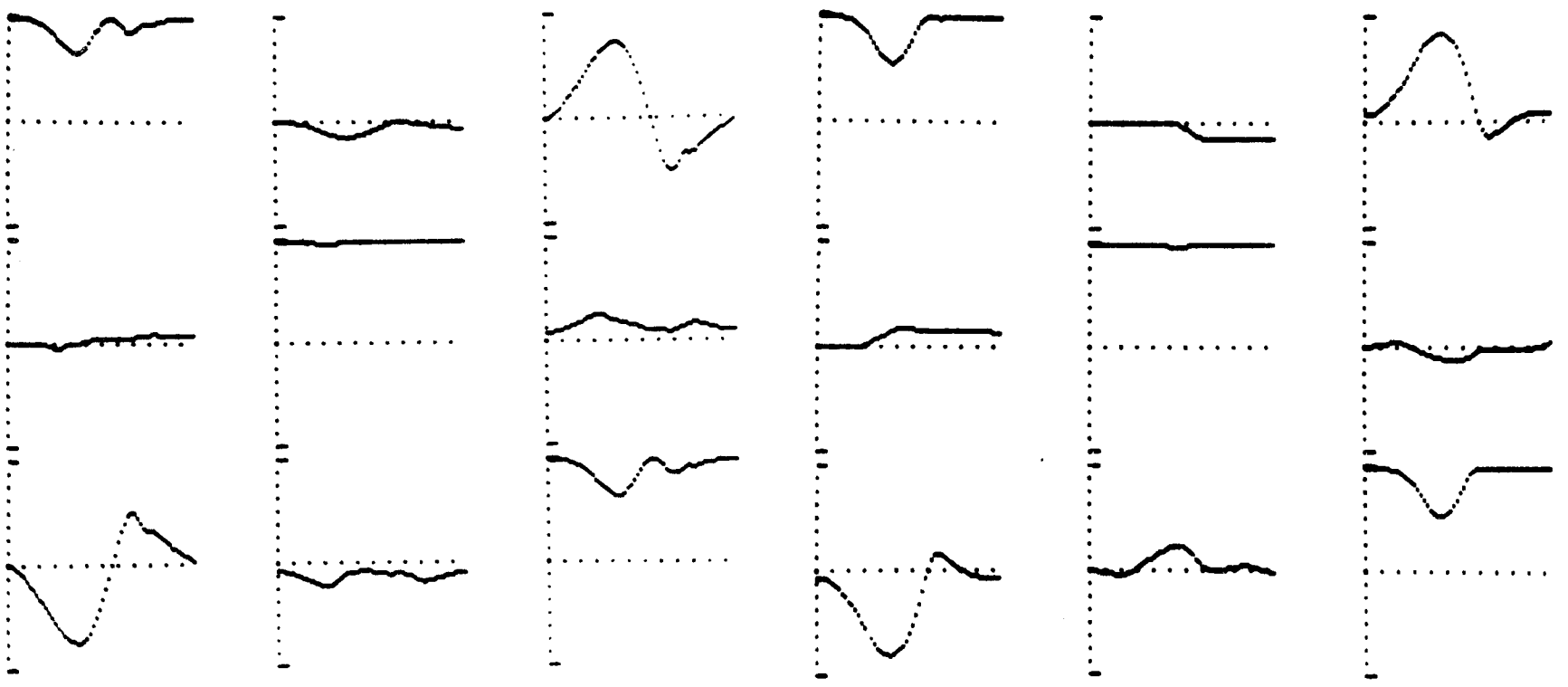
Subject D.B. shows a normal direction cosine matrix (Fig.4.22), and normal forward displacements of the knee and ankle (Fig.4.25),

Figure 4.22 (D.B.) Direction Cosines



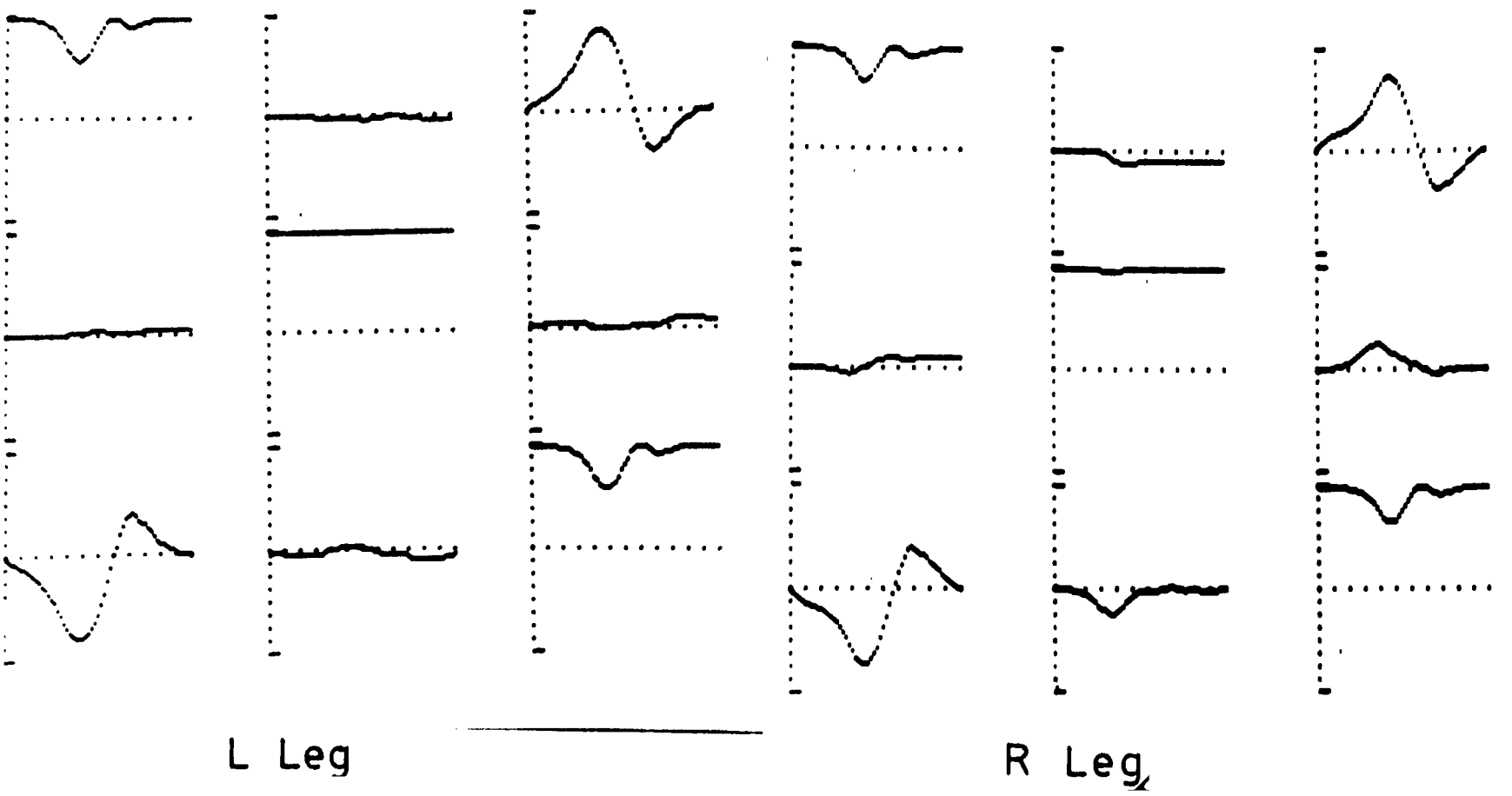
L Leg R Leg

Figure 4.23 (G.F.)



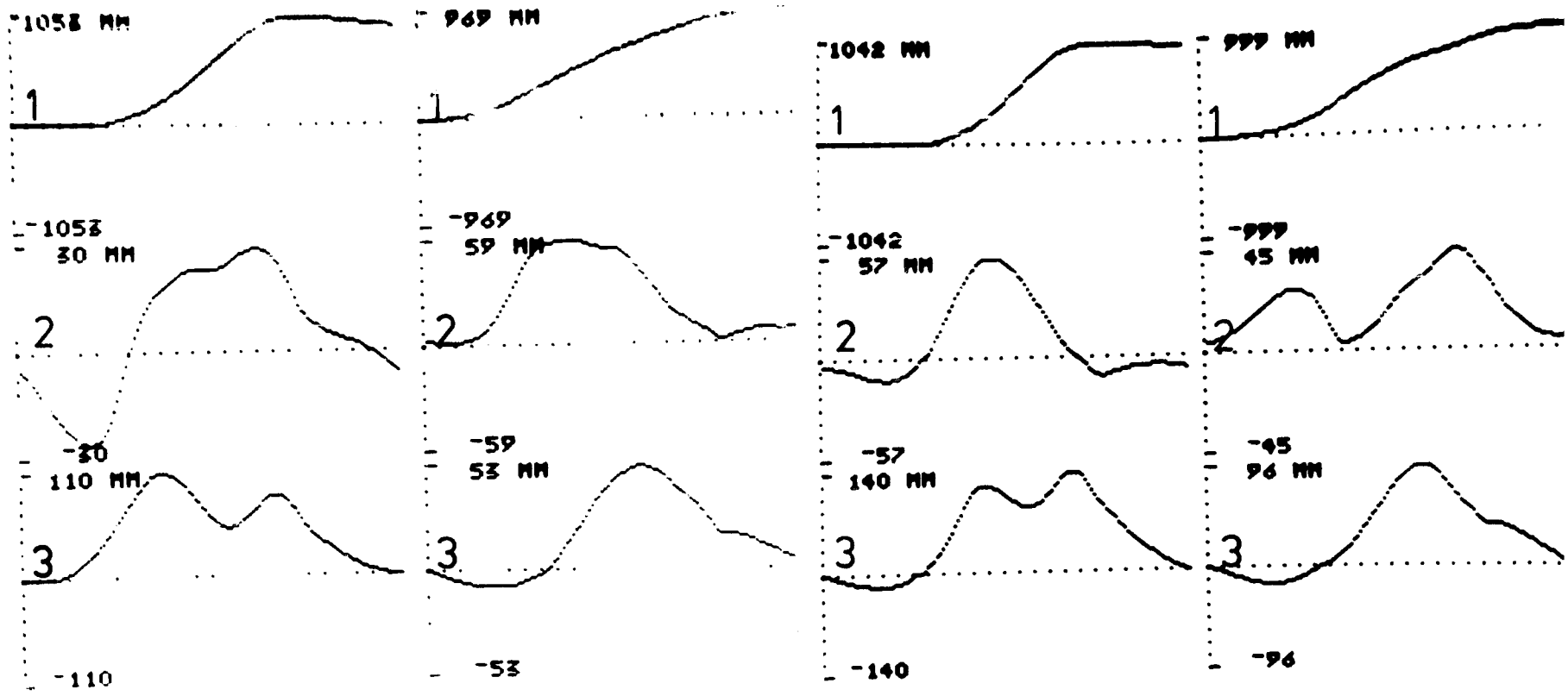
L Leg R Leg

Figure 4.24 (G.P.)



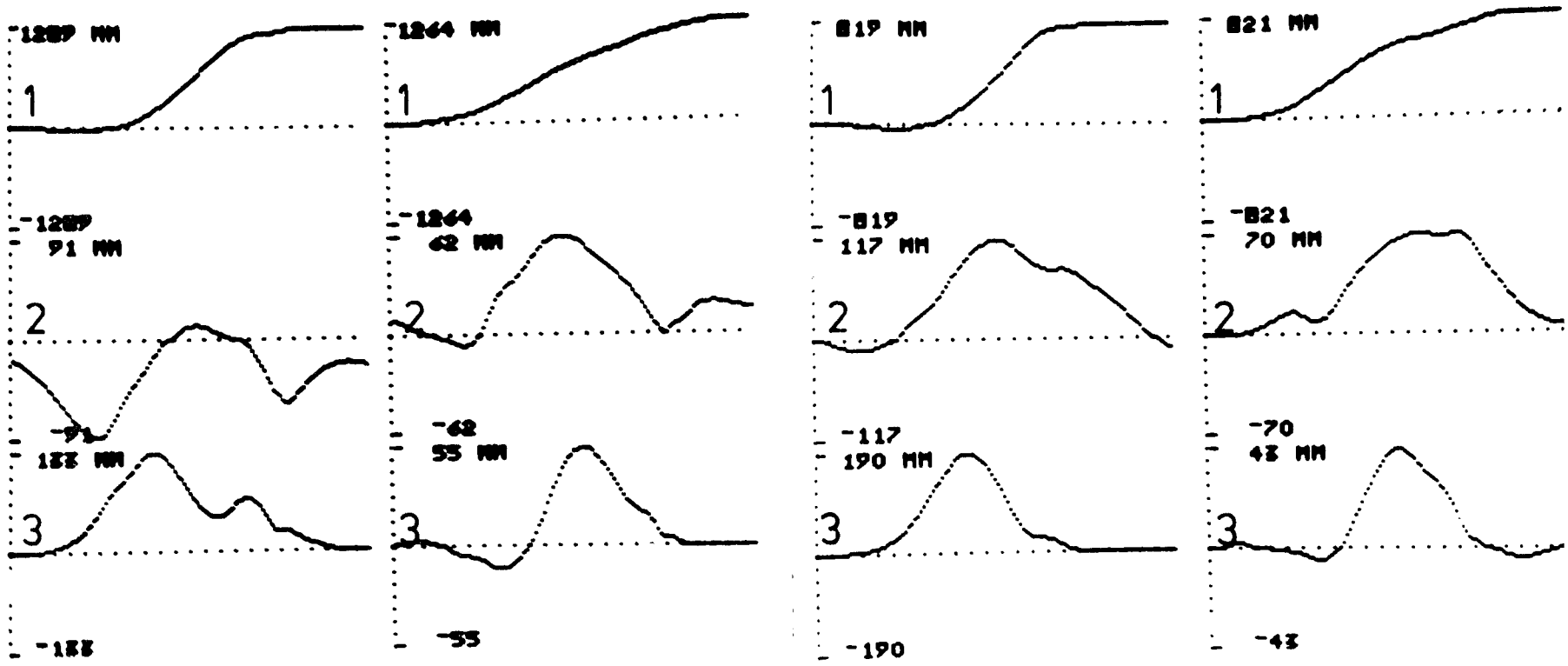
L Leg R Leg

Figure 4.25 (D.B.) Displacements



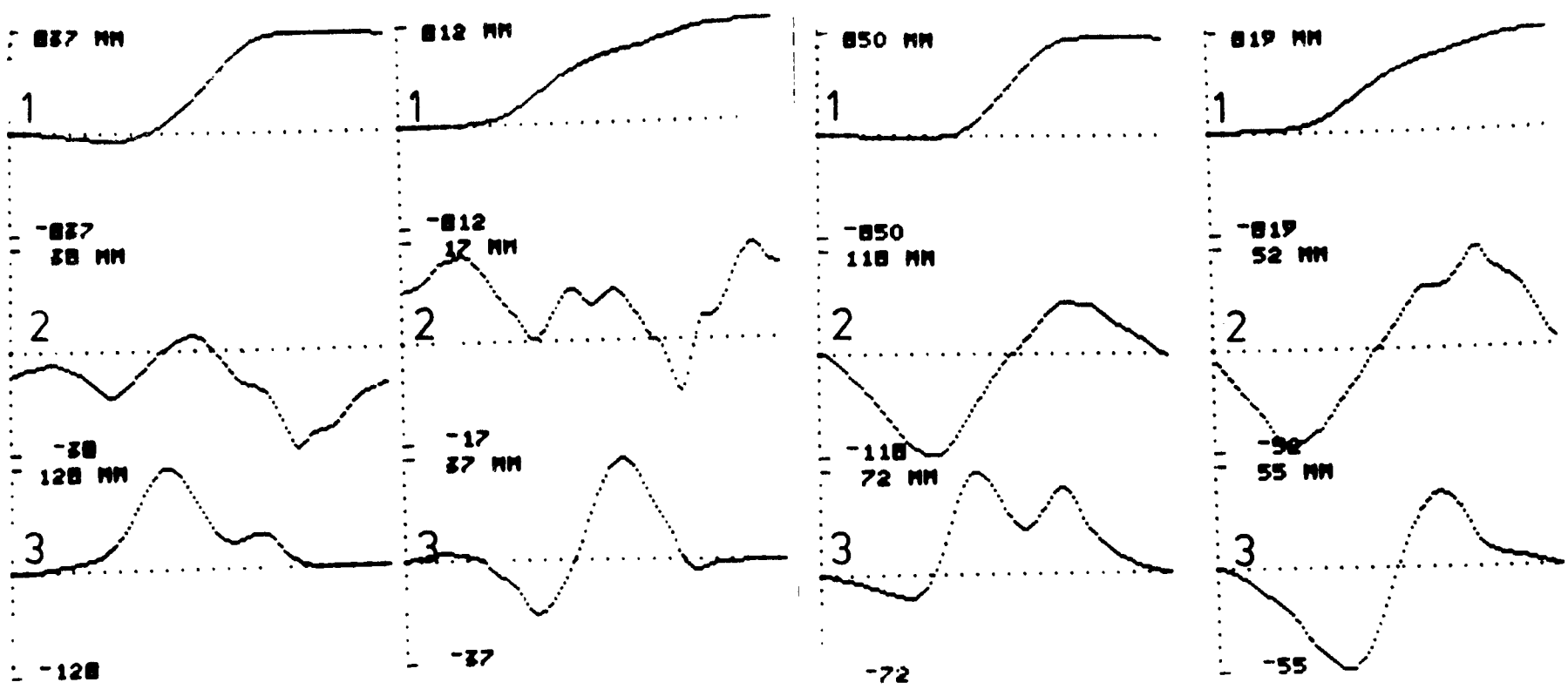
L Ankle L Knee R Ankle R Knee

Figure 4.26 (G.F.)



L Ankle L Knee R Ankle R Knee

Figure 4.27 (G.P.)



L Ankle L Knee R Ankle

but the vertical displacements of both joints are abnormal. Part of this abnormality may be due to an initial condition inaccuracy, as mentioned at the beginning of this section (the right ankle is shown to move 20 mm below its stance phase level), but the second peak of both ankle vertical displacements is markedly larger than normal. The gait is high-stepping. The knees move down very little in the initial swing phase and fall very slowly from their maximum heights. A possible explanation for this is that the subject walked with a flexion contracture of the hips, which may not ever have reached full extension. This is a normal occurrance for a painful osteoarthrotic hip, but what is more surprising is that it occurs bilaterally. The pelvis is rotated forward to prevent full extension of the painful left hip and remains in that position throughout the cycle, thereby preventing full extension of the pain-free right hip.

Subject G.F. (Fig.4.23) shows abnormalities and asymmetries even in the direction cosine matrix. The forward swing of the left leg may be seen to have begun decreasing (λ_{13} and λ_{31}) before heel strike occurs. The very small forward swing of the right leg is also obvious. The only obvious abnormality which may be seen in the ankle and knee displacement data (Fig.4.26) for this subject is the large difference in stride length (1300 mm compared with 800 mm). This could be due, either to a peculiarity of the particular step which was measured, or to errors in the determination of displacements. Since major abnormalities have already been shown to exist in the gait of

this subject, it is interesting to note that Fig.4.26 shows the data of the type which would have been obtained from film, before such data was differentiated. It would therefore seem likely that the high accelerations at heel strike would have been missed by that method.

Finally, Fig.4.24 shows normal direction cosine matrices for subject G.P.,and Fig.4.27 shows the corresponding displacement data for her knees and ankles. The graphs for the left leg are normal, although they indicate a very short pace (800 mm). The right leg displacements are also normal except for the vertical ankle graph which has an abnormally high second peak. However, as the ankle displacement drops during the stance phase, the abnormality is probably due to an initial condition error.

Fig. 4.28. A table indicating how the kinematic variables provide clinically relevant data.

Subject	D.B.	G.F.	G.P.
Ankle Acc. and Knee Acc.	a) High stepping gait b) Bilateral spasm c) Asymmetric gait relieving L side.	a) V.hard L heel-strike	-
Angular Vel.	d) Slightly stiff L knee e) L side apparent shortening due to stance phase flexion	b) Poor control L knee	a) V.stiff knees. R stiffer than L
Ankle Vel. and Knee Vel.	f) Flat-footed gait g) L hip has small range of movement.	c) Small or absent R leg forward swing	-
Direction Cosines	-	d) Abnormal L forward swing	-
Ankle Pos. and Knee Pos.	h) High stepping gait i) Bilateral hip flexion contractures	-	b) Short paces

4.6 Summary of Clinically Relevant Variables

The conclusions which have been drawn from considering all the available variables are summarised in the table in Fig.4.28.

The patients who were studied here in detail were chosen from the dozen, or so, with abnormal gait who have so far been measured, because they represent the major categories of subjects who will be assessed in the future. These comprise: patients with degenerative joint disease for whom surgery is planned, patients with joint disease for whom no surgery is planned, and patients who are rehabilitating after surgery. Clearly, detailed studies of this type are not a practical clinical proposition. This is not because the automatic analysis is time consuming. The measurements take approximately 10 minutes and the computer programs which produce the graphs take approximately 30 minutes, depending on the quality of the recorded data. The time consuming feature of the full assessment is the interpretation of the graphical results. This may take several hours.

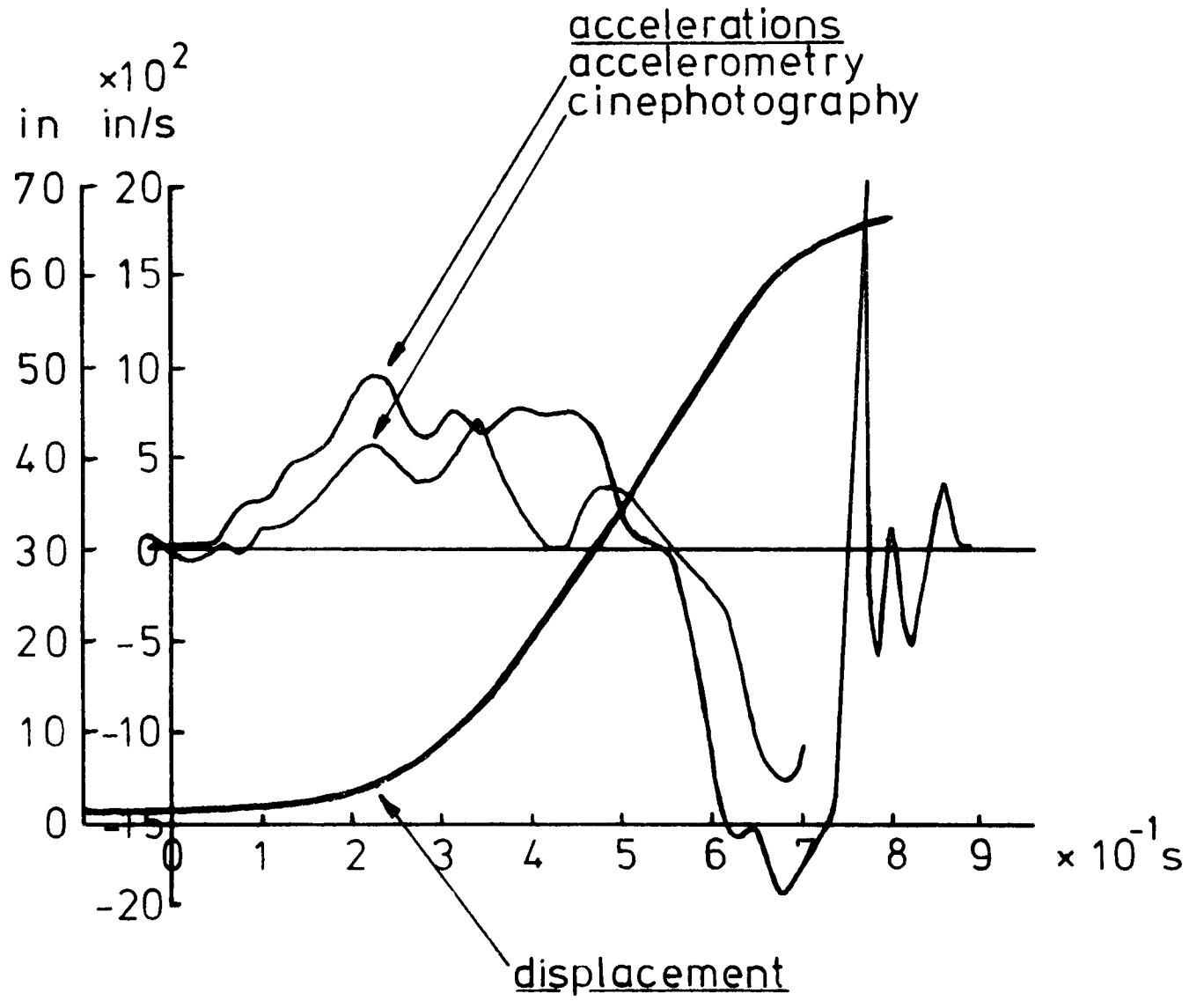
The clinical application of assessments of this type should use an abbreviated set of graphical results which can be interpreted more quickly, but which reveal most of the features of the subject's gait. The elimination of some of the graphical presentations to produce this shortened set is summarised as follows.

The information contained in the position graphs could be presented as mean stride length (1 number) and mean swing phase ankle heights (2 numbers). The direction-cosine graphs

could be left out altogether. Knee and ankle translational velocities could be rationalised from twelve graphs to four, namely bilateral ankle forward/backward and vertical velocities. The sagittal plane angular velocity graph, which analysis of many tens of paces has shown to be the most characteristic and repeatable feature of a subject's gait, must be retained and, from it, the Swing Phase Ratio may be calculated. The coronal plane graph could be left out. Finally, only the peak, heel-strike, ankle a/p and vertical accelerations need be kept, comprising a set of 4 numbers. This leaves a total of five graphs and 9 numbers per patient.

Although the routine clinical use of the system is not yet properly underway, it would seem perfectly feasible to present all this information on a single computer display record as an indication of the patient's progress during treatment.

Figure 4.29 Comparison of ankle anterior accelerations found by two methods (adapted from Paul)



4.7 Heel-Strike

A single published acceleration graph[19], obtained from cinephotographic measurement of the anterior displacement of the ankle, is shown in Fig.4.29 (after Paul). For comparison, an accelerometric graph of the same variable, from a different subject, but for approximately the same cadence and stride length, is also shown.

There are several interesting features in the comparison. There is a general agreement between the shapes of the graphs, although the direct method gives consistently higher values of acceleration. The most interesting feature, however, is that the highest accelerations occur at heel-strike, at a point where the displacement data cannot be relied upon to give sensible results. It may be noted that no estimates are made of the acceleration after a time just prior to heel-strike. The displacements thereafter are so small, being comparable with the errors of measurement, that such estimates would be almost meaningless. This demonstrates a major advantage of direct acceleration measurement, namely that displacement measurements give the least reliable results at the very point where the dynamic components are greatest.

It is now possible to quantify the connection between the magnitude of the peak ankle acceleration at heel-strike and the type of footwear worn by the subject. In bare feet, the peak accelerations are low, in the range 2 - 3g. Although the heel of the foot is relatively stiff by comparison with some shoe-sole materials, the painful consequence of applying high dynamic forces through a small area of the heel is presumably

the main limiting factor. In light footwear with rubber soles, the accelerations are of the order of 4 - 5g. With heavy, stiff footwear on a hard floor, the acceleration of the ankle at heel-strike in normal gait can be 8 - 10g.

Since the energy absorbed in an elastic collision is the integral of force over distance, the energy absorbed by a highly elastic rubber heel with a low peak acceleration will not differ greatly from the energy absorbed by a stiff, steel heel which produces high peaks of acceleration.

The exception to this observed direct relationship between ankle heel-strike acceleration and heel stiffness is the bare-foot case. It was stated in section 1.4 that the role of mechanical factors in the aetiology of degenerative joint disease has not been clearly established. However, it is well known that members of population groups which use little or no footwear are almost completely free from degenerative joint disease. The low acceleration of the ankle at heel-strike is the only mechanical phenomenon in the gait of a subject with bare feet which indicates that joint loading may be lower in this case than in the case of a subject wearing shoes. There seems to be a real possibility that footwear saves the feet at the expense of the joints.

CHAPTER 5

THE TAPE RECORDER

5.1 Introduction

5.2 Possible Recording Systems

5.3 The MRC/Oxford Instruments Tape Recording System

5.4 Duplexing Pulse Width Modulation Coding

5.5 Decommutation and Decoding

5.6 Future systems (the Resistance-Ratio Controlled Oscillator)

5.1 Introduction

This chapter is quite separate in content from those which have preceded it. It contains a general description of a portable tape recording system which would be suitable for use with the accelerometers. A new method of recording eight separate signals on a four track recorder is explained. Other possible ways of recording data from potentiometric transducers are examined in the final section.

5.2 Possible Recording Systems

The initial specification of this project[48] described a telemetry system which would be used to transmit data from the accelerometers to a fixed recording station. The system would have used conventional FM/FM multiplexing techniques with each transducer controlling the frequency of a sub-carrier oscillator. The outputs from a number of oscillators were to be added together and used to frequency-modulate a radio-frequency carrier. Initial experiments were performed using a variable inductance accelerometer* to modulate the frequency of a resonance oscillator. However, a major problem with a telemetry system of this kind is the Post Office regulation on the power of telemetry r.f. transmitters which was apparently formulated in order to meet the requirements of the operators of radio-controlled model aircraft etc. The electromagnetic environment of the open countryside in which these models are normally used is quite different from that existing in a typical modern hospital. Personnel'bleep' systems, X-ray machines, floor-polishers, diathermy machines and a host of other transmitters crowd the e.m. spectrum. Other researchers, in personal communications (most notably Wolff), advised strongly against the use of radio-telemetry monitoring of a widely-moving subject in a hospital environment. Another difficulty with radio telemetry is the high cost of commercial systems. Because of the difficulties that mobile patient monitoring had presented in the past, the M.R.C. were supporting (1970) the development of a portable tape-recording system for use, initially, in the long-

---

* Electromechanisms Type MEM

Figure 5.1 The M.R.C./Oxford Instruments Cassette Recorder

The size of the recorder is shown in relation to the tape cassette mounted on it. Current production models of this machine (now designated MATR : Miniature Analogue Tape Recorder) have a different appearance but are of approximately the same size.



term monitoring of e.c.gs. (Fig.5.1). The project, at the Churchill Hospital, Oxford under the direction of Dr.F.D.Stott, had reached the stage where a prototype recorder was about to be presented to a manufacturer, with a view to commercial production. It was decided to modify a recorder of this type to record signals from the accelerometers. The recording system, as designed by Dr.Stott, is described below, since it has not been described elsewhere.

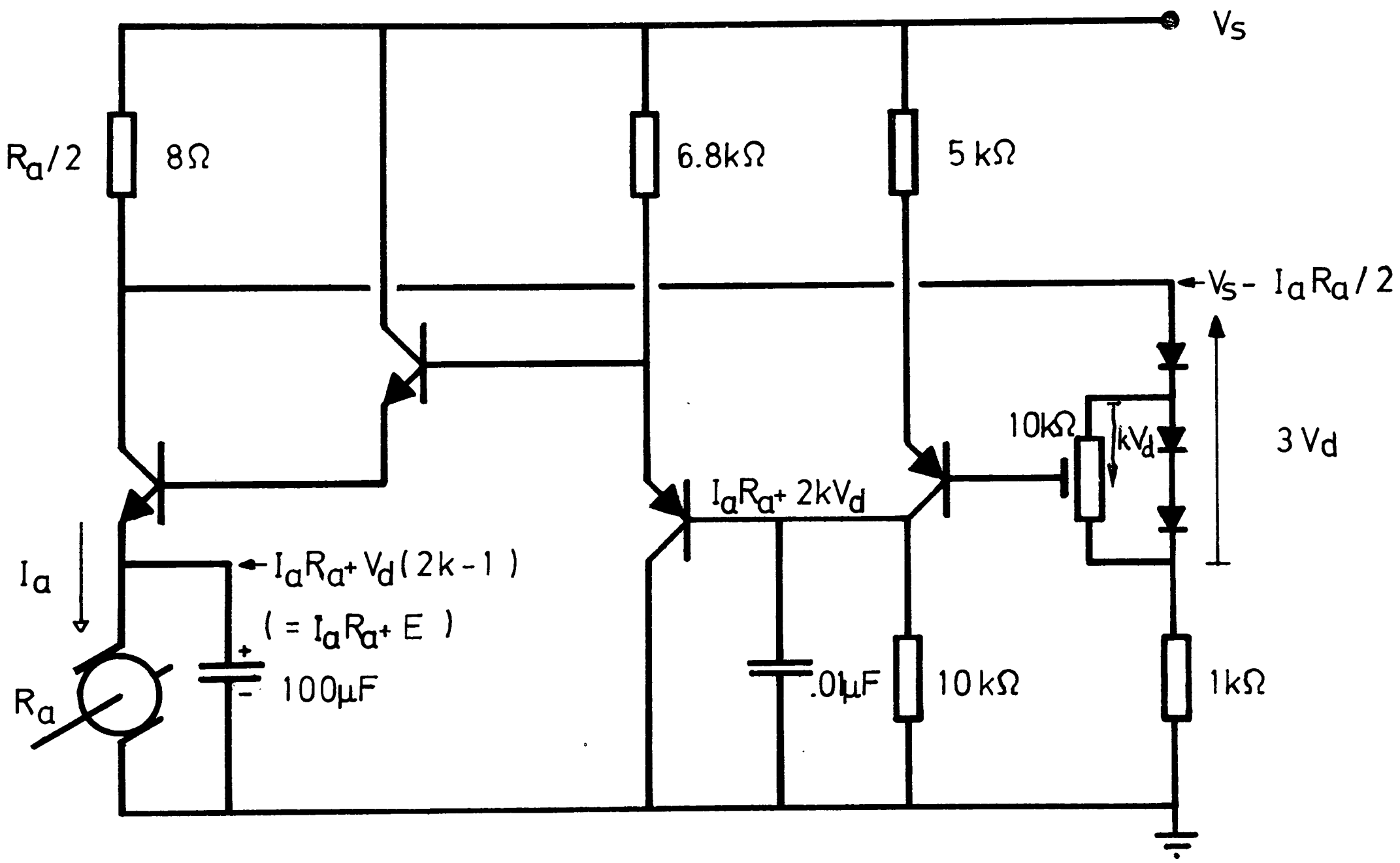
5.3 The MRC/Oxford Instruments Tape Recording System [49]

The recording system is based on the Philips Cassette. Magnetic tape, of width 6.3 mm, is wound from one spindle to another within a flat, rectangular package, passing between spindles, via pulleys, along one edge of the cassette which is cut away to allow access to the tape. The tape is wound with the magnetic coating outermost, so that a recording head may be pressed against this coating from outside the cassette. A felt pressure-pad, built into the cassette and spring-loaded by a variety of methods which differ from one manufacturer to another, keeps the tape in intimate contact with the head. In addition, holes are provided in the cassette casing to allow a drive-capstan to be sited on the uncoated, inner side of the tape. A pinch-wheel squeezes the tape against this capstan so that the tape can be driven at a constant speed.

By comparison with instrumentation tape-transport systems, the cassette system is crude. There is poor control of tape tension and the tape may be fed to the tape head guides at a considerable angle. But in terms of size and convenience, the system has no current rival. Small 'micro-cassettes' have recently become available for use in pocket dictation machines, but were not considered to be suitable for the present purpose because they are not provided with capstan holes. The tape speed is therefore a function the quantity of tape on the take-up spindle. The speed characteristics are understandably poor.

Since four-track heads of suitable quality were not available commercially, these were manufactured specially to meet the requirements of the recorder. These heads proved unsuitable for

Figure 5.2



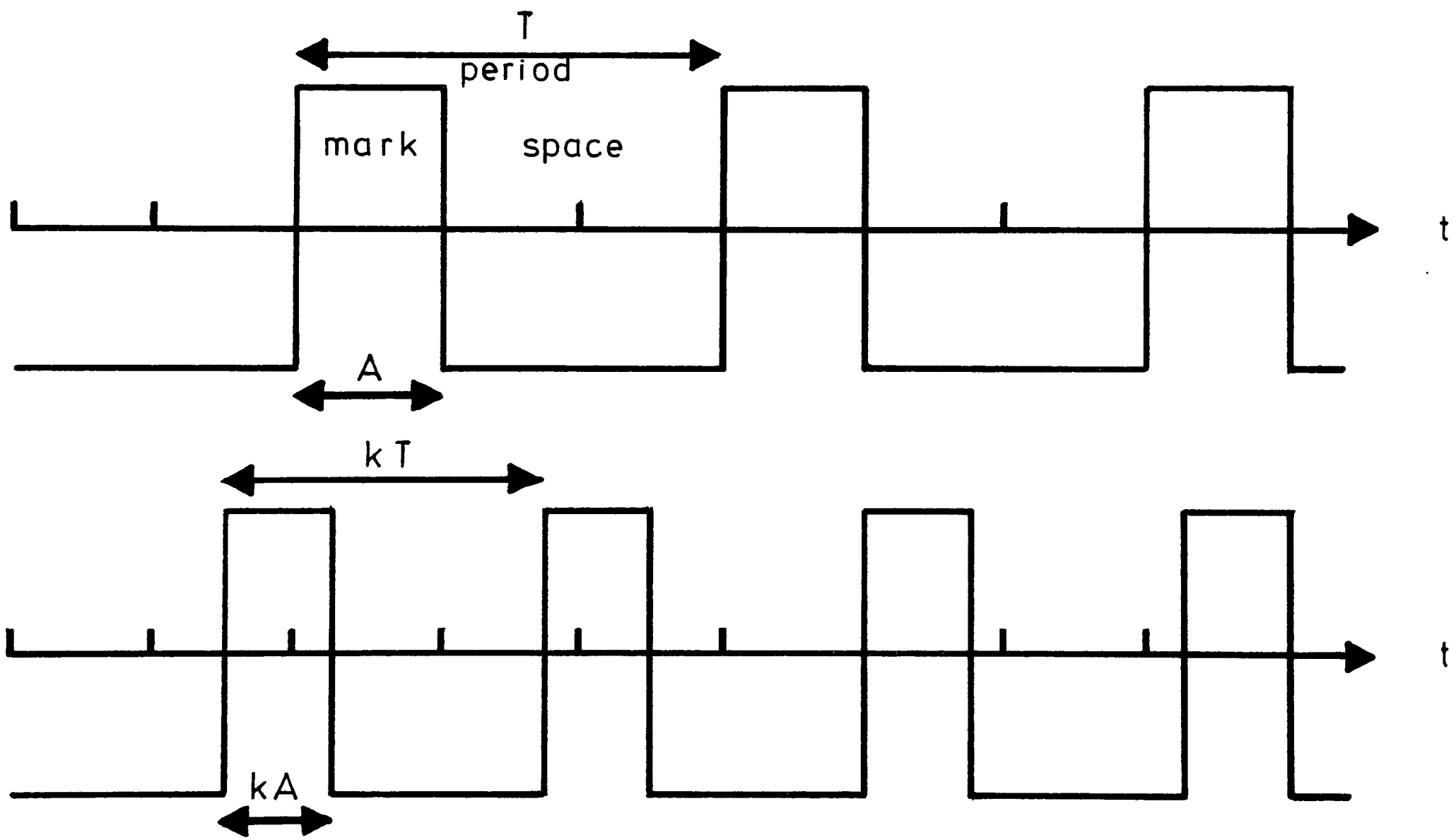
SERVO MOTOR SPEED CONTROL

the modified recorder which was to be used with the accelero-meters for reasons which will be described later, in section 5.6.

The capstan which drives the tape is itself driven by a worm-reduction gearbox which, in turn, is driven by a spur-gearbox stepping-down a small d.c. motor. This motor is driven by the speed-control circuit shown in Fig.5.2. The operation of this novel circuit, apparent from the voltages indicated on the schematic diagram, is independent of supply voltage and motor load within a fairly wide range. However, the current spikes which this controller produces on a battery supply are consider-able, and the resulting voltage variations make the motor power supply unsuitable for powering transducers. The take-up spool is driven by a slipping clutch with a p.t.f.e./brass plate inter-face. The torque provided by this clutch is limited by sliding friction so that a reasonably constant take-up tension is provided in the tape. The feed tension, which is applied through the tape to the recording head, is provided simply by the friction in the feed spindle and pulley of the cassette. As a result, this tension is far from constant.

As is mentioned above, the original recorder was conceived as a monitoring device of long term e.c.gs., and in order to allow the cassette to last up to 24 hrs., a tape speed of 2 mm per second was used. With a packing density of 400 sine-waves per mm for standard thickness recording tape, a recorded signal bandwidth of 800 Hz was anticipated. The modulation system chosen was mark/period ratio, pulse-width modulation (PWM). As is shown in Fig.5.3, the signal, encoded as the ratio A/T, is

Figure 5.3



MARK / PERIOD RATIO
CODING

independent of timebase variations which are slow by comparison with the cycle period, T. If the timebase changes by a factor k, then the durations A and T are both multiplied by k, and the ratio kA/kT is equal to A/T. Variations of tape speed, may be due, for instance, to poor compensation by the speed controller for a lowering of battery voltage with time. A resulting distortion of the time-base is proportional to the speed variation, but the signal amplitude is unaffected.

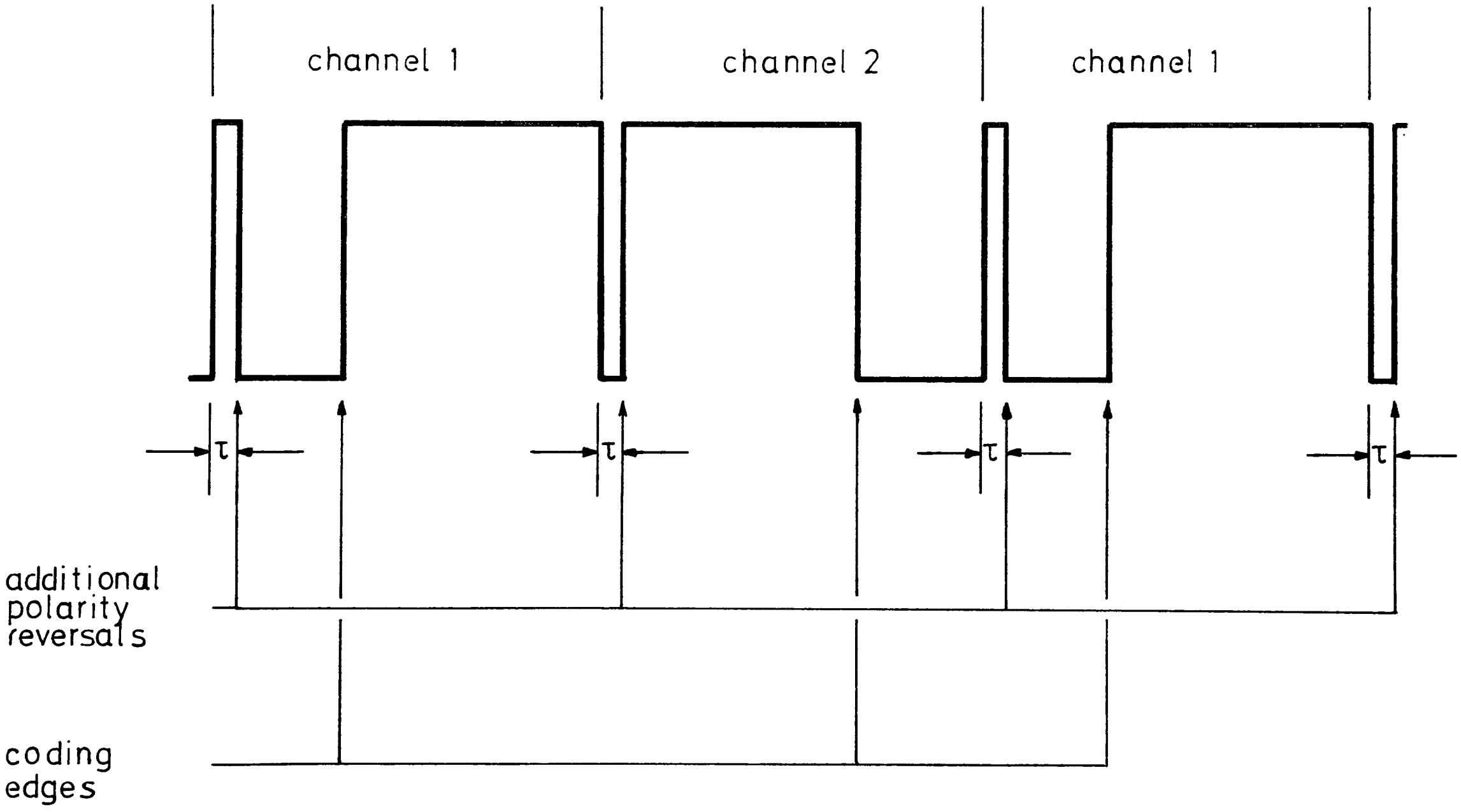
Since the voltage induced in a tape playback head is proportional to the rate of change of flux in the magnetic circuit of that head, recorded magnetisations of the tape at frequencies tending to zero produce little or no output. For this reason, the direct recording process has a lower frequency limit. PWM, however, records steady-state signals. With a recorded signal bandwidth of 800 Hz, it was found possible to record a square-wave carrier of approx. 40 Hz and obtain edges steep enough to measure their relative timing on playback. This is equivalent to a sampling rate of 40 samples/second, and according to the Sampling Theorem, it should be possible to encode a signal of up to 20 Hz on such a carrier. As in all communications systems, this ideal cannot be achieved, but it was found that signals up to 15 Hz could be encoded and decoded. This was considered adequate for e.c.g. recordings.

The decoding of a mark/period ratio signal is very simple. If the amplitude of such a signal is constant, the mean level of the signal is proportional to the mark/period ratio. Decoding is achieved by passing the signal through a low-pass filter which will pass the encoded signal baseband, while attenuating

the carrier.

The recording system, described above, was adapted to record the signals from the accelerometers. The basic system is now (1973) in commercial production but, at the time at which the work was done, it was necessary to assemble the recorder and playback unit using parts copied from a pre-production prototype.

Figure 5.4



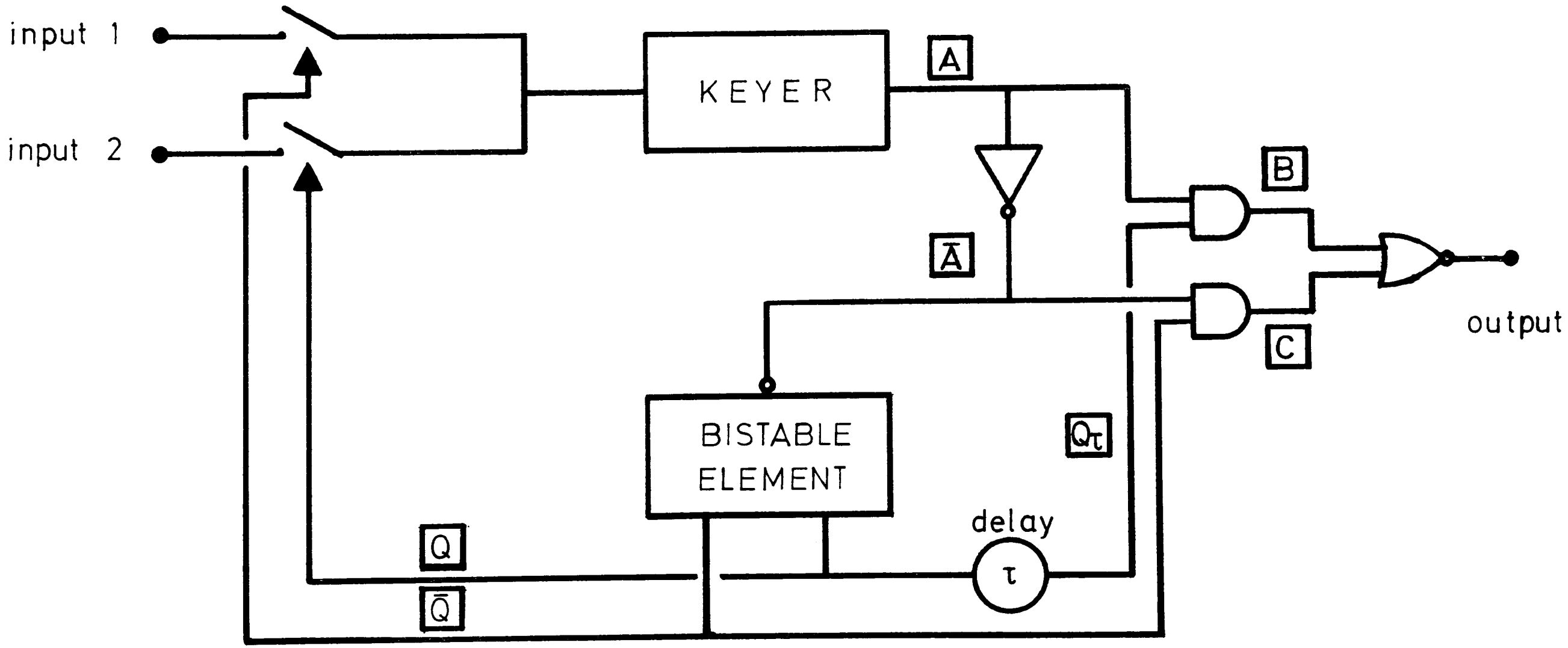
DUPLEXED M/P RATIO SIGNAL

5.4 Duplexing Pulse Width Modulation Coding

It was estimated from the accelerographic data of Gage[25] that a signal bandwidth of approximately 50 Hz was required for the recording of accelerometric data from the shank. In order to perform a full analysis of the movement of the shank, recorded signals from six accelerometers are required. Clearly, the basic tape recorder described in the previous section would need both greater bandwidth, from higher tape speeds, and some form of multiplexing in order to record more than one channel/track. One possible form of duplexing was to keep the mark/period modulation for one channel and modulate the carrier frequency itself with another channel. However, since the basic encoded signal is in digital form, time-division multiplexing seemed more appropriate. Conventionally this involves allocating consecutive samples to different channels and marking the end of a set of channel samples by a synchronization period. It seemed wasteful of tape-time to provide a separate synchronizing period for only two channels, because up to one third of all tape-time would be used solely for synchronizing purposes. Some other way of separating one duplexed channel from another was needed.

A method of channel recognition was devised as follows. Shortly after the pulse edge which marks the beginning of each channel period in the encoded signal, the polarity of the signal is reversed. This reversal results in a signal such as that shown in Fig.5.4. The difference between the two channels is clear in that the period for channel 1 begins with a positive edge, contains its information in the relative position within

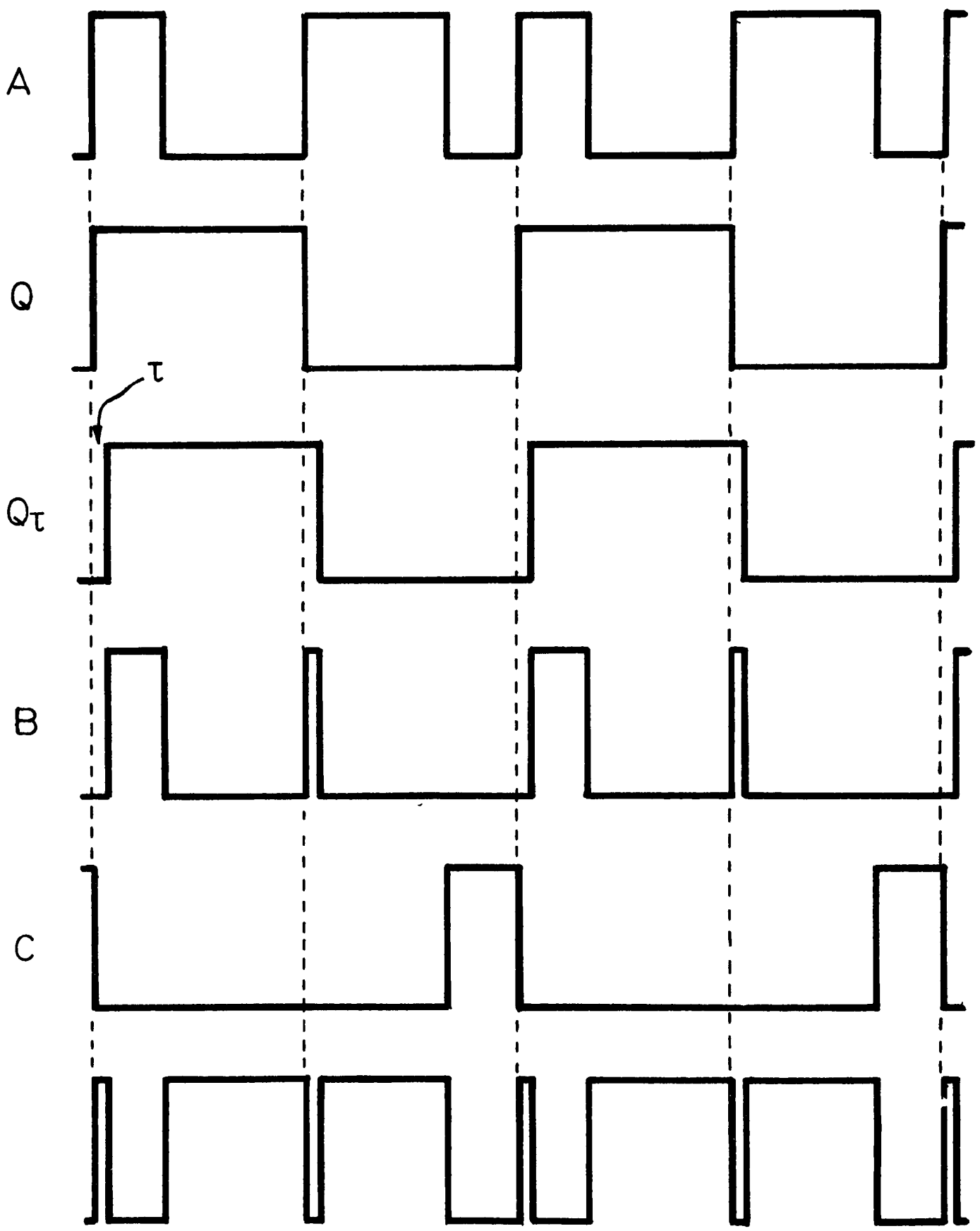
Figure 5.5



DUPLEXER

Figure 5.6

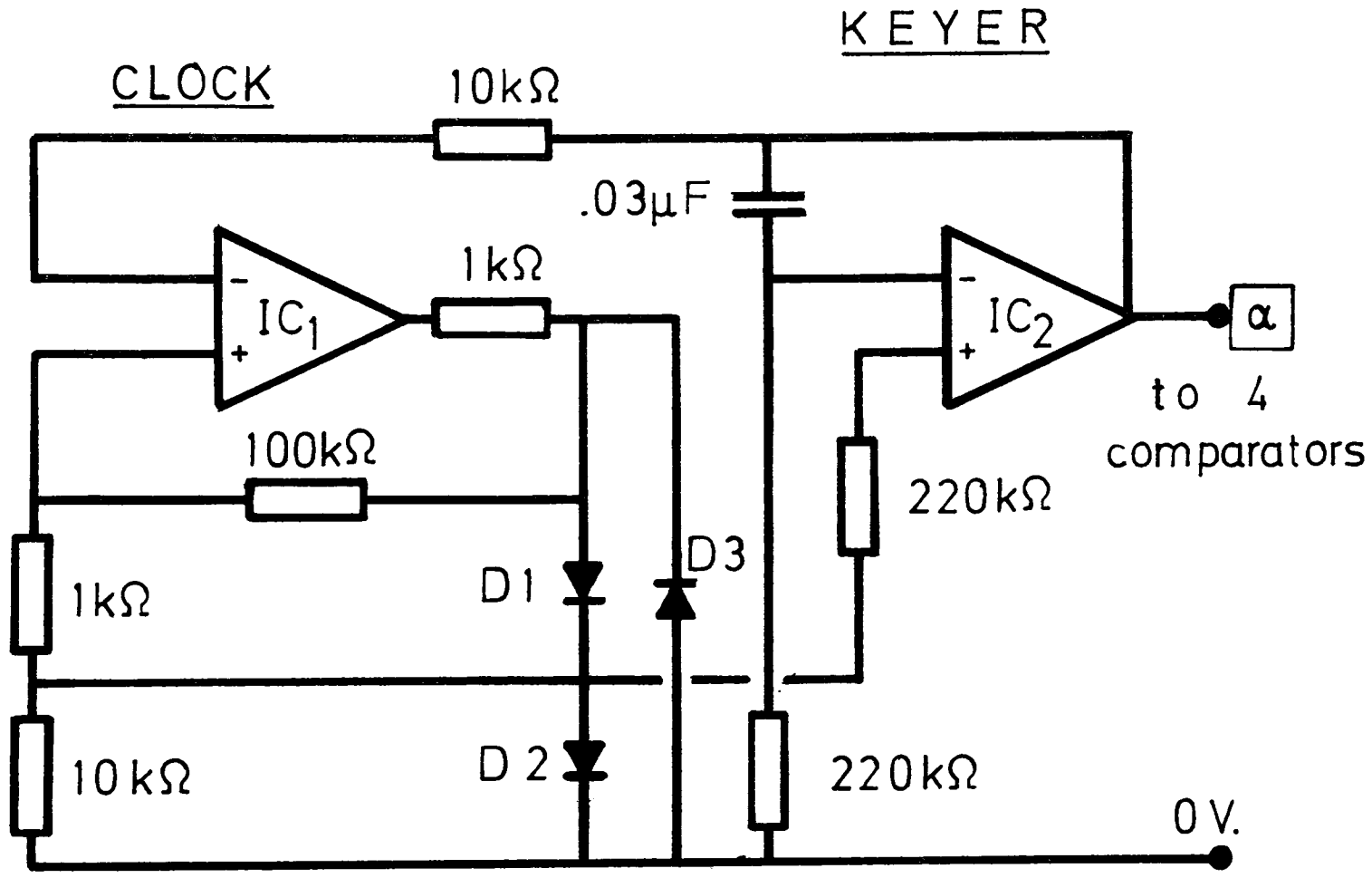
DUPLEXER WAVEFORMS

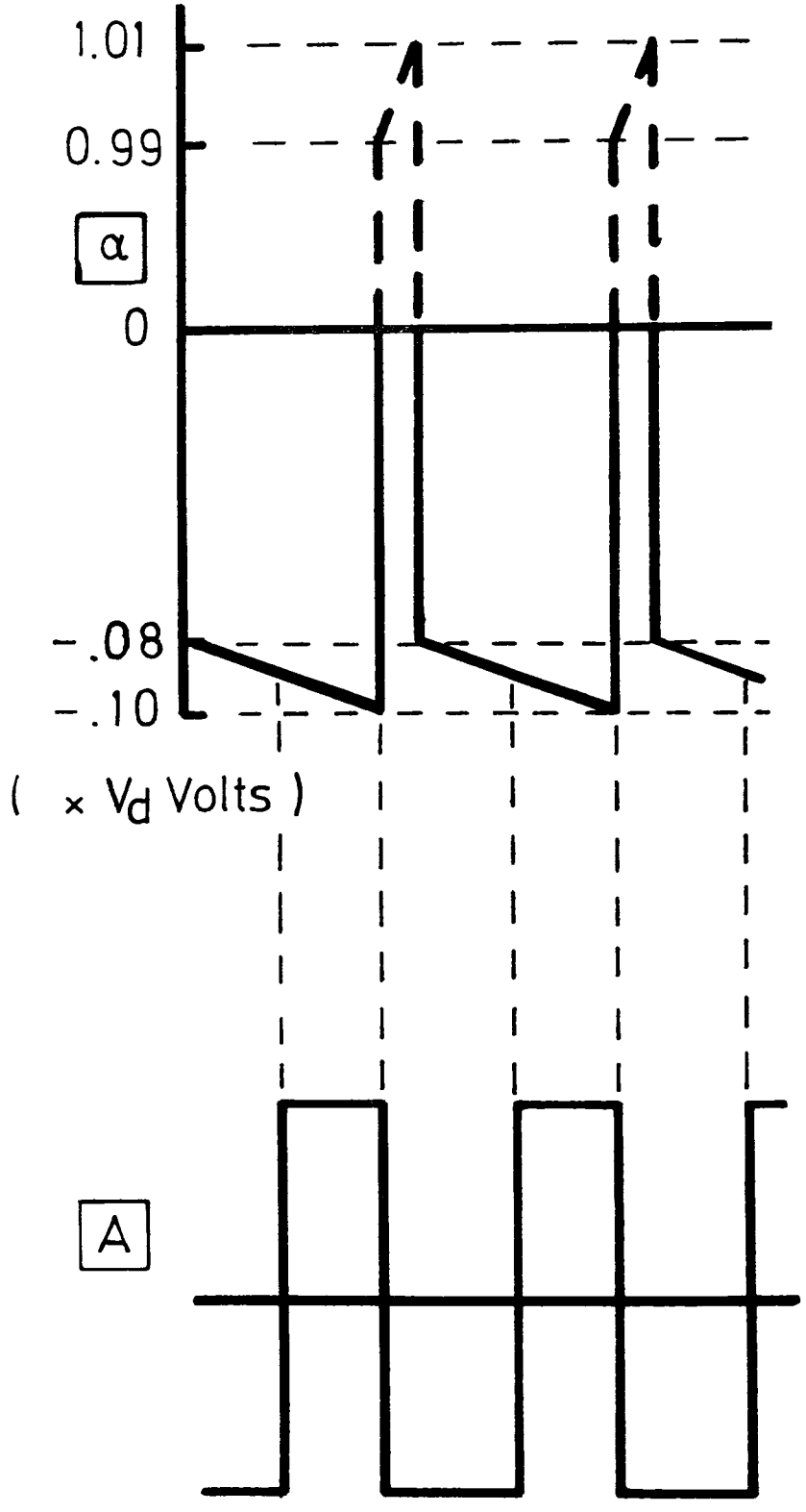


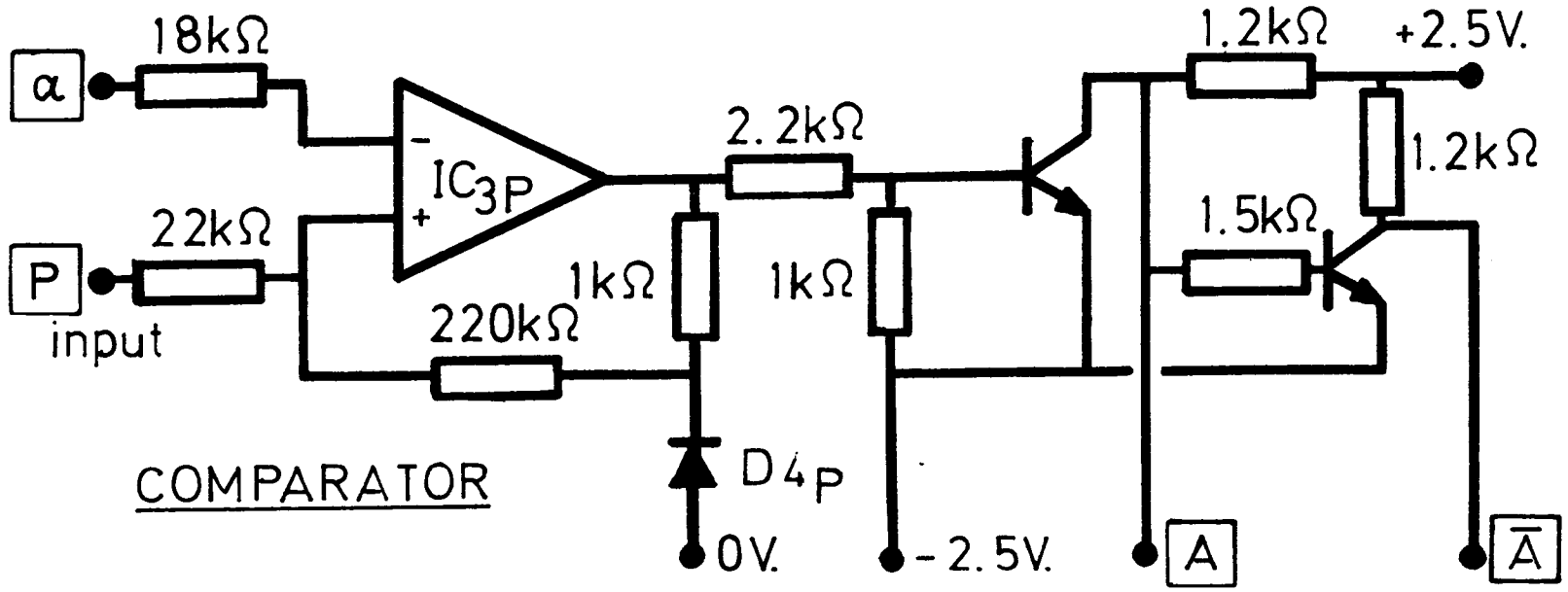
the period of a positive edge, and ends with a negative edge. Exactly the reverse is true for channel 2. The extra edges caused by the polarity changes contain no information and are made to occur as soon after the beginning of the channel period as possible, given the frequency response of the recording medium. This maximises the usable range of modulation.

The circuit which will produce such an encoded output from two analogue voltage inputs is shown in Fig.5.5 in block format, with the signal waveforms from various points in the circuit shown in Fig.5.6. The two data channel inputs, 1 and 2, are switched alternately to the keyer input by the two analogue gates. These gates are driven by a bistable element and are always in complementary states. Whichever channel is currently being encoded, the keyer output, A, will begin a channel period with a positive edge, change state at some point during the period, and commence the next period with a further positive edge. The channel periods can be made to alternate between channels 1 and 2 by driving the negative-edge triggered bistable element with $\bar{A}$, the inversion of A. The system, thus far, is no different from a standard form of time-division duplexing system, with the exception of the absence of a synchronizing period. One of the outputs of the bistable element, in this case Q , is delayed by a time, τ , equal to that required between the beginning of a channel period and the extra signal reversal. The delayed signal, Q_τ , is then combined logically, with A to produce $B = A \circ Q_\tau$. $\bar{A}$ is similarly combined with $\bar{Q}$ to produce $C = \bar{A} \circ \bar{Q}$. When the result of a logical OR operation B and C is derived, it is found, after inversion, to

Figure 5.7


KEYER
CLOCK
10kΩ
.03μF
1kΩ
IC1
IC2
α
to 4
comparators
100kΩ
220kΩ
1kΩ
D1
D3
D2
10kΩ
220kΩ
0V.


1.01
0.99
α
0
-.08
-.10
(× Vd Volts)
A

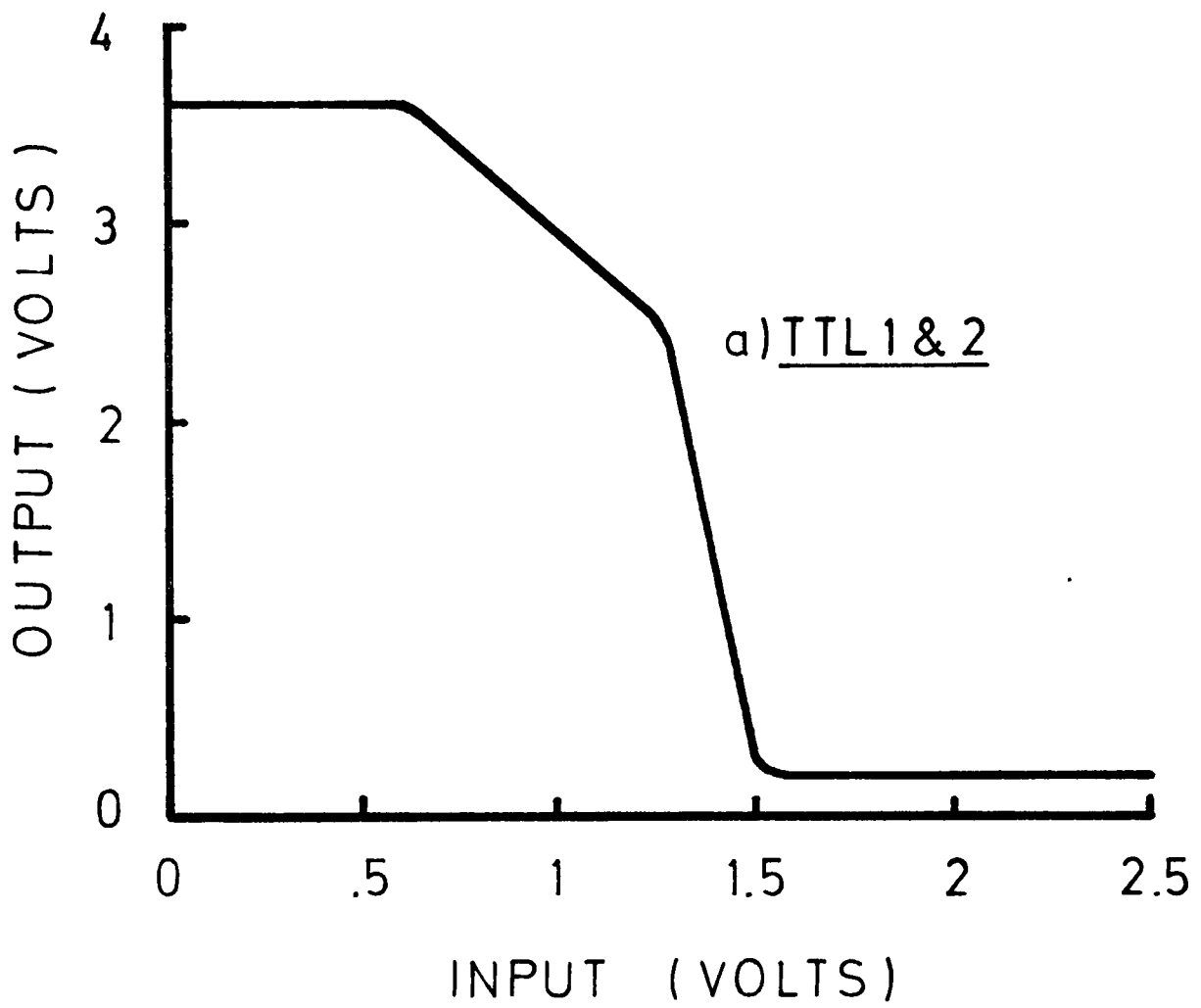

18kΩ
α
IC3P
2.2kΩ
1.2kΩ
+2.5V.
1.2kΩ
22kΩ
P
input
1kΩ
1kΩ
1.5kΩ
220kΩ
D4P
0V.
-2.5V.
A
Ā
COMPARATOR

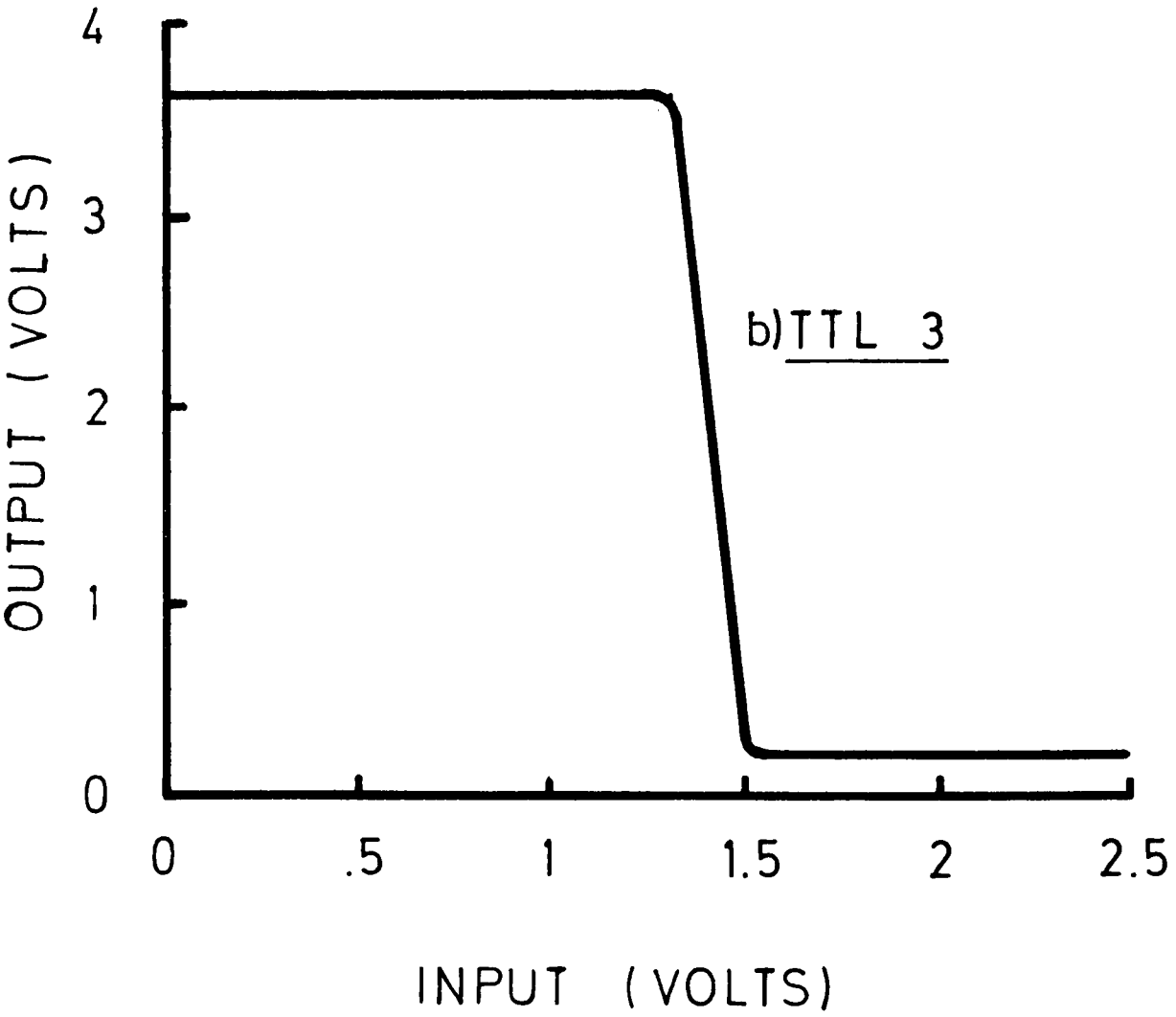
be the signal shown at the bottom of Fig.5.4. The final inversion is not, of course, essential to the system operation but is usually present if the two AND gates and the OR gate form part of a single TTL logic element. (4-input, 2-wide AND-OR-INVERT gate)

The design philosophy behind the encoder and duplexer circuits is that they should be made as simple and small as possible, even at the expense of added complexity in the play-back circuitry. The logic functions required were chosen to be parts of standard integrated circuits (ICs) and the encoder itself used IC operational amplifiers. Fig.5.7 shows the components used to construct the keyer in Fig.5.5. A sawtooth generator is built around IC_1 and IC_2 in the form of a bilateral trigger circuit and an augmenting integrator. Since the trigger circuit positive-feedback voltage and the integrator input voltage are both clamped by D_1,D_2 and D_3, the circuit is independent of supply voltage variations and the circuit output is as shown. This sawtooth generator feeds the inputs of four identical comparators, $IC_{3p} \rightarrow IC_{3s}$, corresponding to the four tracks of the tape recorder. Since the trigger levels of these comparators are controlled by the four inputs, P→S, their outputs are mark/period ratio modulated. The comparator outputs have edges whose speed depends ultimately on the slew rate of the operational amplifiers. The specified slew rate of the 741 amplifier is $0.8V/\mu s$.[50] As may be seen from the block diagram (Fig.5.5), the keyer output is needed to drive the clock input of the bistable element. TTL logic JK flip-flops, of the type used, operate on a stored-charge principle and the clock input signal must

Figure 5.8

TTL LOGIC TRANSFER CHARACTERISTICS





have a fall-time of < 100 nsec.[51] In order to match the slow slew rate of the keyer output to this fast logic element input, the voltage is passed through two overdriven, inverting amplifiers in cascade which speed up the edges as well as providing the required complementary output. The delay element is a simple RC network which produces a signal that rises and falls exponentially about the input logic level of the AND-OR-INVERT gate. The type of TTL which is currently most popular (as exemplified by the Texas 7400 series) has an unsatisfactory transfer characteristic (see Fig.5.8a) for use with this type of delay circuit. The slow, exponential input voltage causes the gate to be, for a time, in an undefined logical state. However, TTL series are available[51] with the transfer characteristic shown in Fig.5.8b, and these will function satisfactorily. MC3020F is a member of such a series.

The two inputs from the transducers are low-level, millivolt signals and, by comparison, the switching voltages from the bistable element are large. Simple junction field-effect transistors may therefore be used as the analogue gate elements. N-channel JFETs (TI BF244A) are used since these have a channel-on resistance of $200\,\Omega$ and may be selected with a pinch-off voltage of < 2V. Positive values of V_{gs} will cause the channel-gate diode to become forward biased. A resistance of $1 M\Omega$, inserted between the flip-flop outputs and the JFET gates, was found to be sufficient to prevent a disturbance of the drain voltage by positive gate voltages of the magnitude encountered here. This concludes the description of the keyer and duplexer circuits used in the tape recorder.

Figure 5.9 Tape Recorder Interior

Shown, left to right, are: 2 duplexer boards, 8 JFET analogue gates, capstan with rubber drive belt to take-up clutch, and motor.
Below: input socket and 4 NiCad cells



Fig.5.9 is a view of the interior of the tape recorder showing the relative positions of the motor, spur gearbox, worm drive, capstan and slipping clutch. All the electronics is built on a plug-in boards. The 'flat-pack' encapsulated logic circuits are on boards mounted above the board of the sawtooth generator and comparators which is therefore hidden in this photograph. The JFET analogue gates hide the motor speed control board. The four cells seen at the bottom of the photograph are Nickel-Cadmium rechargable cells (Ever Ready NC100) with a capacity of 100 mAH. Although the cell capacity is much lower than mercury cells of the same size, which were used in the 24 hr. recorder, the cost saving in rechargability is considerable. Furthermore, NiCad cells are ideally suited to high-discharge rates. The current consumption of the recorder is around 150 mA., giving a charge life of ¾ hr. This corresponds well with the duration of the cassette at the higher speeds used in this machine.

This and the previous section have described in some detail all aspects of the tape recorder except the recording head. The decommutation and decoding process is the subject of the following section.

Figure 5.10

DECODER

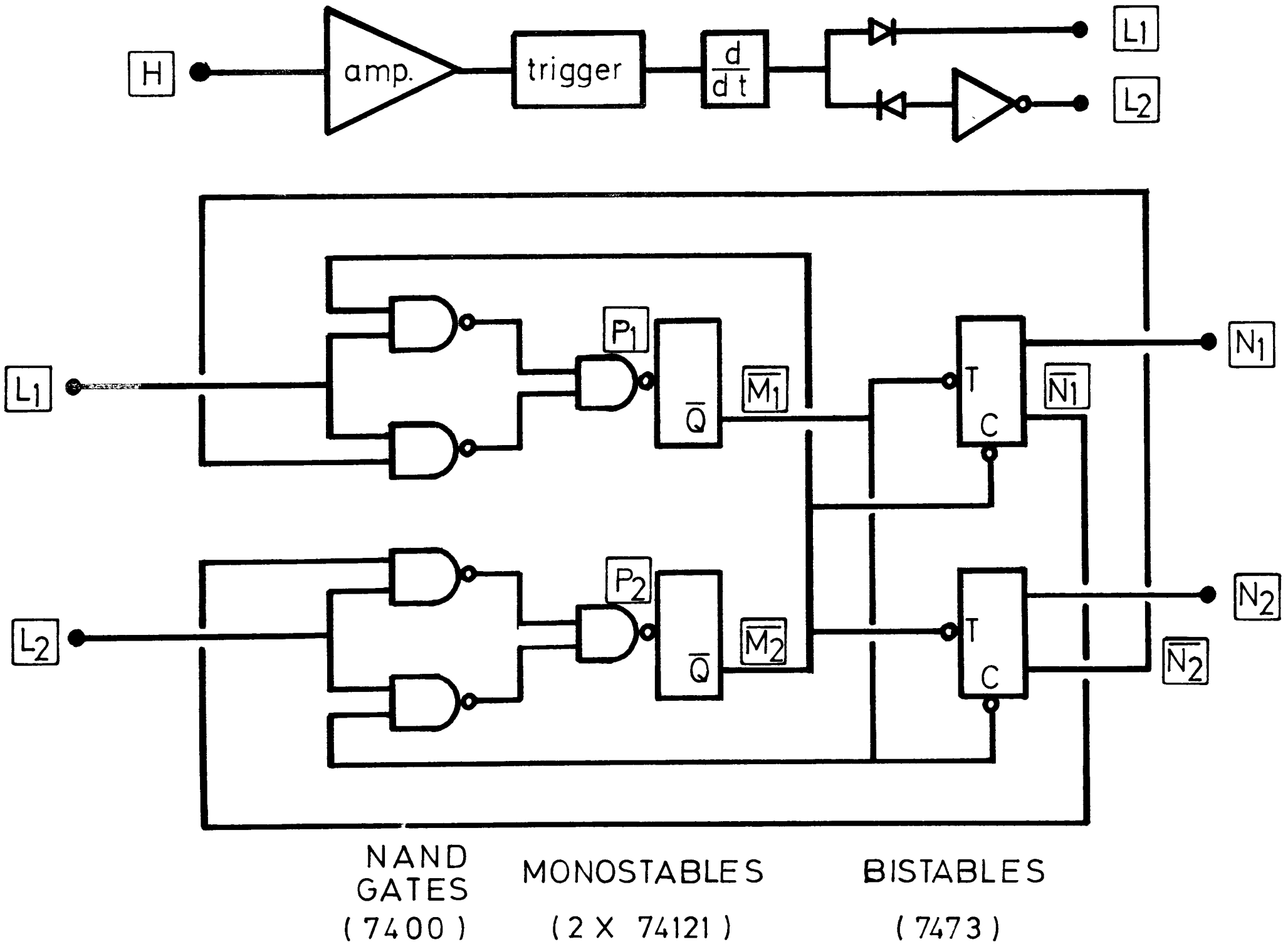
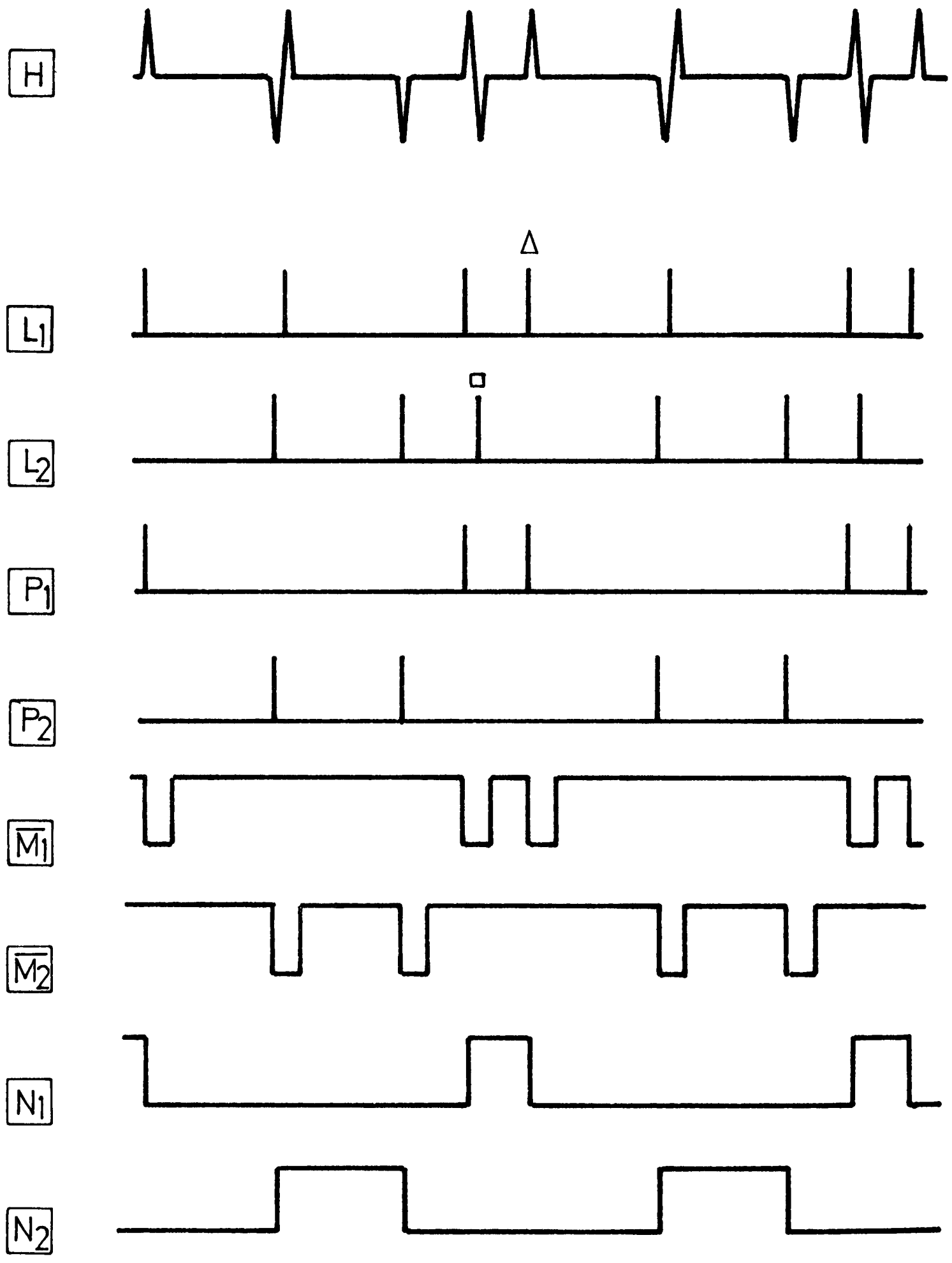


Figure 5.11

DECODER WAVEFORMS



5.5 Decommutation and Decoding

The decommutator of any time-multiplexed information channel must be self-starting and must be able to restart immediately after any combination of signal drop-outs. The comparative complexity of the circuitry described here is due to the necessity of meeting these needs.

Fig.5.10 shows a block diagram of the decommutator/decoder. The first part of this circuit is conventional and should be explained by waveform, H, at the top of Fig.5.11. The two trains of spikes, L_1 and L_2, provide all the timing information necessary to separate the two channels from one another and decode them. As may be seen by comparing L_1 and L_2 with H in Fig.5.11, every fourth spike on L_1 or L_2 is produced by the extra sign change which was introduced in the encoding/duplexing process. These spikes may be recognised as they occur approximately a time, τ , after a spike on the opposite stream. All spikes that are permitted to do so set the monostable element on the appropriate stream. The output pulses of the monostables, M_1 and M_2, have durations slightly greater than τ and these pulses inhibit the access of spikes to the monostable element on the opposite stream. In this way, the monostables will only produce output pulses which start with edges containing information.

The leading edges of the complementary monostable outputs, $\bar{M}_1$ and $\bar{M}_2$, trigger two bistable flip-flops with outputs N_1 and N_2. In the event of a signal drop-out, one pulse in the pairs of pulses in stream $\bar{M}_1$ or $\bar{M}_2$ might be absent. The state of N_1 or N_2 respectively would then be incorrect for the arrival of the next pair. For this reason, the pulses on the opposite channel

are used to 'clear' the incorrect bistable before the pair of pulses arrive. If the bistable element is already in the correct state, the 'clear' signal has no effect. Further examination of pulse streams L,M and N shows that not all spikes which occur within a time, τ , after a spike on the opposite stream need be inhibited. Spike Δ on L_1 may quite correctly occur $< \tau$ after spike $\square$ on L_2. Not to allow this type of possibility would place a restriction on the minimum signal pulse width allowed for either channel, thus limiting the dynamic range of the keyer. L_2 should be inhibited only when M_1 and N_1 are high. If P_1 and P_2 are the spikes which actually set the monostables; then, using Boolean algebra,

$$P_1 = L_1 \circ \overline{(M_2 \circ N_2)} \qquad 5.1$$

$$\therefore \quad P_1 = L_1 \circ (\overline{M}_2 + \overline{N}_2) \qquad 5.2$$

$$= (L_1 \circ \overline{M}_2) + (L_1 \circ \overline{N}_2) \qquad 5.3$$

$$= \overline{\overline{(L_1 \circ \overline{M}_2)} \circ \overline{(L_1 \circ \overline{N}_2)}} \qquad 5.4$$

Similarly: $$P_2 = \overline{\overline{(L_2 \circ \overline{M}_1)} \circ \overline{(L_2 \circ \overline{N}_1)}} \qquad 5.5$$

These expressions (5.4 and 5.5) correspond to the canonical NAND gate realisation of the initial AND/NAND expression. The gates and their inputs are shown in Fig.5.10.

The two output pulse streams, N_1 and N_2, contain the separated, coded, mark/period ratio signals. If the channel period is T and the lengths of the channel pulses are t_1, and t_2

respectively, the mean levels of the two channel voltages are proportional to $t_1/2T$ and $t_2/2T$. Since the data was encoded as proportional to t_1/T and t_2/T, this proportionality is still preserved and the data may be decoded by the low-pass filtering method described in section 5.2.

Not shown in Fig.5.10 is an additional bistable element which may be triggered by the NOR combination of N_1 and N_2. The output of such a bistable is a square-wave of period 4T which could be used to indicate time-base distortion, provided the sawtooth generator of the keyer was appropriately stable. This refinement was tried, but not used.

The efficiency of this duplexed coding system is a function of many variables in the information channel, but, given the same channel parameters, it is certainly considerably more efficient than a duplexed system with a synchronizing period equal to a data period. It is also less complicated than a system where the synchronizing period is made shorter than the data periods.

The identification of either channel in a time-division duplexed system requires a minimum of one bit of information per channel period in order to make the channel identification. The time required to transmit one bit is inversely proportional to the bandwidth of the transmission medium. As stated in the previous section, the delay, τ , of the channel identification polarity reversal is also inversely proportional to the bandwidth of the transmission medium. The extra change in polarity contains one bit of information. Thus, it is clear that, by the adjustment of τ to suit the system bandwidth, this form of duplexing can be made to identify a channel in a time which approaches the theoretical minimum.

Encoder/Decoder Characteristics.

The following characteristics were measured for the tape recorder electronics when driving the decoder directly from the encoder.

Clock frequency: 400 Hz.

Channel Sample Rate: 200 Hz.

Identity Pulse Length, τ: 0.3 ms.

Linear Input Voltage Range: $\pm$ 5 mV.

Frequency Response: 0-50 Hz nominal
-3 db measured @ 30 Hz.
-6 db measured @ 60 Hz.

Phase Response: Linear 0-70 Hz.

Carrier Breakthrough: -40 db (1%).

Cross-talk : not Detectable.

Drift (1m at ambient): -38 db(1.25%).

Drift (10m at ambient): -32 db(2.5%).

Power Requirements (for 4 channel pairs)

Encoder $\pm$ 2.5V : 90 mA symmetrical.

Decoder + 5V : 240 mA and $\pm$ 15V: 120 mA.

5.6 Future systems - the Resistance Ratio Controlled Oscillator*

The bandwidth of a magnetic tape recording system is limited at the lower end of the frequency spectrum by the need for magnetisation changes for any replay voltage. (See section 5.3). At the upper end of the frequency spectrum, there are various limiting factors. The first is the replay "gap-effect" which, as the name implies, causes the replay head output to drop to zero when a whole cycle of magnetisation on the tape lies between the pole-pieces of the replay head. A second phenomenon, known as "slurring", occurs because the sine-wave packing density on the tape is a function of the tape thickness and has a maximum value for a particular magnetic coating material. Since both these phenomena limit the maximum packing density of sign-reversals on the tape, the upper frequency limit can be pushed up by increases in tape speed.

However, a third limitation on the highest frequency available cannot be removed by increases in speed. The magnetising current required to saturate the tape is inversely proportional to the number of turns wound on the head. Since currents in excess of this value serve only to increase inter-track cross-talk, it is usual to adjust the resistance in series with the head, R, to pass this current for maximum applied voltage. Furthermore, since the head inductance, L, will attenuate the current at frequencies above $\omega_0 (=R/L)$, it is desirable to make R/L large. Now; $L \propto N^2$ (N is the number of turns on the head) and $R \propto N$ (with a limitation on the maximum voltage

---

* a paper describing this oscillator has been accepted for publication in Medical and Biological Engineering.

available), so; $\omega_0 \alpha$ 1/N. For the 24 hr. recorder with a supply voltage of 5V., a head inductance of 30 mH was chosen, but when the maximum frequency response is to be increased from 1 kHz. to 5 kHz., this inductance becomes the limiting factor on the system bandwidth. As is shown above, a lower head inductance will increase the frequency response as the number of turns is reduced. A suitable low inductance head (6 mH) is not yet available (1973) and the use of the recorder for monitoring acceleration measurements must await its development. This development is expected to be complete in the near future.

While methods of recording eight channel of data on a four track tape recorder were under investigation, the possibility of using FM recording techniques was examined. The recording of frequency modulation signals, in general, requires a high quality tape transport system, since changes in speed themselves modulate the frequency of the recorded signal. It is possible, however, to compensate for much of the error thus introduced by recording a stable, reference timebase, typically the output of some form of mechanical resonance oscillator, using a crystal or tuning-fork. The demodulation of the frequency of this signal on playback gives a direct indication of the variations of tape speed. The signal thus derived can then be used to remove the error term from the signal-bearing recorded frequencies. The compensation is not perfect, mainly because 'flutter' at frequencies approaching ½ the reference frequency cannot be detected, but may still introduce errors into the encoded signals. Commercial systems using this system quote 'wow-and-flutter

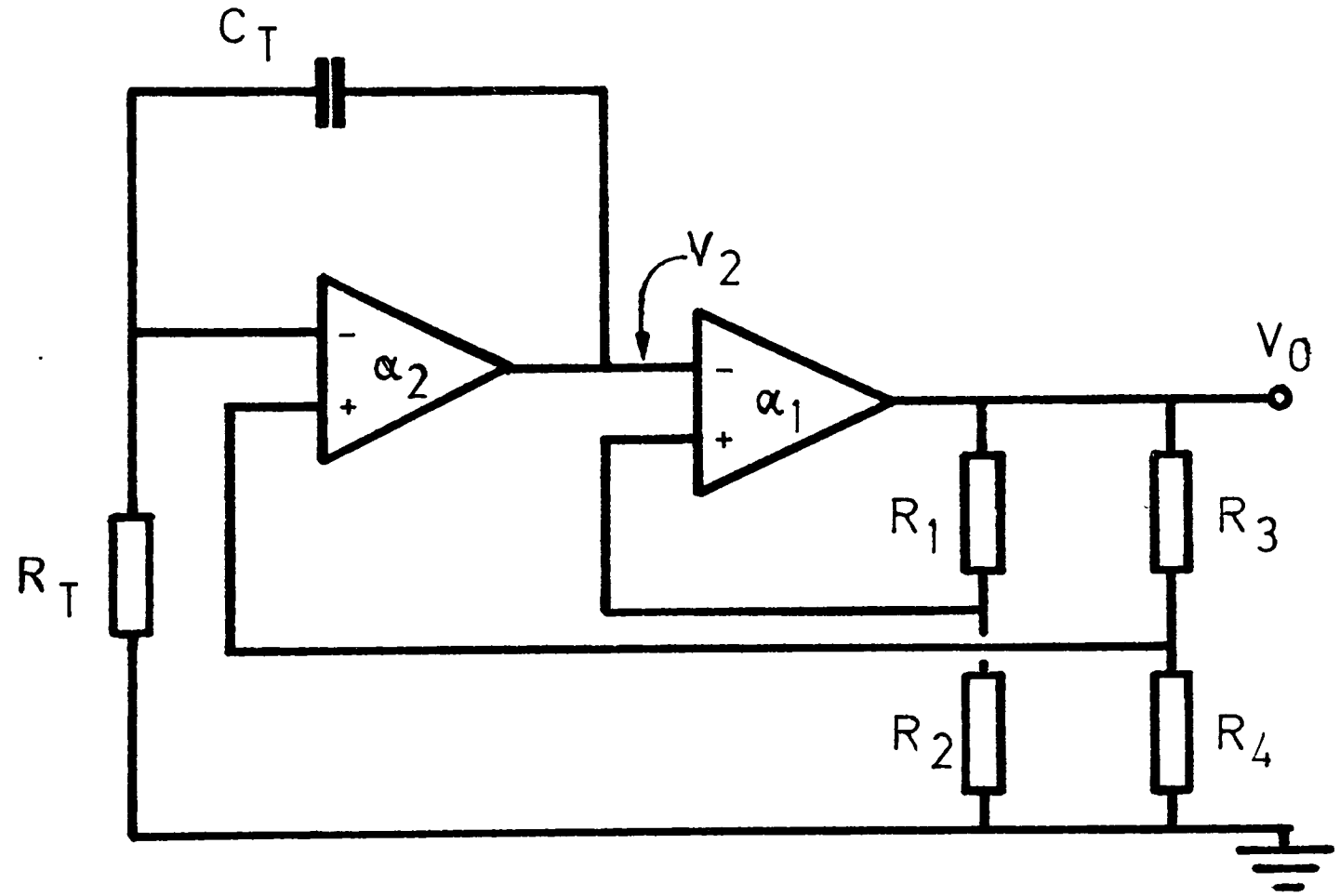


Figure 5.12 Resistance-Ratio Controlled Oscillator

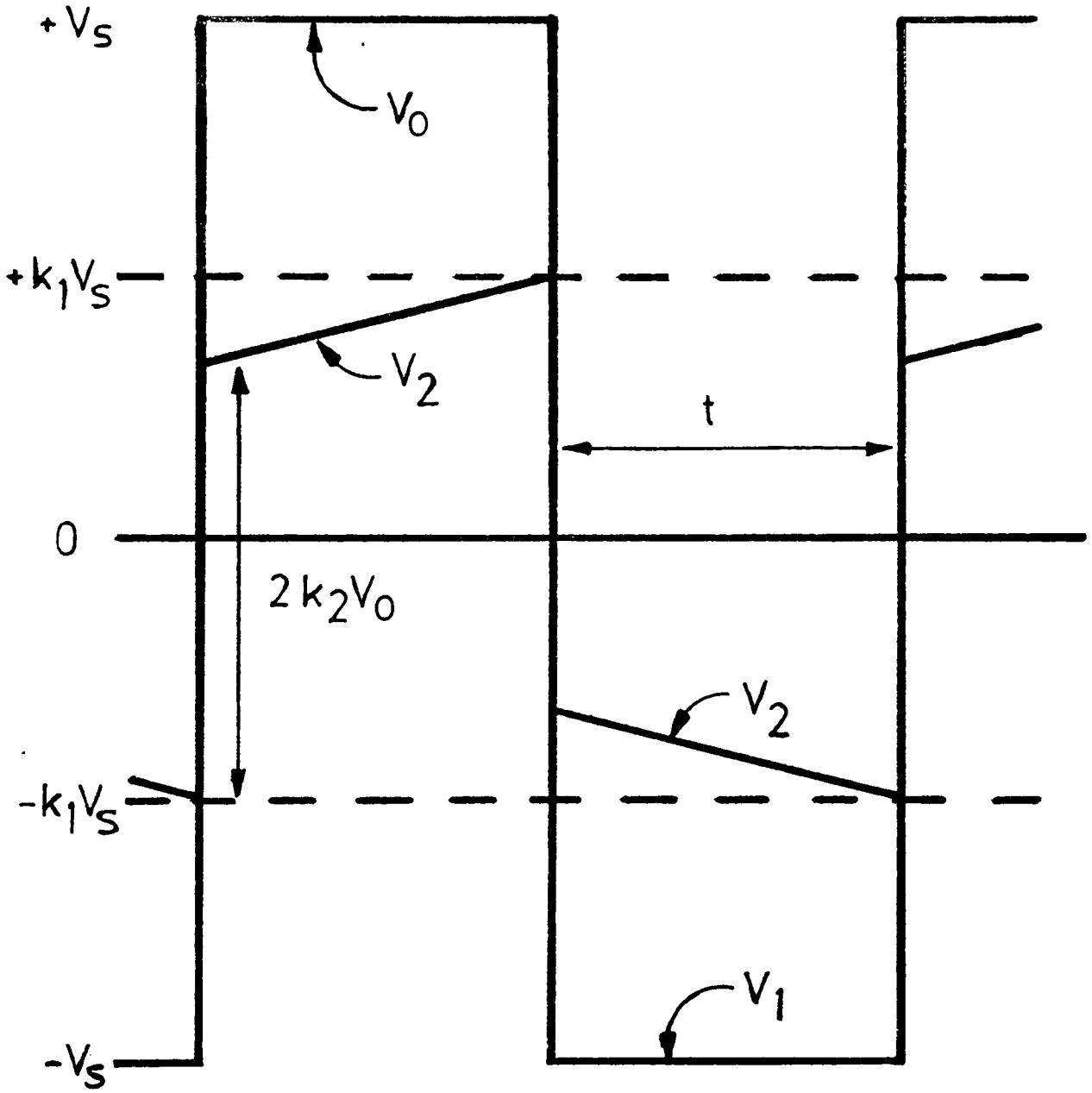


Figure 5.13 Voltage Waveforms for Fig. 5.12

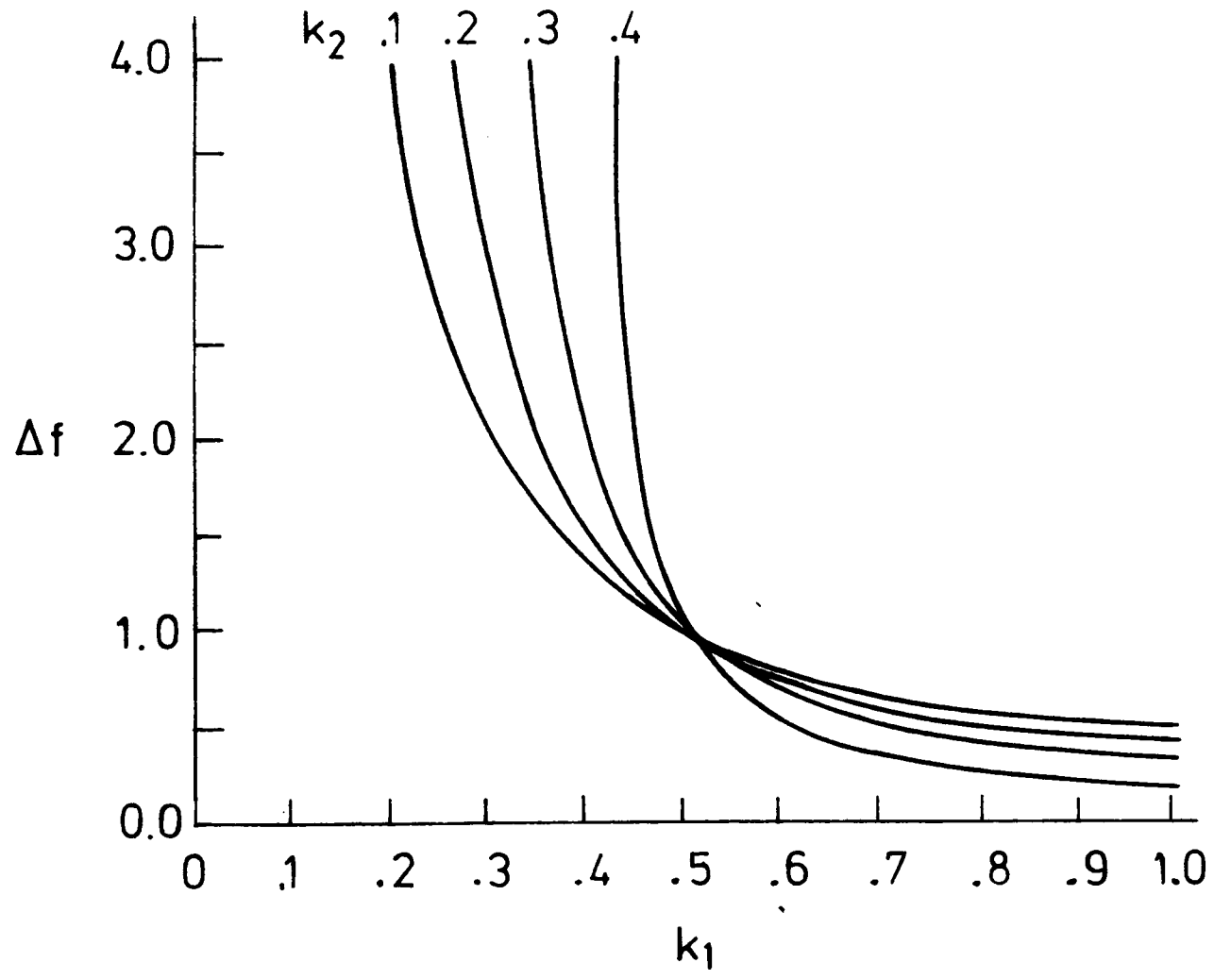
improvements' of around 40 db.

One form of sub-carrier oscillator has already been mentioned in section 5.2; the variable-reactance resonance oscillator. The more common 'voltage-controlled oscillator' (VCO) takes the form of an astable multivibrator, the charging current of whose timing capacitor is controlled by an applied voltage. This type of oscillator requires some form of preamplification when used with a transducer whose output is a few millivolts. The minimum number of components required to realise a wide-deviation, millivolt-sensitive V.C.O. is fairly high.

It seemed that by incorporating the transducer, electrically, within the oscillator (as in the reactance-controlled oscillator) instead of using it simply to obtain a separate, controlling voltage, the complexity and size of the circuit could be reduced. A sufficient reduction in size would allow the attractive possibility of building the oscillator physically around the transducer without a loss of transducer mounting capability. The signal for line-transmission to the tape recorder would then be a high energy modulated frequency instead of a low energy transducer output voltage.

The circuit was eventually reduced to the simple form shown in Fig.5.12. Timing components, R_T and C_T, together with amplifier α_2, form an augmenting integrator. For a step input, the output of such an integrator first changes by an amount equal to the input step. It then follows a linear ramp as the capacitor charges though R_T, the amplifier working to keep its two input terminals at the same voltage. The other

Figure 5.14 Family of Hyperbolae $\Delta f / k_1$



amplifier, α_1 , with R_1 and R_2, forms a symmetrical bilateral trigger circuit. The two potential dividers, R_1 and R_2, and R_3 and R_4, divide the trigger output by the ratios k_1 and k_2, respectively. If the output of the trigger is $\pm V_o$, the hysteresis of the trigger is $2k_1V_o$, and the amplitude of the steps applied to the integrator is $2k_2V_o$. Figure 5.13, which shows the voltages V_o and V_2, indicates that, provided $k_1 > k_2$, the circuit will oscillate. The output of α_1 rises or falls linearly until the trigger level of α_2 is reached. At this moment the output voltage changes by $2k_2V_o$ and then moves linearly to the opposite trigger level. Since the slope of the ramp is $\pm k_2V_o/R_TC_T$, the cycle period of the oscillation is $4T(k_1-k_2)/k_2$, where $T = R_TC_T$. As this period is a function of both k_1 and k_2, either variable may be used to control the frequency of oscillation. It is convenient to use k_1 as the control variable with R_1 and R_2 forming the two arms of a ½-bridge transducer, in this case an accelerometer. If $R_1 \doteqdot R_2$, so that $k_1 \doteqdot ½$, then $k_2 < ½$.

If: $$\Delta f = f/f_o = (k_1' - k_2)/(k_1 - k_2) \qquad 5.6$$

where: $k_1 = k_1'$, when $f = f_o$

then: $$\partial \Delta f / \partial k_1 = (k_2 - k_1')/(k_1 - k_2)^2 \qquad 5.7$$

i.e. $$\left(\partial \Delta f / \partial k_1\right)_{\Delta f = 1} = 1/(k_2 - k_1') \qquad 5.8$$

Figure 5.14 shows a family of hyperbolae for different values of k_2, when $k_1' = ½$.

The sensitivity of the oscillator depends on the slope of the relevant hyperbola at $\Delta f = 1$. Even transducers in which k_1

changes by as little as $\pm$ 5% can be used to deviate the centre frequency by +100%, - 30% ($k_1' = 0.5$; $k_2 = 0.45$).

The circuit has other useful properties. Both k_1 and k_2 are independent of temperature changes provided that R_1 and R_2 (the transducer) are made of the same material, and R_3 and R_4 are similarly matched. The absolute values of R_1,R_2,R_3 and R_4 are determined only by the bias requirements of the amplifiers. The expression for f is independent of V_o, which depends on the supply voltage. Symmetrical changes in the supply voltages of the operational amplifiers do not cause changes in frequency. Thus only two components, R_T and C_T, can effect the frequency by changing their absolute values with temperature. By careful selection, these components can be chosen so that their temperature coefficients are equal but opposite (they are in the range $\pm$ 100 ppm/^oC). The product, R_TC_T(=T), then has a zero temperature coefficient. This leaves only the offsets of the amplifiers as potentially disturbing influences on the frequency of oscillation. The amount by which these will change in normal thermal environments is very small compared with the signal levels at which the amplifiers are operating.

Finally, the physical size of the circuit can be greatly reduced by using operational amplifiers which are currently available, two per substrate. These are manufactured in 8-pin dual-in-line, TO99 or flatpack encapsulations. The timing capacitor is then physically the largest component in the circuit. The circuit has been built and tested with the following component values:

$R_1 \doteqdot 1\ k\Omega$ }
$R_2 \doteqdot 1\ k\Omega$ } accelerometer

R_3 and R_4 2 kΩ cermet potentiometer

$R_T = 1\ M\Omega$

$C_T = 0.01\mu F$

amplifiers : dual 741.

Since the frequency of the oscillator is inversely proportional to k_1, the signal cannot be demodulated in a normal FM detector. A zero-crossing detector is used to drive a resettable ramp generator. The peak values of the ramps are proportional to k_1 and are sampled and held from cycle to cycle.

This chapter has examined some of the problems associated with the recording of signals from transducers, such as accelerometers, which are attached to ambulant subjects. This part of the research project is clearly not complete, but since the principles of accelerometry have been shown to be technically applicable, there is now a good reason for it to continue. With the anticipated continuation of the project as a whole, this further development seems to be a likely probability. The tape recorder will first be tested, using duplexed PWM, with the low inductance recording heads when they become available. If it is then found that the performance of this system is inadequate, the possibility remains of using the resistance-ratio controlled oscillator.

CHAPTER 6

DISCUSSION AND SUMMARY

6.1 Introduction

6.2 A Comment on Methods of Describing Gait

6.3 The Advantages of Accelerometry

6.4 The Disadvantages of Accelerometry

6.5 Extensions of the Present System.

6.1 Introduction

Many bioengineers involved with the study of human movement have at some time attempted to use an accelerometer for the quantitative measure of that movement. Careful searches made at the beginning of this project, and at various times since then, have failed to uncover a single reported instance of the use of accelerometers in conjunction with a systematic analysis of the data which they produce. There are even references[13] to the unsuitability of accelerometers for gait analysis. It was for this reason that the project evolved into a feasibility study in the use of accelerometry. This final chapter will attempt to make a judgement on the usefulness of the method, based on experiences gained from the project as a whole. But first, the description of the step in Chap.1 is briefly discussed.

6.2 A Comment on Methods of Describing Gait

In Chap.1, section 4, the separate processes which together constitute human locomotion are summarised in a new way. There is now a very considerable amount of reliable information available on the functional behaviour of the elements of the locomotor system. Indeed, textbooks[52] have been written on this subject. It is a universal characteristic of these textbooks that they are inhibited by the standard topographical methods of describing the body's anatomy. Each organ, or set of organs, is treated as a separate subject for explanation and there is a danger that the interaction between organs is lost.

There is a strong case for separating anatomical description from functional description. Clearly, a thorough understanding of anatomy is a prerequisite to a proper functional interpretation. However, once the anatomy of a musculo-skeletal system is understood, all functional descriptions are best made as a sequence of interactive events in time. Thus, the action of the legs is best described as a sequence through various periodic activities or activities of finite duration. For instance: a step of walking, a step of running, a step of stair climbing, the act of rising from a chair. Similarly, the action of an arm could be described by: raising the arm to place the hand at some anterior point, the act of raising an object from table to mouth.

It is hoped that the description of the step in Chap.1 demonstrates the method satisfactorily. While most of the information contained in the description is already published, it has not before been collected together in this way.

6.3 The Advantages of Accelerometry

Since almost all the advantages of the method have been described and discussed already, a brief summary of the main points will be made.

1) The method has been shown to be at least as accurate (Chapter 4) as any other method of measuring a range of kinematic gait variables. The method is particularly useful for the study of fast, transient phenomena, such as heel-strike.

2) The technique of accelerometry is ideally suited to use outside the laboratory since the movement of the limbs can be measured without reference to any outside physical constraints. An interesting consequence of this is that the subjects may be normally dressed. It was also found that nervous patients walked most naturally when distracted by a conversation with someone walking alongside them.

3) It has been demonstrated that tests may be made by personnel who need not fully understand the process. Tests may be made quickly and with a minimum of inconvenience to the subject.

4) Kinematic analysis of accelerometric data may be performed on a simple, interactive digital computer. This task is not tiring and is, in fact, very interesting for the operator since he can watch the analysis proceed and study the effects of his interactions with the program. Computer simulation of a leg's movement, which has also been the subject of research[53] elsewhere, is little more than an amusing game.

5) Accelerometry can provide a much needed addition to the current range of gait analysis techniques. It can be used in basic physiological research, in prosthetics research, and in clinical orthopaedics.

6.4 The Disadvantages of Accelerometry

There is a problem in separating the inherent disadvantages of the technique from the difficulties which have been encountered in this project, but which could be overcome by further work. An attempt at a summary of the inherent disadvantages is given here.

1) There is a basic limitation to the number of limb elements, or parts of the body, to which the transducers can usefully be fixed. For instance, the mass of soft tissue on the thigh will effectively mean that it is impossible to determine accurately the movement of the femur from a study of the movement of any part of the surface to which transducers could be attached.

2) It is effectively impossible to analyse the data from accelerometers without the aid of a digital computer. The labour involved would be enormous,

3) It is not possible to estimate the forces and moments in the legs without measuring foot/ground reaction, which is indeterminate whenever the subject has two feet on the ground. The portability of the system is thus only useful for purely kinematic measurement unless a six-component load-shoe can be developed. This seems most unlikely.

Some further items which are seen as difficulties, rather than disadvantages, are discussed in the next section.

6.5 Extensions of the Present System

There are two main directions in which the project can now move. If the work is to continue in Oxford, since it would be supported by the Department of Health and Social Security, there are powerful reasons for the existing system being developed into a service for use in clinical orthopaedic assessment and in the assessment of orthotic appliances. Certainly, it was shown in Chap.4 that the existing system can provide a considerable amount of information on the gait of a subject. The only part of the system which needs to be improved, for this application, is the tape recorder. The way in which this can be done was explained in Chap.5.

Now that the technique has been applied successfully to the shank, it is natural to consider how the movement of other parts of the body can be studied. Since the thigh presents the inherent difficulties mentioned in the last section, the pelvis is the obvious place to make the next attempt.

In normal walking, the pelvis rotates in all three planes; transverse, sagittal and coronal. It was shown in Chap.2 that the analysis of the movement of a body with three rotational degrees of freedom requires the solution of a set of non-linear, first order differential equations. While numerical methods of solution are available, they are complicated and still very much the subject of research in numerical analysis. If it were possible to approximate one of the rotations to zero, the non-linearity could be removed as it was in the case of the shank. It seems quite probable that the sagittal plane rotation of the pelvis can be approximated to zero.

The most suitable site for an accelerometer platform on the pelvis appears to be over the sacrum, just above the gluteal fold and below the L5 - S1 articulation. If no attempt is made to measure the sagittal plane rotation, the platform can be made with the same basic dimensions and transducer positions and orientations as in the present case (see Fig.2.5). The following transformation indicates the pelvic platform orientation: platform axis 3 becomes pelvic axis 2, platform axes 1 and 2 are in the sagittal plane of pelvic axes 1 and 3.

If the movement of the pelvis and both shanks can be calculated, then the movement of the thighs can be interpolated by assuming that the knee and hip are purely rotational joints. A five bar chain (2 shanks, 2 thighs and a pelvis) with four spherical joints has 18 degrees of freedom. This is the same number as the 18 variables determined from the movement of the two shanks and the pelvis. Such a system is kinematically determinate. If the knee joints are both reduced to one degree-of-freedom, the system is over-determined (c.f. 'foot-flat' in Chap.2) by order 4 and the resulting redundancies can be used to correct some of the errors that will have occurred. Such a process would be complicated, but should be possible.

As was mentioned in Chap.3, it is hoped to start using a new type of transducer with lower zero-drift characteristics. The main advantage that should accrue from this change is an improvement in the rotational and translational displacement accuracies, the former being much the more important.

It is planned to build force-plates in the new Orthopaedic Engineering Unit, Oxford. Using the force-plates and a combination

of accelerometry and cinephotography, it will be possible to undertake dynamic analyses of gait. There are two reasons for wishing to repeat experiments which have been performed elsewhere.[19,21]

First, accelerometry will allow the dynamic components of force[54] to be estimated with far greater accuracy than has before been possible. This would be necessary in a study of the effect of footwear on joint forces. Second, the solution of the equations of motion of the various elements of the limbs requires that assumptions be made about the activity of muscles at any moment of time. Unless such assumptions are made, there is an infinite number of solution sets to the underdetermined equations of motion. Until recently, the usual assumption has been that there is a minimum of antagonistic muscular activity between different synergistic groups.[55] It has long been known that pure reflex responses contain nervous, reflex arcs which inhibit the antagonists to the primary muscles of the response. However, walking is not a purely reflex activity and it has been suggested[56] that other criteria might be useful in selecting one of the force solution sets. Possible criteria are: minimum system work, minimum muscle force, minimum joint force, or weighted combinations of these. A selection procedure of this type is known as a 'simplex' selection.

Further into the future, there is the possibility of using accelerometers to study the movement of the head, shoulders or arms, although these last would present a considerable mounting problem. However, since movements at this end of the body are far less periodic than the movement of the legs, the transducers used for such a study would need to be of a much higher quality than those currently in use.

REFERENCES

1 BORELLI G.A. De Motu Animalium Lugduni Bavatorum 1679

2 MUYBRIDGE E. Animals in Motion Chapman and Hall 1925

3 MAREY E.J. De la Locomotion Terrestre chez les Bipeds et les Quadrupedes J.l'Anat.et de la Physiol. IX,42 1873

4 BRAUNE W. and FISCHER O. Uber die Lage des Schwerpunkt des menschlichen Körpers Abh.Math.Phys.Klasse d.Kgl. Saschen, Ges.d.Wiss,15 1889

5 BRAUNE W. and FISCHER O. Der Gang des Menschen, Versuche unbelasten und belasten Menschen Abh.Math.Phys.Klasse d. Kgl.Saschen, Ges.d.Wiss,21 1895

6 DEMPSTER W. Space Requirements of the Seated Operator WADC Tech.Rep. 55:159 1955

7 BERNSTEIN N.A. Investigations of the Biodynamics of Walking, Running and Jumping Pt.II,Moscow, Cent.Sci. Instit.of Phys.Cult. 1940.

8 SCHWARTZ R.P., HEATH A.L., and MISIEK W. The Influence of the Shoe on Gait, as Recorded by the Electrobasograph and Slow-Motion Pictures J.Bone Jnt.Surg. 17 1935

9 SCHERB R. Kinetisch-diagnostische Analyse von Gehstörungen; Technik und Resultate der Myokinesigraphie Zeitschr. Orthop. 82, Supplementum 1952

10 STEINDLER A. and LINDEMANN E. Alteration of the Action Current of Skeletal Muscles following Sympathetic Ramisection J.Bone Jnt.Surg.11 1929

11 SCHWARTZ R.P. and HEATH A.L. A Pneumographic Method of Recording Gait J.Bone Jnt.Surg. 14 1932

12 EBERHART H.D., INMAN V.T., SAUNDERS J.B.de C.M., LEVENS A.S., BRESLER B. and McCOWAN T.D. Fundamental Studies on Human Locomotion and Other Information Relating to Design of Artificial Limbs Report to NRC Comm. on Artificial Limbs Berkeley, California 1947

13 SAUNDERS J.B.de C.M., INMAN V.T. and EBERHART H.D. The Major Determinants of Normal and Pathological Gait J.Bone Jnt.Surg. 35A 1953

14 LEVENS A.S., INMAN V.T., and BLOSSER J. Transverse Rotations of the Segments of the Lower Extremity in Locomotion J.Bone Jnt.Surg. 30A 1948

15 JUDET J., JUDET R. et al. Resection Reconstruction of the Hip. Arthroplasty with Acrylic Prosthesis Livingstone, London 1954

16 CHARNLEY J. A New Arthroplasty for the Hip Lancet,i,1, p.129 1961

17 McKEE G.K. and WATSON-FERRAR J. Replacement for Arthritic Hips by the McKee-Ferrar Prosthesis J.Bone Jnt.Surg.48B 1966

18 McLEISH R. and CHARNLEY J. Abduction Forces in One-Legged Stance J.Biomech. 3.2 1970

19 PAUL J.P. Bioengineering Studies of the Forces Transmitted by Joints II Biomech. and Rel.Bioeng.Topics Pergamon 1965

20 RYDELL N. Forces Acting on the Femoral Head Prosthesis Lytotyp, Gotenburg 1966

21 MORRISON J. The Mechanics of the Knee Joint in Relation to Normal Walking J.Biomech.3.1 1970

22 JOHNSTON R.C. and SMIDT G.L. Measurement of Hip Joint Motion during Walking J.Bone Jnt.Surg. 51A 1969

23 KETTELKAMP D.B., JOHNSON R.J., SMIDT G.L., CHAO E.Y.S. and WALKER M. An Electrogoniometric Study of Knee Motion in Normal Gait J.Bone.Jnt.Surg. 52A 1970

24 WRIGHT D.G., DESAI S.M. and HENDERSO W.H. Action of the Subtalar and Ankle-Joint Complex During the Stance Phase of Walking J.Bone Jnt.Surg. 46A 1964

25 GAGE H. Accelerographic Analysis of Human Gait ASME Paper 64-WA/HUF-8 1964

26 PAUL J.P. Personal Communication 1970

27 SUTHERLAND D.H. and HAGY J.L. Measurement of Gait Movements from Motion Picture Film J.Bone Jnt.Surg. 54A 1972

28 DEANE G. Personal Communication 1972

* 30 SORBIE C. and ZALTER R. Bioengineering Studies of the Forces Transmitted by Joints I Biomech.and Rel.Bioeng. Topics Pergamon 1965

31 HOUTZ S.J. and WALSH F.P. Electromyographic Analysis of the Function of the Musc s Acting on the Ankle during Weight Bearing J.Bone Jnt.Surg. 41A 1959

*29 CLOSE J.R. and TODD F.N. The Phasic Activity of the Muscles of the Lower Extremity and the Effect of Tendon Transfer. J. Bone Jnt. Surg. 40A 1958

32 KENWRIGHT J. Arthrodesis of the Knee and Ankle Joint- A Clinical and Biomechanical Study Ph.D.Thesis to University of Stockholm 1972

33 LIEB F.J. and PERRY J. Quadriceps Function J.Bone Jnt.Surg. 50A 1968

34 SUTHERLAND D.H. An Electromyographic Study of the Plantar Flexors of the Ankle in Normal Walking on the Level J.Bone Jnt.Surg. 48A 1966

35 MANN R. and INMAN V.T. Phasic Activity of Intrinsic Muscles of the Foot J.Bone Jnt.Surg. 46A 1964

36 CUNNINGHAM'S Manual of Practical Anatomy 13th.Ed.Oxford 1966

37 GUTEWORT W. The numerical Presentation of the Kinematics of Human Body Motions Biomechanics II Univ.Park Press 1971

38 KASAVAND T. Pattern Recognition Applied to Measurement of Human Limb Positions during Movement Report to Canadian NRC LTR-CS-41 1970

39 BORTZ J., Snr. A New Concept in Strapdown Inertial Navigation NASA TR R-329 1970

40 GRAMMATICOS A. Gimballess Inertial Systems for Space Navigation NASA CR-71089 Pennsylvania 1969

41 BEGG J.S. Advanced Mechanism pp.66-69 Macmillan 1966

42 BRADNER H. Internal Navigation without Gyros Am.J.Phys. 37.2 pp.169-170 1969

43 JEFFRIES H. Cartesian Tensors pp.9-12 Cambridge 1931

44 HILDEBRAND F.B. Introduction to Numerical Analysis p.73 McGraw-Hill 1956

45 JORDAN J. Direction Cosine Computation Error NASA TR-304 1969

46 IBM 1130 Functional Characteristics GA26-5881 IBM 1970

47 PAUL J.P. Ph.D.Thesis pp.151-153, University of Strathclyde 1965

48 MORRIS J.R.W. and O'CONNOR J.J. O.U.Engineering Lab. Report 1095.69 1969

49 OXFORD INSTRUMENTS Specifications for MATR 1972

50 ANALOG DEVICES Data Sheet C076-15-9/70 1970

51 MOTOROLA The Integrated Circuit Data Book p.4-95 1969

52 HALL M.C. The Locomotor System; Functional Anatomy Charles C. Thomas 1965

53 GARRETT G., REED W.S., WIDULE C., GARRETT R.E. Human Motion: Simulation and Visualisation Biomechanics II Univ. Park Press 1971.

54 RADIN E., PAUL I. and ROSE R. The Role of Mechanical Factors in the Pathogenesis of Primary Osteoarthritis Lancet 7749 pp.519-522 1972

55 MORGAN C.T. Physiological Psychology pp.288-289 McGraw-Hill 1965

56 SEIREG A. and ARVIKAR R.J. A mathematical model for Evaluation of Forces in Lower Extremities of the Musculo-Skeletal System J.Biomech. 6.3 1973

APPENDIX A

A GLOSSARY OF ANATOMICAL TERMS

(Cross-references underlined)

Abduction - Drawing away of any part of the body from the middle line.

Abductor Hallucis - A muscle on the medial side of the foot. Origin:diffuse at the heel. Insertion:1st.phalanx of great toe.

Adduction - Drawing towards the middle line of the body.

Antagonistic - Muscular action which tends to oppose the action of another muscle.

Anterior - Description of the front of the body or limbs.

Biceps Femoris - A hamstring muscle in the thigh. Origin: a) Ischial tuberosity and b) mid femur. Insertion: Head of the fibula.

Coronal Plane - A vertical plane at right angles to the Sagittal Plane.

Distal - Descriptive of a point far from the centre of the body. Opposite of proximal.

Dorsiflexion - Upward flexion of the foot or ankle joint.

Extension - Straightening out of a limb.

Extensor Digitorum Communis - A muscular group of ankle and toe extension. Origin:diffuse in the shank. Insertion: Phalanges of medial 4 digits.

Extensor Hallucis Longus - A muscle of ankle and great toe extension. Origin:mid fibula. Insertion:Distal phalanx of great toe.

Extensor Muscle - A muscle which has a primary effect of extending a limb.

External Rotation - Rotation of a limb about its long axis so that the anterior surface moves laterally.

Femur - The long bone of the thigh.

Flexion - The act of bending a joint so that the parts which it connects approach one another.

Flexor Digitorum Brevis - A muscle in the sole of the foot which flexes the lateral 4 toes. Origin:diffuse at heel. Insertion:2nd.phalanges of lateral 4 toes.

Flexor Hallucis Brevis - A muscle in the sole of the foot which flexes the great toe. Origin: diffuse at heel. Insertion: Proximal phalanx of great toe.

Flexor Muscle - A muscle which has a primary effect of flexing a limb.

Gastrocnemius - A large muscle in the calf which flexes the knee and plantar flexes the ankle. Origin: Posterior, superior points of both femoral condyles. Insertion calcaneus through Achilles tendon.

Gluteus Maximus - A large muscle in the buttock which extends the hip. Origin: diffuse on the posterior pelvis. Insertion: Gluteal tuberosity on femur.

Gluteus Medius - A muscle of the lateral buttock region which abducts the hip. Origin: diffuse on the pelvis. Insertion: Greater trocanter on the femur.

Hamstrings - The tendons on either side of the posterior portion of the knee, which attach the thigh flexor muscles of the knee to their insertions.

Hyperextend - To extend a joint beyond the point at which it may be held by normal muscular action.

Internal Rotation - Rotation of a limb about its long axis so that the anterior surface moves medially.

Insertion - The distal attachment of a muscle to bone.

Ischio-Femoral Ligament - An anterior ligament across the hip joint which limits extension and external rotation.

Lateral - Description of the side of the body or limbs.

Lateral Collateral Ligament - A lateral ligament across the knee joint which prevents adduction of the knee.

Medial - Descriptive of the middle side of an organ or limb.

Medial Condyle - The medial articulating surface of the knee joint, either on the femur or tibia.

Origin - The proximal attachment of a muscle to bone.

Pelvis - The structure of four bony parts (ischium, ilium, sacrum and pubis) between the spine and femora.

Plantar Flexion - Downward flexion of the foot or ankle joint.

Popliteal Nerve - A large nerve supplying many of the muscles of the leg.

Posterior - Descriptive of the rear of the body or limbs.

Posterior Cruciate Ligament - A ligament within the knee joint between the posterior tibial condyles and the anterior femoral condyles.

Proximal - Descriptive of a point closer to the middle of the body.

Quadriceps - A large group of four muscles on the front of the thigh which all extend the knee through the patellar tendon.

Sagittal Plane - A vertical plane which divides the body into left and right halves.

Semimembranosus - A hamstring muscle in the rear of the thigh. Origin:Ischial tuberosity.Insertion:through medial hamstring to the rear of the tibial medial condyle.

Semitendonosus - A hamstring muscle in the rear of the thigh. Origin:Ischial tuberosity.Insertion:through medial hamstring to upper medial surface of tibia.

Shank - A non-anatomical name for the part of the lower limb between knee and ankle, commonly used to avoid ambiguity. Anatomical term is leg.

Soleus - A muscle in the calf which plantarflexes the ankle. Origin:Posterior surfaces of tibia and fibula. Insertion:with Gastrocnemius into calcaneus.

Subtalar Joint - The lower articulation of the ankle joint complex, between the talus and the calcaneus.

Synergistic - The action of an organ (muscle) which is coordinated with that of another organ.

Tibia - One of the long bones of the shank. The tibia has a weight-bearing function whereas the fibula serves only as a muscle attachment.

Tibalis Anterior - A muscle of the lateral, anterior shank which dorsiflexes the foot. Origin:mid tibia.Insertion: 1st.metatarsal and 1st.cuneiform bones.

Tibalis Posterior - A muscle of the posterior shank which plantar flexes the foot.Origin:Posterior tibia and fibula. Insertion:Navicular and other tarsal bones.

Transverse Plane - A plane across the long axis of the body.

Vasti - A group of three muscles in the quadriceps group all with their origins in the thigh. The fourth muscle in the group, rectus femoris, originates at the front of the ilium.

(reference: Butterworths Medical Dictionary, Butterworth,London 1965)

ENDEVCO

MODEL 8210

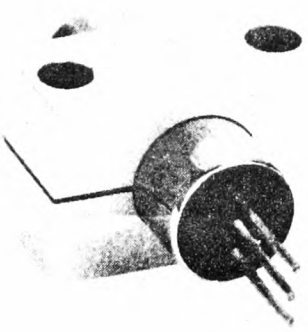
VIBRATION SENSOR

RUGGED

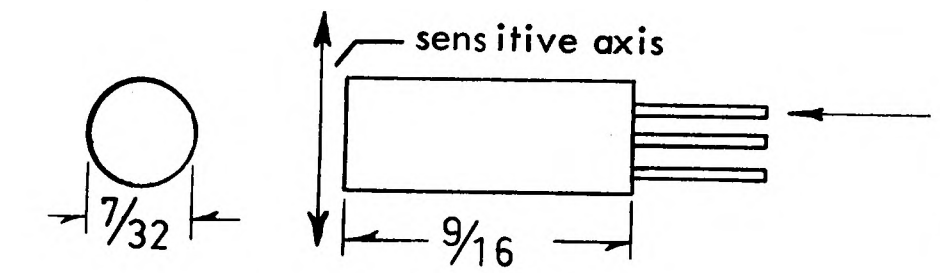
LOW COST

SMALL SIZE

HIGH SENSITIVITY

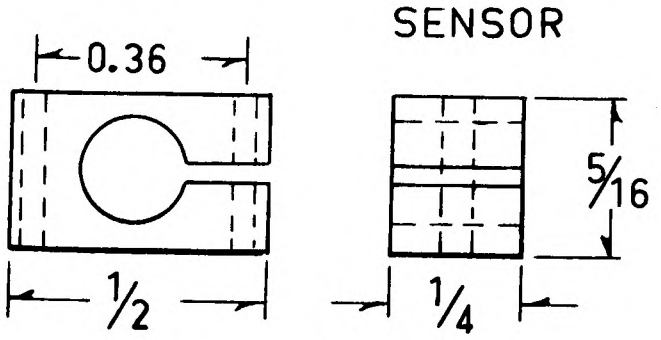


The 8210 is an Industrial Vibration Sensor designed for maximum reliability in a shop type environment, featuring a 250 times scale overload capacity. It is suitable for low frequency applications from a hundredth of a cycle to 300 cycles per second (18,000 revolutions per minute).



SENSOR

3 Pins of 0.017" dia. on 0.050" centers - mate with Barnes MG 314 Transistor Socket (supplied)



MOUNTING BRACKET

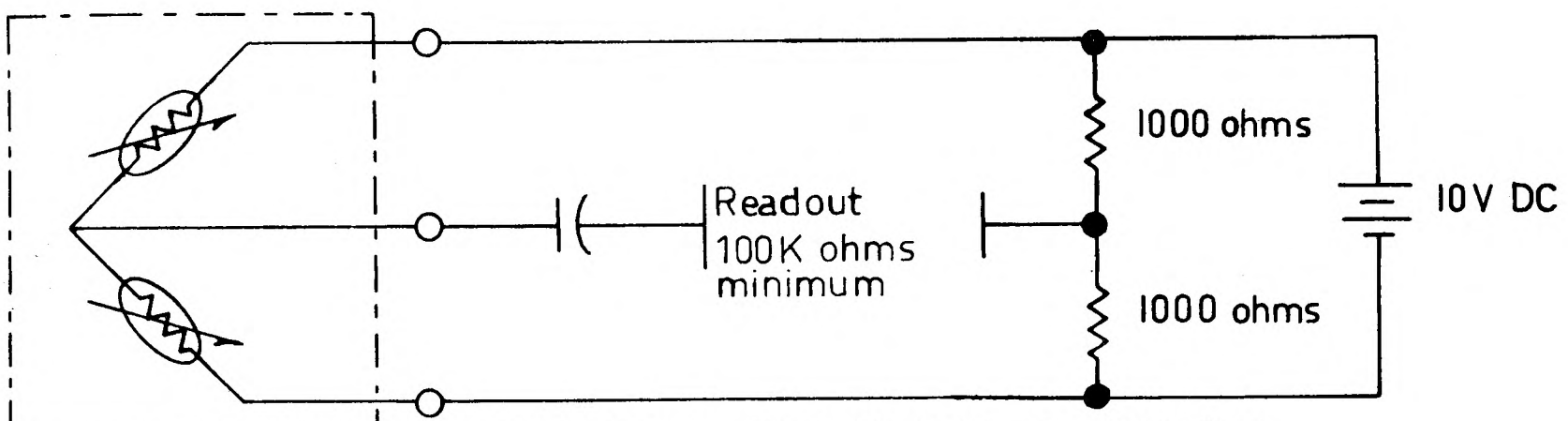
Mounting holes drilled for 2-56 Screw Clearance

Mounting screws and washers furnished.

All dimensions in inches.

SPECIFICATION — MODEL 8210

Sensitivity:	10 mV/g (nominal)
Full Scale Output:	20.0 g's (200 mV with 10 V DC excitation)
Rated Excitation Voltage:	10 V DC
Electrical Configuration:	1/2 Wheatstone Bridge
Resistance per Leg:	1200 ohms (nominal)
Resistance Match:	5% or better at 25°C
Overload Rating:	5000 g's (all axes)
Resonant Frequency:	350 Hz. (cps) (nominal)
Damping:	0.15 of critical (nominal)
Operating Temperature:	0°F to +150°F (-18°C to +66°C)
Cross-Axis Sensitivity:	Less than 5%



SUGGESTED ELECTRICAL SCHEMATIC

RELIABILITY

All sensors are manufactured and tested in accordance with the most stringent Quality Control requirements. All parts, sub-assemblies and finished sensors undergo 100% inspection.

COMPLEMENTARY EQUIPMENT

8630 BRIDGEPAC - 8631 METERPAC

These products provide matching electronics with DC excitation, balance and calibration circuits, along with an output current capability of 0.1 ma.

Terms are 1/4 of 1% 10 Days, net 30 Days, from date of invoice. Continued product improvement necessitates that Endevco reserve the right to change the prices or specifications without notice. Prices of Endevco products for export or purchased with intent to export beyond the territorial limits of the United States are subject to special quotation.

ENDEVCO SENSOR AND CONTROL DIVISION

801 SOUTH ARROYO PARKWAY • PASADENA, CALIFORNIA 91109 • (213) 795-0271

Printed in U.S.A.

Division of Becton, Dickinson and Company BD

APPENDIX C

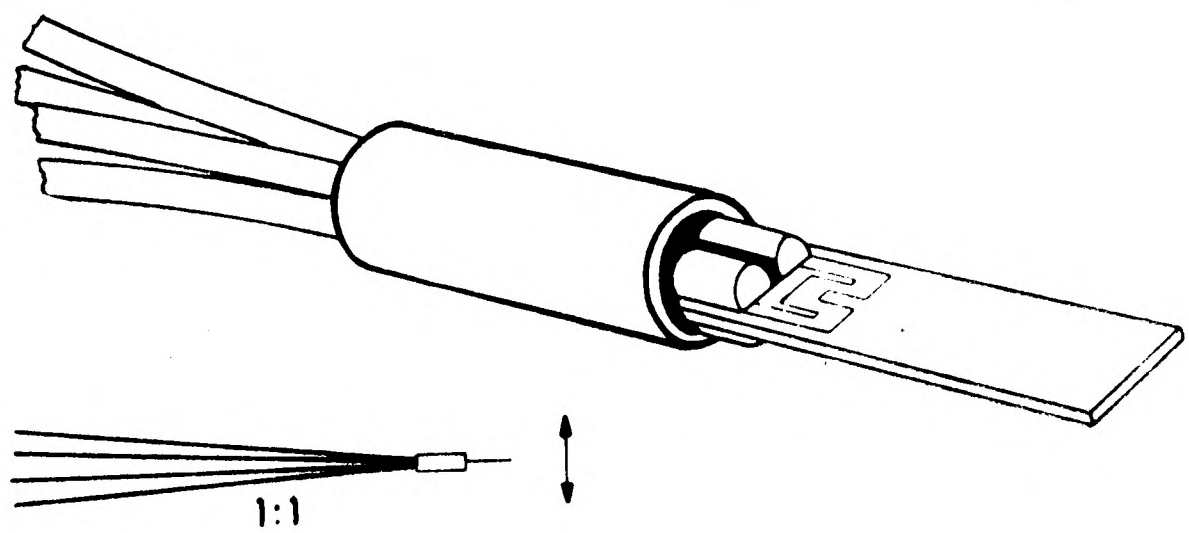
Solid State Products

SEMICONDUCTOR TRANSDUCER ELEMENTS

AE 801
AE 802
AE 803

The **AKERS** 800 series transducer elements represent an improvement in the measuring and control field. A silicon beam with planar diffused resistors is the active element of this new multipurpose transducer element, which converts force, pressure, movement, acceleration and angle etc. to electrical signals.

A deflection of the beam gives a resistance change in the diffused resistors on both sides of the beam. An electrical signal may be obtained which is nearly proportional to the deflection of the beam.



AE 800 features:

LOW IMPEDANCE
HIGH OUTPUT SIGNAL
SMALL SIZE
HIGH FREQUENCY RESPONSE
EASY MOUNTING

AE 800 applications:

PRESSURE TRANSDUCERS
LOAD CELLS
DEFLECTION TRANSDUCERS
ACCELEROMETERS
INCLINOMETERS
etc.

AE 470/1

AKERS ELECTRONICS

Address: 3191 Horten, Norway - Telephone: 4733 42 651 - Telex: Oslo 16527 - Telegrams: Micro

SPECIFICATIONS

Exitation	:	6 V
Nominal resistance	:	1000 ohm
Nominal resistance matching	:	10%
Temperature coefficient of individual resistors	:	$0,8 \cdot 10^{-3}$ per °C
Output voltage	:	25 mV/V
Zero shift of complete element	:	AE801P <0.005% AE802P <0.02% AE803P <0.05% of full scale per °C
Gauge factor of individual resistors	:	55 - 70
Temperature coefficient of gauge factor	:	$2 \cdot 10^{-3}$ per °C
Modules of elasticity	:	$1.6 \cdot 10^{4}$ kp/mm^2
Max dissipation	:	4 mW/°C in oil 1 mW/°C in free air
Non linearity at an output signal of 25 mV/V	:	ca. ±0.25% FS.

MECHANICAL DATA (Standard beam)

Case	: length	:	5 mm
	: diameter	:	1.8 mm$^{\phi}$
Beam	: length	:	5 mm
	: width	:	1 mm
	: thickness	:	0.1 mm ± 10%

Upon request elements with thickness 0,15 mm ±10% can be delivered.

APPENDIX E

Errors may be introduced into the results of experiments such as those described here by two separable sources; namely experimental error and analytical assumptions. When a computer is used to analyse results it is usual to consider the numerical accuracy of the machine as a third potential source of error, but in this case it will be quite apparent that this source of error is insignificant. Indeed, it will be shown that almost all the errors may be traced to the inadequacies of the transducers.

E.1. Errors in the estimates of ω_1 and ω_2

The cross-axis sensitivity of the transducers and any non-orthogonality in their mounting produce equivalent errors whereby a proportion of the net acceleration field in a plane perpendicular to the nominal sensitive axis of a transducer is detected by the transducer. An estimate of the effect of these errors may be made as follows:

Cross-axis sensitivity $\leq$ 5% (Appendix B)

Non-orthogonality $\leq$2% (2^{o} in 90^{o}: p.39)

Since these errors are equivalent, their absolute values may be added. i.e. Total orthogonality error = 7^{o} or 7% (max.)

The angular acceleration $\dot{\omega}_2$ is found from equation 2.25

whence: $$e(\dot{\omega}_2) = e(\alpha m_1 - \beta m_1) + e(L)$$

where: $e(\ )$ is a relative error.

Now: $$\varepsilon(\alpha m_1 - \beta m_1) = \varepsilon(\alpha m_1) + \varepsilon(\beta m_1)$$

where: $\varepsilon(\ )$ is an absolute error.

$$\therefore \quad \varepsilon(\alpha m_1 - \beta m_1) \leq 0.07 \sqrt{\alpha m_2^2 + \alpha m_3^2} + 0.07 \sqrt{\beta m_2^2 + \beta m_3^2}$$

where: $\sqrt{\alpha m_2^2 + \alpha m_3^2}$ is the net acceleration field perpendicular to αm_1.

Since: $\alpha m_2 \doteqdot \beta m_2$ and $\alpha m_3 \doteqdot \beta m_3$ (see graphs opposite p.57)

$$\varepsilon(\alpha m_1 - \beta m_1) \leq 0.14 \sqrt{\alpha m_2^2 + \alpha m_3^2}$$

From equation 2.2 :

$$\underline{\alpha m} = \underline{\alpha} + \underline{g}$$

and from equation 2.9:

$$g_2 = \lambda_{32} \; ; \quad g_3 = \lambda_{33}$$

So: $$\varepsilon(\alpha m_1 - \beta m_1) = 0.14 \sqrt{(\alpha_2 + \lambda_{32})^2 + (\alpha_3 + \lambda_{33})^2}$$

Approximate values are known for $\alpha_2, \alpha_3, \lambda_{32}$, and λ_{33} and any errors in these terms introduces only 2nd. order errors. Using the Binomial Expansion,

$$(\alpha m_1 - \beta m_1) \leq 0.14 \sqrt{\alpha_2^2 + \lambda_{33}^2 + 2(\lambda_{32}\alpha_2 + \alpha_3\lambda_{33}) + \alpha_3^2 + \lambda_{32}^2}$$

$$\leq 0.14 \left(\lambda_{33} + \alpha_3 + \frac{\alpha_2}{\lambda_{33}}(\lambda_{32} + \alpha_2/2) + (\alpha_3^2 + \lambda_{32}^2)/2\lambda_{33}\right)$$

provided: $\lambda_{33} > \alpha_3 > \alpha_2 > \lambda_{32}$, as is usually the case.

Maximum values: $\lambda_{33} \doteqdot 1.0$

$\alpha_3 \doteqdot 0.5$

$\alpha_2 \doteqdot 0.3$

$\lambda_{32} \doteqdot 0.1$

i.e. $\varepsilon_{max.}(\alpha m_1 - \beta m_1) \doteqdot 0.24$

Now $|\alpha m_1 - \beta m_1|_{max} \doteqdot 2.0$ (see graphs opposite p.57)

$\therefore$ $e(\alpha m_1 - \beta m_1) \lesssim 0.12$ or 12%.

This limit is unreasonably high since it assumes that $\lambda_{33}, \alpha_3, \alpha_2$ and λ_{32} all reach maxima at the same instant. In practice, this is not so and $e(\alpha m_1 - \beta m_1)_{max}$ is a function of time. Using data from the subject in Chapter 3, the following values are found:

$e(\alpha m_1 - \beta m_1) \lesssim 6\%$ at max. knee flexion

$e(\alpha m_1 - \beta m_1) \lesssim 0.5\%$ at mid-stance phase.

Now: $e(L) \doteqdot 4\%$ (the exact transducer separation is an unknown function of internal geometry)

$\therefore$ $e(\dot{\omega}_2) \lesssim 10\%$ at max. knee flexion.

and $e(\dot{\omega}_2) \lesssim 5\%$ in mid-stance phase.

The integration of $\dot{\omega}_2$ to ω_2 will preferentially decrease errors at higher harmonics of the step-cycle. An examination of the components of $\varepsilon(\alpha m_1 - \beta m_1)$ shows that the second harmonic predominates in $\varepsilon(\dot{\omega}_2)$, whereas the fundamental is the dominant term in $\dot{\omega}_2$. Thus: $e(\omega_2) < e(\dot{\omega}_2)$.

Whence: $e(\omega_2) < 10\%$ at max. knee flexion.

and $e(\omega_2) < 5\%$ in mid-stance phase

A less fortuitous situation exists when $\dot{\omega}_1$ is integrated to ω_1. The major cross-coupling error is due to terms with the same period as ω_2, namely those with a dominant fundamental, whereas ω_1 is largest in the 2nd. harmonic.

Thus: $e(\omega_1)=e(\dot{\omega}_1)$

Now: $e(\dot{\omega}_1) \doteqdot 5\ e(\dot{\omega}_2)$

since: $|\alpha m_1-\beta m_1| \doteqdot 5|\ \alpha m_2-\beta m_2$ (see graphs opposite p.57)

$\therefore\ e(\omega_1)_{max} > 50\%$ due to orthogonality errors.

It must be noted that ω_1 will also have an error term due to $\int\omega_2\omega_3$ (see p.39), introduced because $\omega_3\neq 0$. As the actual value of ω_3 is unknown, it is not possible to evaluate this term with any accuracy. It would certainly be possible for the total error in the estimate of ω_1 to exceed 100%. While this is certainly a very large relative error, it will be shown in the next section that no variables of large relative magnitude are found solely from ω_1.

E.2 Errors in the estimates of the transformation matrix, $[\lambda]$

Besides the errors due to approximate values of ω_1 and ω_2, the estimates of the elements of $[\lambda]$ may be inaccurate on two counts. First, the initial value of $[\lambda]$ may be in error and second, the assumption that $\omega_3 \equiv 0$ will introduce further errors.

Considering first the initial value of $[\lambda]$; this is found from the measured acceleration in two near-horizontal directions. It has been shown (p.36) that measurements of acceleration with the present transducers may have a zero error of up to 0.1g, or 10% of the maximum possible value in this case. This corresponds to an angular error of 5^{o}-6^{o}.

To this should be added the possible cross-axis sensitivity of 7% (see E.1). However, since the acceleration measurements themselves are approximately zero, this contribution will be neglibible by comparison with the zero error. It is worth noting that this is the only circumstance in which zero errors exceed cross-axis sensitivity errors since the former are otherwise filtered out by the analysis programs.

A determination of the effect of assuming that $\omega_3 \equiv 0$ is complicated by the fact that it is not possible to write down a vector $\underline{\omega}$ as an explicit function of time and to derive a corresponding analytical solution for $[\lambda]$, since $\underline{\omega}$ is an explicit function of $[\lambda]$. To test the effect of making $\omega_3 \equiv 0$ in a numerical solution for $[\lambda]$, exact expressions for $[\lambda]$ and $\underline{\omega}$ were found in terms of three Euler Angles; ϕ, Θ and ψ.

ϕ is a primary rotation about axis 2

Θ is a secondary rotation about axis 1, after rotation ϕ

ψ is a tertiary rotation about axis 2, after rotations ϕ and Θ.

$$[\lambda] = \begin{bmatrix} \cos\phi\cos\psi & \sin\phi\sin\Theta & \cos\phi\sin\psi \\ -\sin\phi\cos\Theta\sin\psi & & +\sin\phi\cos\Theta\cos\psi \\ \sin\Theta\sin\psi & \cos\Theta & -\sin\Theta\cos\psi \\ -\sin\phi\cos\psi & \cos\phi\sin\Theta & -\sin\phi\sin\psi \\ -\cos\phi\cos\Theta\sin\psi & & +\cos\phi\cos\Theta\cos\psi \end{bmatrix}$$

$$\underline{\omega} = \begin{Bmatrix} \dot{\phi}\sin\Theta\sin\psi + \dot{\Theta}\cos\psi \\ \dot{\phi}\cos\Theta + \dot{\psi} \\ -\dot{\phi}\sin\Theta\cos\psi + \dot{\Theta}\sin\psi \end{Bmatrix}$$

A test program has been written in which periodic Euler Angles of different relative amplitudes and frequencies can be used to investigate the difference bttween the exact analytical solution for $[\lambda]$ (given above) and a numerical approximation which uses the same algorithms as M4EXT, the kinematic analysis program. (Trapezoidal integration; sampling at 100 times fundamental frequency; $\omega_3 \equiv 0$).

A number of different functions of time were tried for ϕ, Θ and ψ until the resulting values of ω_1, ω_2 and ω_3 approximated to the real case, i.e. 1.5:7:1. In this case, neglecting ω_3 produced errors in λ_{12} and λ_{21} (as predicted on p.42) which corresponded to maximum angular errors of 8°. These errors increase most rapidly when the instantaneous value of ω_2 is small and ω_1 and ω_3 are relatively large.

It was shown in the last section that ω_1 and ω_2 can have maximum relative errors of ~100% and ~10% respectively. Equations 2.30-2.38 (p.41) indicate that λ_{21}, λ_{22} and λ_{23} will suffer the greatest errors due to ω_1. In equation 2.34 ω_1 is multiplied by near-zero λ_{32}, so that $\lambda_{22} = 0$. In the two remaining equations which contain only ω_1, namely $\dot{\lambda}_{21}=\omega_1\lambda_{31}$ and $\dot{\lambda}_{23}=\omega_1\lambda_{33}$, λ_{21} and λ_{23} may be in error by 100%. However, exact values of λ_{21} and λ_{23} are near-zero so that the errors in λ_{21} and λ_{23} are not unreasonably large.

E.3 Accuracy of Integration and Overall Program Accuracy.

A generalised verification of the analysis programs is almost impossible for the reasons stated in the previous section

namely that is not possible to specify generalised input variables for which there is a known analytical solution. Equations of the form $\ddot{x}+f(t)x+g(t)=0$ are produced for which there are no general solutions.

Simple trapezoidal integration, such as is used throughout the analysis has been tested for accuracy and found to be accurate to within 1% for all frequency components except those which occur in the acceleration values at heel-strike. For instance, the program which has been written to test for the effects of the approximation $\omega_3 \equiv 0$ shows that, provided ω_3 is indeed equal to zero, $[\lambda]$ is found to an accuracy of 0.0012 (0.06^{o}) when ω is 0.01 times the sample rate, and 0.008 (0.45^{o}) when ω is up to 0.2 times the sample rate. Clearly integration errors are extremely small by comparison with other errors introduced into the solutions by inaccurate measurement.

E.4. Summary.

The major sources of error are:

a) Cross-axis sensitivity and non-orthogonal mounting

b) Approximating $\omega_3 \equiv 0$

c) Zero-errors in transducers effecting initial angular displacements.

These combine to produce the following <u>maximum</u> possible errors:

ω_1	~ 100%	($\pm$ 0.5 r/s)
ω_2	~ 10%	($\pm$ 0.5 r/s)
λ	~ 6^{o}	initial error
	$+8^{o}$	cumulative

Errors in translational variables are due almost entirely to the error in $[\lambda]$, e.g. maximum error in ankle height = stride length x $\tan(6^{o}+8^{o}) \equiv 150$ mm. (without periodic correction).

The results presented in Chaps. 3 and 4 are clearly considerably more accurate than is indicated here, and the comparison test with cine photography shows good agreement. It may be concluded that the ability of the experimenter to disregard poor data in the interactive programs introduces an unquantifiable improvement. Data is not rejected unless clearly impossible results are obtained (subject walks down into the ground). In terms of the clinical usefulness of the system, the shape of graphs is as important as their magnitude. In this context, it is interesting to note that the graphs of $\underline{\omega}$ (Figs.4.14-4.16) show clearly the phase characteristics of ω_2 imposed on ω_1, making ω_1 useless for this sort of assessment.

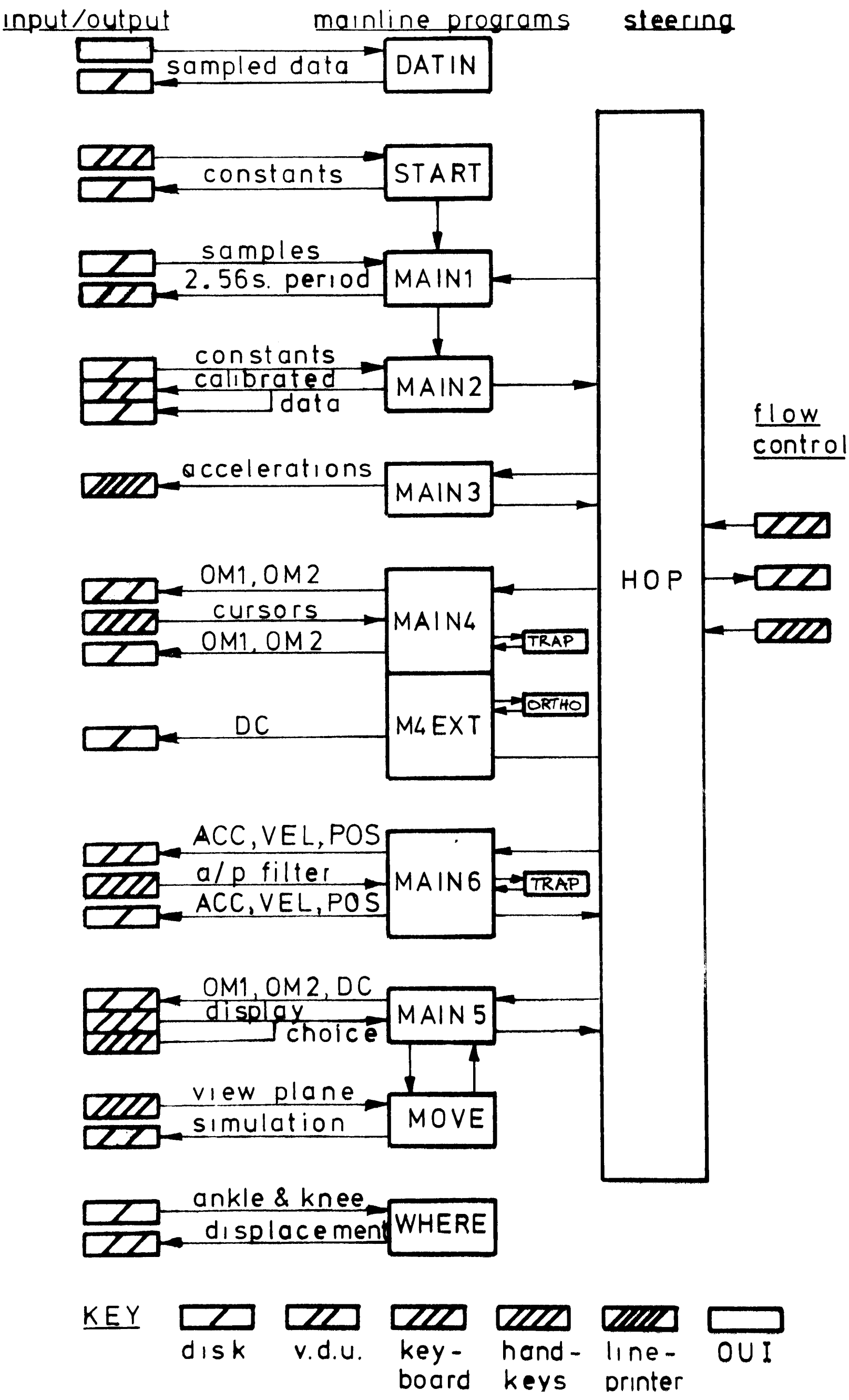
Improved transducers would reduce error (a), eliminate the need for approximation (b) and reduce error (c). There is room for considerable improvements in the accuracy of all these items before other factors become significant.

APPENDIX D

PROGRAM FLOW BLOCK DIAGRAM AND PROGRAM LISTINGS

Program Flow Diagram	A9
TRAP, ORTHO	A10
DATIN	A11
START	A12
MAIN1	A13
HOP	A14
MAIN2	A15
MAIN3	A17
MAIN4	A18
M4EXT	A21
MAIN6	A23
MAIN5	A25
MOVE	A27
FILM	A30
WHERE	A32

Figure D1 PROGRAM FLOW DIAGRAM



```
// FOR
* NAME TRAP
*ONE WORD INTEGERS
      SUBROUTINE TRAP(T,A,B,N)
      DIMENSION A(1000),B(1000)
      DO 11 I=2,N
   11 B(I)=B(I-1)+T*(A(I)+A(I-1))/2.0
      RETURN
      END

// DUP
*DELETE                TRAP
*STORE       WS  UA    TRAP
```

```
// FOR
*ONE WORD INTEGERS
      SUBROUTINE ORTHO(DC,NMAX,QTEST,ISET)
      DIMENSION DC(3,3),DCT(3,3),PROD(3,3),TEST(3,3)
      N=0
    4 DO 5 I=1,3
      DO 5 J=1,3
    5 DCT(I,J)=DC(J,I)
      DO 6 I=1,3
      DO 6 J=1,3
    6 PROD(I,J)=DCT(I,1)*DC(1,J)+DCT(I,2)*DC(2,J)+DCT(I,3)*DC(3,J)
      DO 8 I=1,3
      DO 8 J=1,3
      IF(I-J) 8,7,8
    7 PROD(I,J)=PROD(I,J)-1.0
    8 TEST(I,J)=PROD(I,J)/2.0
      Q=0.0
      DO 10 I=1,3
      DO 10 J=1,3
      IF (ABS(TEST(I,J))-Q) 10,10,9
    9 Q=ABS(TEST(I,J))
   10 CONTINUE
      IF (Q-QTEST)  18,18,11
   11 DO 13 I=1,3
      DO 13 J=1,3
      IF (I-J) 21,12,21
   12 TEST(I,J)=1.0-TEST(I,J)
      GO TO 13
   21 TEST(I,J)=-TEST(I,J)
   13 CONTINUE
      DO 14 I=1,3
      DO 14 J=1,3
   14 DC(I,J)=DC(I,1)*TEST(1,J)+DC(I,2)*TEST(2,J)+DC(I,3)*TEST(3,J)
      N=N+1
      IF (N-NMAX) 15,15,16
   15 GO TO 4
   18 ISET=0
      GO TO 100
   16 ISET=1
  100 RETURN
      END

// DUP
*DELETE                ORTHO
*STORE       WS  UA    ORTHO
```

```
// FOR
*IOCS(TYPEWRITER,KEYBOARD)
*NAME DATIN
*ONE WORD INTEGERS
      DIMENSION L1(322),L2(322),D(322)
      COMMON ISCAN(8)
      EQUIVALENCE (L1(2),D(1)),(L2(2),D(162))
      CALL IREQ
      ISECT=348
      ISCTL=ISECT+370
      L1(321)=ISECT
      L1(322)=0
      CALL FILER(L1(322),1)
      CALL INHIB
      CALL SINT1
      ISECT=ISECT-1
      ISW=1
      I=-4
      L1(322)=320
      L2(322)=320
      PAUSE1111
      CALL ALLOW
      PAUSE2222
      CALL SINT2
      CALL DATSW(0,K)                          <-- A
      GO TO(300,5),K
    5 CALL SCAN                                <-- B
      GO TO (100,200),ISW
  100 I=I+5
      L1(I)=ISCAN(1)
      L1(I+1)=ISCAN(2)
      L1(I+2)=ISCAN(3)
      L1(I+3)=ISCAN(4)
      L1(I+4)=ISCAN(5)
      IF(I-316) 10,110,110
   10 CONTINUE
      PAUSE                                    <-- C
  110 ISECT=ISECT+1
      L1(321)=ISECT
      ISW=2
      I=-4
      IF(ISECT-ISCTL)115,300,300
  115 CALL FILER(L1(322),1)                    <-- D
      PAUSE
  200 I=I+5
      L2(I)=ISCAN(1)
      L2(I+1)=ISCAN(2)
      L2(I+2)=ISCAN(3)
      L2(I+3)=ISCAN(4)
      L2(I+4)=ISCAN(5)
      IF(I-316) 11,210,210
   11 CONTINUE
      PAUSE                                    <-- C'
  210 ISECT=ISECT+1
      L2(321)=ISECT
      ISW=1
      I=-4
      IF(ISECT-ISCTL)215,300,300
  215 CALL FILER(L2(322),1)                    <-- D'
      PAUSE
  300 CONTINUE
      CALL INHIB
      WRITE (1,400)
  400 FORMAT ('TURN OFF INTERRUPTS, THEN LIFT BITSW 15')
  500 CALL DATSW (15,IGO)
      GO TO (700,600),IGO
  600 GO TO 500
  700 CALL EXIT
      END

// DUP
*DELETE              DATIN
*STORECI    WS  UA   DATIN                    N
```

```
// FOR
*NAME START
*IOCS(DISK,1403 PRINTER,KEYBOARD)
*ONE WORD INTEGERS
      COMMON IDUM1(3844),NMAIN,ITEST
      DEFINE FILE 100(15,2,U,II)
      CALL CINIT(3840)
      CALL CON
      CALL CXYST(0,100)
      WRITE (5,100)
  100 FORMAT ('PROGRAM (START) SETS UP INITIAL CONDITIONS',/
     *        'AND THEN LINKS TO PROGRAM (HOP)',//
     *        '(HOP) IS THE MASTER STEERING PROGRAM FOR',/
     *        'ANALYSIS OF DATA FILED BY (DATIN)',//
     *        'PRESS PROG START TO CONTINUE')
      PAUSE
      CALL IREQ
      CALL CLEAR
      CALL CXYST(10,10)
      WRITE(5,200)
  200 FORMAT('ENTER FIXED PARAMETERS FOR THIS RUN'///
     *       'AOS1,BOS1,AOS2,BOS2,AOS3')
      CALL CYINC(16)
      CALL CDATA(5,AOS1,BOS1,AOS2,BOS2,AOS3)
      CALL CYINC(16)
      WRITE(5,300)
  300 FORMAT('AG1,BG1,AG2,BG2,AG3')
      CALL CYINC(16)
      CALL CDATA(5,AG1,BG1,AG2,BG2,AG3)
      CALL CYINC(16)
      WRITE(5,400)
  400 FORMAT('ADC SENSITIVITY (VOLTS), TIBIA ROTATION (DEG),'/
     *       'SAMPLE TIME (SEC),SHANK LENGTH (MM),'/
     *       'PLATFORM/ANKLE DISTANCE (MM)')
      CALL CYINC(16)
      CALL CDATA(5,SENS,THETA,T,SHANK,PAD)
      CALL CYINC(16)
      WRITE(5,500)
  500 FORMAT('CHECK....THEN, PRESS START')
      PAUSE6666
      II=1
      WRITE(100'II) AOS1,BOS1,AOS2,BOS2,AOS3,AG1,BG1,AG2,BG2,AG3,
     *              SENS,THETA,T,SHANK,PAD
      NMAIN=1
      ITEST=0
      CALL COFF
      CALL LINK(HOP)
      END

// DUP
*DELETE                START
*STORECI     WS  UA  START     1              N
*FILES(100,KIN00)
```

```
// FOR
*NAME MAIN1
*ONE WORD INTEGERS
      DIMENSION L(3842),D(1921),ISIFT(16)
      COMMON L,J1,J2,NMAIN,ITEST
      EQUIVALENCE (L(2),D(1))
      DATA ISIFT/0,1,2,4,8,16,32,64,0,-1,-2,-4,-8,-16,-32,-64/
      NMAIN=1
      ISECT=348
      ISCTL=ISECT+370
      J1=1
      J2=J1
      DO 300 I=1,12
      L(320*I+2)=320
      L(320*I+1)=ISECT+(I-1)
      CALL FILER(L(320*I+2),0)
      CALL DBUSY
  300 CONTINUE
    1 CALL HDATA(IAA,IAA,IB,IA)
      IF (IB) 3,3,2
    2 J3=IB
      GO TO 4
    3 J3=J2
    4 CONTINUE
      J4=J3-J2
      J2=J3
      J1=J1+J4
      IA=IA+1
      J1=J1+ISIFT(IA)*5
      IF(J1) 10,10,50
   10 ISECT=ISECT-4
      J1=J1+1280
      GO TO 70
   50 IF(J1-1920) 90,90,55
   55 ISECT=ISECT+4
      J1=J1-1280
   70 CONTINUE
      DO 21 I=1,12
      L(320*I+2)=320
      L(320*I+1)=ISECT+(I-1)
      CALL FILER(L(320*I+2),0)
      CALL DBUSY
   21 CONTINUE
   90 CONTINUE
   95 CALL DATSW(7,JGO)
      GO TO(100,110),JGO
  100 CALL SHOWA(L(J2),192,1,0,12,20)
      GO TO 95
  110 CONTINUE
      CALL SHOWA(L(J1),240,1,0,12,5)
      CALL DATSW(0,IGO)
      GO TO (200,201),IGO
  201 CALL DATSW(1,IGO)
      GO TO (400,1),IGO
  200 ITEST=0
      CALL LINK(HOP)
  400 ITEST=1
      CALL LINK(HOP)
      END

// DUP
*DELETE                MAIN1
*STORECI    WS  UA  MAIN1                    N
```

```
// FOR
*NAME HOP
*IOCS(TYPEWRITER,KEYBOARD,1403 PRINTER)
*ONE WORD INTEGERS
      COMMON IDUM1(3844),NMAIN,ITEST
      IF (NMAIN-1) 5,2,5
    2 IF (ITEST) 4,3,4
    3 CALL IREQ
      CALL LINK(MAIN1)
    4 CALL LINK(MAIN2)
    5 IF (NMAIN-2) 14,6,14
    6 IF (ITEST) 7,81,7
    7 CALL CINIT(2000)
      CALL CON
      CALL CXYST(0,100)
      WRITE (5,8)
    8 FORMAT ('FILES 1 AND 2 UPDATED')
      GO TO 9
   81 CALL CINIT(2000)
      CALL CON
      CALL CXYST(0,100)
    9 WRITE (5,16)
      WRITE (5,160)
      WRITE (5,10)
      WRITE (5,17)
   10 FORMAT ('IF HARD COPY OF FILES 1 AND 2 IS REQUIRED,'/'TYPE 3')
      CALL CYINC(16)
      CALL CXSET(120)
      CALL CDATA(1,1)
      CALL COFF
      IF (I-3) 111,110,111
  110 CALL LINK(MAIN3)
  111 IF (I-2) 12,11,12
   11 CALL LINK(MAIN4)
   12 IF (I-1) 50,3,50
   14 IF (NMAIN-3) 50,15,20
   15 CALL CINIT(2000)
      CALL CON
      CALL CXYST(0,100)
      WRITE (5,16)
   16 FORMAT ('IF NEW DATA IS REQUIRED,  TYPE 1')
      WRITE (5,160)
  160 FORMAT ('IF KINEMATICS ARE REQUIRED,  TYPE 2')
      WRITE (5,17)
   17 FORMAT ('OTHERWISE,  TYPE 0')
      CALL CYINC(16)
      CALL CXSET(120)
      CALL CDATA(1,1)
      CALL COFF
      IF (I-1) 50,3,18
   18 IF (I-2) 50,19,15
   19 CALL LINK(MAIN4)
   20 IF (NMAIN-4) 50,21,25
   21 CALL CINIT (2000)
      CALL CON
      CALL CXYST (20,120)
      WRITE (5,210)
  210 FORMAT('KINEMATICS COMPLETE  - '//
     *       '                FILES 3,4, AND 5 UPDATED')
      WRITE (5,230)
  230 FORMAT ('TO DISPLAY RESULTS,  TYPE 1')
      WRITE (5,17)
      CALL CYINC(16)
      CALL CXSET(120)
      CALL CDATA(1,1)
      CALL COFF
      IF (I-1) 25,24,21
   24 CALL LINK(MAIN5)
   25 PAUSE
   50 CALL EXIT
      END

// DUP
*DELETE                HOP
*STORECI    WS  UA  HOP                      N
```

```
// FOR
*NAME MAIN2
*IOCS(DISK,1403 PRINTER)
*ONE WORD INTEGERS
      DIMENSION L(3842),LL(1280),AM(3,256),BM(2,256)
      DIMENSION AMB1(256),AMB2(256),BUF1(256),BUF2(256)
      COMMON L,J1,J2,NMAIN,ITEST
      DEFINE FILE 100(15,2,U,II)
      DEFINE FILE 1(768,2,U,MM)
      DEFINE FILE 2(512,2,U,NN)
      NMAIN=2
      J3=J1+1-J2
      JK=J3+1279
      DO 11 I=J3,JK
      J4=I-J3+1
      LL(J4)=L(I)
   11 CONTINUE
      II=1
      READ(100'II) AOS1,BOS1,AOS2,BOS2,AOS3,AM1,BM1,AM2,BM2,AM3,
     *             SENS,THETA
      SENS=SENS/4096.0
      DO 15 I=1,256
      J=I*5-4
      AM(1,I)=(LL(J)*SENS-AOS1)/AM1
      BM(1,I)=(LL(J+1)*SENS-BOS1)/BM1
      AM(2,I)=(LL(J+2)*SENS-AOS2)/AM2
      BM(2,I)=(LL(J+3)*SENS-BOS2)/BM2
      AM(3,I)=(LL(J+4)*SENS-AOS3)/AM3
   15 CONTINUE
      THETA=THETA*3.142/180.0                    ]
      C=COS(THETA)                               ]------ A
      S=SIN(THETA)                               ]
      GMAX1=0.0
      GMAX2=0.0
      GMAX3=0.0
      GMAX4=0.0
      GMAX5=0.0
      DO 30 I=1,256
      QAM=AM(1,I)*C+AM(2,I)*S                    ]
      RAM=BM(1,I)*C+BM(2,I)*S                    ]
      AM(2,I)=AM(2,I)*C-AM(1,I)*S                ]------ B
      BM(2,I)=BM(2,I)*C-BM(1,I)*S                ]
      AM(1,I)=QAM                                ]
      BM(1,I)=RAM                                ]
      AMB1(I)=AM(1,I)-BM(1,I)
      AMB2(I)=AM(2,I)-BM(2,I)
      IF (ABS(AM(1,I))-GMAX1) 18,18,17
   17 GMAX1=ABS(AM(1,I))
   18 IF (ABS(BM(1,I))-GMAX1) 20,20,19
   19 GMAX1=ABS(BM(1,I))
   20 IF (ABS(AM(2,I))-GMAX2) 22,22,21
   21 GMAX2=ABS(AM(2,I))
   22 IF (ABS(BM(2,I))-GMAX2) 24,24,23
   23 GMAX2=ABS(BM(2,I))
   24 IF (ABS(AM(3,I))-GMAX3) 26,26,25
   25 GMAX3=ABS(AM(3,I))
   26 IF (ABS(AMB1(I))-GMAX4) 28,28,27
   27 GMAX4=ABS(AMB1(I))
   28 IF (ABS(AMB2(I))-GMAX5) 30,30,29
   29 GMAX5=ABS(AMB2(I))
   30 CONTINUE
      MAX1=IFIX(GMAX1+1.0)
      MAX2=IFIX(GMAX2+1.0)
      MAX3=IFIX(GMAX3+1.0)
      MAX4=IFIX(GMAX4+1.0)
      MAX5=IFIX(GMAX5+1.0)
      GMAX1=FLOAT(MAX1)
      GMAX2=FLOAT(MAX2)
      GMAX3=FLOAT(MAX3)
      GMAX4=FLOAT(MAX4)
      GMAX5=FLOAT(MAX5)
      CALL CINIT(3000)
      CALL CON
      CALL CXYST(6,29)
      WRITE(5,31)
   31 FORMAT('A(1)',/'AND',/'B(1)')
      CALL CXYST(6,115)
      WRITE(5,32)
   32 FORMAT('A(2)',/'AND',/'B(2)')
```

```
      CALL CXYST(6,210)
      WRITE(5,33)
   33 FORMAT('A(3)')
      CALL CXYST(134,29)
      WRITE(5,34)
   34 FORMAT('A(1)',/' - ',/'B(1)')
      CALL CXYST(134,115)
      WRITE(5,35)
   35 FORMAT('A(2)',/' - ',/'B(2)')
      DO 36 I=31,33
      CALL CPUT(I,4)
      CALL CPUT(I,79)
      CALL CPUT(I,90)
      CALL CPUT(I,165)
      CALL CPUT(I,176)
      CALL CPUT(I,251)
   36 CONTINUE
      DO 37 I=159,161
      CALL CPUT(I,4)
      CALL CPUT(I,79)
      CALL CPUT(I,90)
      CALL CPUT(I,165)
   37 CONTINUE
      CALL CXYST(34,4)
      WRITE(5,38) MAX1
   38 FORMAT(I2,' G')
      CALL CXYST(34,90)
      WRITE(5,38) MAX2
      CALL CXYST(34,176)
      WRITE(5,38) MAX3
      CALL CXYST(162,4)
      WRITE(5,38) MAX4
      CALL CXYST(162,90)
      WRITE(5,38) MAX5
      DO 39 I=1,256
      BUF1(I)=AM(1,I)
      BUF2(I)=BM(1,I)
   39 CONTINUE
      CALL CXYST(30,4)
      CALL CXYND(127,79)
      CALL CDISP(34,255,2,-GMAX1,GMAX1,BUF1,BUF2)
      DO 40 I=1,256
      BUF1(I)=AM(2,I)
      BUF2(I)=BM(2,I)
   40 CONTINUE
      CALL CXYST(30,90)
      CALL CXYND(127,165)
      CALL CDISP(34,255,2,-GMAX2,GMAX2,BUF1,BUF2)
      DO 41 I=1,256
      BUF1(I)=AM(3,I)
   41 CONTINUE
      CALL CXYST(30,176)
      CALL CXYND(127,251)
      CALL CDISP(34,255,1,-GMAX3,GMAX3,BUF1)
      CALL CXYST(158,4)
      CALL CXYND(255,79)
      CALL CDISP(34,255,1,-GMAX4,GMAX4,AMB1)
      CALL CXYST(158,90)
      CALL CXYND(255,165)
      CALL CDISP(34,255,1,-GMAX5,GMAX5,AMB2)
      CALL CXYST(158,200)
      PAUSE7777
      CALL DATSW(0,IGO)
      GO TO (43,44),IGO
   43 MM=1
      WRITE(1'MM) AM
      NN=1
      WRITE(2'NN) BM
      ITEST=1
      CALL COFF
      CALL LINK(HOP)
   44 ITEST=0
      CALL COFF
      CALL LINK(HOP)
      END

// DUP
*DELETE                MAIN2
*STORECI    WS  UA  MAIN2      1              N
*FILES(1,KIN01),(2,KIN02),(100,KIN00)
```

```
// FOR
*IOCS(1132 PRINTER,DISK)
*NAME MAIN3
*ONE WORD INTEGERS
      COMMON DUM1(1280),IDUM2(1284),NMAIN,IDUM3
      DEFINE FILE 1(768,2,U,MM)
      DEFINE FILE 2(512,2,U,NN)
      NMAIN=3
      WRITE (3,10)
   10 FORMAT (1H1,45X,'CALIBRATED ACCELERATIONS'/1H ,45X,24(1H*)/////)
      WRITE (3,11)
   11 FORMAT (1H ,111(1H*)/1H ,1H*,1X,'SAMPLE',2X,1H*,7X,'AM(1)',7X,1H*,
     *          7X,'BM(1)',7X,1H*,7X,'AM(2)',7X,1H*,7X,'BM(2)',7X,1H*,
     *          7X,'AM(3)',7X,1H*/1H ,111(1H*))
      MM=1
      NN=1
      DO 13 I=1,256
      READ (1'MM) A,C,E
      READ (2'NN) B,D
      WRITE (3,12) I,A,B,C,D,E
   12 FORMAT (1H ,1H*,3X,I3,3X,1H*,5(5X,F8.4,6X,1H*))
      CALL DATSW (0,K)
      GO TO (15,13),K
   13 CONTINUE
   15 WRITE (3,14)
   14 FORMAT (1H ,111(1H*))
      CALL LINK(HOP)
      END

// DUP
*DELETE                MAIN3
*STORECI     WS  UA  MAIN3     1            N
*FILES(1,KIN01),(2,KIN02)
```

```
// FOR
*NAME MAIN4
*ONE WORD INTEGERS
*IOCS(DISK,1403 PRINTER)
      DIMENSION AM(3,256),BM(2,256),OM1(256),OM2(256)
      DIMENSION CM(256),SCM(256)
      DIMENSION BUF1(256),BUF2(256)
      COMMON IDUM1(3844),NMAIN,IDUM2
      DEFINE FILE 100(15,2,U,II)
      DEFINE FILE 1(768,2,U,MM)
      DEFINE FILE 2(512,2,U,NN)
      DEFINE FILE 3(256,2,U,MN)
      DEFINE FILE 4(256,2,U,NM)
      DEFINE FILE 5(2305,2,U,LL)
      DATA QL/125.0/
      QL=QL/9810.0
      NMAIN=4
      II=13
      READ (100'II) T
      MM=1
      READ (1'MM) AM
      NN=1
      READ (2'NN) BM
      DO 300 I=1,256
  300 CM(I)=AM(1,I)-BM(1,I)
      SCM(1)=0.0
      CALL TRAP(T,CM,SCM,256)
      DO 400 I=1,256
  400 OM2(I)=SCM(I)/QL                          <-- A
      DO 500 I=1,256
  500 CM(I)=AM(2,I)-BM(2,I)
      SCM(1)=0.0
      CALL TRAP(T,CM,SCM,256)
      DO 600 I=1,256
  600 OM1(I)=-SCM(I)/QL                         <-- B
      II=1
      JJ=1
  113 CONTINUE
      OM1MX=0.0
      OM2MX=0.0
      DO 118 I=1,256
      IF (ABS(OM1(I))-OM1MX) 116,116,115
  115 OM1MX=ABS(OM1(I))
  116 IF (ABS(OM2(I))-OM2MX) 118,118,117
  117 OM2MX=ABS(OM2(I))
  118 CONTINUE
      ISCL1=IFIX(OM1MX+1.0)
      ISCL2=IFIX(OM2MX+1.0)
      CALL CINIT (3000)
      CALL CON
      CALL CXYST(4,0)
      WRITE(5,119) ISCL1
  119 FORMAT (I2,' RAD/SEC')
      CALL CPUT(1,0)
      CALL CPUT(2,0)
      CALL CPUT(3,0)
      CALL CXYST(0,0)
      CALL CXYND(255,100)
      RSCAL=FLOAT(ISCL1)
      CALL CDISP(34,255,1,-RSCAL,RSCAL,OM1)
      CALL CPUT(1,100)
      CALL CPUT(2,100)
      CALL CPUT(3,100)
      CALL CXYST(4,110)
      WRITE (5,119) ISCL2
      CALL CPUT(1,110)
      CALL CPUT(2,110)
      CALL CPUT(3,110)
      CALL CXYST(0,110)
      CALL CXYND(255,210)
      RSCAL=FLOAT(ISCL2)
      CALL CDISP(34,255,1,-RSCAL,RSCAL,OM2)
      CALL CPUT(1,210)
      CALL CPUT(2,210)
      CALL CPUT(3,210)
```

```
      CALL CXYST(0,214)
      WRITE (5,101)
  101 FORMAT ('100 MS, LEVEL 3 INTS MOVE CURSORS',/
     *        'START / BS(10)=L / BS(11)=R /',/
     *        'END / BS(14)=L / BS(15)=R /',/
     *        'BS(0) TO LOCK, BS(1) TO MISS',/
     *        'FILTER RECYCLE, PRESS START TO CONT')
      CALL CPOS(IPOS)
      CALL SINT1
      CALL ALLOW
      II=II-1
      JJ=JJ-1
  102 CONTINUE
      DO 103 JK=1,22
      CALL CPUT(II,10*(JK-1))
  103 CALL CPUT(JJ,10*(JK-1))
      CALL DATSW(0,IGO)
      GO TO (109,107),IGO
  107 CONTINUE
      CALL DATSW(10,IGO)
      GO TO (125,124),IGO
  124 CALL DATSW(11,IGO)
      GO TO (126,127),IGO
  125 II=II-1
      GO TO 127
  126 II=II+1
  127 CONTINUE
      CALL DATSW(14,IGO)
      GO TO (105,104),IGO
  104 CALL DATSW(15,IGO)
      GO TO (106,108),IGO
  105 JJ=JJ-1
      GO TO 108
  106 JJ=JJ+1
  108 PAUSE7777
      CALL CRSTR(IPOS)
      GO TO 102
  109 CALL INHIB
      PAUSE1111
      IF(JJ-II) 128,128,1301
 1301 IF(II) 128,1302,1302
 1302 IF(JJ-255) 130,130,128
  128 CALL CINIT(2000)
      CALL CON
      CALL CXYST(0,120)
      WRITE(5,129)
  129 FORMAT ('YOU''VE GOT YOUR CURSORS OVERLAPPED,'/
     *        'BACKWARDS, OR OFF-SCALE.'/
     *        'PRESS PROG START')
      PAUSE
      CALL COFF
      GO TO 113
  130 CALL DATSW(1,IGO)
      II=II+1
      JJ=JJ+1
      GO TO (112,110),IGO
  110 CONTINUE
```

```
      DIF1=(OM1(JJ)-OM1(II))/(JJ-II)
      DIF2=(OM2(JJ)-OM2(II))/(JJ-II)
      DO 111 I=1,256
      OM1(I)=OM1(I)-DIF1*(I-1)
  111 OM2(I)=OM2(I)-DIF2*(I-1)
      IE=JJ-II+1
      DO 1111 I=1,IE
      IJ=I+II-1
      BUF1(I)=OM1(IJ)
 1111 BUF2(I)=OM2(IJ)
      SCM(1)=0.0
      CALL TRAP(T,BUF1,SCM,IE)
      DIF1=(SCM(IE)-SCM(1))/((JJ-II)*T)
      SCM(1)=0.0
      CALL TRAP(T,BUF2,SCM,IE)
      DIF2=(SCM(IE)-SCM(1))/((JJ-II)*T)
      DO 121 I=1,256
      OM1(I)=OM1(I)-DIF1
  121 OM2(I)=OM2(I)-DIF2
      GO TO 113
  112 CONTINUE
      MN=1
      WRITE (3'MN) OM1
      NM=1
      WRITE (4'NM) OM2
      LL=1
      WRITE(5'LL) II,JJ
      CALL LINK(M4EXT)
      END
```

C

D

```
// DUP
*DELETE                MAIN4
*STORECI     WS  UA    MAIN4      1              N
*FILES(100,KIN00),(1,KIN01),(2,KIN02),(3,KIN03),(4,KIN04),(5,KIN05)
```

```
// FOR
*NAME M4EXT
*IOCS(DISK,KEYBOARD,1403 PRINTER)
*ONE WORD INTEGERS
      DIMENSION AM(3,5),BM(2,5),RKAPP(3),DIRC(3,3),A(9),B(9)
      DIMENSION DC(3,3,256),OM1(256),OM2(256)
      COMMON IDUM1(2000),IDUM2(1844),NMAIN,IDUM3
      EQUIVALENCE (IDUM2(2),OM1(1)),(IDUM2(514),OM2(1))
      DEFINE FILE 100(15,2,U,II)
      DEFINE FILE 1(768,2,U,MM)
      DEFINE FILE 2(512,2,U,NN)
      DEFINE FILE 3(256,2,U,MN)
      DEFINE FILE 4(256,2,U,NM)
      DEFINE FILE 5(2305,2,U,LL)
      NMAIN=4
      CALL CLEAR
      II=13
      READ(100'II) T,PAD
      BIT=0.5-PAD/125.0                                          <-- A
      BOT=0.5+PAD/125.0
      LL=1
      READ (5'LL) IS,IF
      MM=3*(IS-3)+1
      READ(1'MM) AM
      NN=2*(IS-3)+1
      READ(2'NN) BM
      MN=1
      READ (3'MN) OM1
      NM=1
      READ (4'NM) OM2
      LL=1
      READ(5'LL) IS,IF
      AA1=0.2*(AM(1,1)+AM(1,2)+AM(1,3)+AM(1,4)+AM(1,5))          <-- B
      AA2=0.2*(AM(2,1)+AM(2,2)+AM(2,3)+AM(2,4)+AM(2,5))
      BB1=0.2*(BM(1,1)+BM(1,2)+BM(1,3)+BM(1,4)+BM(1,5))
      BB2=0.2*(BM(2,1)+BM(2,2)+BM(2,3)+BM(2,4)+BM(2,5))
      DC(3,1,1)=AA1*BIT+BB1*BOT
      DC(3,2,1)=AA2*BIT+BB2*BOT
      DC(3,3,1)=SQRT(1.0-DC(3,1,1)*DC(3,1,1)
     *                   -DC(3,2,1)*DC(3,2,1))
      DC(1,2,1)=0.0
      DC(2,2,1)=SQRT(1.0-DC(3,2,1)*DC(3,2,1))
      DC(2,1,1)=-DC(3,1,1)*DC(3,2,1)/DC(2,2,1)
      DC(1,3,1)=DC(2,1,1)*DC(3,2,1)-DC(2,2,1)*DC(3,1,1)
      DC(2,3,1)=DC(3,2,1)*DC(1,3,1)
      DC(1,1,1)=DC(2,2,1)*DC(3,3,1)-DC(2,3,1)*DC(3,2,1)
      III=IS+1
      B(1)=1.0
      B(2)=0.0
      B(4)=0.0
      B(5)=1.0
      B(9)=1.0
```

```
      DO 1400 L=III,IF
      N=L-IS+1
      B(3)=T*OM2(L)/2.0                    <-------- C
      B(6)=-T*OM1(L)/2.0
      B(7)=-T*OM2(L)/2.0
      B(8)=T*OM1(L)/2.0
      DO 1000 I=1,3
      RKAPP(1)=DC(1,I,N-1)+T*DC(3,I,N-1)*OM2(L-1)/2.0
      RKAPP(2)=DC(2,I,N-1)-T*DC(3,I,N-1)*OM1(L-1)/2.0
      RKAPP(3)=DC(3,I,N-1)+T*(DC(2,I,N-1)*OM1(L-1)
     *          -DC(1,I,N-1)*OM2(L-1))/2.0
      DO 800 J=1,9
  800 A(J)=B(J)
      CALL SIMQ(A,RKAPP,3,0)
      DO 900 J=1,3
  900 DC(J,I,N)=RKAPP(J)
 1000 CONTINUE
      DO 1010 I=1,3
      DO 1010 J=1,3
 1010 DIRC(I,J)=DC(I,J,N)
      CALL ORTHO(DIRC,50,0.005,ITEST)
      IF (ITEST-1) 1013,1011,1013
 1011 CALL CINIT(2000)
      CALL CON
      CALL CXYST(0,120)
      WRITE (5,1012) L
 1012 FORMAT ('ORTHO FAILS ON SAMPLE ',I3,//
     *        'PRESS START TO RECYCLE')
      PAUSE
      CALL COFF
      CALL LINK(MAIN4)
 1013 CONTINUE
      DO 1320 I=1,3
      DO 1320 J=1,3
 1320 DC(I,J,N)=DIRC(I,J)
 1400 CONTINUE
      LL=2
      WRITE(5'LL) DC
      CALL COFF
      CALL LINK(MAIN6)
      END

// DUP
*DELETE                M4EXT
*STORECI    WS  UA     M4EXT      1                N
*FILES(100,KIN00),(1,KIN01),(2,KIN02),(3,KIN03),(4,KIN04),(5,KIN05)
```

```
// FOR
*NAME MAIN6
*ONE WORD INTEGERS
*IOCS(DISK,1403 PRINTER)
      DIMENSION DC(3,3,256),AM(3,256),BM(2,256)
      DIMENSION ALPHA(3,256),VEL(3,256),POS(3,256),BUF(256),BUFA(256)
      DIMENSION TIT(2),TAT(2),TOT(2)
      COMMON IDUM(2000)
      EQUIVALENCE (DC(1),VEL(1))
      EQUIVALENCE (DC(769),POS(1))
      EQUIVALENCE (DC(1537),BUF(1))
      EQUIVALENCE (DC(1793),BUFA(1))
      DEFINE FILE 100(15,2,U,II)
      DEFINE FILE 1(768,2,U,MM)
      DEFINE FILE 2(512,2,U,NN)
      DEFINE FILE 5(2305,2,U,LL)
      DEFINE FILE 6(768,2,U,LM)
      DEFINE FILE 7(768,2,U,LN)
      DEFINE FILE 8(768,2,U,LI)
      DATA TIT/'M/SE',' C**2'/
      DATA TAT/'M/SE',' C   '/
      DATA TOT/'MM  ','     '/
      CALL INHIB
      II=13
      READ (100'II) T
      MM=1
      READ (1'MM) AM
      NN=1
      READ (2'NN) BM
      LL=1
      READ (5'LL) IS,IF,DC
      IL=IF-IS+1
      DO 11 I=1,IL
      DO 11 J=1,3
      IJ=I+IS-1
      ALPHA(J,I)=DC(J,1,I)*((AM(1,IJ)+BM(1,IJ))/2.0-DC(3,1,I))
     *          +DC(J,2,I)*((AM(2,IJ)+BM(2,IJ))/2.0-DC(3,2,I))
     *          +DC(J,3,I)*(AM(3,IJ)-DC(3,3,I))
      ALPHA(J,I)=ALPHA(J,I)*9.81
   11 CONTINUE
```

```
      CALL CINIT(2000)
      CALL CON
      II=1
      JJ=1
      KK=3
      LL=3
      MM=IL
      DO 53 ID=1,3
      DO 50 IP=1,IL
   50 BUF(IP)=ALPHA(ID,IP)
      BUFA(1)=0.0
      CALL TRAP(T,BUF,BUFA,IL)
      DIF=(BUFA(IL)-BUFA(1))/(IL-1)
      DUF=DIF/T
      DO 51 IP=1,IL
      BUF(IP)=BUF(IP)-DUF
      ALPHA(ID,IP)=BUF(IP)
   51 BUFA(IP)=BUFA(IP)-DIF*(IP-1)
      CALL CGRAF(II,JJ,KK,LL,MM,TIT,BUF)
      BUF(1)=0.0
      CALL TRAP(T,BUFA,BUF,IL)
      DIF=(BUF(IL)-BUF(1))/(IL-1)
      DUF=DIF/T
      DO 52 IP=1,IL
      BUFA(IP)=BUFA(IP)-DUF
      BUF(IP)=BUF(IP)-DIF*(IP-1)
      VEL(ID,IP)=BUFA(IP)
      POS(ID,IP)=BUF(IP)
   52 BUF(IP)=BUF(IP)*1000.0
      CALL CGRAF(II,JJ,KK,LL,MM,TAT,BUFA)
      CALL CGRAF(II,JJ,KK,LL,MM,TOT,BUF)
   53 CONTINUE
      PAUSE6767
      LM=1
      WRITE(6'LM) ALPHA
      LN=1
      WRITE (7'LN) VEL
      LI=1
      WRITE (8'LI) POS
      CALL COFF
      CALL LINK(MAIN5)
      END

// DUP
*DELETE                MAIN6
*STORECI     WS  UA    MAIN6     2              N
*FILES(100,KIN00),(1,KIN01),(2,KIN02),(5,KIN05)
*FILES(6,KIN06),(7,KIN07),(8,KIN08)
```

```
// FOR
*IOCS(DISK,TYPEWRITER,KEYBOARD,1403 PRINTER)
*NAME MAIN5
*ONE WORD INTEGERS
      DIMENSION BUF1(256),BUF2(256),DC(3,3,256)
      DIMENSION TIT(2),TAT(2)
      COMMON IDUM1(2000),IDUM2(1844),NMAIN,IDUM3
      EQUIVALENCE (BUF1(1),IDUM2(2)),(BUF2(1),IDUM2(514))
      DEFINE FILE 3(256,2,U,MN)
      DEFINE FILE 4(256,2,U,NM)
      DEFINE FILE 5(2305,2,U,LL)
      DATA TIT/'RAD/','SEC '/
      TAT(1)=0.0
      TAT(2)=0.0
      NMAIN=5
      CALL IREQ
   90 CALL CINIT(2000)
      CALL CON
      CALL CXYST (60,100)
      WRITE (5,100)
  100 FORMAT ('DISPLAY PROGRAM')
      DO 105 I=60,150
  105 CALL CPUT(I,110)
      CALL CXYST(0,120)
      WRITE(5,110)
  110 FORMAT ('CHOICES - ANGULAR VELOCITIES,  TYPE 1!,/
     *          '           DIRECTION COSINES,   TYPE 2!,/
     *          '           MOVEMENT SIMULATION, TYPE 3!,/
     *          '           PROGRAM END,         TYPE 0!)
      CALL CXSET(110)
      CALL CYINC(16)
      CALL CDATA(1,I)
      IF (I-1) 500,120,190
  120 LL=1
      READ(5'LL) IS,IF
      IFIN=IF-IS+1
      MN=IS
      READ(3'MN) (BUF1(IJ),IJ=1,IFIN)
      NM=IS
      READ(4'NM) (BUF2(IJ),IJ=1,IFIN)
      IX=1
      IY=1
      ISX=1
      ISY=2
      CALL CLEAR
      CALL CGRAF(IX,IY,ISX,ISY,IFIN,TIT,BUF1)
      CALL CGRAF(IX,IY,ISX,ISY,IFIN,TIT,BUF2)
      PAUSE1111
      GO TO 90
  190 IF (I-2) 90,200,220
  200 LL=1
      READ(5'LL) IS,IF,DC
      IFIN=IF-IS+1
      CALL CLEAR
      IX=1
      IY=1
      ISX=3
      ISY=3
      DO 211 I=1,IFIN
  211 BUF1(I)=DC(1,1,I)
      CALL CGRAF(IX,IY,ISX,ISY,IFIN,TAT,BUF1)
      DO 212 I=1,IFIN
  212 BUF1(I)=DC(1,2,I)
      CALL CGRAF(IX,IY,ISX,ISY,IFIN,TAT,BUF1)
      DO 213 I=1,IFIN
  213 BUF1(I)=DC(1,3,I)
      CALL CGRAF(IX,IY,ISX,ISY,IFIN,TAT,BUF1)
      DO 214 I=1,IFIN
  214 BUF1(I)=DC(2,1,I)
      CALL CGRAF(IX,IY,ISX,ISY,IFIN,TAT,BUF1)
      DO 215 I=1,IFIN
  215 BUF1(I)=DC(2,2,I)
      CALL CGRAF(IX,IY,ISX,ISY,IFIN,TAT,BUF1)
      DO 216 I=1,IFIN
  216 BUF1(I)=DC(2,3,I)
      CALL CGRAF(IX,IY,ISX,ISY,IFIN,TAT,BUF1)
```

```
      DO 217 I=1,IFIN
  217 BUF1(I)=DC(3,1,I)
      CALL CGRAF(IX,IY,ISX,ISY,IFIN,TAT,BUF1)
      DO 218 I=1,IFIN
  218 BUF1(I)=DC(3,2,I)
      CALL CGRAF(IX,IY,ISX,ISY,IFIN,TAT,BUF1)
      DO 219 I=1,IFIN
  219 BUF1(I)=DC(3,3,I)
      CALL CGRAF(IX,IY,ISX,ISY,IFIN,TAT,BUF1)
      PAUSE2222
 2004 CALL DATSW (4,IGO)
      GO TO (2192,2190),IGO
 2190 CALL DATSW (5,IGO)
      GO TO (2193,2191),IGO
 2191 CALL DATSW (6,IGO)
      GO TO (2194,2204),IGO
 2192 I=1
      GO TO 2195
 2193 I=2
      GO TO 2195
 2194 I=3
 2195 CALL DATSW (8,IGO)
      GO TO (2198,2196),IGO
 2196 CALL DATSW (9,IGO)
      GO TO (2199,2197),IGO
 2197 CALL DATSW (10,IGO)
      GO TO (2200,2204),IGO
 2198 J=1
      GO TO 2201
 2199 J=2
      GO TO 2201
 2200 J=3
 2201 DO 2202 K=1,IFIN
 2202 BUF2(K)=DC(I,J,K)
      CALL CLEAR
      CALL CXYST(20,0)
      WRITE (5,2203) I,J
 2203 FORMAT ('DETAIL DC(',I1,',',',I1,')')
      CALL CGRAF(1,1,1,1,IFIN,TAT,BUF2)
      PAUSE3333
      GO TO 2004
 2204 CALL COFF
      GO TO 90
  220 IF (I-3) 90,230,500
  230 CALL LINK(MOVE)
  500 CALL CLEAR
      CALL CXYST (20,100)
      WRITE (5,600)
  600 FORMAT ('TO RERUN KINEMATICS, TYPE 1')
      CALL CXYST (20,110)
      WRITE (5,650)
  650 FORMAT ('OTHERWISE,           TYPE 0')
      CALL CXSET(110)
      CALL CYINC(16)
      CALL CDATA(1,I)
      CALL COFF
      IF (I-1) 660,670,500
  660 CALL LINK(HOP)
  670 CALL LINK(MAIN4)
      END

// DUP
*DELETE              MAIN5
*STORECI    WS  UA   MAIN5      1                    N
*FILES(3,KIN03),(4,KIN04),(5,KIN05)
```

```
// FOR
*NAME MOVE
*IOCS(DISK,1403 PRINTER)
*ONE WORD INTEGERS
      DIMENSION P(26,3),IPIC(63,26,3)
      DIMENSION DC(3,3,256)
      DIMENSION POS(3,256)
      DIMENSION IQUIX(1638),IQUIY(1638)
      COMMON IDUM(550)
      EQUIVALENCE (DC(1),IQUIX(2))
      EQUIVALENCE (DC(320),IQUIY(2))
      DEFINE FILE 100(15,2,U,II)
      DEFINE FILE 5(2305,2,U,LL)
      DEFINE FILE 8(768,2,U,LI)
      CALL INHIB
      CALL COFF
      IX=0
      IY=0
      II=14
      READ(100'II) SHANK,PAD
      PLAT=3.6-3.6*PAD/SHANK
      SHANK=3600.0/SHANK
      LL=1
      READ (5'LL) IS,IF,DC
      LI=1
      READ(8'LI) POS
      P(1,1)=-0.5
      P(2,1)=-0.7
      P(3,1)=-0.7
      P(4,1)=-0.5
      P(5,1)=-0.7
      P(6,1)=-0.5
      P(7,1)=-0.7
      P(8,1)=-0.7
      P(9,1)=-0.5
      P(10,1)=-0.7
      DO 101 I=11,20
  101 P(I,1)=0.0
      DO 102 I=21,24
  102 P(I,1)=0.4
      P(25,1)=0.9
      P(26,1)=0.9
      P(1,2)=0.0
      P(2,2)=-0.1
      P(3,2)=-0.1
      P(4,2)=0.0
      P(5,2)=0.0
      DO 103 I=11,15
  103 P(I,2)=0.0
      P(6,2)=0.5
      P(7,2)=0.6
      P(8,2)=0.6
      P(9,2)=0.5
      P(10,2)=0.5
      DO 104 I=16,18
  104 P(I,2)=0.5
      P(19,2)=0.4
      P(20,2)=0.5
      P(21,2)=0.0
      P(22,2)=0.0
      P(23,2)=0.3
      P(24,2)=0.6
      P(25,2)=0.1
      P(26,2)=0.4
```

```
      DO 106 I=1,4
      DO 106 J=1,3
      IJ=5*(I-1)+J
  106 P(IJ,3)=PLAT-FLOAT(J-1)
      P(4,3)=PLAT-3.6
      P(9,3)=PLAT-3.6
      P(14,3)=PLAT-3.6
      P(19,3)=PLAT-3.6
      P(5,3)=PLAT-4.0
      P(10,3)=PLAT-4.0
      P(15,3)=PLAT-4.0
      P(20,3)=PLAT-4.0
      P(21,3)=PLAT-3.7
      P(22,3)=PLAT-4.0
      P(23,3)=PLAT-3.7
      P(24,3)=PLAT-4.0
      P(25,3)=PLAT-4.0
      P(26,3)=PLAT-4.0
      III=IF-IS+1
      ILAST=(III-1)/4
      DO 108 I=1,ILAST
      II=(I-1)*4+1
      DO 108 J=1,26
      DO 108 K=1,3
      IPIC(I,J,K)=     IFIX(20.0*(P(J,1)*DC(K,1,II)  <-------- A
     *                           +P(J,2)*DC(K,2,II)
     *                           +P(J,3)*DC(K,3,II)+POS(K,II)*SHANK))
  108 CONTINUE
      MAX=0
      DO 109 I=1,ILAST
      IF(IPIC(I,5,3)-MAX) 324,325,325
  324 MAX=IPIC(I,5,3)
  325 IF(IPIC(I,10,3)-MAX) 326,109,109
  326 MAX=IPIC(I,10,3)
  109 CONTINUE
      DO 338 I=1,ILAST
      IF(IPIC(I,15,3)-MAX) 327,328,328
  327 IPIC(I,15,3)=MAX
  328 IF(IPIC(I,20,3)-MAX) 329,330,330
  329 IPIC(I,20,3)=MAX
  330 IF(IPIC(I,22,3)-MAX) 331,332,332
  331 IDIF=IPIC(I,22,3)-MAX
      IPIC(I,22,3)=MAX
      IPIC(I,21,3)=IPIC(I,21,3)-IDIF
  332 IF(IPIC(I,24,3)-MAX) 333,334,334
  333 IDIF=IPIC(I,24,3)-MAX
      IPIC(I,24,3)=MAX
      IPIC(I,23,3)=IPIC(I,23,3)-IDIF
  334 IF(IPIC(I,25,3)-MAX) 335,336,336
  335 IPIC(I,25,3)=MAX
  336 IF(IPIC(I,26,3)-MAX) 337,338,338
  337 IPIC(I,26,3)=MAX
  338 CONTINUE
      CALL CINIT(550)
      CALL CON
      CALL CXYST (60,120)
      WRITE (5,240)
  240 FORMAT('LIFT BITSW 4 OR 5')
      CALL CXYST (30,140)
      WRITE (5,241)
  241 FORMAT ('PROVIDE 40 MSEC LEVEL 3 INTERRUPTS')
      PAUSE1010
```

```
C***
C***
C***
      CALL SINT1
      CALL ALLOW
      PAUSE7777
      CALL SINT1
      CALL IREQ
      CALL CLEAR
      IKX=120
      IKY=120
      CALL DATSW(4,K)
      GO TO (265,262),K
  262 CALL DATSW (5,K)
      GO TO (280,264),K
  264 CALL INHIB
      GO TO 90
  265 CALL INHIB
      CALL CXYST(20,5)
      WRITE (5,270)
  270 FORMAT('LIMB MOVEMENT  -  A/P VIEW')
      IY=3
      IX=2
      DO 339 IP=1,256,10
  339 CALL CPUT(IP,IKY+1-MAX)
      GO TO 320
  280 CALL INHIB
      CALL CXYST(20,5)
      WRITE (5,290)
  290 FORMAT ('LIMB MOVEMENT  -  LATERAL VIEW')
      IY=3
      IX=1
      DO 341 IP=1,256,10
  341 CALL CPUT(IP,IKY+1-MAX)
      GO TO 320
  320 CALL ALLOW
      DO 321 IP=1,10
  321 CALL CPUT(240,7+IP)
      DO 322 IP=1,9
  322 CALL CPUT(230+IP,17)
      CALL CXYST(238,0)
      WRITE(5,323) IY
  323 FORMAT(I1)
      CALL CXYST(225,12)
      WRITE(5,323) IX
      DO 1212 I=1,ILAST
      DO 1212 J=1,26
      JK=(I-1)*26+J
      IQUIX(JK)=IKX-IPIC(I,J,IX)          <-- B
      IQUIY(JK)=IKY-IPIC(I,J,IY)
 1212 CONTINUE
      CALL CPOS(IPOS)
 3201 I=1
      JK=1
  110 CONTINUE                            <-- C
      CALL CRSTR(IPOS)
      J=1
  111 CALL CPUTF(IQUIX(JK),IQUIY(JK))
      JK=JK+1
      J=J+1
      IF(J-26) 111,111,1111
 1111 I=I+1
      IF (I-ILAST) 112,112,113
  112 PAUSE7777
      GO TO 110                           <-- D
  113 PAUSE1111
      GO TO 3201
   90 CALL INHIB
      CALL LINK(MAIN5)
      END

// DUP
*DELETE                MOVE
*STORECI     WS  UA  MOVE        1          N
*FILES(100,KIN00),(5,KIN05),(8,KIN08)
```

```
// FOR
*NAME FILM
*ONE WORD INTEGERS
*IOCS(1132 PRINTER,1403 PRINTER)
      REAL K1(128),K2(128),K3(128),KE1,KE2,KE3,K11,K21,K31
      DIMENSION A1(128),A2(128),A3(128)
      DIMENSION TIT(12)
      COMMON IDUM(3000)
      DATA TIT/'MM  ','  A1','MM  ','  A2','MM  ','  A3',
     *         'MM  ','  K1','MM  ','  K2','MM  ','  K3'/
      WRITE (3,100)
  100 FORMAT (1H1,40X,'POSITION DATA FROM FILM (MM)',//,
     *        1H ,'FRAME',5X,'ANKLE 1',13X,'ANKLE 2',13X,'ANKLE 3',14X,
     *        'KNEE 1',14X,'KNEE 2',14X,'KNEE 3')
      CALL CINIT(3000)
      CALL CON
      CALL CXYST(40,100)
      WRITE (5,200)
  200 FORMAT ('ENTER DA,DL,HL,N')
      CALL CDATA(4,DA,DL,HL,NN)
      CALL CLEAR
      CALL CXYST(30,100)
      WRITE(5,300) NN
  300 FORMAT ('FRAME ',I3,/'ENTER A1,A2,A3,K1,K2,K3')
      CALL CDATA(6,AE1,AE2,AE3,KE1,KE2,KE3)
      CALL CLEAR
      A11=AE1*(1.0-AE2/DL)*127.0
      A21=AE2*(1.0-AE1/DA)*127.0
      A31=(AE3*(1.0-AE2/DL)+HL*AE2/DL)*127.0
      K11=KE1*(1.0-KE2/DL)*127.0
      K21=KE2*(1.0-KE1/DA)*127.0
      K31=(KE3*(1.0-KE2/DL)+HL*KE2/DL)*127.0
      N=1
  400 CONTINUE
      IF (N-1) 500,500,600
  500 A1(1)=0.0
      A2(1)=0.0
      A3(1)=0.0
      K1(1)=0.0
      K2(1)=0.0
      K3(1)=0.0
      GO TO 700
  600 CONTINUE
      CALL CLEAR
      CALL CXYST(30,100)
      WRITE (5,300) NN
      CALL CDATA(6,AE1,AE2,AE3,KE1,KE2,KE3)
      CALL CLEAR
      A1(N)=AE1*(1.0-AE2/DL)*127.0-A11
      A2(N)=AE2*(1.0-AE1/DA)*127.0-A21
      A3(N)=(AE3*(1.0-AE2/DL)+HL*AE2/DL)*127.0-A31
      K1(N)=KE1*(1.0-KE2/DL)*127.0-K11
      K2(N)=KE2*(1.0-KE1/DA)*127.0-K21
      K3(N)=(KE3*(1.0-KE2/DL)+HL*KE2/DL)*127.0-K31
  700 CONTINUE
      I=1
      J=1
      IX=2
      IY=3
      CALL CGRAF(I,J,IX,IY,N,TIT(1),A1)
      CALL CGRAF(I,J,IX,IY,N,TIT(7),K1)
      CALL CGRAF(I,J,IX,IY,N,TIT(3),A2)
      CALL CGRAF(I,J,IX,IY,N,TIT(9),K2)
      CALL CGRAF(I,J,IX,IY,N,TIT(5),A3)
      CALL CGRAF(I,J,IX,IY,N,TIT(11),K3)
      PAUSE7777
      CALL DATSW(0,IGO)
      GO TO (400,800),IGO
  800 CALL DATSW(15,IGO)
      GO TO (1100,900),IGO
  900 CALL COFF
      WRITE (3,1000) N,A1(N),A2(N),A3(N),K1(N),K2(N),K3(N)
 1000 FORMAT (1H ,I3,3X,F10.3,5(10X,F10.3))
      CALL CON
      N=N+1
      NN=NN+1
      GO TO 400
 1100 CALL COFF
      CALL EXIT
      END
```

```
      CALL CLEAR
      LK=1
      READ (8'LK) POS
      IX=1
      IY=1
      DO 600 I=1,3
      BUFM=(POS(I,1)+DC(I,3,1)*PAD)*1000.0
      BOFM=(POS(I,1)+DC(I,3,1)*PKD)*1000.0
      DO 500 J=1,IL
      BUF(J)=(POS(I,J)+DC(I,3,J)*PAD)*1000.0-BUFM
      BOF(J)=(POS(I,J)+DC(I,3,J)*PKD)*1000.0-BOFM
  500 CONTINUE
      CALL CGRAF(IX,IY,IXM,IYM,IL,TIT(5),BUF)
      CALL CGRAF(IX,IY,IXM,IYM,IL,TIT(5),BOF)
  600 CONTINUE
      PAUSE3333
      CALL COFF
      CALL EXIT
      END

// DUP
*DELETE                WHERE
*STORECI    WS  UA     WHERE      2                *
*FILES(100,KIN00),(1,KIN01),(2,KIN02),(3,KIN03)
*FILES(4,KIN04),(5,KIN05),(6,KIN06),(7,KIN07),(8,KIN08)
```

```
// FOR
*NAME WHERE
*IOCS(DISK,1403 PRINTER)
*ONE WORD INTEGERS
      DIMENSION AM(3,256),BM(2,256),OM1(256),OM2(256),DC(3,3,256)
      DIMENSION TIT(6),ALPHA(3,256),VEL(3,256),POS(3,256)
      DIMENSION BUF(256),BOF(256)
      COMMON IDUM(2000)
      EQUIVALENCE (ALPHA(1),VEL(1),POS(1))
      EQUIVALENCE (OM1(1),BUF(1)),(OM2(1),BOF(1))
      DEFINE FILE 100(15,2,U,II)
      DEFINE FILE 1(768,2,U,MM)
      DEFINE FILE 2(512,2,U,NN)
      DEFINE FILE 3(256,2,U,MN)
      DEFINE FILE 4(256,2,U,NM)
      DEFINE FILE 5(2305,2,U,LL)
      DEFINE FILE 6(768,2,U,LI)
      DEFINE FILE 7(768,2,U,LJ)
      DEFINE FILE 8(768,2,U,LK)
      DATA TIT/'M/SE','C**2','M/SE','C   ','MM  ','    '/
      CALL IREQ
      II=14
      READ (100' II) SHANK,PAD
      MM=1
      READ (1'MM) AM
      NN=1
      READ (2'NN) BM
      LL=1
      READ (5'LL) IS,IF,DC
      LI=1
      READ (6'LI) ALPHA
      PAD=-PAD/1000.0
      PKD=PAD+SHANK/1000.0
      IL=IF-IS+1
      CALL CINIT(2000)
      CALL CON
      IXM=2
      IYM=3
      IX=1
      IY=1
      DO 200 I=1,3
      MN=1
      READ (3'MN) OM1
      NM=1
      READ (4'NM) OM2
      DO 100 J=1,IL
      K=IS+J-1
      DUM=(AM(1,K)-BM(1,K))*9.81*DC(I,1,J)/0.125
     *   +(AM(2,K)-BM(2,K))*9.81*DC(I,2,J)/0.125
     *   -(OM1(K)**2+OM2(K)**2)*DC(I,3,J)
      BUF(J)=ALPHA(I,J)+DUM*PAD
      BOF(J)=ALPHA(I,J)+DUM*PKD
100   CONTINUE
      CALL CGRAF(IX,IY,IXM,IYM,IL,TIT(1),BUF)
      CALL CGRAF(IX,IY,IXM,IYM,IL,TIT(1),BOF)
200   CONTINUE
      PAUSE1111
      CALL CLEAR
      LJ=1
      READ (7'LJ) VEL
      IX=1
      IY=1
      DO 400 I=1,3
      MN=1
      READ (3'MN) OM1
      NM=1
      READ (4'NM) OM2
      DO 300 J=1,IL
      K=IS+J-1
      DUM=OM2(K)*DC(I,1,J)-OM1(K)*DC(I,2,J)
      BUF(J)=VEL(I,J)+DUM*PAD
      BOF(J)=VEL(I,J)+DUM*PKD
300   CONTINUE
      CALL CGRAF(IX,IY,IXM,IYM,IL,TIT(3),BUF)
      CALL CGRAF(IX,IY,IXM,IYM,IL,TIT(3),BOF)
400   CONTINUE
      PAUSE2222
```